Immunity in Breast Cancer

Charting T cell evasion
and exploring new targets for T cells

Dora Hammerl

The studies described in this thesis were performed at the Laboratory of Tumor Immunology in collaboration with the Laboratory of Translational Cancer Genomics, Department of Medical Oncology, Erasmus MC Cancer Institute, within the framework of the Erasmus MC Molecular Medicine gratuate school. These studies were funded by the Dutch Cancer Society (Alpe d'HuZes/KWF 2014-7087)

ISBN: 9789464190779

cover design and layout: Dora Hammerl

printed by: Gildeprint (www.gildeprint.nl)

Immunity in Breast Cancer
Charting T cell evasion and exploring new targets for T cells
-
Immuniteit in borst kanker
In kaart brengen van T cel evasie en verkenning van nieuwe targets voor T cellen

Thesis

to obtain the degree of Doctor from the
Erasmus University Rotterdam
by command of the
rector magnificus

Prof.dr. R.C.M.E. Engels

and in accordance with the decision of the Doctorate Board.
The public defence shall be held on
Friday 18 December 2020 at 13.30hrs

by

Dora M. Hammerl
born in Oberwart, Austria.

Erasmus University Rotterdam

Doctoral Committee:

Promotors:
Prof. dr. J.E.M.A. Debets
Prof. dr. J.W.M. Martens

Other members:
Prof. dr. P.A.E. Sillevis Smitt
Prof. dr. A.W. Langerak
Prof. R.A. Salgado Figueroa

Erasmus University Rotterdam

Thesis Content

Chapter 1
Short introduction to the thesis' research

PART 1. Charting T cell Evasion

Chapter 2
Dora Hammerl, Marcel Smid, Mieke Timmermans, Stefan Sleijfer, John Martens, Reno Debets
'Breast cancer genomics and immuno-oncological markers to guide immune therapies'

Chapter 3
Dora Hammerl, Maarten Massink, Marcel Smid, Carolien van Deurzen, Hanne Meijers-Heijboer, Quinten Waisfisz, Reno Debets*, John Martens*; *joint senior authors
'Differential prognostic value in breast cancer subtypes: not T cell abundance, rather T cell influx, antigen recognition and suppression'

Chapter 4
Dora Hammerl, John Martens, Mieke Timmermans, Marcel Smid, Anita Trapman-Jansen, Renée Foekens, Olga Isaeva, Leonie Voorwerk, Emrah Balcioglu, Rebecca Wijers, Iris Nederlof, Hugo Horlings, Roberto Salgado, Marleen Kok, Reno Debets
'Spatial immunophenotypes predict response to anti-PD1 treatment in Triple Negative Breast Cancer and capture distinct paths of CD8 T cell evasion'

PART 2. Exploring New Targets for T cells

Chapter 5
Dora Hammerl, Dietmar Rieder, Marcel Smid, John Martens, Zlatko Trajanoski, Reno Debets
'Adoptive T cell Therapy: new avenues leading to safe targets and powerful allies'
Trends in Immunology, 2018 39:921-936

Chapter 1

Short introduction to the thesis' research

1

Chapter 1

Short introduction to the thesis' research

Research in this thesis focuses on immunity in breast cancer (BC), zooming in on 2 main aspects, namely: improved understanding of the lack of immune control, particularly lack of T cell control; and the discovery and testing of new targets for adoptive T cell therapy. These 2 aspects are covered by Parts 1 and 2 of this thesis, respectively.

BC is one of the most frequently occurring cancers worldwide. In the Netherlands 1 in 8 women develop BC during their lifetime (source: IKN). In fact, BC is a heterogeneous disease comprising of several molecular and histological characteristics that can be classified into 4 main subtypes according to the expression of estrogen receptor (ER), progesterone receptor (PR) and human epidermal growth factor receptor 2 (HER2). This subtype classification has clinical relevance since it affects prognosis and available treatment options. In example, the BC subtypes luminal-A (i.e., ER+, PR+, HER2-, low proliferation, often measured by the marker Ki67) and luminal-B (i.e., ER+, PR+, HER2 or Ki67hi) have good prognosis (overall survival (OS): 94% and 90% respectively). These 2 subtypes also have fairly good treatment options, including chemotherapy and endocrine therapy given alone or together with modern targeted therapies, such as mammalian target of rapamycin (mTOR) inhibitors and cyclin dependent kinase (CDK4/6) inhibitors. The her2 subtype (i.e., ER-, PR-, HER2+) has an OS of 83%, and is mainly treated with chemotherapy combined with HER2-blocking antibodies. Finally, triple negative breast cancer (TNBC) (i.e., ER-, PR-, HER-) has the poorest survival (OS: 77%) and unfortunately limited treatment options, such as cytotoxic agents and, for specific subgroups, since recently Poly (ADP-ribose) polymerase (PARP) inhibitors and immune checkpoint inhibition (ICI)[1–3].

It has been recognized for several years that tumor infiltrating lymphocytes (TILs) are frequently present in BC (particularly in ER- subtypes) and that their abundance correlates with survival and therapy response[4–8]. Despite variable frequencies of TILs, their prognostic value was observed in all BC subtypes[9–11]. Hence, in the recent years the development of immune therapies for BC received markedly more attention. In a general sense, immune therapies include oncolytic viruses, vaccination, ICI and adoptive T cell therapy. Treatment with oncolytic viruses is considered to specifically infect malignant cells and boost anti-tumor immune responses; cancer

vaccines make use of predefined antigens either directly administered in form of peptide vaccine or loaded onto dendritic cells that are adoptively transferred; ICI represents treatment with monoclonal antibodies that target so called immune checkpoints, which are expressed by T cells and cancer cells, and aims to (re-)activate the anti-tumor T cell response; and adoptive T cell therapy makes use of the patients own T cells which encode for a T cell receptor with pre-defined tumor reactivity[12–15]. The latter two forms of immune therapy are integral components of this thesis. To date, most immune therapy trials have been performed using ICIs in BC, and these trials showed higher initial responses in TNBC when compared to other BC subtypes (see **Chapter 2** for an overview). Notably, objective response (OR) rates to ICI monotherapy in metastatic TNBC (mTNBC) do not exceed 5-25%[16]. These OR rates do increase when ICI is combined with cytotoxic agents (OR: 30-40%)[16] . As a result, anti-programmed cell death receptor ligand 1 (anti-PDL1) antibody atezolizumab combined with nab-paclitaxel, has recently been approved by the food and drug association (FDA) and European medicines agency (EMA) for PD-L1-positive mTNBC. Nevertheless, these OR rates are considered poor in comparison to other immunogenic solid tumor types, such as melanoma (OR: 43-72%), colorectal cancer (OR: 14-78%[17]) lung cancer (OR: 19-33%[18]). Furthermore, it is particularly hard to predict ICI-response in BC. For example, in contrast to the above mentioned tumor types, mutational burden is not predictive for ICI response in TNBC[19–21] and even the currently used biomarker, PD-L1 on immune cells, does not accurately predict non-responders[22].

Rational and scope of Part 1

Collectively, these clinical observations urge for better understanding of the interplay between the immune system and malignant tumor cells in BC which are studied in Part 1 of this thesis. To date, there is little data regarding the shortcomings in CD8 T cell immunity (i.e., what drivers of immune responses are compromised or lacking) and consequences of effective CD8 T cell immunity (i.e., what immune evasive mechanisms come into play) in BC. In this regard, it has been recognized that not only numbers of TILs, but also their composition, spatial localization and activation state matters[23–27] , urging for better understanding of spatial immune contexture in BC. Part 1 of this thesis focuses on these knowledge gaps, which is most critical to explain the variable and low responses to current immune therapies among BC subtypes (explained in detail in **Chapters 2** and **3**), and may contribute to the development of better predictive markers and provide a basis for the development of more effective combination treatments in TNBC according to determinants of CD8 T cell

immunity (see **Chapter 4**).

Study design and methodology: To this end, we utilized several public and proprietary BC cohorts, including node-negative untreated BC comprising all subtypes as well as anti-PD1 treated TNBC and studied antigen load, T cell clonality as well as gene-sets and pathways associated with T cell evasion. Furthermore, we studied the spatial immune contexture and potential drivers of different immunophenotypes using multiplexed immunofluorescent images on TNBC tissues and assessed its prognostic and predictive value. Finally, we evaluated immune evasive strategies using an integrative approach that combines clinical data, omics data and immunological data.

Rational and scope of Part 2

Part 2 of this thesis shifts focus towards the development of another immune therapy, namely adoptive T cell therapy with TCR engineered cells (AT) for the treatment of TNBC. AT has been very successful in different blood cancers (OR for CAR-T cells in B cell malignancies: 90%[28]) as well as solid tumors (OR TCR-T cells in synovial sarcoma: 61% and in melanoma: 50%[29])(reviewed in **Chapter 5**), but has not yet been tested clinically for the treatment of BC. Despite proven clinical efficacy, AT in solid tumors is challenged by lack of suitable target antigens, poor and non-durable responses and sometimes even toxicities[14,28,30–32]. In contrast to CAR-T cells, TCR-T cells have shown superior clinical efficacy and safety in solid tumors due to recognition of a variety of target antigens (i.e. extracellular as well as intracellular proteins presented via MHC), we opted for the latter form of AT in BC (**chapter 6**). New technologies, including TCR editing have been described which potentially further enhance safety and efficacy profiles of engineered T cells (described in **Chapter 7**). In extension, efficacy is sometimes compromised by the immune-suppressive TME, which can limit influx and migration, antigen presentation or suppression of tumor specific T cells (also reviewed in **Chapter 5**). In this regard, T cell evasive strategies, identified in Part 1 provide rational for combination that enhance the efficacy of AT in BC (discussed in **Chapter 8**).

Study design and methodology: We studied gene and protein expression of target antigens for AT in TNBC and healthy tissues using large expression data sets and tissue micro arrays. We selected and applied a variety of in silico and laboratory tools that enable the identification of immunogenic epitopes including epitope predictions, immunopeptidome analysis of BC cell lines that overexpress

target antigens and in vitro binding assays. We identified TCRs using optimized protocols to enrich specific T cells from TILs or PBMC and tested their functionality and specificity in vitro.

Thesis content in a nutshell

Chapter 2 introduces Part 1 by providing a detailed overview of the composition and the prognostic value of TILs among BC subtypes, and informs on the outcome of various immune therapy trials in different BC subtypes.

In **Chapt 3** we have studied large patient cohorts of node-negative untreated BC and interrogated subtypes for the differential prognostic value of various immune parameters and the occurrence of immune evasive strategies using in silico techniques.

In **Chapter 4** we zoomed in on TNBC and have further delineated the prognostic and predictive value of spatial immune contextures (i.e., excluded, ignored and inflamed phenotypes) in untreated and anti-PD1 treated cancers. Furthermore, we performed in-depth analyses of distinct immune determinants and T cell evasive strategies among the different immunophenotypes using NGS data and multiplexed immune stainings.

An introduction to Part 2 is provided in **Chapter 5**. Here we present an overview of new technologies, including various in silico and laboratory tools, to enable on the one hand selection and validation of target antigens, epitopes, and their corresponding TCRs as well as to enable on the other hand choices of combinatorial approaches that counteract immune evasive mechanism**.**

In **Chapter 6**, we have applied these technologies and identified PCT2, a TNBC-specific target antigen with high and homogenous expression in tumor, but not healthy tissue. Using a variety of tools discussed in **Chapter 5**, we have identified safe and immunogenic epitopes and a corresponding TCR which may be further exploited for the development of AT for TNBC.

In **Chapter 7,** new technologies of TCR-editing that can further improve safety and efficacy of the identified TCR are discussed.

The final **Chapter 8** summarizes the main findings of both parts, and discuss how these findings affect future immune therapeutic developments to treat BC and in particular TNBC.

PART1

Charting T cell evasion

Chapter 2

Breast cancer genomics and immuno-oncological markers to guide immune therapies

Dora Hammerl, Marcel Smid, Mieke Timmermans, Stefan Sleijfer, John Martens, Reno Debets

Department of Medical Oncology, Erasmus MC – Cancer Institute, Rotterdam, the Netherlands

Seminars in Cancer Biology, doi: 10.1016/j.semcancer.2017.11.003

Abstract

There is an increasing awareness of the importance of tumor - immune cell interactions to the evolution and therapy responses of breast cancer (BC). Not surprisingly, numerous studies are currently assessing the clinical value of immune modulation for BC patients. However, till now durable clinical responses are only rarely observed. It is important to realize that BC is a heterogeneous disease comprising several histological and molecular subtypes, which cannot be expected to be equally immunogenic and therefore not equally sensitive to single immune therapies. Here we review the characteristics of infiltrating leukocytes in healthy and malignant breast tissue, the prognostic and predictive values of immune cell subsets across different BC subtypes and the various existing immune evasive mechanisms. Furthermore, we describe the presence of certain groups of antigens as putative targets for treatment, evaluate the outcomes of current clinical immunotherapy trials, and finally, we propose a strategy to better implement immuno-oncological markers to guide future immune therapies in BC.

Abbreviations

APC	antigen presenting cell
APOBEC	apolipoprotein B mRNA editing enzyme, catalytic polypeptide-like
BRCA1/2	breast cancer 1/2
BCSS	breast cancer specific survival
CAF	cancer associated fibroblast
CCL	chemokine ligand
CD	cluster of differentiation
CMV	cytomegalo virus
CTLA4	cytotoxic T lymphocyte associated protein 4
CR	Complete response
CXCL	CXC-motif chemokine ligand
DC	dendritic cell
DCIS	ductal carcinoma in situ
DFS	disease free survival
EBV	epstein-barr virus
ECM	extracellular matrix
ELF5	E75 like ETS transcription factor 5
EMT	epithelial - mesenchymal transition
GBP1	interferone induced guanylate binding protein 1
GRZM	granzyme
HER2	human epidermal growth factor receptor 2
HERV-K	human endogenous retro virus K
HLA	human leucocyte antigen
HPV	human papiloma virus
HR	hormone receptor or hazard ratio
hTERT	telomerase reverse transcriptase-
IDC	invasive ductal carcinoma
IDO1	indoleamine-pyrrole-2,3-dioxygenase
IFN	interferon
IGK	immunoglobin kappa locus
IGLL5	immunoglobin lambda like polypeptide 5
LAG3	lymphocyte activation gene 3
MDSC	myeloid derived suppressor cell
MEK	map kinase kinase
MFS	metastasis free survival
MHC	major histocompatibility complex
MMTV	mouse mammary tumor virus
MUC1	mucin 1
MV	measles virus
NK	natural killer cell
NO	nitric oxide
OCLN	occludin
OR	objective response or odds ratio
OS	overall survival
PC	plasma cell
PD1	programmed cell death protein 1
PDL1	programmed death ligand
PI3K	phosphoinositol 3-kinase
PR	progesteron receptor
RFS	relapse-free survival
ROS	reactive oxygen species
SD	stable disease
STAT1	signal transducer and activator of transcription 1
TAA	tumor associated antigen
TAP	transport associated protein
TIL	tumor infiltrating leukocytes
TLS	tertiary lymphoid structures
TGFB	transforming growth factor -beta
TNBC	triple negative breast cancer
TNFa	tumor necrosis factor -alpha
Treg	Regulatory T cell
Tγδ	gamma delta T cell

2.1 Introduction

Cancer immunotherapy is a rapidly emerging field, which has proven successful in the treatment of various tumor types, such as lymphoma, melanoma, renal cell carcinoma, and non-small cell lung cancer [33]. Initially, breast cancer (BC) has been considered a poorly immunogenic tumor type and has therefore not been extensively investigated for its susceptibility to immune therapies. During the past years, however, it became evident that certain cases of BC are strongly infiltrated by immune cells and that the presence of these immune cells has significant prognostic and predictive value. Although many studies are currently examining immune therapies for BC, still only a minority of patients appear to respond, and little is known about the underlying mechanisms of treatment efficacy. Thus, there is an unmet need to get better understanding of the interaction of breast cancer and the immune system in order to identify potential immuno-oncological prognostic and predictive markers as well as novel leads for effective mono or combination immune therapies.

Genomics has improved our understanding of BC biology and revealed 4 intrinsic molecular subtypes: luminal A (resembling: ER+, PR+, HER2-, Ki67-), luminal B (resembling: ER+, PR+, HER+/-, Ki67+), HER2 (resembling: ER-, PR-, HER2+), and basal-like subtype (resembling: ER-, PR-, HER2-). The classification of BC into subtypes bears clinical relevance. For instance, in the treatment of the hormone receptor (HR) positive subtypes (those that are positive for ER and/or PR) endocrine therapy, including aromatase inhibitors or selective estrogen receptor mediators such as Tamoxifen, play an important role. HER2 over-expressing tumors are generally treated with HER2-targeting drugs such as trastuzumab and pertuzumab, whereas triple negative BC (TNBC, largely resembling the basal-like BC subtype) is mostly treated with standard cytotoxic therapies.

Notably, and the focus of the current review, these molecular subtypes also differ with respect to quantity and composition of tumor infiltrating leukocytes (TILs). In BC, an enormous number of studies have been performed in order to evaluate the prognostic and predictive values of TILs, and their specific subsets. Although mononuclear cells can easily be identified by H&E-stainings upon routine diagnostics, this technique does not allow accurate assessment of different immune subsets. Immune stainings have enabled the phenotypic distinction of various cell types, but are often limited to those markers for which well-characterized antibodies are available. Recent advances in immunogenomics have paved the way towards enhanced understanding of specific immune subsets and their interactions with tumor cells based on gene expression data [34–37]. In addition, emerging DNA sequencing data has made it possible to explore mutational landscapes of BC and investigate their relation-

ship with TILs and immune pathways. Here, we discuss TIL profiles, prognosis and prediction based on TIL subsets, antigenicity, immune evasive mechanisms, and current immunotherapy trials. Finally, we propose a strategy to select and implement immune-oncological markers to improve therapy choices for BC patients.

2.2 Normal breast versus (pre)malignant breast tissues: quantity and quality of TILs

Normal breast tissue

Immune cells in the healthy mammary gland form an active and dynamic barrier against microbes in the mucosal layer [38]. In addition, immune cells take part in mammary gland remodeling and are considered to play a role in cancer immune surveillance [39]. In normal breast tissue, one generally finds low numbers of leukocytes, including T cells (typically expressing the markers CD3, CD4 or CD3, CD8), B cells (CD20), macrophages (CD68) and dendritic cells (CD11c) [38]. These immune cells are not found in interlobular stroma but are restricted to the lobules, where T cells directly associate with the epithelial layer [40]. While frequencies of macrophages and CD4 T cells are rather constant, frequencies of CD8 T cells depend on hormonal changes and peak within the luteal phase of the menstrual cycle, coinciding with epithelial cell turnover [41].

Pre-malignant breast tissue

BC formation is a multistep process, including premalignant stages of hyperplasia and ductal carcinoma in situ (DCIS) and the malignant stage of invasive ductal carcinoma (IDC) [42]. The transition from normal breast tissue to malignancy typically goes along with an increased infiltration of leukocytes, including myeloid cells, B cells and cytotoxic CD8 T cells [40]. First, in premalignant DCIS, an increased lymphocytic infiltration is observed [43], which is significantly higher in HER2+ and TN DCIS compared to HR+ DCIS [44]. Numbers of neutrophils are significantly increased compared to normal tissue, however activated T cells represent the dominant lymphocyte population[45], followed by B cells and the immune suppressive regulatory T cells (Tregs: CD4, CD25, FOXP3) [46]. While in normal and premalignant BC the CD4/CD8 T cell-ratio is approximately 2, in IDC this ratio is shifted towards 0.3 [47,48].

Malignant breast tissue

A common feature in IDC is a high overall quantity of TILs. Interestingly, high lymphocytic numbers relate to better prognosis and predict a favorable response to neo-adjuvant chemotherapy [49–51](see also sections 2.3 and 2.4). In fact, in highly inflamed tumors, TIL frequency was found to be a superior prognostic marker in comparison to HR status and lymph node involvement in patients with primary operable BC [47]. Notably, characteristics of TILs vary across molecular subtypes of BC [52,53]. The frequency of TILs is usually high in the more aggressive types of BC, including the ER- subtypes (HER2 and basal) as well as the highly proliferating luminal B subtype, but are low in the less aggressive luminal A subtype [54,55] (**Figure 1A**). Even though, the evaluation of overall TIL frequencies, based on H&E stainings, in feasible and clinically relevant [56,57], it is noteworthy, that TILs represent a heterogeneous collection of immune cells, and not all types or subsets of immune cells are associated with a favorable clinical outcome (**Figure 1B** and explained in more detail in section 2.3).

2.3 Prognosis of breast cancer based on TILs

Numerous studies have investigated the prognostic values of TILs and specific subsets by means of H&E- and immune stainings, flow cytometry or analyses of gene expression. We evaluated 33 of such studies and schematically categorized different TIL subsets based on hazard ratios (HR) for ER- and ER+ BC (**Figure 1B**).

2.3.1 Prognostic TILs in ER- breast cancer

ER- tumors typically show higher numbers of TILs when compared to ER+ tumors. Especially numbers of T- and B cells, macrophages and myeloid derived suppressor cells (MDSC) are higher in ER- compared to ER+ BC [53].

Favorable outcome

Adaptive immune cells, including cells of T- and B cell lineages, are typically found in sites of prior, or ongoing immune reactions. High numbers of such lymphocytes are associated with a better prognosis in lymph node negative, primary BC patients including those with stages I-III [47,58–60]. Moreover, numerous studies show that high frequencies of CD8 effector T cells and T helper type-1 gene signatures (Th1: IFNG, STAT1, GRZM, CXCL9) are correlated with favorable clinical outcome, particularly

in ER- tumors [62] . In contrast, high numbers of Tregs in tumor tissue and blood are correlated with favorable outcome in ER- tumors, which may reflect the initiation of negative feedback since numbers of Tregs strongly correlate with those of CD8 T cells and are correlated with poor prognosis in the absence of CD8 T cells [62–64]. B cell and plasma cell (PC: CD138) gene signatures are especially significant prognostic factors in ER- BC, but also in highly proliferating luminal B BC [54]. Macrophages are enriched in basal-like BC and associate with survival according to immune stainings [47,50,60]. In agreement, myeloid and macrophage/dendritic cell signatures (oa. MHCII, CD11c, CD11b) were found to have overall prognostic value in BC according to large gene-expression cohorts [54,65]. Notably, higher blood lymphocyte to monocyte ratio (LMR) correlates with overall survival (OS) in 1570 BC patients (HR: 1.63, 95% CI: 1.07-2.49), in particular in TNBC patients (HR: 3.05, 95% CI: 1.08-8.61) [66].

Unfavorable outcome

Frequencies of immature immune cells, such as MDSC (CD33) which can originate from monocytic or granulocytic lineages, are enriched in highly proliferating ER- tumors [53], and intra-tumoral numbers of these cells are correlated with poor survival in ER- tumors [67]. Elevated numbers of MDSCs are also found in peripheral blood of BC patients when compared to healthy controls [68]. Strikingly, also in the blood compartment frequencies of MDSCs are associated with later stage tumors, metastatic tumor burden, and are correlated with reduced survival [69,70]. Also, numbers of intra-tumoral neutrophils (N, CD16) are associated with poor BC-specific survival [47], and meta-analysis revealed significant unfavorable prognosis in case of a high neutrophil to lymphocyte ratio (NLR, HR(OS): 2.03, 95% CI: 1.41-2.93) [71]. High frequencies of undifferentiated macrophages and alternatively activated, M2 macrophages (CD163) are inversely correlated with survival [67].

2.3.2 Prognostic TILs in ER+ BC

In comparison with ER- BC, less studies found significant correlations between immune cell subsets and clinical outcome in ER+ BC. Overall, mostly innate immune cells cluster to the ER+, luminal A tumors and correlate with good prognosis [53].

Favorable outcome

NK cells are shown to have anti-tumor activity in ER+ BC [72,73], yet their numbers

are decreased in later tumor stages [74]. Signatures of B cells including plasma cells, plasmablasts and immunoglobulin not only correlate with favorable outcome in ER-, but also ER+ tumors [20,32,40].

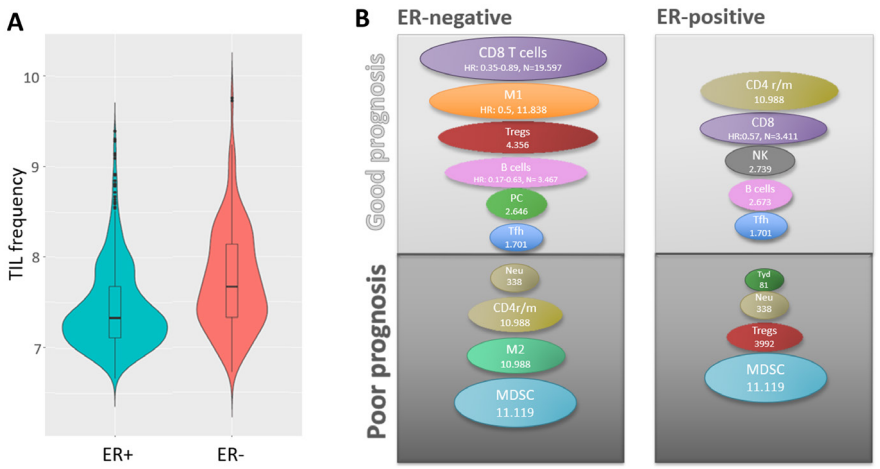

Figure 1. TIL frequencies and prognosis in ER+ and ER- BC: Violin plots based on average RNA expression of TIL gene signature [>100 leukocyte related genes, manuscript in preperation] on a log scale, per patient based on ER-status. (Data from NCBI's Gene Expression Omnibus, accessions GSE2034, GSE5327, GSE2990, GSE7390 and GSE11121.) (**A**). Leukocyte subsets which are significantly correlated ($p<0.05$) with overall survival, or metastasis free survival (*), in ER+ and ER- tumors. Hazard ratios of multivariant regression analyses are shown between brackets [HR]. Circle sizes are indicative of cohort-size (N), based on numbers of patients evaluated in one or more studies [13, 18-43]. Studies include gene expression based analysis, immunohistochemistry and/or flow cytometry (**B**).

Unfavorable outcome

Gamma delta T cells (Tγδ, TCRγ/δ) are more frequent in BC compared to other immunogenic tumors, such as melanoma, suggesting a unique role of these T cells in BC [77]. Moreover, numbers of a subset of Tγδ cells, the so-called regulatory Tγδ, correlate with advanced cancer stages, lymph node involvement and numbers of FOXP3+ cells in ER+ BC, whereas numbers of this subset inversely correlate with those of CD8 T cells in these tumors [78]. It is important to note that while Tregs are correlated with good prognosis in ER- tumors, these cells are strongly associated with adverse clinical outcome in ER+ tumors [62,64]. Even though numbers of MDSC are generally lower in ER+ tumors, their presence is correlated with poor OS [67].

2.4 Prediction of breast cancer therapies based on TILs

Many studies show that standard neo-adjuvant therapies can recruit TILs and modify the tumor microenvironment. Vice versa, TILs, when present prior to therapy, were found to be predictive for clinical response to neo-adjuvant therapies.

2.4.1 Prediction of neo-adjuvant therapies based on TILs

Besides surgical resection and radiotherapy (RT), primary operable BC patients are frequently treated with neo-adjuvant chemotherapy (NAC) and/or targeted therapies. It is of interest to note that numerous studies suggest that the immune system is required to boost the efficacy of NAC. Sequential treatment with anthracycline- or taxane-based drugs is a common form of NAC used to treat BC, with pathological complete responses (pCR) ranging from 10 to 30%. NAC based on anthracyclines and taxanes can directly induce immunogenic tumor cell death, resulting in increased antigen presentation. Moreover, NAC was found to induce inflammatory pathways in tumor associated fibroblasts, such as interferon, Wnt and TGFβ signaling pathways [79], which can enhance recruitment of TILs. Consequently, immune gene signatures have been revealed to predict the response to NAC across various studies, regardless of molecular subtypes or treatment regime [54,80,81]. Also, high TIL frequencies (>60%), as assessed by H&E stainings were predictive for response to NAC82. In fact, a 10% increase in TIL frequencies resulted in 16% increase in pCR rates in TNBC (OR: 1.16), 13% in HER2 (OR: 1.13), and 33% in ER+/ HER2- BC (OR: 1.31). In the latter subtype no survival benefit was noted, which may be attributed to differences in TIL composition (as explained in more detail in sections 2.3.1 and 2.3.2). The predictive value of TILs in the setting of NAC is mainly attributed to high numbers of CD8 T cells (odds ratio (OR) for pCR: 1.59-3.36, [83,84]) but also the presence of follicular T helper cells (Tfh: CD200, CXCL13), were found to have predictive value in ER- (OR(pCR): 1.34-1.85) as well as ER+ (OR(pCR): 2.52) BC patients, across different studies, using both immune stainings and genomic approaches [67,73,83]. Vice versa, chemotherapy can change the immune cell composition in tumor tissue and blood. For example, within 2 weeks after NAC, B-, T- and NK cells were found significantly depleted from peripheral blood compared to pre-treatment levels, with numbers of B and CD4 T cells remaining low up to 9 months post chemotherapy [85], whereas numbers of MDSCs were increased [69]. Numbers of intra-tumoral CD68 macrophages were found significantly decreased to NAC, while those of intra-tumoral CD8 T cells were increased compared to pre-NAC frequencies [50,69]. Strikingly, high intra-tumoral numbers of CD3, CD4 and CD20 as well as high CD4/CD8 ratios prior to therapy predict clinical benefit following NAC independently

of subtype or clinical parameters (OR(pCR): 17.84 [50]). In ER- tumors, pre-therapy T- and B cell signatures were found to predict long-term (> 6 year) outcome to anthracycline-based chemotherapy (OR(pCR):6.33 [86]).

Similar to NAC, RT can also induce immunogenic cell death, antigen release and local inflammation, and consequently evoke an innate and adaptive immune response directed against the tumor [87]. Interestingly, in an ER-, HER2+ patient, who showed a clinical complete response following neo-adjuvant (paclitaxel) and RT, the production of Th1-type cytokines by tumor-specific T cells was enhanced compared to pre-treatment [88]. Immune responses may also predict clinical responses to endocrine therapy [89,90]. In example, OS of post-menopausal women treated with aromatase inhibitors, which block the conversion of androgens into estrogens, is correlated with high numbers of TILs, in particular high numbers of Tregs [91]. In contrast, treatment with tamoxifen (an ER antagonist) shifts immune response from Th1- towards Th2-type T cell responses in an estrogen-independent manner, and may promote immune escape [92]. Treatment with trastuzumab, a humanized antibody directed towards HER2, is at least in part dependent on the immune system as this treatment induces influx of T cells, macrophages and NK cells into tumor tissue and promotes cell-mediated cytotoxicity [93]. Vice versa, pre-existing lymphocytic infiltrate can predict response to trastuzumab treatment [94,95], altough clinical studies provide somewhat contradictive data. While in certain trials higher TIL frequencies [7] or high expression of TIL gene signatures [96] at diagnosis were significantly associated with good response when treated with trastuzumab in combination with CT, in another large clinical trial the presence of TILs was associated with survival in patients treated with chemotherapy only, but not in patients treated with CT plus trastuzumab [97]. Interestingly, in the same study expression of genes related to immune function, did correlate with survival in the CT plus trastuzumab treated group [98], suggesting that particular TIL subsets, rather than bulk TIL predict response. These conflicting results between different studies, may be explained by differences in treatment regime and HR status of patients [99], because the latter correlates with CT response as well as TIL frequency and composition, potentially favoring that patients treated with trastuzumab should be stratified according to HR status. Further research is required to better define the predictive value of particular TIL subsets in this patient group.

Overall, the above findings suggest that standard care of treatments can modulate the tumor microenvironment and may sensitize tumors towards immune therapies. In fact, combination of RT and NAC with immune therapies has already shown promising results in mouse models of BC, and is currently investigated in a number of clinical trials (Table 1), [100–102].

2.4.2 Prediction of immune therapies based on TILs

Thus far, immunotherapeutic approaches to treat BC include: peptide vaccines; autologous transfer of T cells, NK cells or DCs; and application of checkpoint inhibitors. An overview of these treatments is given in **Table 1**. Vaccinations in BC have been focusing mainly on targeting the over-expressed HER2/neu antigen, for which successful treatment has been achieved in DCIS, usually resulting in lesion shrinkage along with activation of HER2-specific CD8 T cells [103–105]. In later stage tumors, however, at best stable disease (SD) has been achieved using similar approaches. Adoptive transfer of autologous HER2-specific T cells resulted in the killing of BC cells that were metastasized to bone marrow, but these T cells were unable to penetrate and resolve liver metastases [106,107]. In contrast, adoptive transfer of allogeneic T cells or NK cells to metastatic BC patients (all subtypes) did not result in T cell persistence and frequently led to graft versus host disease [108,109]. Promising clinical responses have been observed for checkpoint inhibition in the advanced metastatic BC setting. For example, blockade of CTLA-4 (Tremelimumab) has led to SD for >12 weeks in 42% of heavily pre-treated ER+ patients [110]. Even better responses, including a few complete responses and several partial responses, were observed upon treatment with a PD-1 blocking antibody (Pembrolizumab) in TNBC patients with PD-L1-positive tumors in 2 trials (objective response (OR): 18.5%, [111]; OR: 23%, [112]). Combinations of CTLA-4 (Tremelimumab) and PD-L1 (Durvalumab) blockade even reached OR in 43% of stage IV, TNBC patients, however, no OR was observed in any of the 11 HR+ patients, [113] which may be due to low numbers of CD8 T cells in these tumors (**Figure 3**). In contrast, blockade of PD-L1 (antibody not specified) in a small group of 4 stage IV BC patients (unknown HR status) did not result in any clinical response [114]. Notably, in that study, PD-L1 expression had not been assessed prior to PD-L1 treatment, which may have contributed to these contradicting results. Another large trial with a PD-L1 blocking antibody (Avelumab), in 168 BC patients, which were not selected for BC subtype nor PD-L1 expression, resulted in a low OR of 4.8%, including 1 CR and 7 PR [115]. When evaluating BC subtypes in that study, TNBC patients had an OR of 8.6% while HR+ patients had an OR of 2.8%. Even though >10% PD-L1 expression on immune cells in TNBC tumors correlated with response, interestingly, there was no overall association of PD-L1 expression and OR [116]. Due to the dynamic nature of PD-L1 expression (explained in section 2.5), we propose to take caution when using this molecule to stratify BC patients for treatment with checkpoint inhibitors. The presence of TILs, in particular CD8 T cells, and (co-)expression of checkpoint molecules on these cells may serve as a more discriminatory marker than tumor cell PD-L1 expression. In fact, high stromal TIL numbers were significantly correlated with a better response to PD-1 blockade (Pembrolizumab) when administered as monotherapy in a first-line setting for meta-

static TNBC (OR: 39.1% above median stromal TIL; OR: 8.7% below median stromal TIL), while PD-L1 expression did not add to the response prediction in that cohort [117]. Promising results have also been observed when combining checkpoint blockade with standard chemotherapies in the neo-adjuvant, as well as the advanced disease setting of TNBC: Upon combination of neo-adjuvant paclitaxel and PD-1 blockade (Pembrolizumab), an impressive OR of 71% was observed in stage II/III TNBC patients, and an OR of 28% was seen in HR+ patients, which were both significantly increased when compared to paclitaxel monotherapy (OR: 19% and 14% in both patient groups, respectively) [118]. In addition, combination of nab-paclitaxel and PD-L1 blockade (Atezolizumab) in metastatic TNBC reached comparable results (OR: 70%) independent of PDL-1 status [119]. Notably, the OR-rates where higher in early lines of therapy in patients with a lower disease burden, reaching 11% CR and 78% PR in patients with one lesion, in contrast to 0% CD and 43% PR in patients with 3 lesions. When treating mainly HR+ metastatic BC with a combination of LAG3Ig fusion protein (IMP321) with paclitaxel, an OR of 50% was achieved which was 25% higher compared to a historical paclitaxel treatment results [120]. These data strongly encourage the rational of combination therapies, particularly in BC where initial TIL numbers are low (HR+) and sensitization of the tumor micro environment may be required for effective immune therapies (**Figure 4**).

At the moment, an increasing number of clinical studies are focusing on immune therapies for BC of various subtypes. A main category of immune treatments is represented by (combinations of) antibodies blocking the checkpoints PD-1, PD-L1, CTLA-4, and LAG-3. In addition to the checkpoint blockade studies mentioned above, another 91 trials are currently being scheduled (blockade of PDL-1: 13x; CTLA-4: 10x; PD-1: 62x; LAG3: 6x, according to clinicaltrials.gov). In addition to checkpoint blockers, vaccine studies are performed directed against over-expressed antigens other than HER2, such as hTERT, surviving and p53. And finally, adoptive transfer studies with T cells have started, either those with T cells engineered with a Chimeric Antigen Receptor (directed against: HER2 (3x), EpCAM, ROR1, MUC1 and CD133) or a T cell Receptor (directed against: survivin or Cancer Germline Antigens: Mesothelin, NY-ESO1:3x, MAGE-A4, PRAME and SSX1), (according to clinicaltrials.gov).

Type of immune therapy	Target	Stage / type	Patients	Clinical outcome
DC vaccination				
Her2 peptides (MHCI and II) [103]	HER2	0 / HER2	11	PR: 64%
Her2 peptides (MHCI and II) [104, 105]	HER2	0 / HER2	27	PR:88%,CR:40%(ER-); 5.9%(ER+)
autologous APC + Her2/neu cDNA [121]	HER2	IV / HER2	18	PR: 5%, SD: 16%
autologous DC [122]		II,IIIA / ER-, PR-	31	PD: 100%
wt p53 peptide (MHC II) [123]	P53	IV	26	SD: 30%
Vaccination (not DC)				
Mam-A cDNA [124]	Mam-A	IV	7	NA
E75 Her2 peptide (HLA-A2/A3) [125]	HER2	0 / HER2	182	DFS: 94.3%
MDA-MB-231 (CD80+, HLA-A2, HER2) cell line [126]	HER2	IV	30	SD: 30%
AE37 Her2/neu peptide (MHCII) [127]	HER2	0	15	NA
Checkpoint inhibitors				
anti PD-L1 (not specified) [144]	PDL1	IV	4	PD: 100%
tremelimumab [110]	CTLA4	IV / ER+	26	SD: 42%
pembrolizumab [111]	PD1	IV / TNBC	27	CR: 2.7%, PR: 15%, SD:26%
pembrolizumab [112]	PD1	IV/TNBC	52	CR: 4% PR: 19%, SD: 17%
pvelumab [115]	PDL1	II/IV	168	CR:0.6% PR: 4.8% SD:24%
pembrolizumab + paclitaxel [118]	PD1	II, III/ Her2-	69	CR: 71.4% (TNBC), CR: 28% (HR+)
durvalumab + tremelimumab [113]	PDL1, CTLA4	IV/ ER+, TNBC	18	PR: 43% (TNBC), 0% ER+
atezolizumab + nab-paclitaxel [119]	PDL1	IV TNBC	32	CR: 4,2% PR:66.7% SD: 20.8%
Adoptive Transfer of immune cells				
autologous T cells [106]	HER2	IV / HER2	1	NA
allogenic T cell mix		IV	9	PR: 56%
autologous T cells + bispecific antibody [107]	HER2, CD3	IV / HER2+/-	23	SD: 27%
allogenic NK cells [109]		IV	6	NA
Other therapies				
oxidized mannam MUC1 [128]	MUC1	II / MUC1+	31	NA
zoledronate (ydT cell agonist) + IL2 [129]		IV	10	PR: 10%, SD: 20%
IMP321 (LAG3Ig fusion protein) + paclitaxel [120]	MHCII	IV	30	PR: 50% SD:40%

Table 1. Overview of immune therapy clinical trials in BC. NA, not assessed; PR, partial response; CR, complete response; SD, stable disease; PD, progressive disease; DFS, disease free survival; DTH, delayed type hypersensitivity; Tγδ, gamma delta T cell.

2.5 Immunogenicity of breast cancer knows several flavors

Immunogenicity of tumor tissue determines the initiation of an anti-tumor adaptive immune response, and depends on various factors, including the quantity and quality of TAA and their presentation to infiltrating immune cells. TAAs are typically categorized in different groups of antigens, including shared antigens which are generally over-expressed in tumors, but not restricted to malignant tissues (and also expressed by normal tissues). Some shared antigens, such as oncoviral antigens and Cancer Germline Antigens (CGAs), are predominantly expressed in tumors and, in case of CGAs, also in immune privileged tissues of the germline. Besides shared antigens, TAAs also include non-shared antigens, such as tumor-specific neo-antigens, which derive from mutated proteins, and are absent in normal tissues.

Most of these groups of TAAs have been exploited for their use as immunotherapeutic targets in many different tumors. In BC most experience has been gained with the targeting of over-expressed antigens. Even though over-expressed antigens are not tumor-specific, cancer vaccines directed towards such antigens, including HER2, MUC1, and hTERT, could induce partial regression and induce immune responses against these antigens in a number of BC patients without major side effects (reviewed in [130,131]). Virus specific DNA can drive tumor formation and lead to expression of oncoviral antigens. Virus specific DNA (EBV, HPV and MMTV) is significantly more frequently detected in BC compared to normal breast tissues [132]. For instance, expression of human retrovirus type K (HERV-K) is enriched in BC, including BC cell lines, and antibody titers are significantly increased in women with DCIS and IDC when compared to healthy controls [133]. Also, Measle Virus (MV) was detected in 64% of BC including DCIS, and its expression correlated with younger age and lower grade tumors [134]. Notably, human cytomegalovirus (CMV) is expressed in 100% of primary BC specimens and 95% of lymph node metastases [135], while it is generally not expressed in normal tissues [136]. Although in general the presence and reported immunogenicity of viral antigens is evident, the therapeutic potential of this class of TAAs in BC is not clear, nor have these antigens yet been targeted in BC patients. CGAs have not yet been targeted frequently either, while the majority of BC express at least a single CGA [137]. Although CGAs are expressed throughout all tumor stages, including DCIS and all histotypes [138], expression levels and number of expressed CGAs are significantly increased in high grade and ER- BC (highest in basal-like BC) (**Figure 2A**). Interestingly, especially TNBC patients and BRCA carriers often co-express multiple CGAs [139,140]. Besides their high and tumor-specific expression of at least some CGAs, these antigens represent therapeutically relevant target antigens since they have been reported to elicit humoral immune response and were shown in some instances to contribute to BC development. In example, patients with

CGA+ BC have demonstrated enhanced antibody titers against these antigens, and CGAs, have been reported to be associated with increased EMT, genomic instability, angiogenesis and tissue invasion in BC [141–143]. Not surprisingly, expression of these CGAs is often linked to adverse outcome. With respect to neo-antigens, expression of these antigens is governed by the mutational load of tumors. Compared to other cancer types, BC has an average mutational load of 1 somatic mutation per Mb, which ranks these tumors among the lower half of a large series of different human cancer types [144]. A mutational load of 10 somatic mutations per Mb (= 150 non-synonymous mutations in all expressed genes) is considered sufficient to elicit a T cell response in melanoma [145]. This suggests that the overall chance of T cells recognizing neo-antigens in BC is rather low. Within BC, however, the median mutational load increases upon higher tumor grades, and the mutational load is significantly increased in ER- subtypes (highest in Basal-like BC), compared to ER+ subtypes, regardless of BC histotypes [146], (**Figure 2B**). These findings suggest that more aggressive, ER- BC may be susceptible for the immunological targeting of neo-antigens. Besides the number of mutations, some mutational signatures were found to be more immunogenic than others. The most prevalent mutational signatures in BC are age-, APOBEC- and BRCA1/2-related signatures [144]. APOBEC3B (A3B) expression is enhanced in ER-, HER2+ subtypes, and correlates with lymph node metastasis [147] and poor prognosis [148]. Interestingly, we have shown previously that APOBEC signatures may create positively charged, neo-antigens, which are associated with increased T cell infiltration in ER+ BC [149]. A3B deletion, on the other hand, leading to hyper-mutation, correlates with IFNy/STAT1 expression and immune cell signatures [147]. The exact mechanism and role of A3B and APOBEC mutagenisis in BC immunogenicity requires further research.

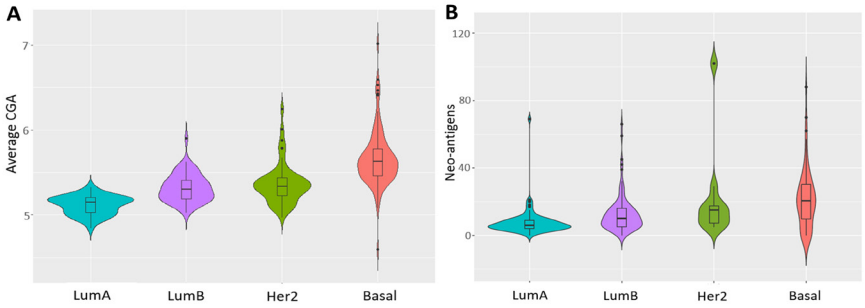

Figure 2. Antigen expression across BC subtypes. Violin plots show average CGA gene expression on a log scale, per patient, based on molecular subtypes. Differences in CGA frequency per molecular subtype are significant (p<<0.0001, Kruskal Wallis test). CGA genes list was derived from CT Database and include CGA genes that were available on Affymetric U133a chip, data from GSE2034, GSE5327 (**A**). Violin plots show the total number of predicted neo-antigens [149] per patient, based on molecular subtypes. Differences in neoantigen frequency per subtype are significant (p<0.0001, Kruskal Wallis test) (**B**).

2.6 Immune evasion of breast cancer counteracts effective therapy

High expression levels of tumor associated antigen (TAA) in late stage and HER2+, ER- BC or TNBC, and high frequencies of TILs in these subtypes do not correlate with each other [150], suggesting that either not all TAAs are equally immunogenic and/or that these tumors have undergone immune editing. The latter generally refers to the shaping of tumor antigenicity under the selective pressure of effector immune cells, and ultimately gives way to the establishment of immune evasive mechanisms [151,152]. Such immune evasive mechanisms may include down-regulation of antigen presentation, lack of immune effector cells, enrichment of immune suppressor cells, and up-regulation of checkpoint molecules [34,35].

Antigen presentation

Critical for the recognition of tumor cells by T cells is that peptides derived from TAAs are presented on human leukocyte antigen (HLA) molecules expressed on the surface of tumor cells or antigen-presenting cells. In fact, expression of genes related to the HLA-A antigen presentation pathway correlates with expression of genes related to T cells, and was found to be most significantly associated with survival within TNBC patients [153]. Especially higher grade BC often (30-40% of tumors) down-regulate classical HLA-A, HLA-B, HLA-C molecules, which are required for the activation of CD8 T cells, and up-regulate non-classical HLA-E, HLA-F, HLA-G molecules, which may promote immune escape [154–156]. Besides HLA-A, expression of transport-associated proteins (TAP1/TAP2), which are required for proper antigen loading, is also down-regulated in high-grade BC [157]. TAP1/TAP2 down-regulation, however, is independent from HLA-A, B, C down-regulation [158], pointing to lack/absence of redundancy of various components of the HLA antigen presentation pathway with respect to immune escape. Besides downregulation of antigen presentation, mutations in antigen presentation (B2M) and IFN response genes (JAK1/2) pathways may provide yet another mechanism of immune escape. Mutations in JAK1/2 can lead to primary as well as acquired resistance to checkpoint blockade[159,160] and potentially other immune therapies. While JAK1/2 mutations affect only a minority of primary BC, and only truncated mutations (1.3% of BC) are associated with poor prognosis[159], BC metastases were found to have acquired additional JAK/STAT driver mutations [161].

Immune effector and suppressor cells

The frequency of clonally expanded, activated T cell is decreased in IDC compared to DCIS45, suggesting that clonal selection for less immunogenic TAAs may occur,

and/or that there is a lack of T cell recruitment or active suppression. In general, exclusion from tumor tissue or compromised activity of intra-tumoral CD8 T cells may in some cases be the direct consequence of aberrant expression of chemokines, adhesion molecules and/or extracellular matrix components (ECM), which to our knowledge has not been investigated yet in BC. There is increasing evidence that oncogenic pathway alterations may contribute to T cell exclusion or comprised activity[152]. PI3K pathway alterations are the most common driver mutations in BC, affecting 49% of luminal A tumors while affecting only 7% of basal like BC162. Interestingly, PTEN loss, which was found to correlate with a lack of TILs in melanoma [163], frequently occurs in basal-like BC (35%)[162] and may contribute to heterogeneity with respect of TILs in this BC subtype. In addition, in TNBC, a lack of T cells is associated with RAS/MAPK pathway activation [164]. Exclusion or compromised activity of CD8 T cells, in other cases, may also be the indirect consequence of enhanced presence of M2 macrophages, MDSC, Tregs and/or cancer associated fibroblasts (CAFs) [31]. CAFs can promote angiogenesis and/or endothelial to mesemchymal transition (EMT), and release suppressive cytokines, such as IL1, IL6 and TGFβ, which can drive the formation of immune suppressor cells [165,166]. In BC, immune suppressor cells, including MDSC and M2, can promote tumor growth and metastasis and suppress T- and NK cell function by releasing suppressive mediators, such as IL10, IDO1, reactive oxygen species (ROS) and nitric oxide (NO) [167,168]. Enhanced recruitment of MDSC is considered to be related to increased expression of ELF5 and CCL2 in ER- BC, and enhanced IFN-signaling was found to induce immune suppressive activities of MDSC [169]. Tregs are recruited by CCL5 and CCL22, which are produced by CD8 T cells and DC [170]. Next to inhibition of CD8 T cells, Tregs can directly promote BC metastasis in a paracrine manner [170].

Checkpoint molecule

As a consequence of an ongoing adaptive immune response, CD8 T cells, but also their target cells, up-regulate the expression of a number of immune checkpoint molecules, which slow down and ultimately inhibit active tumor killing by T cells. PD-L1, for instance, is expressed in a quarter of all BCs and high expression levels correlate with poor OS across all subtypes [171]. PD-L1 expression is particularly high in inflammatory BC (IBC, defined by symptoms resembling an inflammation, mostly ER-), and correlates with T- and B- cell signatures, most significantly those covering cytotoxic T cells, interferon and TNFα pathways [172]. Early BC stages, such as DCIS do not yet express PD-L1, however, in triple negative DCIS, APCs do already show strong PD-L1 expression [46]. Besides acquired expression of PD-L1 by the inducers IFNα/β or IFNγ, which are well-recognized products of activated immune cells or resident stromal cells, also mutations in PTEN and PI3K which occur in 30%

and 40% of BC, respectively, were found to provide inherent expression of PD-L1 [173]. Moreover, EMT was found to induce PI3K and MEK-dependent up-regulation of PD-L1 in BC [174]. PD-L1 expression in BC is accompanied by expression of other immune suppressive checkpoints, like IDO1 and TGFb, as well as the expression of T cell co-inhibitory receptors, such as PD-1, CTLA-4, TIM-3 and LAG-3 [172,174]. PD-1 expression is commonly up-regulated after T cell activation and PD-1 positive T cells can be detected in blood of early stage BC patients, while peripheral changes in the expression of other checkpoint molecules such as CTLA-4 are not observed [175].

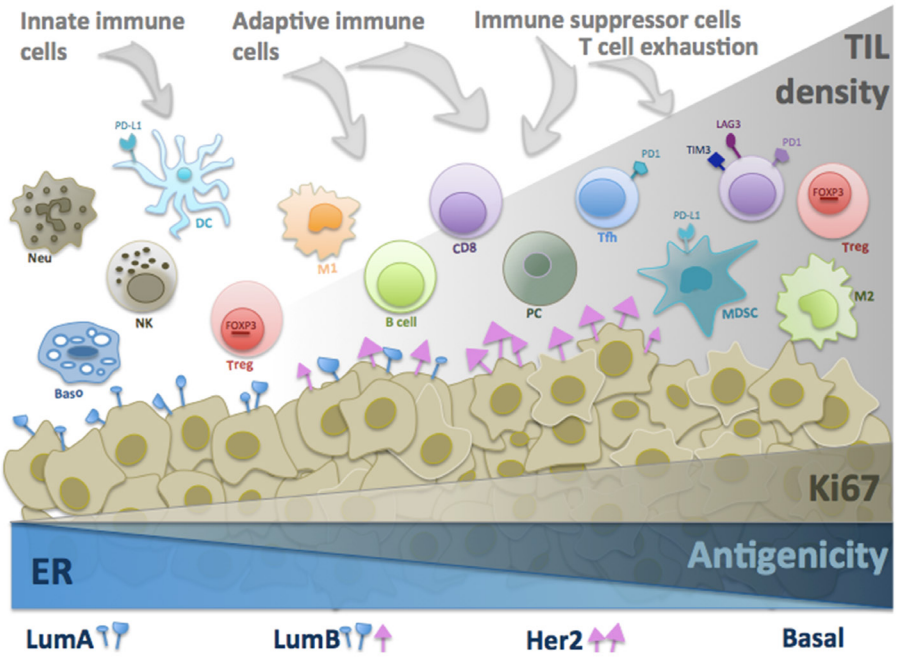

Figure 3. Schematic illustration of immunity and evasive mechanisms in BC. BC subsets are categorized according to hormone receptor ER and PR (blue) or HER2 (pink) expression of tumor cells (brown). Antigenicity (ao. CGAs and neo-antigens) increases from luminal to basal type BC. Overall TIL quantity (gray background) increases from lumA to basal type BC, and its increase is related to tumor cell proliferation (Ki67). With respect to TIL quality, lumA tumors have relatively more innate immune cells, whereas the highly proliferating lumB, her2 and basal BCs are enriched for adaptive immune cells and immune suppressor cells. In particular, basal BC is enriched for exhausted CD8 T cells.

Within tumors, T cells positive for PD-1 are generally restricted to tertiary lymphoid structures (TLS), which are present in tumor stroma and composed of B- and T cells. TLS are often representative of a strong and ongoing immune response, and are present in 60% of BC, including all molecular subtypes [176]. In TNBC, the ex-

pression of PD-1 and LAG-3 tends to be associated with good prognosis. PD-1 and LAG-3 positive TILs were found in 30% and 18% of BC, respectively, and 15% of tumors were double positive for these markers, most likely indicating the presence of exhausted T cells [177]. Checkpoint molecules are not only up-regulated on CD8 T cells as PD-1 and TIM-3 were also found to be up-regulated on CD4+ Tfh cells in BC, which was associated with both a reduced CXCL13 production and a reduced capability of stimulating B cells [178]. Interestingly, in metastatic lesions, only 5% and 3% were found positive for the PD-1 and PD-L1, respecievely, arguing that other immune evasive mechanism may be more dominant in advanced diseases [179].

2.7 Future therapies should combine tumor sensitization and T cell treatments

Here we propose a strategy that implements immune-oncological markers to better select immune therapies in BC subtypes, and rationalize whether or not there is a requirement for sensitization for immune therapies based on our current understanding of BC's immune evasion and immunogenicity. In **Figure 4**, we have distinguished ER+ and ER- BC, and described steps in selecting (combination) immune therapies:

Across BC subtypes, ER+ tumors, in particular luminal A BC, are the least immunogenic since they have the lowest number of TILs and the lowest levels of expression of CGAs and neo-antigens (**Figure 3**). Because of the low abundance of antigen, immune therapies targeting TAAs in ER+ BC require extensive screening for pre-defined antigens, which is costly and time consuming. Therefore, immune therapies using checkpoint inhibition, which do not directly target TAAs, but rather TILs, may show more potential in ER+ BC, since the presence of TILs can easily be assessed by H&E or immune stainings of routine biopsies. Thus far checkpoint blockade as monotherapy in ER+ tumors has resulted in SD at best (see section 2.4.2). In a subset of ER+ BC patients with deficiency in DNA mismatch repair (MMR) genes 180, mutational load may represent an independent parameter for therapy selection. In general, however, we argue that the presence of TILs rather than mutational load serves as a robust marker for patient stratification in BC. Even though TILs in ER+ BC are generally scarce and composed of innate rather than adaptive immune cells, it is important to note that there exists significant heterogeneity with respect to quantity and quality of TILs (own observations; manuscript in preparation). The presence of effector CD8 T cells, and the expression of immune checkpoint molecules on these T cells are indicative of an antigen-initiated immune response, which is anticipated to robustly predict success of checkpoint blockade in patients with these tumors. Therefore, the presence of these markers, in particular CD8 T cells

(which reflects an ongoing immune response) should be assessed in the first step when designing therapies (**Figure 4**, step1). In case CD8 T cells are absent one could opt for combinitation therapies since checkpoint blockade with NAC was found to increase TIL levels [181] and to enhance the CD8/Treg ratio (see section 2.4.1), may further enhance treatment efficacy in ER+ BC. In fact, such combinations have shown to increased pCR rates by 13-25%, when compared to NAC monotherapy (**Table 1**). The immunogenicity of tumors may also be increased by epigenetic drug treatment, including DNA-methyltransferase and/or histone deacetylase inhibitors, which were found to promote expressions of CGAs, MHC-I as well as co-stimulatory molecules in particular in tumor cells [182,183]. A few clinical studies are currently examining the combination of epigenetic drugs and checkpoint inhibitors in ER+ BC [184]. Even though results have not yet been published, combining cytotoxic therapies and/or epigenetic drugs with checkpoint inhibitors should be considered interesting strategies to treat ER+ BC.

In contrast to ER+ tumors, ER- tumors (HER2, TNBC) are intrinsically more immunogenic. Among all BC subtypes, TNBC bear the highest numbers of T cells, which are accompanied by the highest frequencies of neo-antigens and CGAs, and intra-tumoral CD8 T cells are often present with an exhausted T cell phenotype (**Figure 3**). Thus, TNBCs may represent a subtype of BC most sensitive to immune therapeutic interventions. However, antigenicity does not always predict response to checkpoint inhibition [185]. Even though clinical trials have resulted in higher response rates to checkpoint blockade in TNBC tumors when compared to ER+ tumors (**Table 1**), the majority of metastatic patients, however, does not show any clinical benefit to checkpoint blockade as monotherapy. This lack of response may be due to heterogeneity with respect to expression of checkpoint molecules or numbers of TILs. Indeed, high numbers of TILs and CD8 were predictive for response to checkpoint inh as first-line and second-line (following irradiation and chemotherapy) treatment for metstatic TNBC [117,186]. Therefore, also in ER- tumors, the presence of CD8 T cells should be assessed first. Most likely T cells are present. In case checkpoint molecules are present, one could again opt for therapy with checkpoint inhibitors. Multiple checkpoint molecules should be evaluated, since ER- tumors often co-express these molecules, which may prevent an effective monotherapy-approach. Indeed, the combination of durvalumab and tremelimumab resultated in an about 2-fold increased OR of 43% in TNBC patients [113] when compared to monotherapy approaches. In case these checkpoint moelcules are not expressed, but immune suppressor cells are present (assessed in step 3), inhibitors of these suppressor cells provide a therapeutic option [187,188]. In some cases CD8 T cells are absent. An underlying reason for CD8 T cell exclusion in a subset of TNBC patients, despite expression of TAAs, could

be lack of or a compromised antigen presentation by tumor cells and/or activation of oncogenic pathways. When CD8 T cells are absent, we suggest to assess MHC expression (which reflects capability of antigen presentation). In case MHC class I is expressed, then in the next steps assessments (of TAAs and corresponding T cells) inform on the option to implement adoptive therapy of T cells. In case MHC class I is not expressed, one could opt for therapy with PI3K and MEK-inhibitors that are found to up-regulate expression of MHCI and PD-L1 in TNBC. In more general terms, epigenetic drugs, RT and/or NAC are other therapeutic options to sensitize tumors for T cell treatments, such as adoptive T cell therapy.

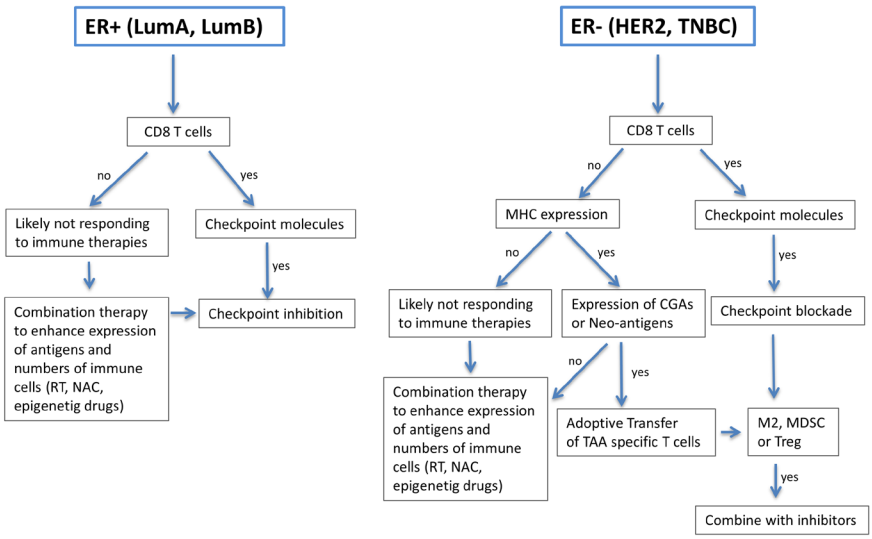

Figure 4. **Strategy to optimally implement immuno-oncological markers to guide selection of therapies for ER+ and ER- BC patients**. Thick arrows indicate the most likely path. Strategies are explained in more detail in section 2.7.

In conclusion, BC subtypes are heterogenous with respect to quantity and quality of TILs, occurrence of immune evasive mechanisms, and antigenicity. Therefore all these factors should be assessed and taken into account when designing and selecting optimal (combination-) immune therapies for a selected group of BC patients.

Conflict of interest: The authors declare that there are no conflicts of interest

Chapter 3

Differential prognostic value of CD8 T cells in breast cancer subtypes: not only T cell abundance, rather T cell clonality, antigen recognition and suppression

Dora Hammerl[1], Maarten P.G. Massink[3], Marcel Smid[1], Carolien H.M. van Deurzen[1], Hanne Meijers-Heijboer[2], Quinten Waisfisz[2], Reno Debets[1]*, John W.M. Martens[1]*

[1]Department of Medical Oncology, Erasmus MC Cancer Institute and Cancer Genomics Netherlands, Erasmus University Medical Center, Rotterdam, The Netherlands; and [2] Department of Clinical Genetics, Amsterdam UMC, Vrije Universiteit, Amsterdam, The Netherlands; [3]Department of Genetics, University Medical Centre Utrecht, Utrecht, The Netherlands.*shared senior authors.

Clinical Cancer Research, doi: 10.1158/1078-0432.CCR-19-0285

Abstract

Purpose: In breast cancer (BC), response rates to immune therapies are generally low and differ significantly across molecular subtypes, urging a better understanding of immunogenicity and immune evasion.

Experimental Design: We interrogated large gene-expression datasets including 867 node-negative, treatment-naïve BC patients (micro-array data) and 347 BC patients (whole-genome sequence and transcriptome data) according to parameters of T cells as well as immune micro-environment in relation to patient survival.

Results: We developed a 109 immune-gene signature that captures abundance of CD8 TILs and is prognostic in basal-like, her2 and luminal-B BC, but not in luminal-A nor normal-like BC. Basal-like and her2 are characterized by highest CD8 TIL abundance, highest T cell clonality, highest frequencies of memory T cells, highest antigenicity, yet only the former shows highest expression level of immune and metabolic checkpoints and highest frequency of myeloid suppressor cells. Also, luminal-B shows a high antigenicity and T cell clonality, yet a low abundance of CD8 TILs. In contrast, luminal-A and normal-like both show a low antigenicity, and notably, a low and high abundance of CD8 TILs, respectively, which associates with T cell influx parameters, such as expression of adhesion molecules.

Conclusion: Collectively, our data argue that not only CD8 T cell presence itself, but rather T cell clonality, T cell subset distribution, co-inhibition and antigen presentation reflect occurrence of a CD8 T cell response in BC subtypes, which have been aborted by distinct T cell suppressive mechanisms, providing a rational for subtype-specific combination immune therapies.

Translational relevance:

In breast cancer (BC) current immunotherapy trials focus on checkpoint inhibition in basal-like BC, and despite high levels of CD8 TILs, clinical benefit is rarely observed. Here, we show that basal-like BC is characterized by high antigenicity and T cell clonality, prerequisites and markers of an anti-tumor CD8 T cell response, but also by enhanced expression of immune and metabolic checkpoints and the presence of myeloid-derived suppressor cells, which represent actionable targets for combination therapies. Moreover, we observed high antigenicity and T cell clonality in her2 and luminal-B subtypes, yet these subtypes show distinct T cell evasive mechanisms, indicating that at least a subgroup of her2 and luminal-B patients may benefit from biomarker guided (combination) immune therapies. Lastly, luminal A and normal-like subtypes, do not express genes related to a CD8 T cell response, which may instruct towards sensitization strategies prior to combination (immune) therapies.

3.1 Background

Numerous immunotherapy approaches are currently being exploited for a variety of human malignancies, including hematologic as well as solid tumors. These approaches generally include oncolytic viral therapy, cancer vaccines, adoptive T cell therapy and application of checkpoint inhibitors (CI). Particularly the latter two have demonstrated impressive objective response rates (OR) of up to 80%, including several complete responses in advanced disease stages [189,190].

Breast cancer (BC) has initially been considered poorly immunogenic due to its low average mutational burden when compared to other tumor types [144]. More recently, it has been acknowledged that some breast tumors are extensively infiltrated by immune cells [8] and it became evident that density of tumor infiltrating lymphocytes (TIL), in particular CD8 T cells, has prognostic value and predicts response to neo-adjuvant chemotherapy as well as immune modulating therapies [5,84,191–193]. Building on the revisited immunogenicity, several studies are currently exploiting cancer vaccines, adoptive T cell therapies or CI for the treatment of BC [194]. Unexpectedly, ORs remain variable, and generally do not exceed 20% for CI mono-therapy [195].

BC is a heterogeneous disease comprising several histological and molecular subtypes. The most well recognized subtypes include luminal-A and normal-like (largely resembling the histological phenotype: ER+, PR+ and HER2-), luminal-B (ER+ PR+ KI67hi and/or HER2+), her2 (ER-, PR-, HER2+), and basal-like subtype (largely resembling the triple negative (TN) phenotype: ER-, PR-, HER2-) [196,197]. This subtype classification has clinical relevance with respect to prognosis and choice of targeted therapies [197]. Notably, it has been observed that TN tumors respond better to CI treatment when compared to ER+ BC [113]. Nevertheless, responses to immune therapies are not restricted to TNBC patients, as it has been reported that a metastatic luminal-A BC patient showed complete regression following adoptive T cell therapy [198].

Immune parameters that can be decisive towards an effective anti-tumor response, such as those reflecting immunogenicity as well as occurrence of T cell evasion, are poorly characterized in case of BC and thus critical factors determining tumor immunogenicity poorly understood. Tumor immunogenicity, which is the extent to which adaptive immune responses are triggered, depends on multiple factors including the expression, processing and presentation of tumor antigens and the presence, type and antigen specificity of TILs. Immunogenic tumor antigens can include oncoviral antigens, cancer germline antigens (CGA), and neo-antigens, which all have been reported to elicit T cell responses in cancer patients [199,200]. Besides immunogenicity, immune evasive mechanisms can affect numbers and anti-tumor activity of T cells. Several evasive mechanisms have been described that limit influx and migration

(e.g., lack or down-regulated expression of chemo-attractants and/or adhesion molecules), antigen recognition (e.g., lack or down-regulated expression of molecules involved in antigen processing and/or presentation), and/or function of CD8 T cells (e.g., presence of immune-suppressor cells, altered expression of immune or metabolic checkpoints, and/or activation of oncogenic pathways) [31,201].

Current reports on prognostic and predictive value of TILs in BC subtypes to a certain extent refer to some of the above mechanisms yet remain inconclusive and sometimes even contradictory [58,191]. In the current study, we have comprehensively assessed immunogenicity as well as T cell evasive mechanisms in BC subtypes with respect to characteristics of TILs and the tumor micro-environment (TME). To this end, we applied a series of omics analysis tools on large publicly available datasets and demonstrated that BC molecular subtypes significantly differ with respect to extent of immunogenicity and occurrence of dominant T cell evasive mechanisms, qualities that go beyond the mere presence of TILs. These novel findings may aid future immune therapy trial design and rationalize implementation of differential combination-immune therapies for BC subtypes.

3.2 Results

TIL signature is prognostic for basal-like, her2 and luminal B, but not luminal A nor normal-like BC

We have built a 109-gene (120-probe) signature (additional file 1) that captures stromal TIL abundance, according to the guideline method from Salgado and colleagues [56] (**Figure 1A-E**). Since TILs can be highly heterogeneous with respect to their composition of T cells and other immune cells, we performed immune fluorescence staining followed by digital image analysis and observed strong correlations between the TIL score and numbers of CD8 T cells ($r=0.82$, $p<0.0001$) as well as CD4 T cells ($r=0.74$, $p<0.0001$), but not macrophages ($r=-0.031$, $p=0.9$) (**Supplementary figure S2**). We further assessed this signature using the omics tools miXCR [202] and CIBERSORT [203]. The first tool, which enumerates the sequence reads of T cell receptor alpha and beta chains (TCRα and β) from RNAseq data (Cohort B), revealed that the number of TCR-Vβ reads in a specimen strongly correlated with the TIL score (computed as average of all 109 genes per sample) of the same specimen ($r=0.91$, $p<0.0001$, **Figure 1D**). The second tool, a deconvolution algorithm that extracts relative proportions of 22 major immune cell populations from microarray data (Cohort A), revealed that proportions of CD8 T cells, activated memory CD4 T cells, naive B cells, gamma/delta T cells and M1 macrophages positively correlated with

TIL scores, whereas proportions of resting DC, Neutrophils, Monocytes, M0 Macrophages, and activated mast cells negatively correlated with these scores (**Supplementary figure S3**). Collectively, these findings point out that TIL-high samples (median of 35% sTIL) are enriched for activated lymphocytes and reflect frequencies of αβ T cells, and that TIL low samples (median of 5% sTIL) are enriched for immune suppressor cells.

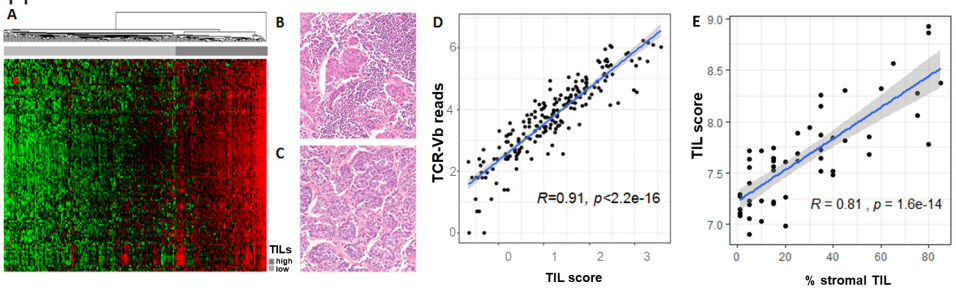

Figure 1. TIL signature captures frequencies of CD8 T cells. A, Hierarchical clustering of normalized gene expression values of a TIL signature in BC samples from Cohort A, discovery set (344 LNN and treatment-naive BC patients). Sample assignment is as follows: dark-grey marks high-TIL samples (containing median of 35% sTILs), light-grey marks low-TIL samples (median of 5% sTIL), based on hierarchical clustering. Figures **B** and **C** show high-magnification close-ups (100X) of H&E stained slides of BC with high and low TIL abundance, respectively. TILs are identified as small round dark stained cells amidst the cancerous tissue. **D**, Scatterplot with pearson correlation (blue line) between TIL score and number of total TCR-Vβ reads extracted from RNAseq data (n= 347, cohort B). **E**, Scatterplot with correlation (blue line) between the percentage of stromal TILs assessed using HE-stainings and TIL score (n=60, cohort A).

Next, we assessed the prognostic value of our TIL signature and observed an association with distant MFS in the discovery set of 344 LNN primary BC (p=0.009, **Supplementary figure S4A**). To validate our findings, we performed similar analyses in a dataset of 523 primary operable, LNN BC and verified a significant association between TIL abundance and MFS (p=0.016, **Supplementary figure S4B**). Following this validation, and to increase statistical power for subgroup analysis, we combined the discovery and validation sets of samples (Cohort A, n=867) and explored the association between TIL scores and MFS in the different molecular BC subtypes (for hormone receptor status per molecular subtypes see **supplementary figure S1**). Basal-like and her2 had equally high TIL scores followed by normal-like BC, whereas luminal-A and B subtypes showed the lowest TIL scores (p<0.0001, **Figure 2A**). TIL scores had prognostic value in univariate cox regression only in basal-like (log-rank p=0.002), her2 (log-rank p= 0.04) and luminal-B (log-rank p=0.02) subtypes, but not in luminal-A or normal-like subtypes (**Figure 3 B-F**). Notably, TIL scores remained significant for basal-like (p=0.025) and luminal-B (p=0.02), but not her2 (p=0.2) in a

multivariable cox regression including tumor size and age (**Table 1A**). To investigate the biological basis of differential prognostic values of TILs we subsequently evaluated TIL and TME characteristics among BC subtypes.

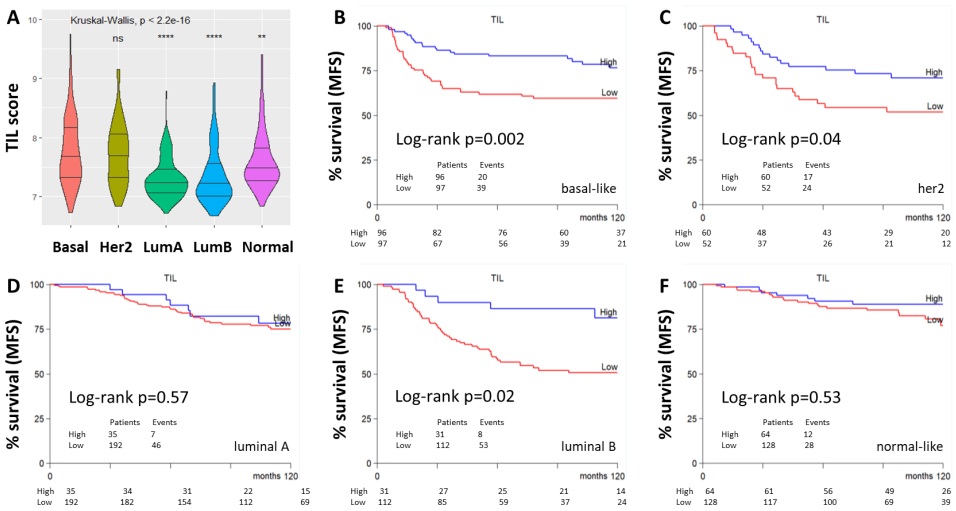

Figure 2. TIL abundance provides differential prognostic values across BC subtype. A, Violin plots with TIL-scores per BC subtype (molecular subtypes according to AIMS). Statistical differences were calculated using Kruskal-Wallis test among subtypes, and Wilcoxon rank sum test for pairwise comparison relative to basal-like BC; p-values are indicated as: '***'<0.001, '**'<0.01, '*'<0.05. Figures **B-F** show Kaplan Meier curves of Cohort A (867 LNN BC patients) by subtype with high versus low TIL scores. TIL-status was assigned as explained in legend to figure 1.

Numbers of clonally expanded T cells were high in basal-like but low in luminal-A BC

Since T cell clonality can be indicative for tumor reactivity of TILs [204], we assessed TCR-Vβ reads in TIL-high samples of different BC subtypes. Basal-like BC showed the highest number of different T cell clones (i.e., highest TCR repertoire diversity, average number=109), which was significantly higher than her2 (61), normal-like (50), luminal-A (39) and luminal-B BC (35) (**Figure 3A**). In agreement, basal-like BC showed the highest read-counts of the 10 most abundant clones per sample (**Figure 3B**). Highly expanded clones (HEC), which were defined as clones with read-counts > 10% of total clone reads, were present in basal-like, her2 and luminal-B tumors. Interestingly, luminal-B but not A tumors harbored HECs (**Figure 3C**), whereas both tumor types had equally low TCR repertoire diversity. Notably, in all subtypes, individual cases with expanded clones (EC, 5-10% of total clone reads) were present.

Expression of neo-antigens and CGAs is highest in basal-like and her2 BC, yet independent of TIL abundance

To evaluate antigenicity we assessed expression of two categories of recognized targets for CD8 T cells, namely neo-antigens and CGAs. We used non-synonymous mutations (cohort B, see Materials and Methods) and evaluated CGA expression (cohort B, average expression of 239 CGAs per sample). Neo-antigen expression was significantly higher in basal-like BC (average number=21.5) compared to luminal-A (7) and B (17), and normal-like BC (15), but not compared to her2 BC (17.5) ($p<0.001$, **Figure 3D**). CGA expression was again significantly higher in basal-like BC compared to luminal-A and B and normal-like BC, but not her2 BC ($p<0.002$, **Figure 3F**). When correlating antigen expression to TIL-scores, we observed a slight positive correlation with neo-antigen expression ($r=0.2$, $p=0.0017$, **Figure 3E**). Interestingly, CGA expression was inversely correlated to TIL-score ($r=-0.21$, $p=0.00082$, **Figure 3G**).

Genes related to T cell evasion are differentially expressed among BC subtypes

Besides parameters of immunogenicity, we evaluated differential expression of genes related to three main categories of T cell evasion (influx and migration of T cells; antigen processing and presentation; and function of T cells, **Figure 4**). With respect to influx and migration of T cells, basal-like BC showed the highest expression of chemo-attractants, which was significantly lower in other subtypes. Normal-like tumors showed the highest expression of T cell adhesion genes (followed by basal-like BC) and those related to cancer associated fibroblasts and extracellular matrix products (**Figure 4A**). With respect to antigen recognition by T cells, basal-like BC showed the highest expression of antigen processing and presentation (APP) genes, which was significantly lower in all other subtypes (**Figure 4B**). Type-I IFN gene products, which are recognized for their effects towards antigen priming [205], were equally high in basal-like, her2 and luminal-B, but expressed to significantly lower levels in luminal-A and normal-like subtypes. With respect to T cell function, we evaluated the expression of co-stimulatory ligands and receptors (for co-stimulatory and inhibitory receptors which are expressed by T cells, we compared TIL high samples only), immune mediators of the TME, components of oncogenic pathways (see additional file 2 for details), and frequencies of immune (-suppressor) cells (based on CIBERSORT deconvolution). Again, basal-like tumors showed the highest expression of co-inhibitory receptors and ligands as well as co- stimulatory receptors and ligands. Expression levels of co-inhibitory/stimulatory receptors were significantly lower in all

other subtypes, while expression of corresponding ligands was equally high in her2, but not other subtypes. Expression levels of mediators such as IL10, IDO-1, VEGF, components of adenosine and glycolysis pathways, which can all limit T cell function, were also highest in basal like BC, and significantly decreased in all other subtypes. Interestingly, while M0 macrophages were significantly enriched in basal-like BC, frequencies of regulatory T cells, monocytes and M2 macrophages were highest in luminal-B tumors (**Figure 4C**).

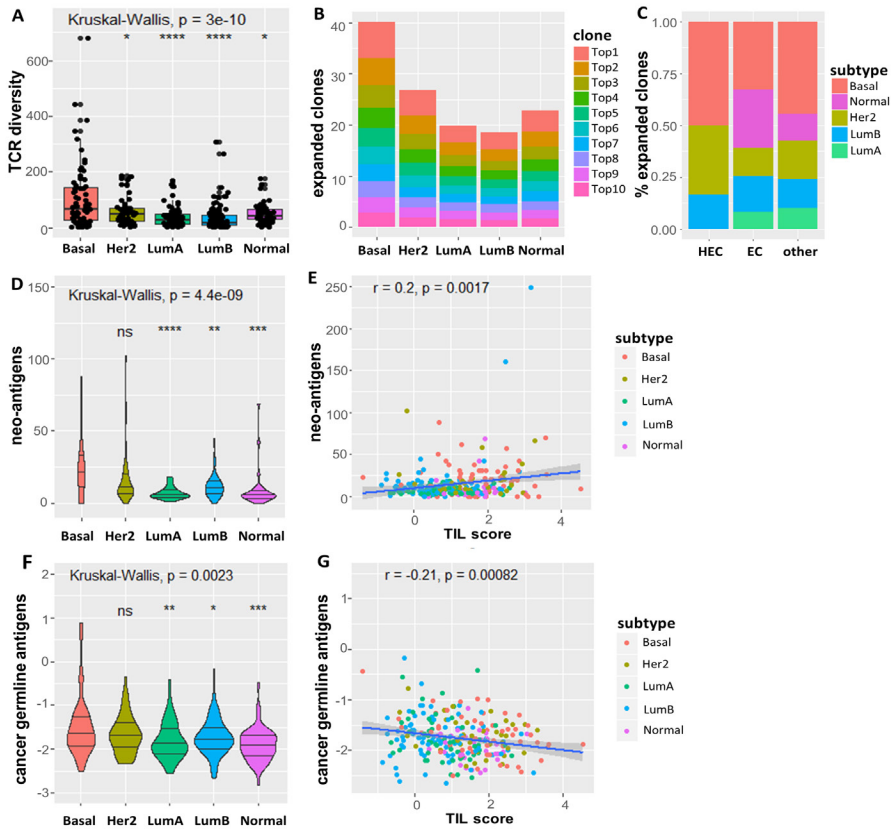

Figure 3. T cell clonality and antigen expression is highest in basal, her2 and luminal B subtypes. **A,** Boxplots with total number of unique TCR-Vβ reads per BC subtype. **B**, Stacked bar charts with the average read numbers of the 10 most abundant T cell clones (according to TCR-Vβ reads) per BC subtype. **C**, Bar charts with proportions of BC subtypes with highly expanded clones (HEC, >10% of all clone reads), expanded clones (EC, 5-10% of all clone reads) and other clones (<5% of all clone reads). **D** and E show total number of neo-antigens per BC subtype and its correlation with TIL abundance on a log scale (Pearson, r=0.2, p=0.0017, CI: 0.95). **F** and **G** show CGA expression (average of all CGAs per sample) per BC subtype and its correlation with TIL abundance on a log scale (Pearson, r=-0.21, p=0.00082, CI: 0.95). Statistical differences were calculated using Kruskal-Wallis test among subtypes, and Wilcoxon rank sum test for pairwise comparison relative to basal-like BC; p-values are indicated as: '***' <0.001, '**'<0.01, '*'<0.05.

When interrelating TIL score with above-mentioned gene sets in a subtype-independent manner, we observed that this score correlated significantly with co-inhibitory/stimulatory receptors and NFKB-pathway (r>0.7), which may be expected because all of these gene-sets can be expressed by T cells. Weaker correlations (r<0.6) were observed between the TIL score and antigen processing, and IFN signatures. For other gene-sets we observed weak (adenosine, immune mediators), no (glycolysis) or even inverse correlations (M0, WNT-pathway) with TIL-scores (see supplementary **Figure S5** for details, interactions between gene-sets and TIL score and subtypes are indicated in **Figure 4**).

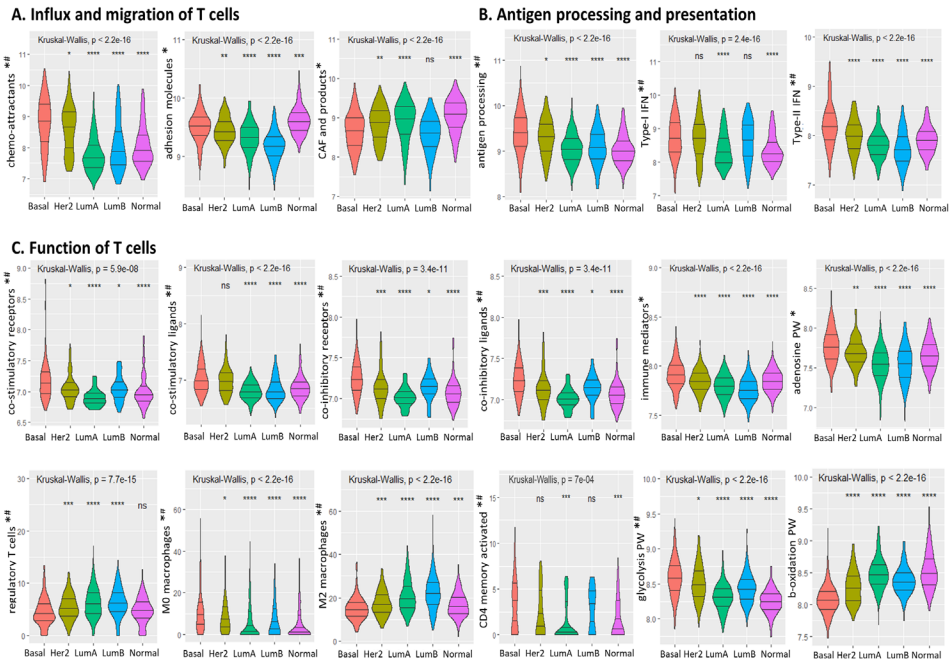

Figure 4. Immune and metabolic checkpoints as well as M0 macrophages are enriched in basal-like, T cell adhesion molecules are enriched in normal-like, and regulatory T cells and M2 are enriched in luminal-A and B BC. Violin plots with expression levels per BC suptype of Cohort A. **A,** Chemo-attractants, adhesion molecules, Cancer associated fibroblast and their products; **B**. Antigen processing and presentation, Type-II interferon genes; **C**. co-stimulatory receptors (TIL-high samples only), co-stimmulatory ligands, co-inhibitory receptors (TIL-high samples only), co-inhibitory ligands, immune mediators , adenosine pathway as well as immune cell frequencies from CIBERSORT deconvolution, as well as glycolysis- and beta-oxidation pathway (for details of gene-sets see additional file 2). Statistical differences were calculated using Kruskal-Wallis test among subtypes, and Wilcoxon rank sum test for pairwise comparison relative to basal-like BC; p-values are indicated as: '***' <0.001, '**'<0.01, '*'<0.05. * indicates a significant interaction with the TIL-score. # indicate a significant interaction with the TIL score and BC subtype.

Finally, we performed Cox regression analyses with MFS to determine the prognostic value of the above gene-sets in uni- and multivariable settings (**Tables 1A** and **1B**; for prognostic value of single genes, see additional file 3). Besides TIL scores, we found significant associations with MFS (Hazard Ratio (HR) <1, $p<0.05$) for the following gene sets: Type-II IFN in BC (not differentiated per subtype), as well as her2 and luminal-B subtypes; co-inhibitory/stimulatory receptors and ligands in BC, as well as basal-like, her2 and luminal-B subtypes; antigen processing and presentation in BC, as well as basal-like and luminal-B subtypes; and NFKB pathway in BC as well as basal-like subtype. In addition, activated memory T cells were significantly associated with MFS in BC and basal-like, in the multivariable analysis. Interestingly, we found significant inverse associations with MFS (HR>1, $p<0.05$) for M2 macrophages in BC; M0 macrophages in normal-like subtype; glycolysis and adenosine pathway in BC; and WNT pathway in the BC, basal-like and luminal-A subtype.

Table 1A Cox regression analyses between immune gene sets and MFS across BC subtypes (univariate model).

	All subtypes		Basal		Her2		LumA		LumB		Normal	
Gene-sets	HR (95% CI)	p.value	HR (95% CI)	p.value	HR (95% CI)	p.value	HR (95% CI)	p.value	HR (95% CI)	p.value	HR (95% CI)	p.value
TIL score	0.6 (0.46-0.79)	0.00022	0.52 (0.32-0.85)	0.002	0.46 (0.24-0.88)	0.04	0.92 (0.41-2.1)	0.57	0.43 (0.23-0.8)	0.02	0.74 (0.36-1.5)	0.53
Plasma cells	0.66 (0.51-0.84)	0.00097	0.72 (0.43-1.2)	0.22	0.55 (0.29-1)	0.069	0.8 (0.46-1.4)	0.43	0.62 (0.37-1)	0.066	0.93 (0.5-1.8)	0.83
Adhesion molecules	0.68 (0.53-0.87)	0.0022	0.92 (0.55-1.5)	0.75	0.89 (0.48-1.6)	0.7	0.6 (0.34-1)	0.069	0.89 (0.54-1.5)	0.66	0.81 (0.43-1.5)	0.51
Type-II IFN	0.69 (0.54-0.89)	0.0036	0.84 (0.5-1.4)	0.5	0.42 (0.22-0.8)	0.0082	0.84 (0.49-1.4)	0.52	0.42 (0.25-0.73)	0.0018	0.67 (0.36-1.3)	0.22
Macrophages M2	1.4 (1.1-1.8)	0.0045	1.2 (0.71-2)	0.52	1.8 (0.97-3.4)	0.063	1 (0.59-1.8)	0.94	1.3 (0.78-2.1)	0.33	1.8 (0.97-3.5)	0.063
Co-stimulation	0.72 (0.56-0.92)	0.0081	0.49 (0.29-0.83)	0.0086	0.42 (0.22-0.79)	0.0077	0.81 (0.47-1.4)	0.45	0.66 (0.4-1.1)	0.11	0.78 (0.41-1.5)	0.44
Antigen processing	0.72 (0.56-0.92)	0.0085	0.4 (0.23-0.68)	0.00089	0.83 (0.45-1.5)	0.55	0.79 (0.46-1.4)	0.4	0.63 (0.38-1.1)	0.078	1.3 (0.68-2.4)	0.45
Monocytes	0.73 (0.57-0.93)	0.013	1 (0.6-1.7)	0.99	0.99 (0.53-1.8)	0.97	0.56 (0.32-0.98)	0.042	0.88 (0.53-1.5)	0.62	0.77 (0.41-1.5)	0.43
CD8 T cells	0.75 (0.58-0.96)	0.021	0.4 (0.23-0.69)	0.001	0.89 (0.48-1.6)	0.71	0.9 (0.52-1.5)	0.69	0.58 (0.35-0.97)	0.039	1.1 (0.61-2.1)	0.69
NFKB-PW	0.75 (0.59-0.97)	0.025	0.62 (0.37-1)	0.072	0.58 (0.31-1.1)	0.088	0.77 (0.45-1.3)	0.36	0.69 (0.41-1.2)	0.16	0.69 (0.36-1.3)	0.25
Co-inhibition	0.76 (0.59-0.97)	0.029	0.55 (0.32-0.93)	0.026	0.56 (0.3-1.1)	0.074	1.1 (0.63-1.9)	0.76	0.78 (0.47-1.3)	0.34	0.88 (0.47-1.7)	0.69
WNT-PW	1.3 (0.99-1.6)	0.06	1.7 (1-2.9)	0.04	1.3 (0.71-2.5)	0.37	1.5 (0.87-2.6)	0.15	1.2 (0.74-2.1)	0.41	0.96 (0.51-1.8)	0.89
Type-I IFN	1.2 (0.97-1.6)	0.081	0.77 (0.46-1.3)	0.32	0.65 (0.35-1.2)	0.17	1.1 (0.64-1.9)	0.72	0.95 (0.58-1.6)	0.85	1.2 (0.62-2.2)	0.65
Glycolysis	1.2 (0.97-1.6)	0.082	0.91 (0.54-1.5)	0.7	1.4 (0.75-2.6)	0.29	1.1 (0.64-1.9)	0.71	0.79 (0.47-1.3)	0.35	1.3 (0.67-2.4)	0.46
Macrophages M0	1.2 (0.96-1.6)	0.099	1.3 (0.75-2.1)	0.39	0.98 (0.53-1.8)	0.94	0.87 (0.5-1.5)	0.61	1.4 (0.86-2.4)	0.17	2 (1-3.8)	0.043
Regulatory T cells	1.2 (0.95-1.6)	0.11	1.7 (1-2.8)	0.051	1.8 (0.97-3.5)	0.064	1 (0.58-1.7)	0.99	1 (0.62-1.7)	0.93	1.1 (0.57-2)	0.83
b-oxidation	0.85 (0.67-1.1)	0.2	1.4 (0.81-2.3)	0.25	0.89 (0.48-1.7)	0.72	0.97 (0.56-1.7)	0.91	1.8 (1.1-2.9)	0.031	0.95 (0.51-1.8)	0.88
Adenosine-PW	1.2 (0.9-1.5)	0.25	0.96 (0.57-1.6)	0.86	1.2 (0.68-2.3)	0.48	1.5 (0.84-2.5)	0.18	1.1 (0.68-1.9)	0.64	0.63 (0.33-1.2)	0.15
Immune mediators	0.89 (0.7-1.1)	0.36	0.98 (0.59-1.6)	0.94	0.43 (0.23-0.83)	0.012	0.95 (0.55-1.6)	0.85	0.8 (0.48-1.3)	0.39	1.1 (0.57-2)	0.82
Act. Memory CD4	1.1 (0.85-1.4)	0.5	1.5 (0.92-2.6)	0.098	1.3 (0.72-2.5)	0.37	1.2 (0.72-2.2)	0.43	0.77 (0.46-1.3)	0.32	0.84 (0.44-1.6)	0.58
PI3K neg. regulator	0.99 (0.77-1.3)	0.94	1.1 (0.69-1.9)	0.6	0.86 (0.47-1.6)	0.63	0.93 (0.54-1.6)	0.81	1.3 (0.76-2.1)	0.36	1 (0.53-1.9)	0.99

Table 1B Cox regression analyses between immune gene sets and MFS across BC subtypes (multivariable model).

	All samples		Basal		Her2		LumA		LumB		Normal	
Gene-sets	HR (95% CI for HR)	p-value	HR (95% CI for HR)	p-value	HR (95% CI for HR)	p-value	HR (95% CI for HR)	p-value	HR (95% CI for HR)	p-value	HR (95% CI for HR)	p-value
TIL score	0.6 (0.44-0.82)	0.002	0.5 (0.28-0.91)	0.025	0.61 (0.29-1.28)	0.2	0.74 (0.30-1.79)	0.51	0.38 (0.17- 0.85)	0.02	0.70 (0.32-1.5)	0.38
Adhesion molecules	0.67 (0.51-0.89)	0.006	1.3 (0.7-2.4)	0.4	1 (0.5-2.2)	0.89	0.45 (0.22-0.9)	0.033	0.7 (0.29-1.7)	0.45	0.56 (0.26-1.23)	0.15
Type-II IFN	0.64 (0.48-0.85)	0.002	0.63 (0.34-1.1)	0.1	0.41 (0.19-0.8)	0.02	0.9 (0.47-1.7)	0.75	0.38 (0.19-0.76)	0.006	0.86 (0.38-1.93)	0.72
Macrophages M2	1.6 (1.22-2.14)	0.001	1.5 (0.86-2.7)	0.14	2.7 (1.27-5.8)	0.01	0.92 (0.49-1.74)	0.8	1.5 (0.8-2.8)	0.2	2 (0.96-4.35)	0.06
Co-stimulation	0.69 (0.52-0.91)	0.01	0.6 (0.33-1.1)	0.08	0.55 (0.26-1.19)	0.13	0.7 (0.35-1.4)	0.3	0.59 (0.33-1.06)	0.08	0.84 (0.39-1.8)	0.67
Antigen processing	0.7 (0.53-0.93)	0.015	0.38 (0.2-0.7)	0.002	0.57 (0.26-1.23)	0.16	0.82 (0.43-1.6)	0.56	0.56 (0.3-1)	0.05	1 (0.43-2.47)	0.95
NFKB-PW	0.72 (0.54-0.95)	0.02	0.45 (0.24-0.86)	0.01	0.8 90.37-1.75)	0.58	0.95 (0.48-1.89)	0.9	0.55 (0.28-1.1)	0.07	0.8 (0.3-1.5)	0.34
Co-inhibition	0.69 (0.52-0.91	0.009	0.38 (0.19-0.72)	0.003	0.59 (0.28-1.24)	0.16	1 (0.53-1.9)	0.98	0.38 (0.19-0.72)	0.003	0.8 (0.38-1.7)	0.55
WNT PW	1.3 (0.99-1.7)	0.05	2.1 (1.25-3.8)	0.006	1 (0.45-2.52)	0.9	2 (1.06-4.2)	0.03	1.1 (0.62-1.9)	0.76	0.86 (0.4-1.86)	0.7
Type-I IFN	1.14 (0.8-1.5)	0.355	0.91 (0.51-1.6)	0.7	0.73 (0.43-1.56)	0.41	1.54 (0.81-2.9)	0.18	1 (0.60-1.8)	0.8	0.66 (0.31-1.37)	0.27
Glycolysis	1.2 (0.91-1.6)	0.18	0.68 (0.35-1.3)	0.26	1.16 (0.51-2.65)	0.71	0.98(0.5-1.89)	0.95	1 (0.61-1.88)	0.78	0.91 (0.34-2.4)	0.85
M0 macrophages	1.16 (0.88-1.5)	0.27	0.9 (0.47-1.7)	0.77	0.78 (0.36-1.65)	0.5	0.89 (0.46 -1.7)	0.73	1.6 (0.93-2.8)	0.08	1.16 (0.51-2.63)	0.71
Regulatory T cells	1.12 (0.86-1.5)	0.4	1.6 (0.93-3)	0.08	1 (0.48-2)	0.99	0.75 (0.4-1.4)	0.37	0.7 (0.38-1.2)	0.25	0.72 (0.34-1.53)	0.4
b-oxidation	0.85 (0.64-1.13)	0.28	1 (0.44-2.61)	0.8	0.88 (0.4-1.9)	0.74	0.78 (0.4-1.5)	0.46	1.5 (0.86-2.8)	0.13	0.76 (0.34-1.65)	0.5
Adenosine PW	1.23 (0.95-1.65)	0.1	1 (0.53-1.9)	0.95	1.77 (0.8-3.9)	0.16	2 (1.07-3.7)	0.029	1.2 (0.7-2.11)	0.5	0.76 (0.36-1.6)	0.46
Immune mediators	0.9 (0.68-1.2)	0.47	1.2 (0.63-2.27)	0.57	0.54 (0.26-1.16)	0.12	0.75 (0.4-1.41)	0.4	1.23 (0.66-2.3)	0.5	0.94 (0.45-2)	0.9
PI3K neg. regulator	1.12 (0.85-1.47)	0.42	1 (0.58-1.9)	0.85	1 (0.46-2.21)	0.97	0.84 (0.45-1.5)	0.6	1.36 (0.78-2.3)	0.28	1.12 (0.53-2.37)	0.76
Act. memory CD4	0.72 (0.53, 0.98)	0.04	0.37 (0.2-0.66)	0.001	0.63 (0.29-1.4)	0.25	1.5 (0.7-3.2)	0.29	0.73 (0.39-1.4)	0.35	0.95 (0.42-2.15)	0.9
Plasma cells	0.6 (0.45-0.79)	0.0001	0.56 (0.32-1)	0.05	0.53 (0.24-1.17)	0.12	0.67 (0.35-1.3)	0.23	0.52 (0.27-1)	0.05	1.22 (0.57-2.61)	0.6
CD8 T cells	0.78 (0.59-1)	0.07	0.48 (0.26-0.89)	0.021	0.8 (0.37-1.74)	0.59	1.2 (0.66-2.24)	0.53	0.52 (0.29 -0.92)	0.026	1.54 (0.74-3.2)	0.25
Monocytes	0.75 (0.6-0.98)	0.04	1 (0.57-1.8)	0.9	0.64 (0.28-1.4)	0.27	0.71 (0.38-1.32)	0.29	1 (0.6-1.8)	0.9	0.58 (0.27-1.22)	0.15

3.3 Discussion

CD8-positive TILs in BC are generally associated with a favorable clinical course, yet response to immune therapies is overall low, does not go hand-in-hand with CD8 TIL abundance, and differs significantly across subtypes. Tumor-immune interactions are not well understood and are expected to contribute to lack of response to immune therapies. In this study, we have addressed immunogenicity and T cell evasive mechanisms according to multiple parameters in a cohort of 867 LNN, untreated primary BC and a cohort of 437 primary BC with WGS data. To this end, we have built a 109-gene TIL signature that preserves differential prognostic value of TILs across molecular BC subtypes. We found that T cell clonality, antigenicity, frequency of immune suppressor cells as well as expression of genes related to influx/migration, antigen recognition or suppression of T cells provide significant determinants of individual subtypes and may explain the differential prognostic value of TILs.

The TIL signature used in this study was based on quantitative pathological assessment of TILs on HE-stained BC [206]. TILs generally comprise a variety of different immune cell population including subsets with pro-and anti-tumor activity [207]. Nevertheless, we found that this signature correlated very well with numbers of CD8 T cells, frequencies of activated lymphocytes (cell types associated with good prognosis) and inversely correlated with immune suppressor cells (cells associated with poor prognosis), suggesting that it may be used to assess T cell abundance when tissues are not available. Moreover, we observed a near perfect correlation between TIL score and TCR-Vβ read counts, suggesting that TCR-Vβ read counts also act as a surrogate for TIL abundance in silico (correlations between TIL density and either TIL score ($r=0.82$, $p<0.0001$) or TCR-Vβ read counts ($r=0.76$, $p<0.0001$) are comparable). TIL scores were high in basal-like, her2 and normal-like BC. T cell abundance, however, was not a prerequisite for prognosis since TIL scores were only associated with MFS in basal-like, her2 (univariate analysis only) and Luminal-B subtypes, but not in luminal-A, nor normal-like subtypes.

Assessment of immunogenicity and T cell evasive mechanisms per subtype revealed that basal-like, her2 and normal-like tumors harbor the highest TCR repertoire diversity. TCR clonality, however, was highest in basal-like, her2 and luminal-B tumors, which suggests that a tumor-specific T cell response has taken place in the latter three BC subtypes and to lesser extent in luminal-A and normal-like tumors (despite high TIL score and TCR diversity in normal-like tumors). Even though T cell clonality assessment based on bulk RNAseq analyses has several limitations [208] and should be interpreted with caution, it is interesting that a recent study by Scheper and colleagues is in line with our findings and revealed that the tumor-re-

active capacity of TILs is highly variable in different cancers and that a proportion of TILs represents true bystander T cells [209], which may be the case for the majority of TILs in normal-like tumors. In line with T cell clonality, basal-like BC showed the highest expression of neo-antigens and CGAs, followed by her2 and luminal-B tumors. These observations suggest that a certain level of antigen expression, which is considered a pre-requisite for an anti-tumor T cell response, and the presence of clonally expanded T cells, which is a consequence of T cell responses, may at least in part explain the prognostic value of TILs in basal-like, her2 and luminal-B subtypes. Nevertheless, when correlating neo-antigens to TIL scores or T cell clonality we only observed a weak correlation, which did not hold true upon subtype stratification (except for luminal-B tumors, which may be due to overrepresentation of APOBEC-driven neo-antigens that are considered more immunogenic than other neo-epitopes [149]), suggesting that, at least in other subtypes, predicted antigens are not truly immunogenic. Undoubtedly, the landscape of antigens goes beyond CGAs and classical neo-antigens (derived from non-synonymous mutations), to which end we have evaluated correlations between TILs and alternative mutations (i.e., frameshifts, indels, drivers, passengers) which did not improve correlations with TILs (data not shown). The lack of strong correlations between antigenicity and TILs may hint to the occurrence of immune editing or other immune evasive mechanisms.

When evaluating genes related to T cell evasion, we observed that expression of chemo-attractants was highest in basal-like BC followed by her2. T cell adhesion molecules on the other hand, were highest in normal-like BC, which may explain the relatively high TIL scores as adhesion molecules may enhance T cell retention [210] irrespective of antigen-specificity. Vice versa, low expression levels of adhesion molecules in luminal-B tumors may explain the low TIL score measured for this subtype. Looking into antigen recognition by T cells, we demonstrated that APP was lowest in luminal-A, -B and normal-like tumors. Nevertheless, we observed a significant association of the APP gene set with survival in luminal-B tumors, suggesting that APP is functional in at least a subset of these patients. Loss of function mutations in APP genes have been reported to result in immune resistance towards CI therapies in melanoma [159,160]. Along this line, it is noteworthy that we found 1 or more mutations in APP genes in 10% of basal-like patients, a fraction of patients that is 2 to 5-fold higher compared to the other BC subtypes (see **Supplementary figure S6**). Type I interferons, such as IFNα and IFNβ, produced either by tumor cells or dendritic cells, are critical for priming of CD8 T cells and significantly impact natural as well as therapy-induced immune control of tumors [205]. Moreover, it has been shown that mice lacking type I IFNs spontaneously develop breast tumors [211]. Expression of type-I IFN genes were equally high in basal-like, her2 and luminal-B tumors and showed significant interaction with the TIL score, which may further support the prognostic

value of TILs in these subtypes. Interestingly, we observed that the abundance of memory CD4 T cells was associated with better survival in BC and basal-like BC, which has recently also been shown by others [212]. We found that this T cell subset was enriched in TIL-high samples of basal, her-2 and luminal-B tumors, which suggest that not only quantity but also quality of the T cell infiltrate matters.

Lastly, when analyzing modes of T cell suppression, we observed that gene-sets for both co-inhibitory/stimulatory receptors showed significant interaction with TIL scores and were associated with survival in basal, her2 and luminal-B tumors (as were TIL scores), which is in agreement with the concept that immune checkpoints become expressed following a tumor-specific T cell response, since these molecules are often expressed in response to IFNγ [213]. M0 and M2 macrophages, cell types which have been associated with various modes of immune suppression and tumor progression in BC [214], were inversely correlated with MFS in BC, which is in agreement with findings by Ali and colleagues [67]. Immune inhibitory mediators, which can be secreted by MDSC or tumor cells, were also expressed at the highest level in basal-like BC, and as a gene set demonstrated a high HR in this subtype. Next to suppressor cells, also oncogenic and metabolic pathways have been linked to T cell evasion. In example, increased glycolysis has been linked to decreased trafficking and cytotoxicity of T cells in other malignancies [215]. Intrestingly, it has been observed that glycolysis signaling can induce MDSC development, via induction of G-CSF and GM-CFS in BC [216]. In line, we observed co-expression of MDSC and glycolysis signatures as well as inverse correlations with TIL scores. Notably, these observations could be caused by a single common process or due to the co-existence of multiple biological processes, indicating that mechanistic conclusions should be drawn with caution. Components of oncogenic pathways, such as WNT and adenosine, were expressed at the highest level in normal-like and basal-like BC, respectively, and remarkably WNT genes were associated with poor prognosis in BC, basal like BC, and luminal-A BC. WNT has been linked to decreased recruitment of T cells in melanoma and it has been shown recently, that WNT signaling can modulate PD-L1 expression in cancer stem cells of BC [217], suggesting that WNT plays a role in multiple modes of T cell evasion.

In **Figure 5**, outcomes of parameters of TILs and tumor micro-environment are summarized per BC subtype, and pointing to the differential qualities of TILs and occurrence of T cell evasive mechanisms, which may represent important biomarkers when monitoring patient responses to immune therapies. Based on our multi-parameter analyses in relation to subtypes, TIL scores and prognosis, we argue that in particular T cell clonality, expression of co-inhibitory molecules, type-I IFN, APP and frequencies of activated memory T cells better reflect the qualities of TILs.

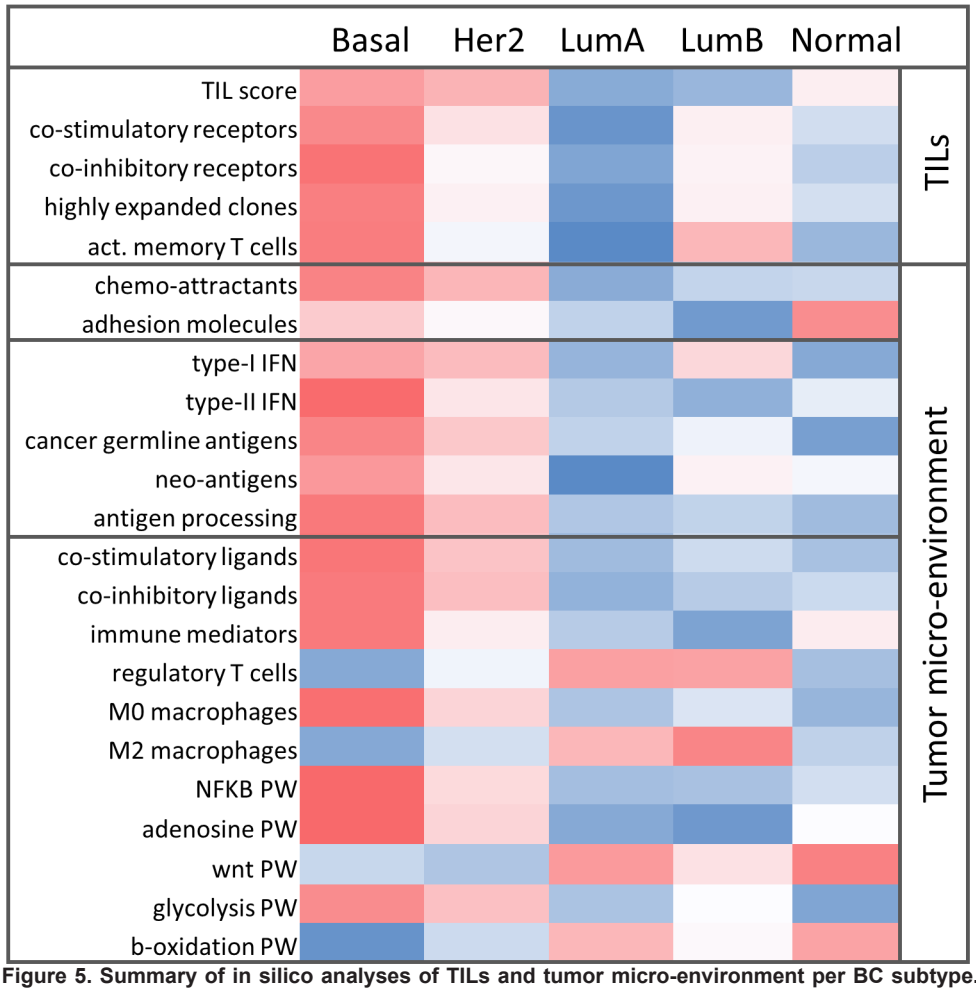

Figure 5. Summary of in silico analyses of TILs and tumor micro-environment per BC subtype. Heat maps with normalized expression of immune gene-sets (high expression in red, low expression in blue). Cohort A was used to calculate average gene expression per BC subtype, except for highly expanded clones (HEC), neo-antigens and CGAs for which Cohort B was used (for individual analyses, see Figures 1-4). **Abbreviations.**: NFKB, nuclear factor kappa-light-chain-enhancer of activated B cells; PW, pathway; WNT, wingless-type MMTV integration site

In agreement, recent results of the TONIC trial showed that T cell clonality correlated with response to pembrolizumab, when combined with chemotherapy, in TNBC [218]. A recent trial in which trastuzumab-resistant Her2+ patients were treated with pembrolizumab showed clinical benefit for patients whose tumors were positive for PD-L1 [219], a marker that is frequently up-regulated following anti-tumor T cell responses [213]. Moreover, the Impassion130 trial, in which 902 TNBC patients were treated with atezolizumab with/without nab-paclitaxel, revealed that only patients

with PD-L1-positive immune infiltrate showed clinical benefit [220]. In line with our study, these findings argue that the mere presence of CD8 TILs is not sufficient to accurately chart immune responses, and that markers that reflect the quality of TILs should be included to monitor future trials. In extension to this concept, our findings on the quality of TILs and the immune micro-environment, in particular with regard to subtype specific differences in metabolic and oncogenic pathways as well as recruitment of different types of suppressor cells may aid the design and translational testing of subtype-specific (combination-) therapies (see examples below). Of note, despite good concordance between subtyping methods and highly similar results for immune-gene analysis in histological and corresponding molecular subtypes (**supplementary Figure S7**), the here presented subtypes do not fully resemble the subtypes used in daily clinical practice. Moreover, we have used gene expression data at bulk level to interrogate BC subtypes for their immunogenicity and immune evasive mechanisms, which subsequently need to be validated in future studies.

Based on this study, in basal-like BC, there is a strong rationale for testing combinations of checkpoints with inhibitors of oncogenic pathways, MDSC or immune mediators. Possible combinations include drugs targeting VEGF or adenosine receptors, which are FDA approved for other implications and showed synergistic effects with CI in pre-clinical models and early clinical studies, including TNBC [221]. Furthermore, several WNT-PW inhibitors, which are currently in clinical trials (including studies in breast cancer) or drugs depleting MDSC [222], which are mainly in preclinical development, may increase efficacies of ICI in basal-like BC.

In Her2 BC, even though generally being immunogenic, there may be insufficient numbers of tumor reactive T cell clones when compared to basal-like BC (despite equally high TIL scores). Given the high antigenicity and relatively low frequencies of immune-suppressor cells, adoptive T cell therapy with TCR-engineered T cells may be considered to treat this tumor type. In fact, chimeric antigen receptor (CAR) T cells targeting her2 effectively kill BC in mouse models, however, in patient studies severe on-target toxicities have been observed [223]. Nevertheless, based on our data, CGAs and neo-antigens are frequently expressed in her2 BC and may represent safe targets for AT.

In luminal-B BC, at least a subset of tumors may very well be immunogenic and may benefit from immune therapies. In fact, TIL scores and expression of APP genes, although being low, were prognostic, and TIL scores correlated to the presence of neo-antigens in this tumor type. The generally low frequencies of T cells, which may be due to low expression of chemo-attractants and adhesion molecules, argues in favor of treatments that enhance accumulation of T cells (chemotherapy or epigenetic drugs), antigen presentation (CDK4/6 inhibitors) [224] and/or adoptive T cell therapy.

In addition, Luminal-B tumors were enriched for M2 macrophages and regulatory T cells, which also represent targets in this tumor type for combinatorial treatments [225].

In Luminal-A BC and normal-like BC, we observed the least signs of immunogenicity and immune evasion implying that these tumor types are unlikely to respond to immune therapies. A recent case study, on the other hand, reported complete regression of a luminal-A patient following treatment with tumor reactive TILs [198]. Importantly, however, this patient had an exceptionally high number of mutations, indicating that these results may not be generally translatable to other luminal-A tumors.

Finally, normal-like BC, demonstrated enrichment for CAF and their products as well as T cell adhesion molecules, which is suggestive for enhanced T cell retention and may explain relatively high TIL scores. This, together with the low expression of antigens and markers for ongoing immune responses, suggest that normal-like tumors are also unlikely to respond to immune therapies, but may benefit from therapies that target CAFs and/or their products.

3.4 Conclusion

Our data suggest that not frequencies of TILs per se, but rather qualities of TILs (i.e. T cell clonality, T cell subset distribution, APP, expression of type-I IFNs and immune checkpoints); and immune micro-environments (in particular oncogenic- and metabolic pathways as well as types and frequencies of suppressor cells) discriminate BC subtypes. Furthermore, our data suggest that evaluation of multiple immune parameters using NGS data enables charting of immunogenicity and immune evasive mechanisms, and provide a guide to select combinatorial approaches which may enhance the efficacy of future immune therapy trials.

3.5 Materials and Methods

Gene expression datasets

Cohort A: Gene expression data (HG-U133-A array) of lymph node–negative (LNN) BC patients (who did not receive any adjuvant systemic treatment) were retrieved through GEO Series accession numbers: GSE2034 (n=286) [226,] GSE5327 (n=58) [227],

GSE11121 (n=200) [228], GSE2990 (n=125) [229] and GSE7390 (n=198) [230]. To assess the prognostic value of TILs in different BC subtypes, GSE2034 and GSE5327 constituted a discovery cohort (n=344), whereas GSE11121, GSE2990 and GSE7390 (n=523) constituted a validation cohort. Raw cel files of all GSE-entries were downloaded and data were normalized using fRMA [231] and corrected for batch effects using ComBat [232]. Subsequently, to retain significant power, the combined cohort of 867 LNN primary BC was used for in depth analyses of TILs and the TME within BC subtypes as described below.

Cohort B (BASIS): Secondly, a unique dataset was retrieved from primary BC cases with both WGS (n=560) and in depth RNA sequencing data (n=347) and which is accessible through EGAS00001001178 [149,233]. From cases for which both WGS and RNAseq were available (n=266), the data were used for predicting neo-antigens and from the cases which had just RNAseq data (n=347), the data were used for analysis of T cell clonality.

Ethics statement

This study has been approved by the medical ethical committee at Erasmus MC (MEC.02.953), and was performed according the Declaration of Helsinki and the "Code for Proper Secondary Use of Human Tissue in The Netherlands" (FMWV, version 2002, update 2011) of the Federation of Medical Scientific Societies in The Netherlands (http://www.federa.org/), the latter aligning with authorized use of coded spare tissue for research.

TIL signature

To assess TIL abundance, we used a previously published [206], but slightly modified TIL signature. In brief, the signature was built based on assessment of the proportion of TIL nuclei of total nuclei (including TIL, tumor and resident stromal cells) for multiple representative areas of H&E stained slides from 96 familial BC samples by an experienced pathologist (CD). Gene-expression data (Affymetrix HG-U133_plus_2.0 array) from GEO54219 [234] of corresponding samples was split in two groups based on TIL abundance (high and low TIL count, median split), and tested for differential gene expression, which resulted in a 152 probe signature that highly correlates with TIL percentages in the specimen ($r=0.74$, p-value < 0.001)[206]. From the 152 HG-U133_plus_2.0 array immune infiltrate signature probe-sets, 120 (resembling

109 genes, see additional file 1) were found to overlap with the HG-U133_A array (Cohort A), and were used to classify samples based on TIL abundance according to average linkage hierarchical clustering (correlation as distance metric) in this study. TIL high samples contained a median stromal TIL count of 35% whereas TIL-low samples had a median stromal TIL count of 5%. The limitation to 120 probes in this study did not affect TIL scores calculated from either RNA–seq or microarray data (correlations between original and modified signatures, r=1, p-value < 0.001).

Assessment of prognostic value of the TIL signature

The prognostic value of this signature according to distant metastasis-free survival (MFS) was tested with cohort A. In the discovery set, mean age at time of surgery was 53 years (standard deviation (SD), 12); 221 patients (64%) were ER-positive; 120 patients were assigned to the TIL-high cluster (35%); 198 patients were pre-menopausal (58%). T1 tumors (<=2 cm) were present in 168 patients (49%), T2 tumors (>2–5 cm) in 163 patients (47%), T3/4 tumors (>5 cm) in 12 patients (3%), and unknown tumor stage in 1 patient. With respect to disease spread, 226 patients (66%) did not develop metastasis at a distant organ during follow-up (median follow-up time of patients still alive was 101 mo; range, 61–171 mo). In the validation set, 404 patients were ER-positive (77%); 166 patients were assigned to the TIL-high cluster (32%); and 387 patients (74%) did not have metastasis at a distant organ during follow-up (median follow-up time of 124 months). An overview of clinical characteristics per molecular subtype is given in **supplementary table 1**. To reduce inter-experimental variation and minimize biases, both datasets were combined by batch mean centering [235], and subsequently used for hierarchical clustering to divide samples in high and low TIL abundance groups using the 120 probe sets of the TIL signature.

Subtyping breast cancer

Samples were assigned to subtypes according to BC intrinsic molecular subtypes (AIMS) as described by Paquet and colleagues [196] using the Bioconductor R package genefu [236]. AIMS subtyping is considered the most stable subtyping based on expression data, as it is not affected by normalization or subtype frequencies in the cohort. It is noteworthy that AIMS subtyping has good concordance with PAM50 molecular subtypes as well as histological subtypes and preserves prognosis of subtypes [196]. For a breakdown of hormone receptor status (ER, PR and Her2) per molecular subtype, see **supplementary Figure S1** and for a comparison of several im-

mune-gene sets in AIMS and histological subtypes see **supplementary Figure S7**.

Immunogenomic tools

T cell clonality (TCR repertoire diversity and convergence): T cell receptor-β chain (TRB) reads were extracted from RNA-seq (Cohort B, n=347) using the miXCR [202] algorithm, available at https://github.com/milaboratory/mixcr. In brief, the software aligns the sequencing reads to reference V,D,J and C genes of the T-cell receptors (TCR), assembles the clonotypes and exports the clones per sample. Since total TCR-Vβ reads significantly differed among BC subtypes, we used only TIL-high samples to compare TCR clonality.

Antigen/mutational load: DNAseq and RNAseq data (Cohort B, n=266) were used to determine load of neo-antigens and expression of cancer germline antigens (CGAs). Neo-antigens and epitopes were predicted as described in [149]. Briefly, 17-mers of amino acids containing an amino acid arisen through a non-synonymous mutation at the center position were run through the online prediction server Net-MHC to predict EC50 values of all possible 9-mer peptides for HLA-class I molecules, and a peptide with a predicted EC50<50 nM was considered a possible neo-epitope. List of CGAs (n=239) was extracted from CT database (http://www.cta.lncc.br/), and their expression levels were determined relative to expression of all CGAs per patient.

Frequencies of immune cell populations: Microarray samples (Cohort A, n=867) were used for deconvolution of 22 immune cell populations (LM22) using CIBERSORT ([203], https://cibersort.stanford.edu/). Prognostic values of immune cell populations towards MFS were assessed by Cox regression analysis following classification into “high” and “low” groups, split by the median frequency.

Genes related to T cell evasion

Genes related to T cell evasion (n=850, see additional file 2) were selected from reports from others [34,35,160] as well as the Laboratory of Tumor immunology (PI: RD), Dept Medical Oncology, Erasmus MC (reviewed in [31,201]). These genes represent different T cell evasive mechanisms, and can be divided into 3 main categories, namely genes related to: (1) influx and migration of T cells; (2) antigen processing and presentation; and (3) function of T cells, with each category having various sub-

categories (see additional file 2). Notably, 4/24 genes of the category immune checkpoints were also present in the TIL signature. Differential gene expression analysis was performed for Cohort A in R using Limma [237]. Genes that were differentially expressed among BC subtypes (Benjamini-Hochberg adjusted P-value <0.05) were grouped according to above-mentioned categories of T cell evasion. Gene-sets with a clear direction (>90% up- or downregulated) were displayed using violin plots and heat maps. Heat maps were made using average expression of gene-sets per BC subtype. For comparison of gene-sets expressed by T cells, only TIL high samples were considered.

Statistical analysis

Differential gene expression was tested using Kruskal-Wallis tests, and comparisons of gene expression levels versus basal-like BC were performed with Wilcoxon tests. Distant MFS was used as endpoint for prognosis and log-rank tests were used to test survivor functions. Cox regression analyses were performed to assess prognostic value of gene-sets (and single genes, see additional file 3) in a uni- as well as multivariable (stratified for tumor size and age) model for the entire cohort A and per individual subtype. An interaction test was performed for all covariates with molecular subtypes. Kaplan-Meier curves were used to plot survival probabilities of subtypes/patients selected based on gene expression. Stata v13 (StataCorp, College Station, Texas, USA) was used to calculate differences and 2-sided p-values of < 0.05 were considered statistically significant.

Conflict of interest: Authors declare no confliict of interest.

3.6 Supplementary Data

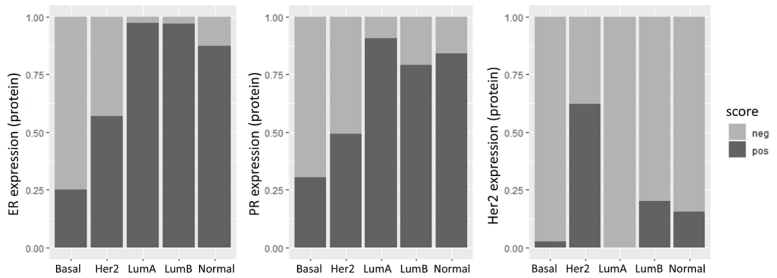

Figure S1. Hormone receptor status per BC molecular subtype. Stacked bar-plots show percentage or estrogen receptor (ER, left), progesterone receptor (PR, middle) and human-epidermal growth factor receptor (Her2, right) as assessed by immune histochemistry of the same patients, per BC subtype.

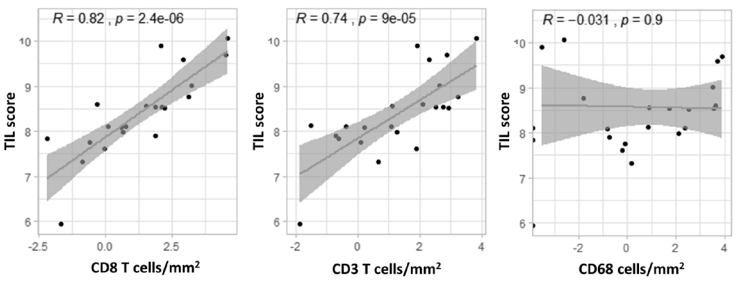

Figure S2. Scatterplots with pearson correlations (blue lines) between immune cell densities (cells/µm2) of A, CD8 T cells (identified as CD3+ CD8+); B, CD4 T cells (CD3+ CD8-) or C, macrophages (CD68+) and TIL scores in 30 BC patients.

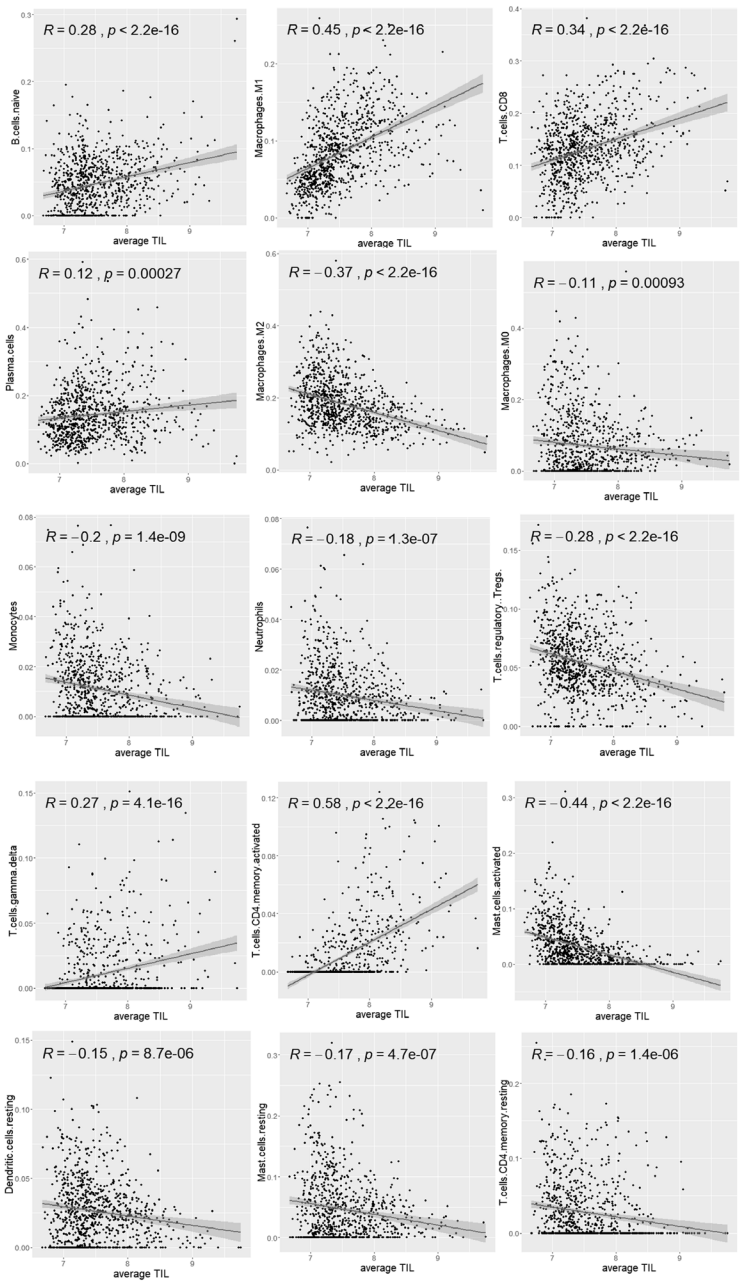

Figure S3. Correlations between proportions of immune cell populations and TIL score in BC. Scatter plots with correlations (blue lines) between fractions of immune cell subsets and TIL-scores (only displayed when pearson-correlation was significant, p<0.05).

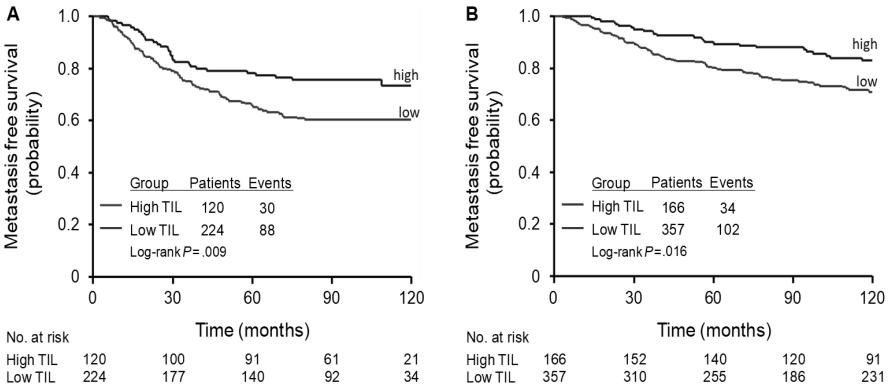

Figure S4. Prognostic value of TIL signature in LNN BC. **A**, Kaplan-Meier curves of estimated MFS for patients in Cohort A, discovery set (n=344, p=0.009). **B**, Kaplan-Meier curves of estimated MFS for patients in Cohort A, validation set (n=523, p=0.016).

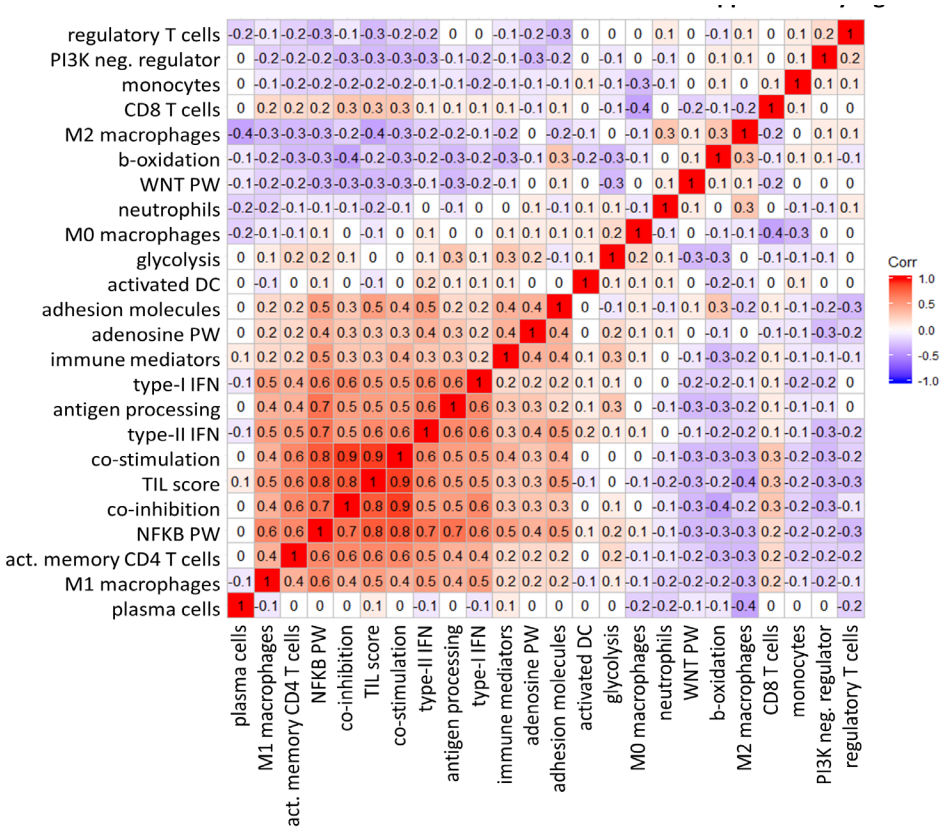

Figure S5. Correlation matrix of gene-sets related to T cell evasion. Numbers represent correlation coefficients (r-values). Negative correlations are shown in blue; positive correlations are visualized in red.

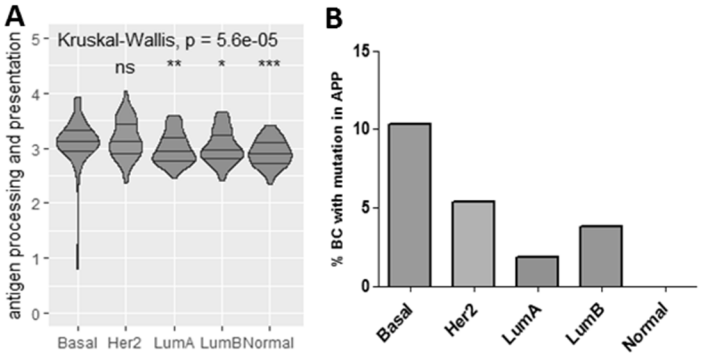

Figure S6. Mutations or down-regulated expression of antigen processing and presentation genes in BC subtypes. **A**, Expression of genes related to APP. **B**, Proportion of BC patients with one or more mutations in APP genes. Statistical differences were calculated using Kruskal-Wallis test among subtypes, and Wilcoxon rank sum test for pairwise comparison relative to basal-like BC; p-values are indicated as: '***'<0.001, '**'<0.01, '*'<0.05.

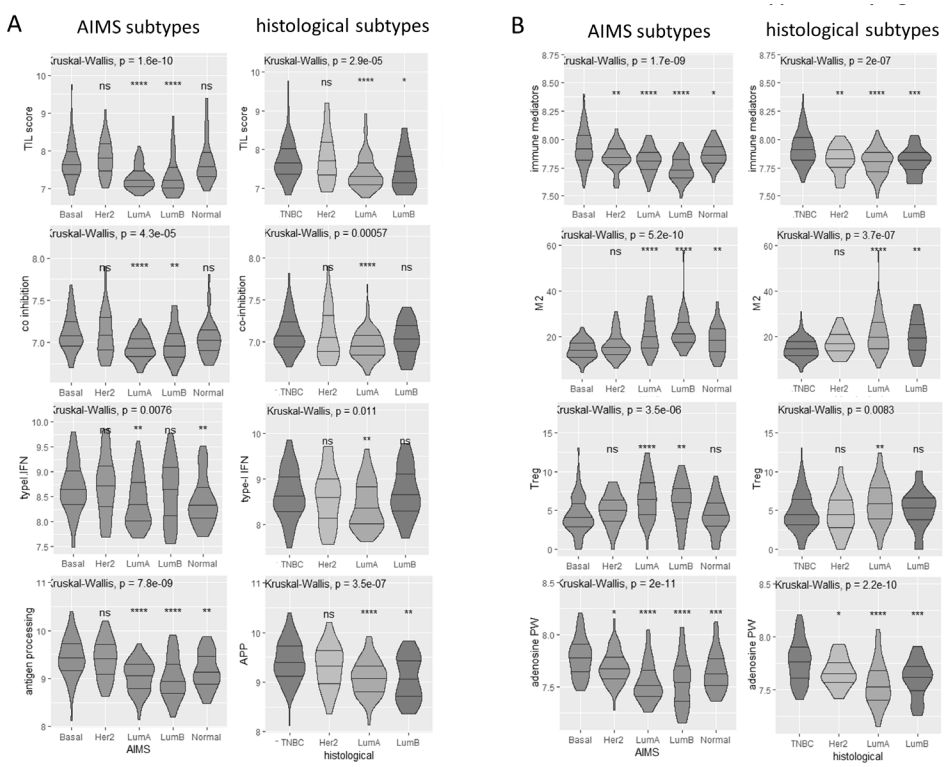

Figure S7. Sets of immune genes show similar levels of expression between molecular (AIMS) and histological subtypes (hormone receptors). **A**. selected gene-sets associated with immune response. **B**. selected gene-sets associated with immune suppression (n=247, cohort A).

Supplementary Table 1. Clinical characteristics of Cohort A per molecular subtype.

Clinical characteristics	Basal		Her2		LumA		LumB		Normal	
	samples	%	samples	%	samples	%	samples	%	samples	%
ER-	138	71.5	50	44.6	9	4	6	4.2	30	15.6
ER+	23	11.9	33	29.5	166	73.1	101	70.6	105	54.7
n.d.(ER)	9	4.7	29	25.9	52	22.9	36	25.2	57	29.7
PR-	73	37.8	31	27.7	14	6.2	19	13.3	16	8.3
PR+	16	8.3	15	13.4	74	32	34	23.8	42	21.9
n.d.(PR)	104	53.9	66	58.9	139	61.2	90	62.9	134	69.8
HER2-	71	36.8	18	16.1	63	27.8	32	22.4	33	17.2
HER2+	1	0.5	22	19.6	0	0	4	2.8	3	1.6
n.d.(HER2)	121	62.7	72	64.3	164	72.2	107	74.8	156	81.3
T1	75	38.9	53	47.3	137	60.4	68	47.6	123	64.1
T2	116	60.1	56	50	82	36.1	75	52.4	65	33.9
T3	1	0.5	2	1.8	6	2.6	0	0	3	1.6
T4	1	0.5	1	0.9	1	0.4	0	0	1	0.5
G1*	1	0.5	3	2.7	27	11.9	3	2.1	15	7.8
G2*	9	4.7	10	8.9	32	14.1	23	16.1	16	8.3
G3*	64	33.2	27	24.1	8	3.5	18	12.6	9	4.7
G1#	3	1.6	2	1.8	35	15.4	6	4.2	45	23.4
G2#	28	14.5	28	25	82	36.1	54	37.8	75	39.1
G3#	68	35.2	102	91.1	12	5.3	24	16.8	8	4.2

Abbreviations: ER: estrogen receptor; Her2; human epidermal growth-factor receptor 2; G: clinical grade; n.d.: not determined; PR: progesterone receptor; T: tumor size.

*clinical grade determined by Bloom-Richardson grading

#clinical grade obtained via public repository (unspecified GSE11121, Elston and Ellis method for GSE7390 and GSE2990)

Chapter 4

Spatial immunophenotypes predict response to anti-PD1 treatment and capture distinct paths of T-cell evasion in triple negative breast cancer

Dora Hammerl[1], John WM Martens[1], Mieke Timmermans[1], Marcel Smid[1], Anita M Trapman-Jansen[1], Renee Foekens[1], Olga I Isaeva[2,5], Leonie Voorwerk[2], Hayri E Balcioglu[1], Rebecca Wijers[1], Iris Nederlof[2], Roberto Salgado[6,7], Hugo Horlings[2,4], Marleen Kok[2,3*], Reno Debets[1*]

[1]Department of Medical Oncology, Erasmus MC Cancer Institute, Rotterdam, the Netherlands [2]Division of Tumor Biology & Immunology, and Departments of [3]Medical Oncology, [4]Pathology, and [5]Molecular Oncology & Immunology, The Netherlands Cancer Institute, Amsterdam, the Netherlands;[6]Department of Pathology, GZA-ZNA Ziekenhuizen, Antwerp, Belgium;[7]Division of Research, Peter Mac Callum Cancer Center, Melbourne, Australia

Nature Communications, in revision

Abstract

Only a subgroup of triple-negative breast cancer (TNBC) responds to immune checkpoint inhibitors (ICI). To better understand lack of response to ICI, we analyzed 669 TNBCs for spatial immune cell contextures in relation to clinical outcomes as well as pathways of T-cell evasion. Excluded, ignored and inflamed phenotypes were captured by a gene classifier that predicts prognosis of various cancers as well as anti-PD1 response of metastatic TNBC patients in a phase II trial. The excluded phenotype, which was associated with resistance to anti-PD1, demonstrated deposits of collagen-10, enhanced glycolysis, and activation of TGFβ/VEGF pathways; the ignored phenotype, also associated with resistance to anti-PD1, showed either high density of CD163+ myeloid cells or activation of WNT/PPARγ pathways; whereas the inflamed phenotype, which was associated with response to anti-PD1, revealed necrosis, high density of CLEC9A+ dendritic cells, high TCR clonality independent of neo-antigens, and enhanced expression of T-cell co-inhibitory receptors.

Significance

Spatial immunophenotypes predict prognosis in TNBC and other malignancies. This is the first report demonstrating that these phenotypes predict response to anti-PD1 treatment in TNBC. Importantly, our in-depth analyses revealed distinct T cell evasive pathways that advocate phenotype-specific combinations to boost the efficacy of ICI in TNBC.

4.1 Background

Triple negative breast cancer (TNBC) is an aggressive form of breast cancer (BC) (accounting for 10-20% of all BCs) that is characterized by absence of hormone receptors and has limited therapeutic options. TNBC is considered the most immunogenic BC subtype based on relatively high numbers of tumor-infiltrating lymphocytes (TILs), which is reflected by a higher likelihood of response to immune checkpoint inhibition (ICI) when compared to other BC subtypes[207]. Nevertheless, objective response rates (ORR) to ICI in metastatic TNBC are variable, and do not exceed 24% when administered as mono-therapy[195]. Clinical benefit has been observed for first-line treatment with the programmed-cell death ligand (PD-L1) blocking antibody (atezolizumab) in combination with nab-paclitaxel, which has recently been approved by the EMA and FDA for PD-L1-positive metastatic TNBC. Although this combination therapy induces survival benefit in PD-L1-positive TNBC[238], still a significant proportion of TNBC patients does not benefit from anti-PD1. Moreover, preliminary data of primary TNBC treated with anti-PD1 plus chemotherapy in the neoadjuvant setting suggest that PD-L1 expression is not associated with benefit of ICI[239,240]. Collectively, these findings point towards the need for better predictive markers and understanding of the underlying immune cell contextures to select TNBC patients for ICI.

Several studies have examined the predictive value of tumor mutational burden (TMB) and TIL abundance in TNBC. While a high TMB has been associated with response to ICI-based therapies in melanoma, lung cancer, and colorectal cancer[19], no significant association between TMB and ICI response has been found for TNBC[20,21,218]. TILs are frequently present in primary TNBC and correlate with good prognosis as well as response to neoadjuvant chemotherapy and ICI in the metastatic setting[5,7,9,10,207,218,241]. Furthermore, TILs predict overall survival (OS) to anti-PD1 as a monotherapy independent of PD-L1 expression[242]. Emerging evidence now suggests that next to abundance of TILs, also the composition and activation state of TILs contribute to clinical outcome. For example, the tissue-resident memory subset of CD8+ T-cells provides more prognostic information when compared to CD8+ T-cells[243], and marks of an ongoing immune response, such as clonal T-cell expansion correlate to anti-PD1 response[218]. In addition, the spatial localization of TILs has prognostic value in TNBC[27,244]. In this regard, three main spatial phenotypes have been identified and recognized for their association with clinical outcome in different cancer types including TNBC[27,245,246]: inflamed (also reffered to as “hot”; characterized by the presence of intratumoral lymphocytes), excluded (also referred to as “altered”; lymphocytes are restricted to the invasive margin) and ignored (also reffered to as “cold” or “desert”; characterized by lack of lymphocytes). Immune evasive mechanisms, including intrinsic as well as acquired mechanisms, and their

contribution to numbers, cell states and locations of TILs have been described[247,248]. Such mechanisms include those that inhibit influx and migration of T-cells, antigen recognition by T-cells or suppression of T-cell function[31,160,249–253]. Collectively, the above studies describe spatial phenotypes in cancers[27,245,246], however, so far it has not been studied whether these phenotypes are predictive of response to ICI and which immune evasive processes underpin these phenotypes in TNBC.

Here, we determined spatial immunophenotypes in four large cohorts of TNBC patients using multiplexed immunofluorescent imaging and next-generation sequencing (NGS). We demonstrated that inflamed, excluded and ignored phenotypes can be accurately assigned by a gene classifier, differentially correlate with prognosis in TNBC and other tumor types, and predict response to anti-PD1 treatment in metastatic TNBC and melanoma. Importantly, spatial immunophenotypes in primary TNBC are characterized by distinct immune determinants as well as tumor micro-environment (TME) and immune response-mediated paths of T-cell evasion. These immunophenotypes provide a rationale to develop therapies specifically for spatial immunophenotypes to enhance response to ICI in TNBC.

4.2 Results

Spatial contexture of lymphocytes but not myeloid cells is prognostic in TNBC

In order to assess tumor-immune interactions in TNBC, CD8+ T-cell presence and spatial organization were studied in 236 untreated, primary TNBC using immunohistochemical staining (IHC) of whole slides (Cohort A; for study design see **Figure S1** and for clinical details of cohorts see **Table S1**). These patients did not receive adjuvant chemotherapy enabling the testing of pure prognostic value of potential biomarkers. We defined three spatial immunophenotypes: excluded (26%; predominant location of CD8+ T-cells at tumor border not center); ignored (28%; negligible presence of CD8+ T-cells neither at border nor center) and inflamed (46%; CD8+ T-cells evenly distributed across border and center) (see M&M section for detailed criteria of spatial phenotypes) (**Figure 1A, Figure S2A**). These spatial phenotypes were significantly associated with survival (distant metastasis-free survival (MFS), disease-free survival (DFS), and overall survival (OS), p≤0.009, n=122 lymph node-negative TNBC): tumors with an inflamed phenotype had the best prognosis (10-year OS: 80%), excluded phenotypes intermediate (10-year OS: 60%, HR:1.45, 95% CI: 0.84-3.3), and ignored phenotypes the worst prognosis (10-year OS: 40%; HR:3, 95% CI: 1.5-5.9) (**Figure 1B**). Prolonged survival of excluded versus ignored phenotypes was statistically significant for OS, but not MFS nor DFS. In addition to

CD8+ T-cells, we assessed the presence of other immune effector cells using multiplexed immunofluorescence (IF) imaging of 64 tumors (**Figure 1C, Figure S2B**). CD4+ T-cells and CD20+ B cells generally co-occurred with CD8+ T-cells at the tumor border and center, whereas CD56+ NK cells were hardly present in TNBC (**Figure 1D, Figure S3A-D**). For instance, at the tumor border numbers of stromal CD20+ B cells, CD4+ and CD8+ T-cells did not differ between excluded and inflamed phenotypes, yet the excluded phenotype had significantly fewer intratumoral B and T-cells (**Figure S3A,C**). Moreover, distances between CD8+ T-cells and tumor cells (CK-positive cells) were significantly larger in excluded versus inflamed phenotypes (**Figure 1E, Figure S3E**). Interestingly, despite a lack of lymphocytes in the ignored phenotype, we did observe stromal and intra-tumoral CD68 macrophages (**Figure 1D, Figure S3A-D**). Notably, densities of stromal CD8+ T-cells and intratumoral CD4+, CD8+ T and CD20+ B cells, but not CD68 macrophages, demonstrated significant correlations with OS or MFS (**Figure S3F**). Next, we evaluated the presence of tertiary lymphoid structures (TLS), defined as focal areas that are positive for CD4 T and CD20 B cells, which are considered important sites for T cell priming and initiation of anti-tumor immune response[254–257]. Interestingly, we observed a high number of TLSs at the border of tumors of both the inflamed and excluded phenotype, but not in the ignored phenotype (**Figure 1F**).

A gene classifier of spatial phenotypes predicts outcome to anti-PD1 treatment in TNBC patients

We developed a gene-expression classifier to be able to assess prognostic and predictive values of the spatial immunophenotypes without the need for CD8+ T-cell stainings. Briefly, we selected most discriminative genes (according to differential expression, DE) for the excluded, ignored and inflamed phenotypes in a discovery set for which both gene expression data and CD8+ T cell stainings were available (Cohort A1, n=101). Using DE and rank-correlations with phenotypes from the discovery set, we assigned spatial phenotypes in an independent validation set (Cohort A2, n=43, gene expression data and CD8+ stainings available), which resulted in correct assignment of spatial phenotypes in 81% of cases, whereby all excluded cases and 80% of the inflamed cases were correctly predicted (**Table 1A**; see M&M section for details on classification).

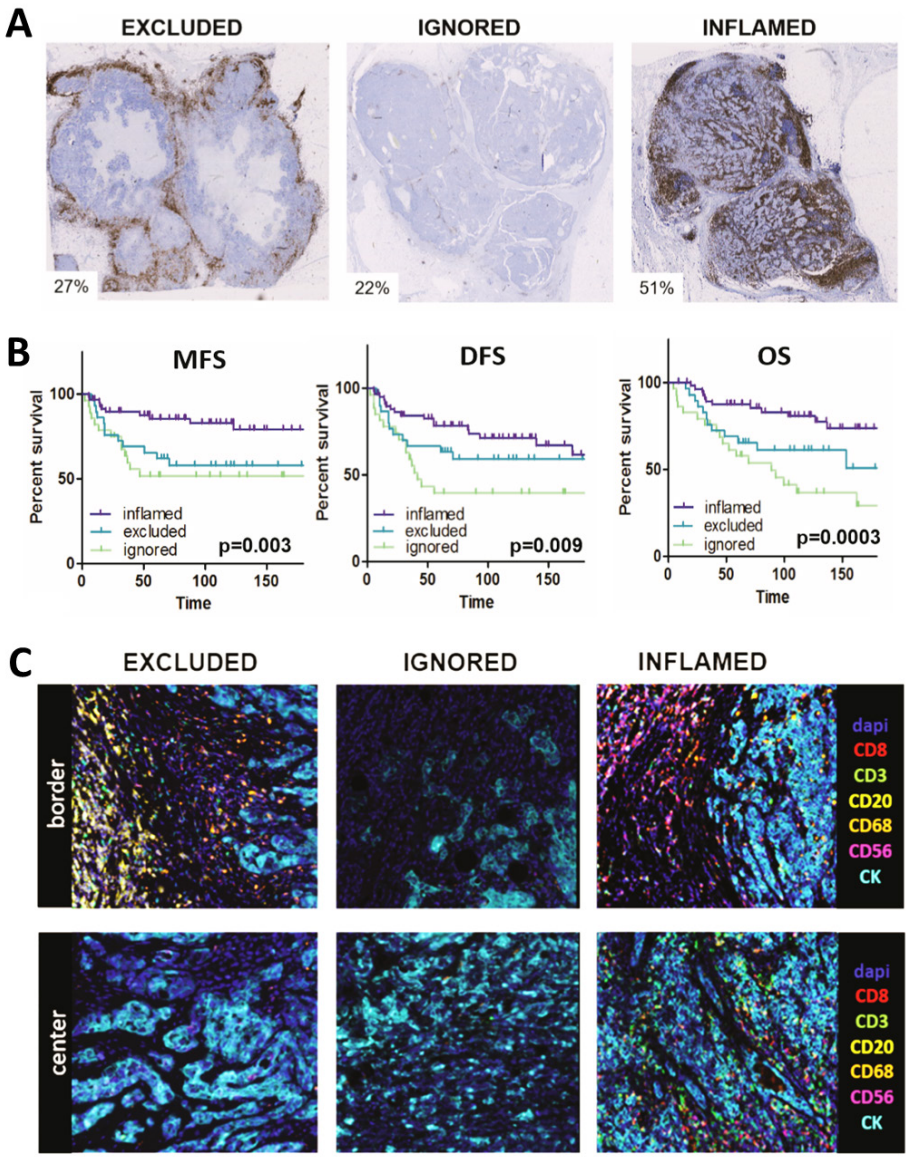

Figure 1. **Spatial immune contexture is prognostic in TNBC**. **A, B.** Representative whole slide images of CD8+ T-cell spatial phenotypes with percentage of patients per phenotype (**A**) and corresponding Kaplan-Meier curves for metastasis-free survival (MFS), disease-free survival (DFS) and overall survival (OS) (**B**, p-values show log-rank test for trend; time is displayed in months). **C**. Representative multiplex IF images of immune effector cells at the tumor border and center of each spatial phenotype.

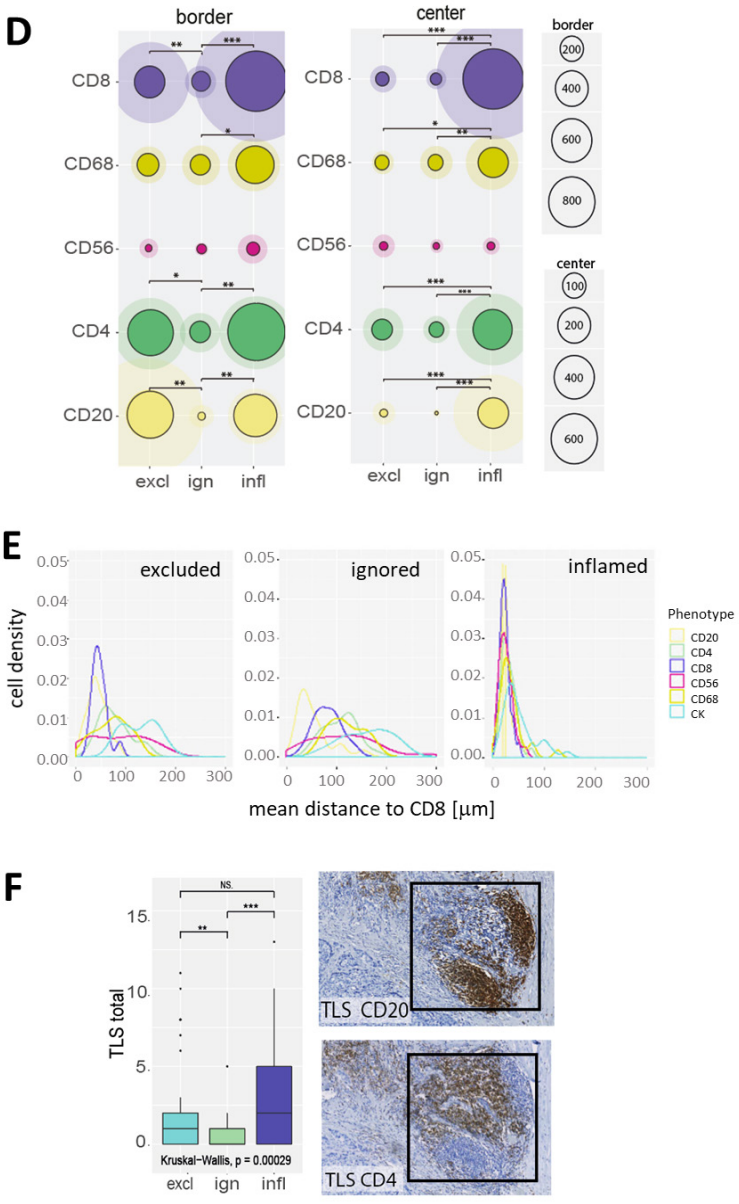

D. Circle plots show mean and SD of immune cell densities (cells/mm2) at border and center. **E**. Histograms show mean distances in µm between CD8+ T-cells and other cell types (x-axis) versus cell densities (cells/mm2, y-axis). **F**. Boxplots show total number of tertiary lymphoid structures (TLS, identified by consecutive stainings of CD20+ B cells (top) and CD4+ T-cells (bottom), see black squares in images). Significant differences are: ***, p<0.001; **, p<0.01; *, p<0.05, NS, p>0.5.

A	spatial immunophenotype (gene classifier)				
CD8 stanings	excl	ign	infl	total	sensitivity
excl	18	0	0	18	**100**
ign	4	5	0	9	**55.6**
infl	3	0	12	15	**80**
total	25	5	12	43	
specificity	**72**	**100**	**100**		

B	spatial immunophenotype (gene classifier)		
anti-PD1 treatment	excl & ign	infl	total
non-responders	35	4	39
responders	4	6	10
total	39	10	49
PVV	**0.6**		
NPV	**0.9**		

Table 1. Performance and clinical validation of gene classifier. Gene classifier (as described in Results section) was tested for the following parameters. **A**. Correct assignment of spatial immunophenotypes. **B**. Prediction of response to anti-PD1 treatment. Abbreviations: PPV: positive predictive value, NPV: negative predictive value.

Subsequently, the prognostic value of this spatial-phenotype-classifier was tested in a second, independent cohort of primary, lymph-node negative, systemically untreated BC (Cohort B, n=196 basal-like tumors[9]). Gene-sets representing the excluded and ignored phenotypes were associated with poor prognosis (excluded: HR=1.8, CI:1.2-2.7; ignored: HR=1.6, CI:1.1-2.4), whereas the gene-set of the inflamed phenotype was associated with good MFS (HR=0.62, CI:0.45-0.86) (**Figure 2A**). Upon testing the performance of the gene classifier in a third cohort of primary TNBC patients (**Figure 2B**, Cohort E, n=137), we validated the prognostic value of the spatial-phenotype-classifier (logrank, p=0.001). It is noteworthy that among all BC, basal-like BC had the highest proportion of the inflamed phenotype followed by her2 and luminal-B subtypes (**Figure S6A**).

To test the capacity of the spatial-phenotype-classifier to predict outcome after anti-PD1 treatment in TNBC, we applied the classifier to a dataset of metastatic patients from the TONIC trial[218]. In this phase II trial, all patients received anti-PD1 after a short (2 weeks) immune induction treatment with low dose chemotherapy or irradiation (cohort D, n=53, biopsies from pre- and post- induction treatment metastatic lesions, see for details). It is noteworthy that we observed significantly higher frequencies of the excluded (41%) and ignored phenotypes (37%), and decreased

frequencies of the inflamed (21%) phenotypes when metastasized TNBC was compared to primary TNBC, not dependent on biopsy sites, which supports the prognostic nature of the classifier (**Figure S4C,D**). Expression of the exclusion gene-set was significantly higher in non-responding (progressive disease, PD patients) patients (odds-ratio (OR): 3.5; CI: 1.2-11.9), whereas expression of the inflamed gene-set was significantly higher in responding patients (complete response, CR; partial response, PR; stable disease, SD for > 24 weeks according to iRECIST criteria258) (OR: 0.4; CI: 0.18-0.92) (**Figure 2C, D**). No association with therapy response was found for the ignored gene-set (OR=0.9; CI: 0.5-1.85). When assessing receiver operating characteristic (ROC) as a measure of predictive value of the excluded, inflamed or combined gene-sets, we observed areas under the curve (AUC) of 0.72 (CI:0.52-0.89), 0.73 (CI: 0.54-0.94) and 0.75 (CI: 0.55-0.95), respectively, whereas PD-L1 expression on immune cells, the biomarker that is currently used in the clinical setting had an AUC of 0.66 (CI: 0.51-0.82) (Figure 2E). The AUC for sTIL, another marker considered to stratify patients was 0.67 (CI: 0.48-0.82) (Figure 2E). In addition, the non-responders group was enriched for the excluded and ignored phenotypes (90% of the cases), whereas in anti-PD1-responders the inflamed phenotype was enriched (60% of the cases, Chi-square, p=0.007, Figure 2F). In fact, using the spatial-phenotype-classifier we were able to predict outcome after anti-PD1 treatment, i.e., the negative predictive value (NPV) of the inflamed phenotype to therapy response is 0.9, while the positive predictive value (PPV) is 0.6 (**Table 1B**). In line, patients with the excluded and ignored phenotypes had shortened OS when compared to the inflamed phenotype (logrank, p=0.05, Figure 2G). Of note, spatial phenotypes predict clinical outcome independent of immune cell PD-L1 but not sTIL (**Figure S5C,D**).

Prognostic and predictive value of spatial phenotypes in multiple cancers

We applied the spatial-phenotype-classifier to other tumor (sub-)types to assess the prognostic and predictive value in a pan-cancer setting. Spatial phenotypes were significantly prognostic not only in invasive breast cancer BRCA (all subtypes, including ER+), but also in bladder cancer (BLCA), skin cutaneous melanoma (SKCM), cervical squamous cell carcinoma and endocervical adenocarcinoma (CESC), head and neck squamous cell carcinoma (HNSC) and kidney cancer (KICH), but despite similar trends not in prostate (PRAD), pancreatic (PAAD), lung (LUAD) or colon cancer (COAD) (Cohort E, **Figure S6B**). Although spatial immunophenotypes have been described for various cancers[249,259], they have not directly been related to response to PD1 treatments. Here we demonstrate that tumors generally responding poorly to ICI, such as pancreas and prostate cancers, had the highest proportions of excluded

or ignored phenotypes, while tumors generally responding well to ICI, such as skin cutaneous melanoma, kidney and lung cancers, had the highest proportions of the inflamed phenotype (**Figure S6A**). In line with TNBC, in advanced and metastatic melanoma, where RNAseq data of ICI-treated patients is publicly available[260,261], we observed that expression of the gene-set of the excluded phenotype was significantly increased in tumors of patients not-responding to ICI, and the gene-set of the inflamed phenotype was significantly increased in tumors of patients responding to ICI (**Figure S6C**).

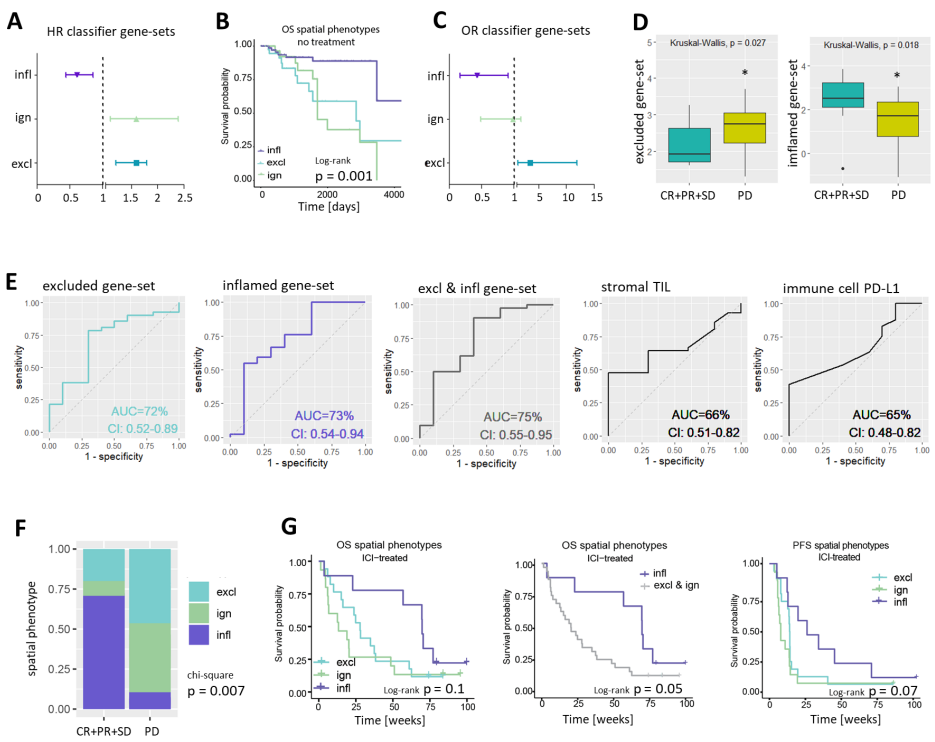

Figure 2. Gene classifier assigns spatial phenotypes of CD8+ T-cells and stratifies metastasized TNBC patients according to ICI response A. Forestplots showing HRs and CIs of classifier gene-sets (Cohort B). **B**. Kaplan Meier curves of assigned spatial phenotypes in primary TNBC patients (Cohort E). **C**. Forest-plots showing Odds Ratios (OR) for response to anti-PD-1 treatment of classifier gene-sets (Cohort D, TONIC trial). **D**. Boxplots displaying average expression of classifier gene-sets in responding (CR + PR + SD > 24 weeks) and non-responding (PD) patients (Cohort D). **E**. ROC curves with area under the curve (AUC) and CIs for the excluded-, inflamed- or a combination if excluded and inflamed gene-sets, and ROC curves of predictive markers, such as frequency of stromal TILs and PDL1 positivity of immune cells (Cohort D). **F**. Proportions of assigned spatial phenotypes in patients with metastatic TNBC responding or not responding to anti-PD-1 treatment (pre-treatment biopsies) and **G**. corresponding survival curves (Cohort D).

Spatial phenotypes differ in TCR repertoire skewness and mutational signatures but not mutational burden

In order to test for potential drivers of spatial phenotypes, we first studied clinicopathological and genomic features in lymph node negative, systemically untreated, primary TNBC (Cohorts A and C). Spatial phenotypes were not associated with mitotic activity index (MAI), tumor grade, tumor stage or histological subtypes, except for tumors with medullary features that were (as expected) solely comprised of the inflamed phenotype (**Figure S7A-D**). In addition, following assignment of spatial phenotypes to Cohort C (RNAseq and WGS data, n=66), we observed that spatial phenotypes did not differ with respect to frequency of BRCA1 or BRCA2 germline mutations (**Figure 3A**), frequency of β2Microglobulin loss (**Figure 3B**) nor TMB or types of genomic alterations, including non-synonymous SNV (passenger and driver mutations combined), exonic frameshifts, indels (**Figure 3C**) or predicted neo-antigens (**Figure 3D**). In contrast, spatial phenotypes did differ with respect to mutational signatures and TCR clonality (**Figure 3E-I**). For instance, mutational signature-3 (related to homologous recombination deficiency) was enriched in the inflamed phenotype and signature-5 (related to age) was significantly enriched in the ignored and excluded phenotypes (**Figure 3F,G**). The highest TCR-Vβ diversity as well as the most skewed TCR-Vβ repertoire (most clonally expanded reads) were observed in the inflamed phenotype, and both these parameters were equally low in the excluded and ignored phenotypes (**Figure 3H,I**).

Spatial phenotypes are characterized by distinct immune evasive pathways

Next, we studied whether spatial phenotypes capture different modes of immune-evasion (Cohort A, **Figure 4, Figure 5**). Immune cell deconvolution by Cibersort73 confirmed above observations (**Figure 1D**) with respect to the abundance of immune effector cells and particularly revealed differential frequencies of plasma cells, activated memory T-cells, follicular helper T-cells, activated dendritic cells (DC), and M1- and M2 macrophages (**Figure 4A**). When evaluating expression of gene-sets related to various mechanisms of T-cell evasion[9], as well as Ingenuity Pathway Analysis (IPA®), we observed that the excluded phenotype was characterized by enhanced expression of genes associated with endothelial barrier, glycolysis, serine protease inhibition (SPI), and extracellular matrix (ECM) remodeling (**Figure 4B-D**, see Figure 4C for examples of individual genes, **Figure S8A**); notably all these pathways were inter-linked with the TGFβ pathway (**Figure 4D, E, Figure S8B**). One of the most up-regulated genes in the excluded phenotype (compared to the inflamed phenotype) was COL10A1 (**Figure 4C**), the expression of which was strongly cor-

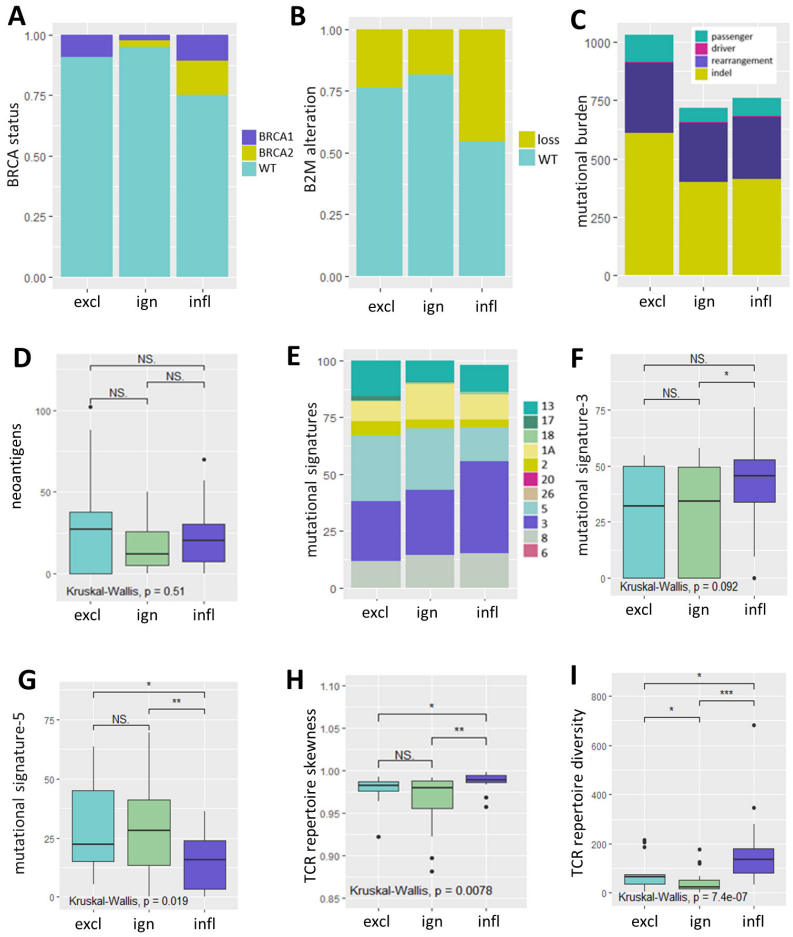

Figure 3. Genomic features of spatial phenotypes. The following parameters were tested for differential presence in spatial phenotypes (determined by the gene-classifier) in TNBC: **A**. BRCA status (proportion). **B**. Loss of β2-microglobin (copy number). **C**. Total number of different types of mutations. **D**. Total number of predicted neo-antigens. **E**. Proportions of most abundant mutational signatures. **F,G** Frequencies of signatures-3 and 5. **H**. TCR repertoire skewness (based on the gini-simpson index). **I**. Total number of different TCR-Vβ reads. For all above parameters Cohort B was used, spatial phenotypes were assigned according to classifier. Significant differences are: ***, p<0.001; **, p<0.01; *, p<0.05, NS, p>0.5.

related to the TGFβ- and VEGF- signaling pathways while being inversely correlated to the expression of CD8A (**Figure 4E,H**). The ignored phenotype was characterized by increased expression of genes associated with β-oxidation (**Figure 4B**) as well as the WNT, PPAR and LXR/RXR pathways (**Figure 4C,D**). Moreover, the ignored phenotype showed enhanced gene expression of S100A7 (**Figure 4C**), a molecule that has been reported to promote oncogenesis and act as chemo-attractant for M2 macrophages and other suppressive myeloid cells[262].

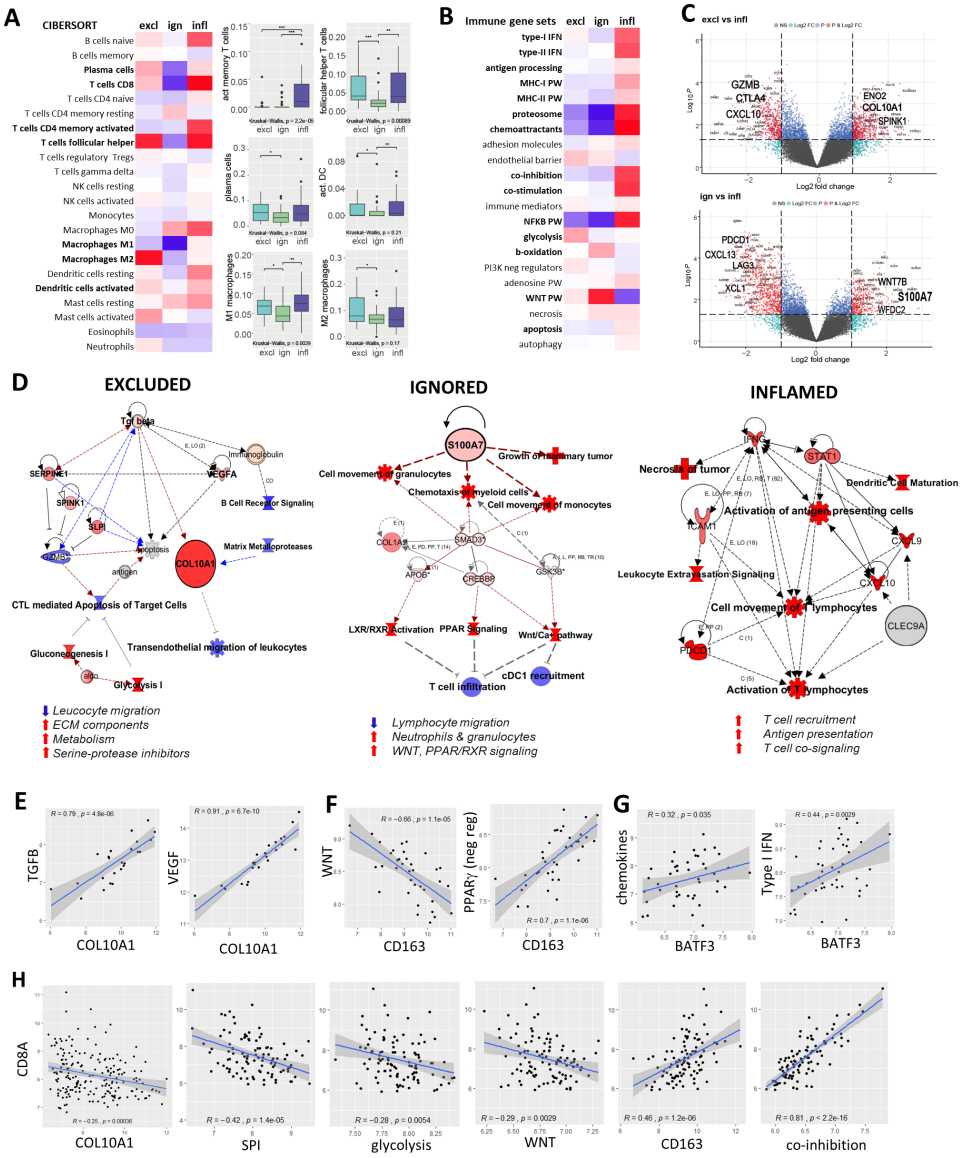

Figure 4. Spatial phenotypes interrogated for immune determinants and evasive pathways. A. Heatmap showing scaled average frequencies of immune cells based on Cibersort deconvolution (red: high, blue: low, immune cell subsets with significant differences among spatial phenotypes are indicated in bold); corresponding boxplots show immune cell subsets with differential abundances among spatial phenotypes. **B**. Heatmap showing scaled average expression of gene-sets related to T-cell evasion (differential gene-sets are indicated in bold). **C**. Volcano plot of differential gene expressions between excluded and inflamed (upper), and ignored and inflamed phenotypes (lower); top DE genes related to T-cell evasion are shown in bold. **D**. IPA analyses of cells, molecules and pathways associated with spatial phenotypes; and lists of major characteristics per spatial phenotype (bottom). **E**. Correlations between

expressions of COL10A1 and TGFB- or VEGF-signaling in the excluded phenotype. **F**. Correlations between expressions of CD163 and WNT targets or negative regulators of PPAR genes in the ignored phenotype. **G**. Correlations between presence of activated dendritic cells (according to BATF3 expression) and expressions of chemokines or type-I IFN genes in the inflamed phenotype. **H**. Correlations between expressions of CD8A and various T-cell evasive genes/gene-sets (all phenotypes) (all correlations show regression coefiicients and p-values).

Of the above oncogenic pathways in particular WNT was inversely correlated with expression of CD8A as well as CD163 (**Figure 4F,H** and **S8B**). Lastly, the inflamed phenotype showed enhanced expression of genes associated with necrosis, type-I and type-II IFN, antigen processing and presentation, T-cell co-stimulation but also co-inhibition (**Figure 4B,C**), which were all inter-related (**Figure S8B**). Importantly, the inflamed phenotype showed high gene expression of the T-cell chemo-attractants CXCL9, CXCL10 (**Figure 4C**), which according to our immune cell deconvolution and pathway analyses are derived from activated (BATF3/CLEC9A-positive) conventional DC (cDC1, **Figure 4G**). Immune response-mediated markers, such as CD163 and T-cell co-inhibition[213] were correlated with the expression of CD8A (**Figure 4H**).

Multiplex IF demonstrated that the enhanced expression of collagen-10 in the excluded phenotype, led to deposits into stromal areas between tumor and immune cells at the tumor center (Figure 5A,B). To assess how entry of T-cells may be affected by a physical barrier, we evaluated the presence of high endothelial venules (HEV, identified via MECA-79 stainings), and observed that these were present at high numbers at the border as well as center of excluded phenotypes (Figure 5D). In the ignored phenotype, IF showed (albeit only in subset of ignored tumors) that very high S100A7 expression by tumor cells (highest of all spatial phenotypes) was accompanied by high frequencies of CD163+ macrophages (Figure 5A, middle panel, Figure 5B). Even though tumor-associated macrophages were not unique for the ignored phenotype, and were present at particularly high densities in the center of inflamed and to a lesser extent in excluded phenotypes, nearest-neighbor analysis revealed that macrophages and myeloid cells showed relatively low distances to CD8+ T-cells, regardless of frequencies and spatial phenotypes (Figure 5C). CD66b+ neutrophils (another immune cell type that has been reported for its immune-suppressive effects in the TME263) co-occurred with macrophages and myeloid cells and were found to be present at high numbers in the same subset of the ignored phenotype (Figure 5E). Notably, the ignored phenotypes that did not show high M2 and neutrophil densities were characterized by enhanced expression of WNT targets. In the inflamed phenotype, IF revealed significantly enhanced numbers of stromal as well as intratumoral CLEC9A+ DC (**Figure 5A.B**). Interestingly, and despite overall

low abundances of these cells (regardless of spatial phenotype), CLEC9A+ DC were found in relatively close proximity to CD8+ T-cells (**Figure 5C**) and their cell densities significantly correlated with those of CD8+ T-cells (**Figure S8C**), pointing to the recognized immune-enhancing action governed by cDC1 cells[264]. Nevertheless, and despite high densities of T-cells and TLS, only a small fraction of CD4+ and CD8+ T-cells in the inflamed phenotype expressed the co-stimulatory receptors ICOS or 41BB, which co-ocurred with a significantly decreased MHC-II expression by tumor cells (**Figure 5D,F**).

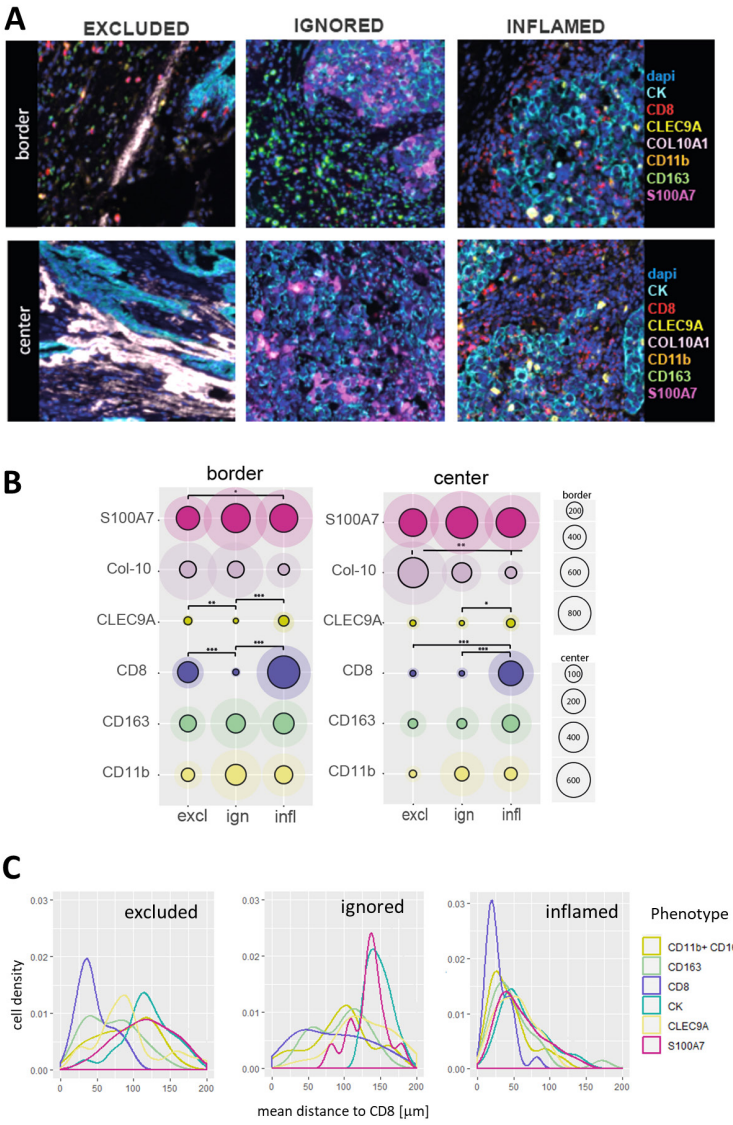

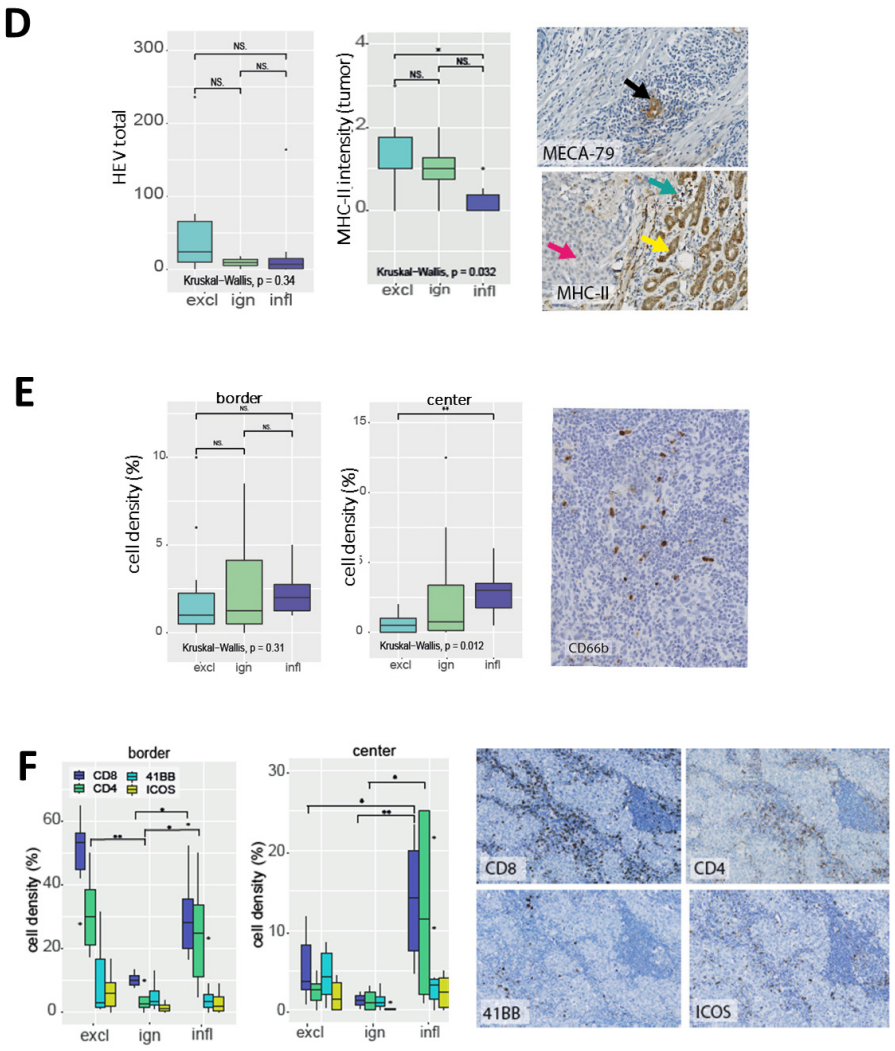

Figure 5. Spatial immunophenotypes are characterized by distinct T-cell evasive mechanisms. A. Representative images of cells and molecules related to spatial phenotypes (spatial phenotype panel) at the tumor border and center. **B**. Circle plots show mean and SD of cell densities at border and center regions per mm2; Collagen-10 was positive tissue area in µm2/100 for visualization purpose. C. Histograms show mean distances in µm between CD8+ T-cells and other cell types (x-axis) versus cell densities (y-axis). **D**. Boxplots show numbers of high endothelial venules (HEV, identified via MECA-79 staining, black arrow) and MHC-II expression of tumor cells (no distinction between border and center, pink arrow: tumor cells; yellow arrow: adjacent normal breast lobules; green arrow: immune cells). **E**. Neutrophil densities at border and center and representative image is shown. **F**. Boxplots show numbers of different T-cell markers stained on consecutive slides, and representative images are shown. Significant differences are: ***, p<0.001; **, p<0.01; *, p<0.05, NS, p>0.05.

4.3 Discussion

In this study, using cohorts of in total 669 patients with TNBC, 2706 with other types of BC and 4003 with other cancers, we present in-depth analyses of spatial immunophenotypes in relation to prognosis and response to anti-PD1 treatment as well as T-cell evasion. Our results, to the best of our knowledge, present for the first time that spatial immunophenotypes predict response to ICI in TNBC, and are characterized by distinct T-cell evasive pathways that provide a rationale to develop spatial phenotype-specific therapies for ICI-refractory TNBC.

We have developed and validated a novel spatial-phenotype-classifier that accurately predicts spatial localization of CD8+ T-cells. Next to its prognostic value in TNBC, this classifier has prognostic value in various tumor types (BC, CESC, HNSC, KICH, BLCA, SKCM) which is in line with recent reports[27,245,265], and suggests that the classifier can be applied to different histologies. Strikingly, we found that this classifier predicts resistance to anti-PD1 treatment in metastatic TNBC as well as melanoma. In case of TNBC, we report an NPV as high as 0.9, which is not achieved with the currently used marker PD-L1. In fact, this classifier acts independently of PD-L1 (**Figure S5C**) and our observations imply that it would enable early identification of non-responders and facilitate decision-making of clinical oncologists with respect to treatment of TNBC patients with ICI; thereby preventing non-responding patients to receive ineffective and expensive treatment, and potentially challenging the diagnostic need for tissue stainings and training of pathologists.

In addition to the predictive value of spatial phenotypes, in the TONIC trial, we observed that proportions of inflamed phenotype increase following induction treatment with cisplatin and doxorubicin (**Figure S4E**), suggesting that spatial phenotypes show plasticity and non-inflamed phenotypes can be primed for treatment with ICI. In this regard,the distinct paths of T-cell evasion that characterize these phenotypes provide novel and actionable targets in order to prime for treatment with ICI (illustrated in **Figure 6**, and discussed below). In case of the excluded phenotype, we argue that inhibitors of TGFβ, such as the bifunctional anti-PDL-1 mAb/TGFβ trap M7824, and inhibitors of VEGF receptor kinases, such as cediranib, both being in clinical development for TNBC[266,267] and the latter being FDA-approved for other malignancies[268,269], can potentially prime for ICI. In case of the ignored phenotype, further developing blockers of the WNT pathway, such as WNT974 and/or drugs that target M2 macrophages, such as pexidartinib, a CSF1R inhibitor that depletes M2 macrophages are of interest, especially since these are currently being tested in TNBC[217]. The inflamed phenotype, being enriched in patients responding to anti-PD1 treatment, would be the phenotype of choice to start combination ICI treatment. In

case ICIs are not effective, this phenotype could potentially benefit from combining multiple ICIs or priming with CSF1R inhibitors that target M2 macrophages. Another actionable target for the inflamed phenotype could be the reactivation of type I/II IFN pathways, thereby re-boosting antigen presentation as well as recruitment and function of intratumoral CD8 T-cells[40]; to this end, an option could be the epigenetic drug decitabine that is approved for other indications and has shown promising results in preclinical studies of TNBC[270].

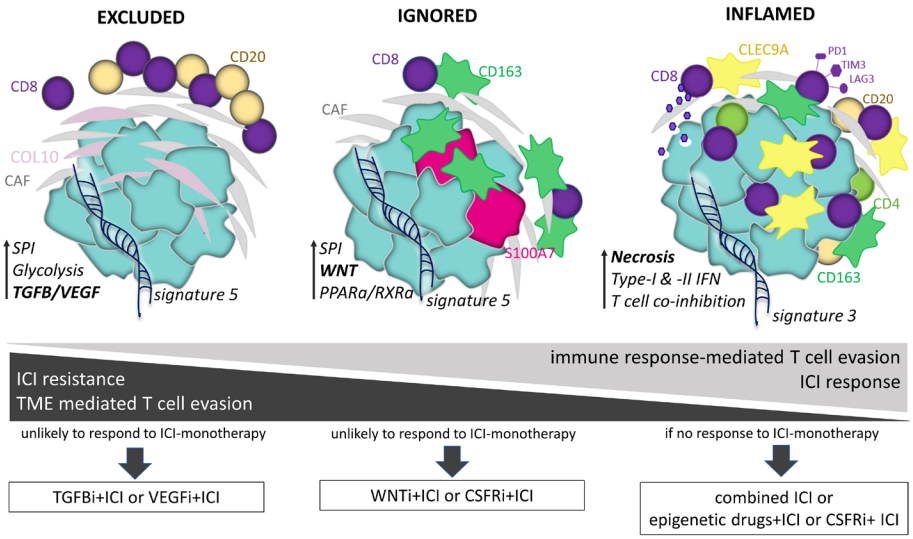

Figure 6. Illustration of immune contextures per spatial phenotype in relation to paths of T-cell evasion as well as response to ICI. Distinctive and dominant pathways (in bold), when targeted in an immunophenotype-specific manner (in boxes), would sensitize TNBC to ICI (see Discussion section for details).

The above-mentioned targets are part of larger immune networks that were revealed upon integrative analyses of TNBC samples using NGS and multiplexed IF. The charting of these larger networks enabled the identification of TME- and immune response-mediated paths of T-cell evasion and their relationship to ICI response. Following this approach, we observed that the excluded phenotype was characterized by CD4+, CD8+, CD20+ and CD56+ lymphocytes that were preferentially located at the tumor border at large distances from tumor cells. This phenotype had high expression of collagen-10, which is not present in normal tissues[271], is associated with epithelial-to-mesenchymal transition[272], as well as poor survival in TNBC and various other tumor types[273]. Recently, it has been suggested, based on collagen fiber density (not further specified) and in silico modeling of T-cell influx, that T-cell exclusion in TNBC is regulated by chemorepellents rather than barriers of extracellular matrix[274]. In contrast, our gene expression and in situ stainings (**Figure 4C,H,**

Figure 5A,B) strongly suggest that T-cell exclusion is due to collagen-10 deposition, possibly hinting towards a unique role of collagen-10 imposing a physical barrier to T-cell influx. Next to the collagen barrier, our data point to enhanced tumor cell glycolysis, which has been reported to suppress T-cell-mediated apoptosis of TNBC in vitro[275], and which may further promote T-cell exclusion. In addition, several serpins and other protease inhibitors, such as SERPINE1, SPINK1 and SLPI, demonstrated high gene expression. These enzyme inhibitors limit the activity of matrix metalloproteases or inactivate granzymes, thereby again potentially inhibiting T-cell influx or T-cell-mediated apoptosis of tumor cells[276]. All immune evasive pathways associated with the excluded phenotype are inter-related (**Figure S8B**) and strongly correlate to TGFβ and VEGF (**Figure 4E**) expression, which most likely represent upstream regulators that contribute to TME-mediated T-cell evasion. Interestingly, a study by Mariathasan and colleagues showed that T-cell exclusion in bladder cancer patients was attributed to stromal remodeling via TGFβ and revealed in a mammary mouse model that pharmacological blockade of TGFβ promotes T-cell inflammation[277].

The ignored phenotype was characterized by no or very low densities of CD8+ T-cells and either showed high expression of target genes of the WNT and PPARγ/RXR pathways or contained CD163+ macrophages and CD66b+ neutrophils. Activation of the WNT pathway promotes T-cell exclusion in bladder cancer[250] and melanoma, and in the latter, the mechanism has been attributed to failure of cDC1 recruitment[252]. In line with these data, we found inverse correlations between WNT pathway activity and presence of CLEC9A+ DC and CD8+ T-cells as well as TCR repertoire skewness. Also activation of the PPARγ/RXR pathway has been related to T-cell exclusion and resistance to ICI in bladder cancer[278], suggesting that the occurrence of both WNT and PPAR pathways are representative of pan-cancer mechanisms of TME-mediated T-cell evasion. Notably, we observed strong inverse correlations with either pathway and the abundance of CD163+ cells (**Figure 4F**), and argue that the presence of M2 macrophages represents a second immune escape mechanism within the ignored phenotype. Murine models of BC revealed that S100A7 expression induced M2 macrophage recruitment and promoted metastasis[262]. In the current study with patient materials, however, we found that numbers of S100A7+ tumor cells as well as CD163+ cells, located at the border, were positively correlated with MFS (**Figure S9G**) and (low) frequencies of CD8+ T-cells, arguing that recruitment of these myeloid cells is part of a negative feedback loop that follows an initial immune response.

Finally, the inflamed phenotype was characterized by high numbers of intratumoral CLEC9A+ DC and lymphocytes. The prognostic value of TILs was mainly attributed to T and B cells located in tumor regions, a finding that is in line with earlier observa-

tions showing that proximity to tumor cells is a pre-requisite for effective anti-tumor activity of lymphocytes[42]. The inflamed phenotype had a high TCR clonality independent of the level of neo-antigens and showed highest expression of genes associated with immunogenic cell death, type I/II IFNs and chemo-attractants. Interestingly, we observed that gene sets associated with necrosis, but not any other forms of cell death, strongly correlated with densities of CD8+ T-cells (**Figure S8C**), suggesting that immunogenic cell death may be a trigger of the cDC1-initiated adaptive immune response. Despite high numbers of DCs, TILs in the inflamed phenotype over-expressed genes encoding for various immune checkpoints and only a minority expressed ICOS or 41BB (**Figure 5F**). In fact, a large fraction of the inflamed phenotype showed genetic alterations in MHC-I (**Figure 3B**) and down-regulated expression of MHC-II by tumor cells (**Figure 5E**). All the above changes are inter-related (**Figure S8B**) and considered part of an immune response-mediated negative-feedback loop and may contribute to the relatively low frequency of sustained clinical responses to ICI even in the inflamed phenotype.

Our study has a number of limitations. For instance, the predictive value of our classifier is based on relatively small numbers of patients in a phase II trial. In addition, performance of the gene classifier in other tumor types requires validation with IHC. And lastly, the proposed spatial phenotype-specific treatments require functional and clinical validation.

In conclusion, patients with TNBC can be classified into three distinct spatial immunophenotypes that have prognostic value in this tumor type as well as other malignancies. These phenotypes, when captured by a gene classifier, predict response to anti-PD1 treatment in TNBC, and are accompanied by distinct T-cell evasive pathways. The excluded phenotype is characterized by a TGFβ-mediated program that prevents T-cells from reaching and/or killing tumor cells; the ignored phenotype is characterized by either a WNT-mediated program that results in complete lack of immune cells or a S100A7-mediated program that recruits M2 macrophages and blocks T-cell responses; whereas the inflamed phenotype is characterized by a program typical for an adaptive negative feedback loop, indicating that spatial phenotype-specific combination treatments could sensitize TNBC for ICI.

4.4 Materials and Methods

Cohorts of patients

Cohort A: Node-negative, primary TNBC from patients who did not receive adjuvant treatment. FFPE resection materials were used for whole tissue stainings for CD8+ (n=228), stainings for multiple immune cells/molecules on consecutive sections (n=30), multiplexed stainings for immune effector cells (n=64) and cells/molecules related to spatial phenotypes (n=69), microarray gene expression analysis (n=101, A1) as well as RNAseq data analysis (n=43, A2). Complete clinicopathological records were available with >10 year follow up (n=122).

Cohort B: Node-negative, primary BC from patients who did not receive adjuvant treatment (n=867 of which n=196 basal-like BC) with microarray data retrieved from gene expression omnibus GSE2034, GSE5327, GSE11121, GSE2990 and GSE7390. Details of combined cohort have been described previously[9].

Cohort C: Node-negative, primary BC from patients who did not reveive treatment with RNAseq and WGS data (n=347 of which n=66 TNBC)[233] accessible through European genome-phenome archive EGAS00001001178.

Cohort D: Metastatic TNBC from patients treated with anti-PD1 antibody in the TONIC-trial (n=53, of which n=44 paired samples)[218] with processed transcriptome data of pre- and post-induction treatment biopsies retrieved via controlled access (available through EGAS00001003535). Stromal TILs were scored independently by RS and HH, according to an accepted international standard from the International Immuno-Oncology Biomarker Working Group (see www.tilsinbreastcancer.org for all guidelines on TIL assessment in solid tumors). PD-L1 stainings (22C3 assay) were assessed independently by RS and HH and the percentage of positive tumor-infiltrating immune cells was scored.

Cohort E: TCGA data[279] as well as sample annotation data of TNBC were retrieved from the USCS xena browser (n=5194 of which 1284 BC of which in turn 137 TNBC). Transcriptome data of anti-PD1 pre-treatment biopsies from melanoma patients (n=28) or treated with anti-PD1 antibody (n=65) were retrieved from GSE-78220261and GSE91061260.

See **Table S1** and **Figure S1** for clinical details and application of these cohorts.

Ethics statement

This study has been approved by the Medical Ethical Committee at Erasmus MC (MEC.02.953), and was performed according to the Declaration of Helsinki and the "Code for Proper Secondary Use of Human Tissue in The Netherlands" (version 2002, update 2011) of the Federation of Medical Scientific Societies in The Netherlands (http://www.federa.org/), the latter granting authorized use of coded spare tissue for research.

Tissue stainings and image analysis

Immunohistochemistry (IHC): IHC stainings were performed on consecutive whole tissue sections (FFPE) following heat-induced antigen retrieval for 20 min at 95°C. After cooling to RT, staining was visualized by the anti-mouse EnVision+® System-HRP (DAB) (DakoCytomation). The following primary antibodies were used: CD8 (C8/C144B, Sanio, 1:100, pH 9); CD3 (PS1, Sigma, 1:25, pH 6); CD4 (4B12, DAKO, 1:80, pH 9), CD137 (BBK-2, Santa Cruz, 1:80, pH 6), CD278 (SP98, Thermo Fisher, 1:50, pH 9), CD66b (80H3, BIO-RAD, 1:100, pH 9), MECA-79 (C111-6, Santa Cruz, 1:50, pH 9), and MHC-II (LN3, Thermo Fisher, 1:50, pH 9).

Multiplexed immunofluorescence (IF): Multiplexed IF was performed using OPAL reagents (Akoya Biosciences) on whole slides (using a randomly selected subset of cohort A with comparable fractions of all spatial phenotypes). In brief, stainings included multiple cycles of: antigen retrieval (15 min boiling in antigen retrieval buffer, pH 6 or pH 9 depending on primary antibodies) followed by cooling, blocking, and consecutive staining with primary antibodies, HRP-polymer and Opal fluorophores; cycles were repeated until all markers were stained. Finally, nuclei were stained with DAPI.

Immune effector panel (number indicates position of primary antibody):

1. CD56 (MRQ-42, Sanbio, 1:500) – OPAL620; 2. CD3 (SP7, Sigma, 1:350) – OPAL520; 3. CD20 (L26, Sanbio, 1:1000) – OPAL650; 4. CD8 (C8/144b, Sanbio, 1:250) – OPAL570; 5. CD68 (KP-1, Sanbio, 1:250) – OPAL540; 6. Cytokeratin-Pan (AE1/AE3, Thermofisher, 1:200) – OPAL690; 7. DAPI.

Spatial phenotype panel (number indicates position of primary antibody):

1. CLEC9A (sheep polyclonal*, R&D Systems, 1:600) – OPAL570; 2. S100A7 (47C1068, Biotechne, 1:1000) – OPAL650; 3. CD11b (EP1345Y, Abcam, 1:200) –

OPAL690; 4. CD8 (C8/144b, Sanbio, 1:250) – OPAL540; 5. CD163 (MRQ26, Cell Marque, 1:50) – OPAL520, 6. COL10A1 (X53, Life Technologies, 1:50) – OPAL620; 7. Cytokeratin-Pan (AE1/AE3, Thermofisher, 1:200) – Coumarin; 8. DAPI.

* Sheep IgG VisUCyte HRP polymer (R&D Systems) was used as secondary antibody.

Manual scoring: IHC was scored for the frequency of CD8+ T-cells at the border (invasive margin, including ~50% tumoral area (tumor cells and stroma) and ~50% peritumoral area (no or only isolated tumor cellsand in the center (non-necrotic regions containing tumor and stroma) by DH and AMT, independently of each other (illustrated in **Figure S2A**). Spatial phenotype of CD8+ T-cells was determined using whole slide scans (Hamamatsu slide scanner) at 1x magnification and using at least 8 regions of interest at 20x magnification in border and center. Scoring criteria were as follows: inflamed: almost equal frequencies of CD8+ T-cells at the border and center; excluded: >10 times more CD8+ T-cells at the border compared to center; and ignored: hardly any CD8+ T-cells present at the border and center. All immune markers stained on consecutive slides were scored at 20x magnification (at border and center) and reported as percentage of positive cells (of total nuclei). TLS were identified as dense clusters of CD4+ T-cells and CD20+ B cells on consecutive slides (as shown in **Figure 1G**), whereas HEV were identified as vessels that were MECA-79 positive (frequently found in TLS), and both TLS and HEV were reported as total number per tumor.

Digital image analysis:Following whole slide scans using VECTRA 3.0 (Akoya Biosciences), at least 8 stamps (regions of interest; stamp size: 670x502 µm2; resolution: 2 pixels/µm2; pixel size: 0.5x0.5 µm2) were set in non-necrotic areas at the tumor border (containing 50% peritumoral region) and center (illustrated in **Figure S2B**). In case parts of the tissue were disrupted or lost due to repeated staining cycles, fewer stamps were set or tissues were excluded from analysis (the latter in case of <3 stamps at either border or center). Tissue-segmentation, cell-segmentation and phenotyping of individual cells was performed using Inform software, and enumerations at borders (tumor and stroma) and centers (umor and stroma) were summarized for all stamps per sample. Spatial phenotypes were determined according to median CD8+ T-cell density at border and center as follows: inflamed, >200 cells/mm2 at border and ratio between border and center <10; excluded, >200 cells/mm2 at border and ratio between border and center >10; ignored <150 cells/mm2 at border and center. All scans fulfilled either of these 3 spatial phenotypes.

Collagen-10 was identified through tissue seqmentation and quantified as collagen-10-positive tissue area. Nearest-neighbor analysis was performed in R using the PhenoptR package, to which end, the number of non-CD8+ T-cells within a 10 µm radius of CD8+ T-cells were calculated from the Inform-derived cell segmentation files in Phyton.

Gene expression and DNA mutational analysis

Data normalization: Microarray data were normalized using fRMA[231] and corrected for batch effects using ComBat. RNAseq data (cohorts A2, C, D E (TNBC)) were aligned with GRCh38 using the STAR algorithm (version 2.4.2a) and geTMM normalized[280] for DE analyses. For pan-cancer analyses (**Figure S6**) pre-processed data was used (i.e., TCGA other than BRCA: EB++Adjusted; and ICI-treated melanoma patients: FPKM normalized).

TCR repertoire, neo-antigen, and mutational signature analysis:TCR clonality was estimated using the MIXCR algorithm as described previously[9]; output was processed with tcR package in R and reported as TCR diversity (total number of TCR-Vβ reads per sample) and TCR repertoire skewness (Gini-Simpson index of TCR-Vβ reads per sample). Prediction of neo-antigens was performed with netCTLpan as described previously [9,149]. Identification of mutational signatures was described elsewhere[281].

Differential gene-, pathway- and immune cell subset analyses: Differential gene expression (DE) analysis was performed in R using limma/voom. Differentially expressed genes ($p<0.05$, $logFC>1$) were used for ingenuity pathway analysis (IPA software, core analysis). Spatial phenotypes were also interrogated for DE of gene-sets related to T-cell evasion[9]. Expression of a gene-set was determined as average expression of all genes in the respective set. Immune cell frequencies were estimated using the CIBERSORT algorithm in absolute mode.

Gene classifier to assign spatial phenotypes: In a discovery set (Cohort A1, n=101), we selected top differentially expressed genes between inflamed, excluded and ignored phenotypes (based on highest logFC between phenotypes and $padj<0.05$) of samples with microarray data and corresponding CD8+ T-cell stain-

ing data. Expressions for each classifier gene were averaged for each of the three spatial phenotypes, ranks of gene expressions were calculated per spatial phenotype, and assignments were based on highest Spearman rank-correlations between each unknown sample and ranked expressions of classifier genes per spatial phenotypes of the discovery set. In a validation set (Cohort A2, n=43), RNAseq data of independent samples with corresponding CD8+ T-cell staining data were used to assign phenotypes based on highest rank-correlations with the discovery set (A1), and yielded 81% accuracy with the following sensitivities/specificities: excluded, 1.00/0.72; ignored, 0.55/1.00; and inflamed, 0.80/1.00. Assignment to inflamed versus other phenotypes (either ignored or excluded) yielded 91% accuracy with the following sensitivities/specificities: inflamed, 0.80/1.00; and others, 1.00/0.91. Correct assignment of unknown samples from Cohort B (RNAseq data) was verified by comparison of T-cell characteristics, such as TCR-Vβ repertoire diversity and numbers of intra-tumoral T-cells, with those of Cohort A2 (RNAseq and CD8+ T-cell stainings), and the classifier-assigned samples were found non-different compared to those from the validation set (see **Figure S4A,B**). Clinical validation was done using metastasized lesions from TNBC patients treated with anti-PD1 antibody (Cohort D, pre-treatment), from which 3 out of 53 samples were excluded because of equally high rank-correlations. Assignment of spatial phenotypes in metastatic lesions did not depend on lesion site yet significantly different proportions (decreased frequency of inflamed, as expected) were observerved in the metastasized (cohort D) versus primary setting (Cohorts A1 and C) **(Figure S4D and E**). Predictive value of classifier gene-sets was determined by fitting ROC curves for different parameters; excluded and inflamed gene-sets were calculated as average scores of all respective genes, and PD-L1 and sTIL scores were scored as described before[218]. Responders (CR, PR, SD > 24 weeks) and non-responders (PD) were separated using the pROC package in R.

Statistical analysis

Statistical analysis was performed in R version 3.5.1 or GraphPad Prism 6. Log-rank test for trend was used to compare Kaplan-Meier curves; Cox-regression analysis was used to assess HR of cell types or gene-sets; and Logistic regression was used to determine OR of gene-sets (glm.OR function). Multiple testing correction was performed for differential gene-expression analysis using the Benjamini-Hochberg method. Kruskal-Wallis test was used to assess differences in gene expression and immune cell densities among spatial phenotypes; Pearson-correlation was used to assess linear relationships between continuous variables; and Chi-Square test or Fishers' exact test (in case of small sample sizes) were used to assess relationships

among factorial variables. The following significance levels were used: *, $p<0.05$; **, $p<0.01$; ***, $p<0.001$; ****, $p<0.0001$; NS, $p>0.5$.

Data availability

All WGS, RNAseq and microarray data are available at the European-Genome Phenome Archive and USCS Xena browser (see Supplementary Table 1 for details). All other code and data will be made available upon request.

Author contributions

DH and RD conceptualised and designed NGS and tissue staining experiments towards spatial immunophenotypes in TNBC. DH and MS designed and tested classifier of spatial phenotypes for various malignancies, TNBC and mTNBC treated with anti-PD1. DH wrote the main manuscript, and JM, MK and RD performed initial editing. DH, AM, RF, RW, and AT performed immune stainings; DH, AM, HH and RS performed histological scoring; DH, HB, AM, and RW performed image analysis; and DH, MS, and OI analysed bioinformatic data. JM, LV, IN and MK provided and discussed data. JM, MK and RD provided facilities and supervised the study. Finally, all authors edited and approved the manuscript.

Competing interests: Authors declare no competing financial interest.

4.5 Supplementary data

Cohorts	Cohort A	Cohort B	Cohort C	Cohort D	Cohort E
Tumor types and number of patients	n=228 TNBC	n=867 BC of which n=196 basal-like	n=347 BC of which n=66 TNBC	n=53 TNBC from phase II clinical trial (n=44 paired samples from metastatic lesions pre- and post-induction treatment)	n=1284 BRCA of which n=137 TNBC; n=477 SKCM; n=454 BLCA; n=877 LUAD; n=623 PRAD; n=567 HNSC; n=91 KICH; n=309 CESC; n=183 PAAD; n=329 COAD; n=93 anti-PD1 treated metastatic SKCM
Disease stage*	primary	primary	primary	metastatic	primary
Treatment*	none	none	none	anti-PD1 preceded by 2-weeks cisplatin (n=9); cyclophosphamide (n=12); doxorubicin (n=11); irradiation (n=10); or no induction (n=11) (for details see ref[218])	variable
Age (mean)*	52	53	54	51	58
Tumor size*	33% T1; 47% T2; 4% T3; 1% T4; 15% NA	39% T1; 60% T2; 0.5% T3; 0.5% T4	24% T1; 37% T2; 5%T3; 4% T4; 30% NA	NA	NA
Nodal status*	70% LN0; 16% LN+; 14% NA	100% LN0	45% LN0; 24% LN+; 31% NA	all M1	65% LN0; 35% LN+
Datasets	prognosis discovery: n=122 (LNN with clinical records >10 year follow up); gene classifer discovery: n=101 (microarray); classifier validation: n=43 (RNAseq); immune effector panel: n=64; spatial phenotype panel: n=69; IHC (multiple markers): n=30	prognosis validation: n=786 (microarray and clinical records)	genomic features: n=347 (WGS and RNAseq)	predicton: n=53 (RNAseq, PD-L1 staining, clinical records)	prognosis/prediction (RNAseq, clinical records, anti-PD1 response)
Determination of spatial immunophenotypes	CD8 stainings	gene-classifier	gene-classifier	gene-classifier	gene-classifier
Access	Datasets available upon request	GSE2034, GSE5327, GSE11121, GSE2990, GSE7390	EGAS00001001178	EGAS00001003535	https://xenabrowser.net/, GSE7822036, GSE9106135

Supplementary Table 1. Overview of study cohorts. Clinical features and access of the different cohorts. *characteristics for TNBC patients. **Abbreviations**: LN0: lymph-node negative; LN+: lymph-node positive; NA: not available; BRCA: breast cancer; BLCA: bladder cancer; SKCM: skin-cutaneous melanoma; LUAD: lung adenocarcinoma; HNSC: head and neck squamous-cell carcinoma; PRAD: prostate adenocarcinoma; PAAD: pancreatic adenocarcinoma; COAD: colorectal adenocarcinoma; CESC: cervical squamous cell carcinoma and endocervical adenocarcinoma; KICH: chromophobe renal cell carcinoma.

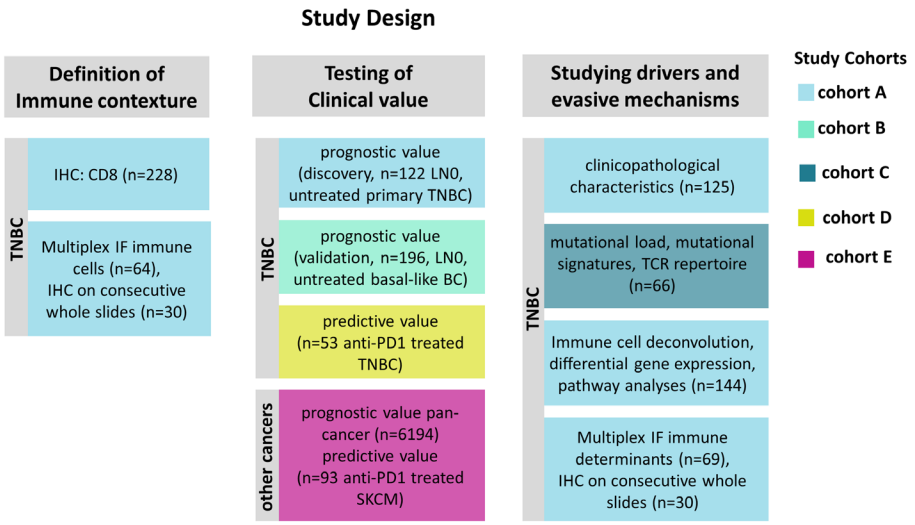

Figure S1. Study Design. Different steps and types of analyses regarding spatial immunophenotypes. Colors of boxes reflect the cohorts used for each step (for details and clinical characteristics of cohorts see M&M section and Supplementary Table 1). For cohort A spatial phenotypes were identified using IHC of CD8+ T-cells on whole slides and for cohort B-E spatial phenotypes were assigned using the gene-classifier.

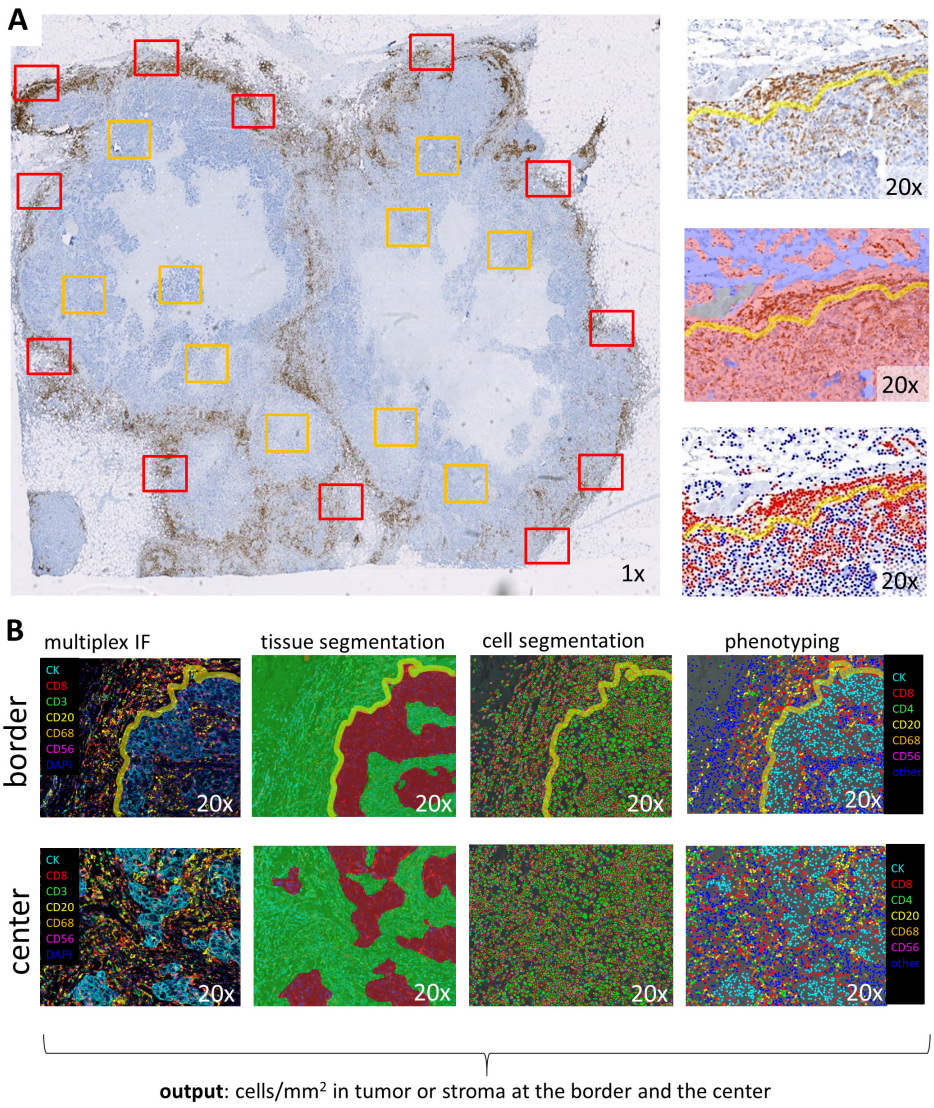

Figure S2. Workflow for digital image analysis of immune stainings. A. Whole slide images of CD8+ T-cell IHC with border and center stamps (regions of interest, red and yellow, respectively) with close-up (20x magnification) of one border stamp (top), separation of tissue (red) and empty space (blue) (middle) and identification of CD8-positive (red) and negative (blue) cells (bottom). Yellow line indicates outer tumor margin. **B**. Image analysis for multiplex IF of immune effector cell panel at border and center of an inflamed TNBC; from left to right: multicolour IF image, tissue segmentation (red: tumor; green: stroma; orange: empty space, yellow line: outer tumor margin); cell segmentation; and individually phenotyped cells (Inform software). Stamp size: 670x502 µm2; resolution: 2 pixels/µm2; pixel size: 0.5x0.5 µm2.

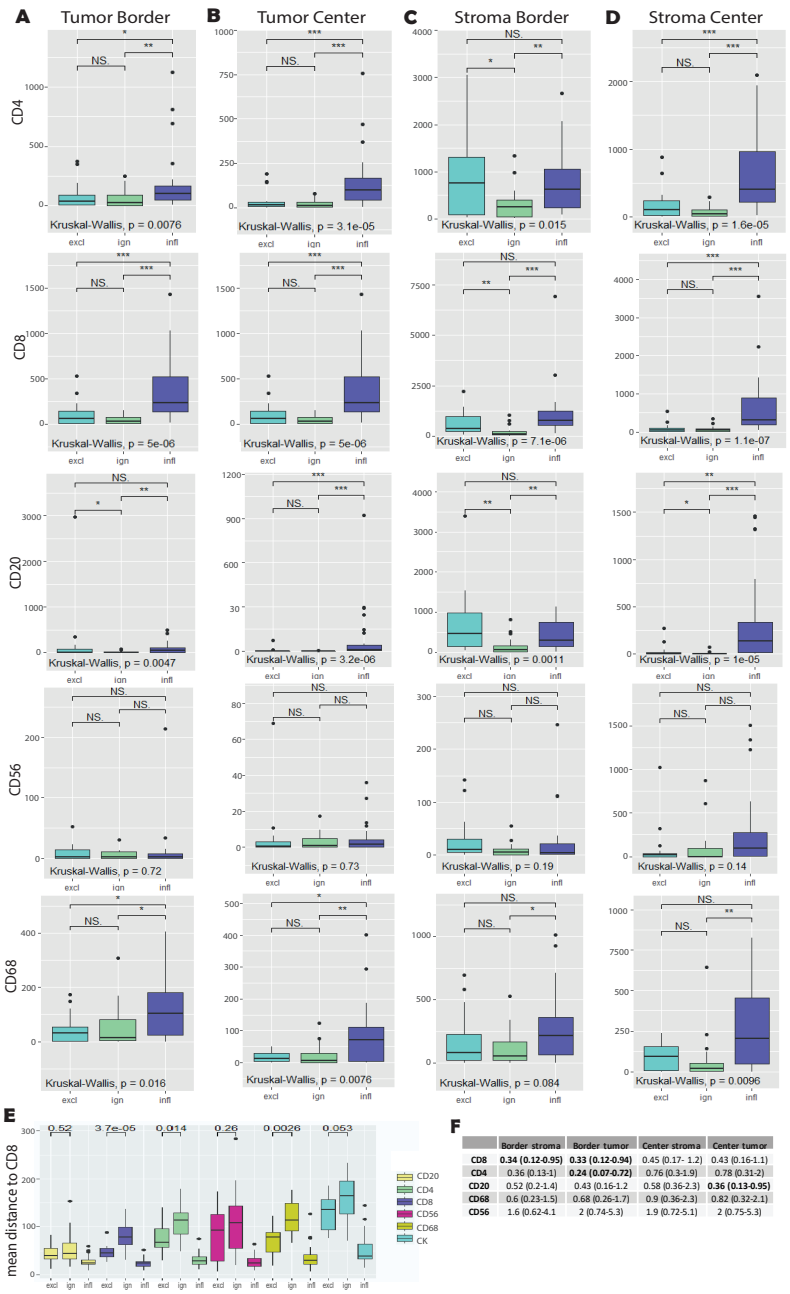

	Border stroma	Border tumor	Center stroma	Center tumor
CD8	**0.34 (0.12-0.95)**	**0.33 (0.12-0.94)**	0.45 (0.17- 1.2)	0.43 (0.16-1.1)
CD4	0.36 (0.13-1)	**0.24 (0.07-0.72)**	0.76 (0.3-1.9)	0.78 (0.31-2)
CD20	0.52 (0.2-1.4)	0.43 (0.16-1.2	0.58 (0.36-2.3)	**0.36 (0.13-0.95)**
CD68	0.6 (0.23-1.5)	0.68 (0.26-1.7)	0.9 (0.36-2.3)	0.82 (0.32-2.1)
CD56	1.6 (0.62-4.1	2 (0.74-5.3)	1.9 (0.72-5.1)	2 (0.75-5.3)

Figure S3. Immune effector cells according to spatial phenotypes in TNBC. Boxplots show cell densities (in cell number/mm2) following staining and analysis using immune effector panel. **A**. Tumor border. **B**. Tumor center. **C**. Stroma border. **D**. Stroma Center. **E**. Boxplots show mean distances between CD8+ T-cells and other cell types. F. Table with Hazard Ratios (HR) and 95% confidence intervals (CI, between brackets) for MFS of immune cell densities (significant HR values are shown in bold, analyses not corrected for multiple testing). Significant differences are: ***, p<0.001; **, p<0.01; *, p<0.05; NS, p>0.5.

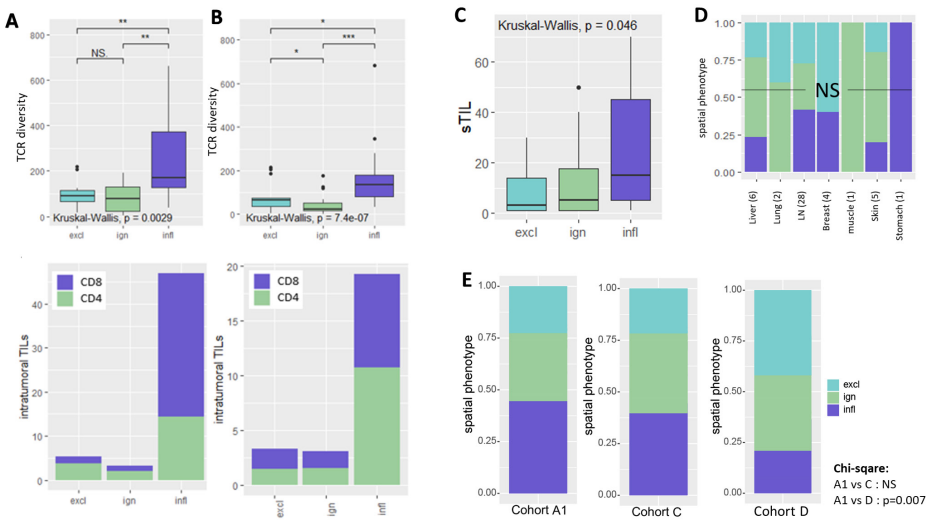

Figure S4. Spatial phenotypes according to CD8 staining and gene classifier are non-different with respect to TCR repertoire and presence of TILs. **A** and **B**. Diversity of TCR-Vβ read counts (top) and intra-tumoral T-cells (cells/mm2, bottom) of spatial phenotypes that were either based on CD8+ T-cell stainings (A, Cohort A2) or gene classifier (B, Cohort C). **C**. Stacked bar graphs show frequencies of spatial phenotypes assigned via gene classifier in different metastatic lesions (number indicates total number of lesions). **D**. Frequencies of spatial phenotypes in Cohort A1 (CD8 stainings, primary tumors), Cohort C (gene-classifier, primary tumors) and Cohort D (gene-classifier, metastatic lesions). **E**. Paired frequencies of spatial phenotypes pre- and post-induction treatments (number indicates a change to inflamed phenotype). Significant differences are: ***, p<0.001; **, p<0.01; *, p<0.05; NS, p>0.05. Abbreviations: cis: cisplatin; cycl: cyclophosphamide; dox: doxorubicin; irr: irradiation; none: no induction.

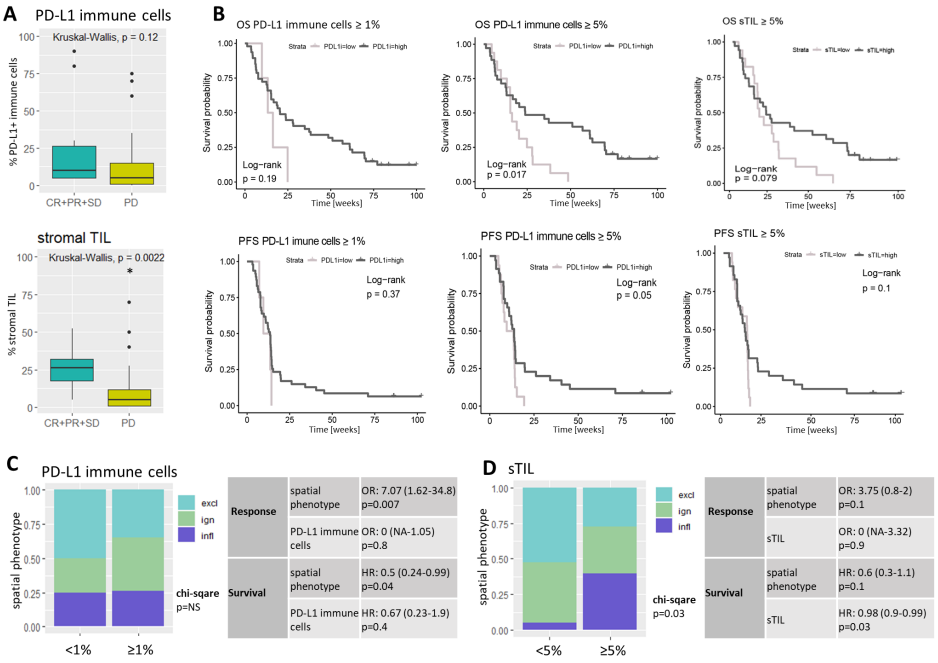

Figure S5. Standardly used predictive markers of ICI response in patients with metastatic TNBC. **A**. Boxplots show fraction of PDL1-positive immune cells (upper plot) and fraction of stromal TIL (sTIL) per response group (all Cohort D). **B**. Kaplan-Meier curves for OS and PFS with different cutoffs (≥1%, left) for PDL1 and sTIL (≥5%). **C**. Stacked bar graphs show frequencies of spatial phenotypes stratified by immune cell PD-L1≥1%; table shows spatial phenotypes and immune cell PD-L1 in multivariable models according to prognostic value (hazard ratio (HR), 95% confidence interval (CI) between brackets and p-value) as well as predictive value (odds ratio (OR), 95% CI and p-value). **D**. Stacked bar graphs show frequencies of spatial phenotypes stratified by sTIL≥5%; table shows spatial phenotypes and sTIL in multivariable models according to prognostic value (HR, CI and p-value) as well as predictive value (OR, CI and p value).

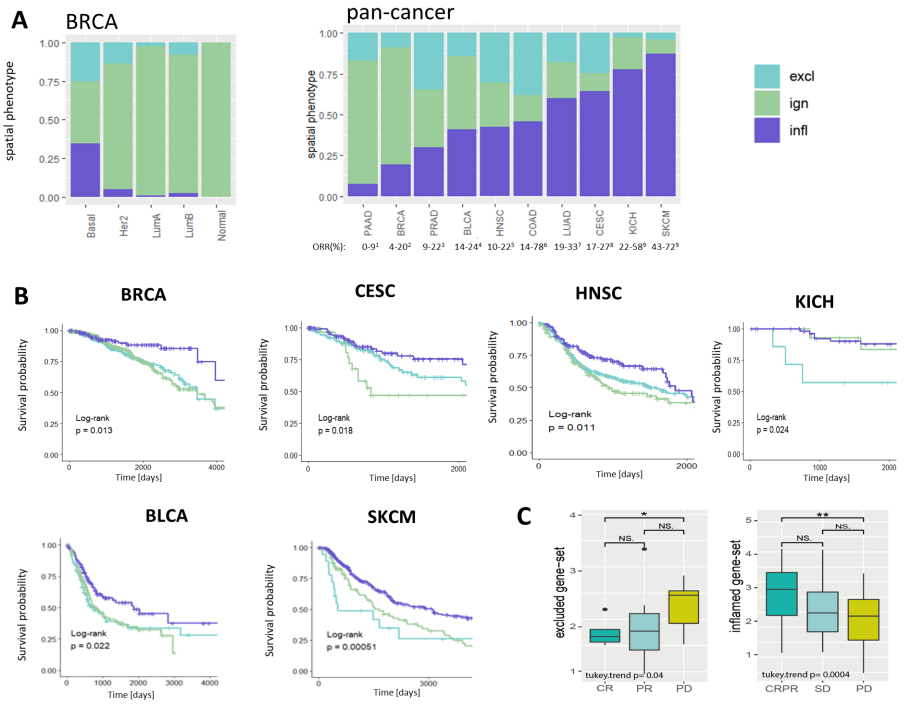

Figure S6. Spatial phenotypes in non-TNBC cancers. A. Stacked bar-graphs show frequencies of spatial phenotypes in different breast cancer subtypes (left, Cohort B) and various cancer types (right, Cohort E); below right panel objective respons rates (ORR) are listed for ICI treatments of respective cancer types (references listed below legend). **B**. Kaplan-Meier curves for OS stratified per spatial phenotype in various cancer types (Cohort E). **C**. Boxplots displaying average expression of gene-sets for the esxcluded as well as inflamed phenotype in responding and non-responding melanoma patients following ICI treatment (left, Hugo Cohort; right, Riaz Cohort). Significant differences are: **, p<0.01; *, p<0.05; NS, p>0.5. **Abbreviations**: PAAD: pancreatic adenocarcinoma; BRCA: breast carcinoma; PRAD: prostate adenocarcinoma; BLCA: bladder urothelial carcinoma; HNSC: head and neck squamous cell carcinoma; COAD: colon adenocarcinoma; LUAD: lung adenocarcinoma; CESC: cervical squamous cell carcinoma and endocervical adenocarcinoma; KICH: chromophobe renal cell carcinoma; SKCM: skin cutaneous melanoma.

References for ORR: 1: Henriksen et al., Can Treat Review, 2019; 2: Kwa et al., Cancer, 2018; 3: Fay et al., Ann Transl Med, 2019; 4: Olivia et al., Annals Oncol, 2019; 5: Kamatham et al., Cur Col Can Rep, 2019; 6: Kim et al., Invest Clin Urol, 2018; 7: Regzedmaa et al., Oncotargets Ther, 2019; 8: Liu et al., Frontiers Pharmacol, 2019; 9: Flynn et al., Ther Adv Med Oncol, 2019.

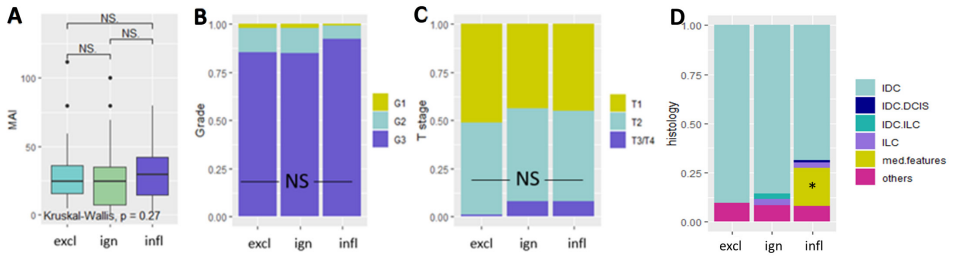

Figure S7. Clinicopathological features of spatial phenotypes. **A**. Mitotic activity index (MAI). **B**. Tumor grade. **C**. Tumor stage. **D**. Histological subtypes. Significant differences are indicated: *, p<0.5, NS, p>0.5. **Abbreviations**: DCIS: ductal carcinoma in situ; IDC: invasive ductal carcinoma; ILC: invasive lobular carcinoma; med. features: medullary features.

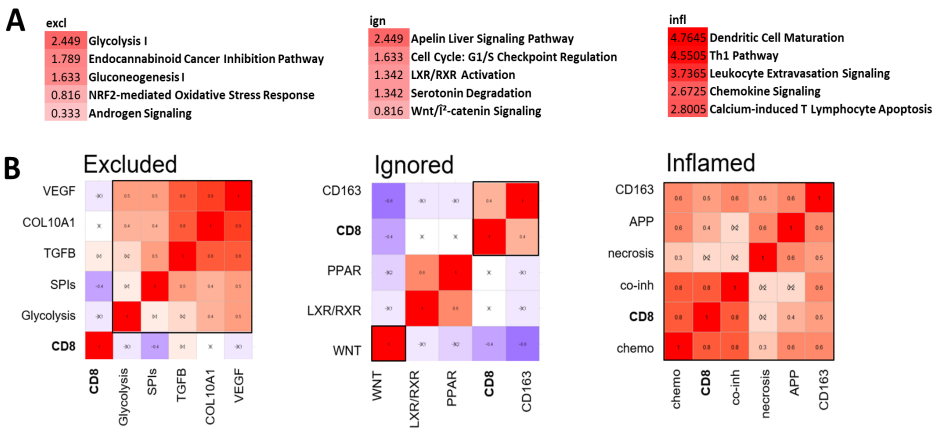

Figure S8. Immune determinants of spatial phenotypes and their inter-relationships in TNBC. A. Top differentially up-regulated canonical pathways per spatial phenotype (IPA, based on DE analyses). **B**. Correlation matrices of pathways in relation to CD8+ T-cells per spatial phenotype (Pearson-correlation; red: positive correlation; blue: negative correlation; crossed R-value: insignificant correlation).

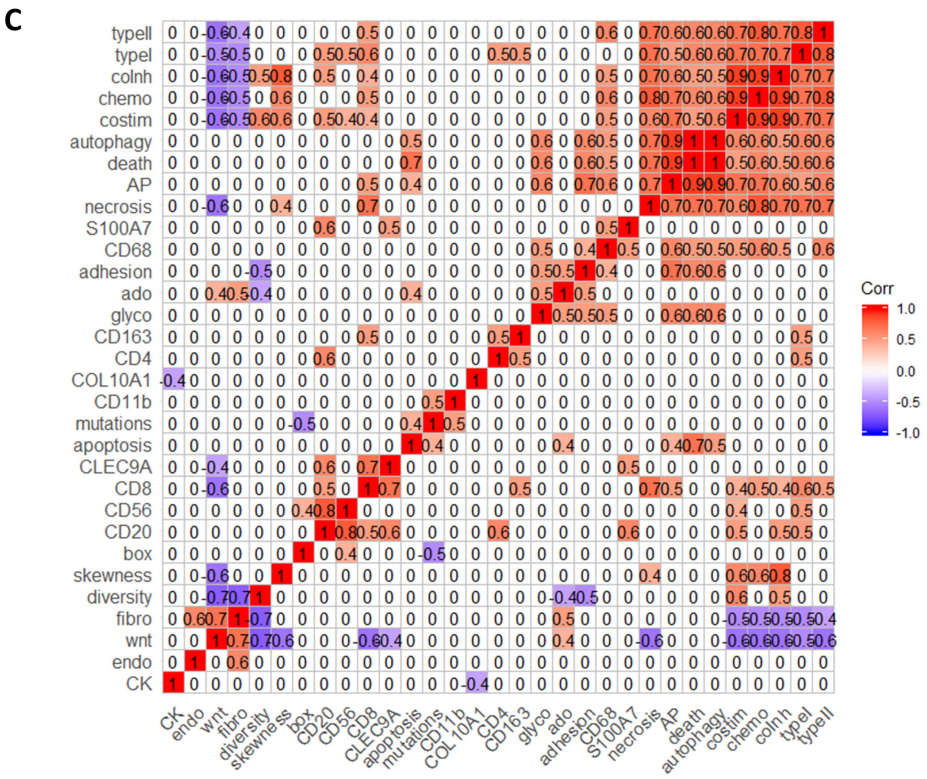

Figure S8C. Integrated correlation matrix of pathway and immune contextures of matched samples (n=30, cohort A; red: significant positive correlation blue: significant negative correlation; white = no correlation).

Abbreviations: SPI: serine protease inhibitor gene-set; CK; cytokeratin; endo: endothelial cell barrier gene-set; wnt: WNT-signaling gene-set; fibro: ffibroblast barrier gene-set; diversity: TCR repertoire diversity; skewness: TCR repertoire clonality (gini-simpson index); box: beta-oxidation gene-set; CD20: CD20+ B cells/mm2; CD8: CD8+ T cells/mm2; CLEC9A: CLEC9A+ DC/mm2; apoptosis: apoptosis gene-set; mutations: total number of expressed mutations; CD11b: CD11b+ cells/mm2, COL10A1: collagen-10 area, CD4: CD4+ T cells/mm2; Cd163: CD163+ cells/mm2; glycol: glycolysis gene-set; ado: adenosine signalling gene-set; adhesion: cell adhesion signalling gene-set; CD68: CD68+ cells/mm2, S100A7: S100A7+ cells/mm2, AP: antigen-processing and presentation gene-set, autophagy: autophagy gene-set; costim: T cell co-stimulation gene-set; chemo: T cell chemokine gene-set; coinh: T cell co-inhibition gene-set; typeI: type-I interferon gene-set; typeII: type-II interferone gene-set

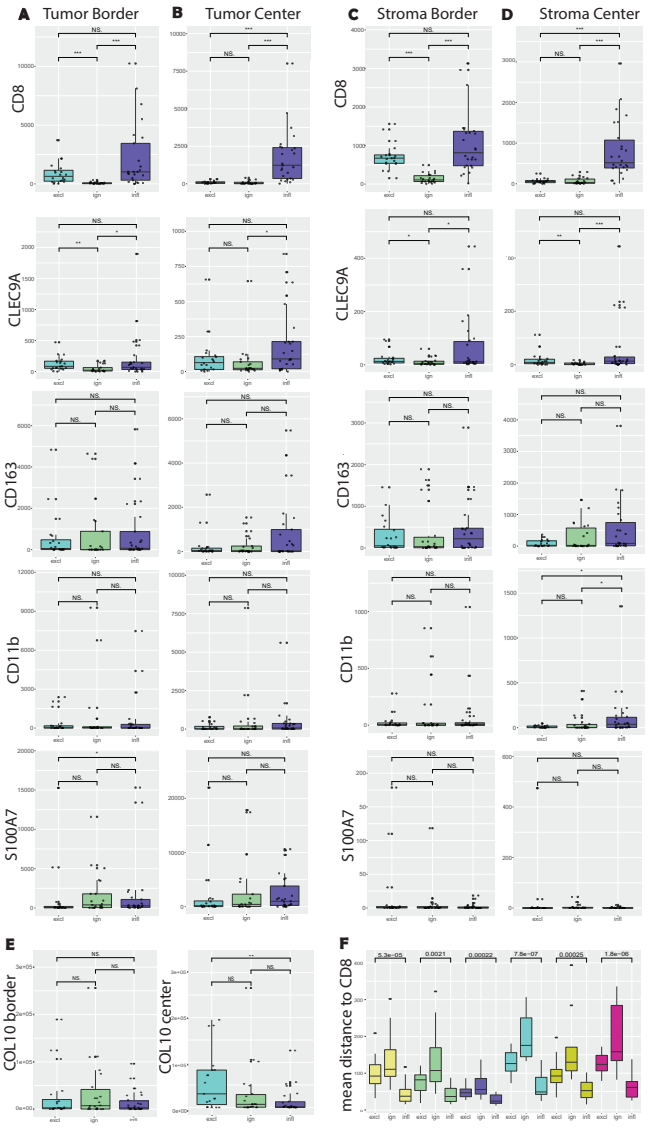

G

	Border stroma	Border tumor	Center stroma	Center tumor
CD8	0.42 (0.15-1.2)	**0.34 (0.12-0.98)**	0.46 (0.17-1.2)	0.46 (0.17-1.3)
CLEC9A	0.38 (0.13-1.1)	1.3 (0.5-3.5)	0.53 (0.2-1.4)	0.59 (0.23-1.6)
CD11b	0.69 (0.26-1.8)	0.48 (0.18-1.3)	0.46 (0.17-1.2)	0.5 (0.19-1.3)
CD163	0.51 (0.19-1.4)	**0.35 (0.12-1)**	0.37 (0.13-1.1)	0.71 (0.27-1.9)
S100A7	1.4 (0.52-3.6)	**0.26 (0.085-0.8)**	0.87 (0.33-2.3)	0.48 (0.18-1.3)

Figure S9. Immune determinants according to spatial phenotypes in TNBC. Boxplots show cell densities (cell number/mm2) following staining and analysis using spatial phenotype panel. **A**. Tumor border. **B**. Tumor center. **C**. Stroma border. **D**. Stroma Center. **E**. boxplots show collagen-10 area per phenotype. **F**. Boxplots show mean distances between CD8+ T-cells and other cell types. **G**. Table with Hazard Ratios (HR) and 95% confidence intervals (CI, between brackets) for MFS of immune cell densities (significant HR values are shown in bold, analyses not corrected for multiple testing). Significant differences are: ***, p<0.001; **, p<0.01; *, p<0.05, NS, p>0.5.

PART 2

Exploring new Targets for T cells

Chapter 5

Adoptive T Cell Therapy: New Avenues Leading to Safe Targets and Powerful Allies

Dora Hammerl[1], Dietmar Rieder[3], John W. M. Martens[2], Zlatko Trajanoski[3], and Reno Debets[1]

[1]Laboratory of Tumor Immunology, [2]Department of Medical Oncology, Erasmus MC-Cancer Institute, Rotterdam, the Netherlands; and [3]Division of Bioinformatics, Biocenter, Innsbruck Medical University, Innsbruck, Austria.

Trends in Immunology, 2018, DOI: 10.1016/j.it.2018.09.004

Abstract

Adoptive transfer of TCR-engineered T cells is a potent therapy, able to induce clinical responses in different human malignancies. Nevertheless, treatment toxicities may occur and, in particular for solid tumors, responses may be variable and often not durable. To address these challenges, it is imperative to carefully select target antigens and to immunologically interrogate the corresponding tumors when designing optimal T cell therapies. Here, we review recent advances, covering both omics- and laboratory tools that can enable the selection of optimal T cell epitopes and TCRs as well as the identification of dominant immune evasive mechanisms within tumor tissues. Furthermore, we discuss how these techniques may aid in a rational design of effective combinatorial adoptive T cell therapies.

Highlights

1) Novel algorithms that surpass the mere binding to HLA- I and integrate multiple immune parameters, including immunopeptidomes and TCR:peptide binding modes, are expected to accelerate the selection of valid target epitopes and corresponding TCRs for AT.

2) Immunophenotyping combining laboratory and in silico tools is required to assess and understand local T cell immunity, and where the tumor evades T cell control, and provide a rationale for combination AT.

3) In silico tools guide qualitative assessment T cell infiltration, antigen recognition and T cell function.

4) Advanced imaging techniques enable simultaneous acquisition on the spatial distribution of hundreds of (immune) markers and provide a detailed view of the tumor micro-environment.

5.1 Successes and Challenges of TCR-engineered T Cells

Adoptive T cell therapy (AT) refers to the infusion of tumor-reactive T cells that can recognize and kill malignant cells. AT requires T cells to be isolated from a patient, expanded and activated ex vivo, and re-infused back into the patient. This therapy, when using T cells with introduced genes encoding T cell receptors (TCRs), has already resulted in impressive clinical responses in a number of human malignancies, such as metastatic synovial sarcoma, melanoma and multiple myeloma [190,389]. Besides clear objective responses (OR: 55-80%), these studies demonstrated durable complete regressions (CR: 2-20%) [31].

While TCRs targeting the tumor antigen new york esophageal squamous cell carcinoma-1 (NY-ESO-1) have been proven successful without treatment toxicities, targeting melanoma antigen recognized by T cells 1 (MART-1) [284] or melanoma-associated antigen 3 (MAGE-A3) [30,375] has led to severe toxicities caused by recognition of cognate antigens (see **Glossary**) or highly similar antigens outside tumor tissues. In addition to side-effects, multiple clinical trials demonstrated variable therapeutic efficacy (OR and CR as low as 12% and 0%, respectively), which in case of solid tumors has been largely attributed to the suppressive nature of the tumor micro-environment (TME) [31].

In recent years, next-generation sequencing (NGS) techniques as well as those to detect and localize markers in tissues, have developed tremendously fast and yielded an overflow of valuable immune-genomic and proteomic data. These data, when analyzed with the appropriate and latest tools, enable researchers to address the above challenges of AT with TCR-engineered T cells. Here, we provide an overview of novel omics and laboratory tools, and discuss how to implement these tools to select truly tumor-specific epitopes and TCRs, as well as to detect tissue profiles and identify immune evasive mechanisms. Furthermore, we present a new strategy to define patient subgroups according to target epitopes, TCRs and immune evasive mechanisms to maximally sensitize the TME for T cells, while minimizing treatment-related toxicities and therapy resistance.

5.2 Avenues to Selecting Target Epitopes and TCRs

Target Antigens for AT: Not a Blind Choice

T cell target antigens should ideally be selected according to the following features: the ability to elicit a cytotoxic CD8 T cell (CTL) response; a high and homogeneous expression in the tumor but not in healthy tissues; and preferably shared by many patients. Numerous tumor antigens have already been tested in AT (includ-

ing those listed above), and despite being generally immunogenic and shared by many patients, only a small fraction of these antigens is truly tumor-selective (absent in healthy tissue) [286]. Among various tumor antigens, one can broadly distinguish between antigens that are shared and non-shared among patients. Shared antigens, such as those that are over-expressed, as well as differentiation antigens, are also expressed in healthy tissues, and targeting such antigens can result in severe on-target toxicities [287]. Cancer Germline Antigens (CGAs), even though generally considered to be tumor-selective, CGAs are not in all cases completely absent from healthy tissues [288]. In fact, only 60 of the 276 known CGAs are transcriptionally silent in normal human, non-germline tissues [152]. Non-shared neo-antigens, as well as a number of shared CGAs and oncoviral antigens, are tumor-selective (see for details 287). In this review, we focus on these last three classes of antigens as targets for TCR-engineered T cells. An overview of reported immune as well as clinical features of these classes of human antigens is given in **Table 1**.

Workflow for Target Antigen and Epitope Selection

Recent technical advances in NGS and 'omics' tools have facilitated selections of target antigens. In a first step, DNA and RNA sequencing of tumors and healthy tissues can enable the identification as well as expression analysis of antigens. Identification of potential neo-antigens requires comparison of DNA changes identified in tumor- with matched normal samples. Identification of oncoviral antigens requires mapping of DNA against the gene information broker for viruses (GIB-V) database [289]. Besides the use of NGS data, CGA expression in tumors and healthy tissues can also be analyzed by the use of gene expression platforms or public databases, such as the Cancer Genome Atlas (TCGA) [279] or the Expression Atlas [290]. In extension to NGS and gene expression data, we recommend verifying antigen expression in tumors as well as absence in healthy tissues by quantitative PCRs and, whenever possible, via immunohistochemistry.

In a second step, candidate epitopes (from the selected target antigens) can be predicted in silico. In general, human leukocyte antigen (HLA) class I epitopes are 8-11 amino acids long, and their immunogenicity depends on the level of expression as well as efficiency of processing and presentation, while the latter events in turn, can depend on: proteasomal cleavage; post-proteasomal trimming; binding affinity for transport associated proteins (TAP, required for epitope loading onto HLA); and binding affinity for HLA [291]. In silico prediction requires the integration of various computational tasks and the proposed workflow for selecting tumor-specific epitopes is illustrated in **Figure 1A**. This workflow starts with typing of restrictive HLA elements;

at the moment, there are 22 different algorithms for HLA-typing which can be used for mapping sequencing reads against the ImMunoGeneTics (IMGT-HLA) database (https://omictools.com/hla-typing-category). For instance, HLA-miner, POLYSOLVER, seq2HLA, and OptiType can be used for NGS-data, whole exome sequencing (WES) data as well as RNA sequencing (RNAseq) data. Next, the prediction of antigen-processing and presentation is covered by numerous algorithms that assess different parameters of epitopes, including the occurrence of proteasomal cleavage sites (NetChop), the binding affinity for HLA-I (MSIntrinsicMC, NetMHC, SYFPEITHI, RANKPEP), and the binding affinity for TCR (Repitope). Finally, prediction of HLA affinities of identical and highly similar epitopes (e.g. using Expitope 2.0 [292] and the SysteMHC Atlas [293]) should be performed to limit risks of toxicities[294].

Most of the above epitope selection algorithms capture binding to common HLA alleles quite accurately, yet have been less trained for antigen processing and presentation of native epitopes (see **Table 2** for a comprehensive list of algorithms). In fact, the presence and immunogenicity of only a minority of predicted epitopes has been validated in vivo, which may, in addition to suboptimal epitope prediction or lack of high-throughput methods to detect low frequencies of epitope-specific T cells, be due to immune editing[295]. Of note, currently available tools cannot yet predict faithfully HLA-II-restricted epitopes due to the lack of training data.

Recently, a number of NGS-based pipelines for in silico prediction of neo-epitopes with different degrees of functionality have been developed [296]. These include newer and potentially improved algorithms that incorporate additional parameters, such as: RNA expression levels[297]; TCR-peptide interaction[298,299]; and the modelling of immunological fitness of tumor antigens[300]. In addition to these in silico developments, progress in the fields of immunopeptidomics and TCR structure might further enhance predictions of peptide presentation and recognition. For example, mass spectrometry (MS)-based methods can nowadays deliver and identify sequences of a significant part of the entire proteome within a few days, which allows high throughput measurements of natively presented peptides[297,301,302]. Upon immune precipitation of HLA molecules and subsequent sequencing of eluted peptides, one can measure the immunopeptidome of tumors or antigen presenting cells (APCs)[303]. At present, the large number of cells required for MS methods still presents a limitation. Moreover, studies of TCR structure, currently covering 345 crystal structures of human TCRαβ's (www.rcsb.org/pdb) and increasing numbers of molecular-dynamics simulations, have increased our knowledge of TCR-peptide binding modes and common structural motifs[304,305]. These binding modes and structural motifs may aid the future creation of homology models of newly sequenced TCRs and the prediction of peptide specificity based on molecular docking rules[306].

		neo-antigens	oncoviral antigens	cancer germline antigens
Immune features (pre AT)	Naturally eliciting a T cell response	Yes [199,200]	Yes [364]	Yes [200,288]
	Frequency of expression/sharing in tumor	most frequent: KRASG12C (2.8% across all cancers) [365] <0.003% shared in more than 5% patients [336]	HPV: 5% of all cancers [364] HTLV: 10% of HTL [366] EBV: 95% of NPC (1.5% of all cancers) [367]	NY-ESO-1: 80% of SCC; 20-35% of NSCLC; 42% of BC [368] MAGE-A3: 33% of NSCLC [369] MAGE-C2: 40% of met melanoma, 20% of HNSCC; 30% of ER- BC; 15% of Bladder cancer [370]
	Tumor selectivity	yes	Some [371]	Some [288]
Clinical features (post AT)	TAnti-tumor response	Neo-antigen T cells: case reports in melanoma and cholangiocarcinoma [372]	HPV TILs: 30% OR in cervical cancer [373] EBV T cells: 63% OR in NPC [355]	NY-ESO-1 TCR T cells: 55% OR in met melanoma; 61% in SS; 80% in MM [190] MAGE-A3 TCR T cells: 55% OR in melanoma [374]
	Treatment toxicity	none	None 373	NY-ESO-1: none [283] MAGE-A3: neurologic and cardiac toxicities [30,285]
	Immune editing	recurrence of mutation-negative tumors [375]	occurrence of escape mutations [376]	recurrence of antigen-negative tumors [283]

Table 1. Three Classes of T Cell Target Antigens: Immune and Clinical Features. **Abbreviations**: BC: breast cancer; EBV: Epstein-Barr Virus; HPV: Human Papilloma Virus; HTLV: Human T-Lymphotropic Virus; met: metastasized; MM: multiple myeloma; NPC: nasopharyngeal carcinoma; NSCLC: non-small cell lung cancer; SCC: squamous cell carcinoma; SS: synovial sarcoma.

Workflow for TCR Selection

Once epitopes have been selected, the next step is to obtain corresponding TCRs. One can obtain TCRs either from autologous patients' tumor infiltrating lymphocytes (TILs) or from naïve T cells derived from HLA-matched healthy donor peripheral blood mononuclear cells (PBMCs). The latter represents a viable source of T cells that have been observed to recognize more predicted epitopes compared to autologous TILs [307], possibly as a result of a less skewed TCR repertoire. Various in vitro protocols to acquire epitope-specific T cells have been established and generally include several rounds of stimulation with autologous- or artificial APCs that are loaded with an epitope or transfected with a minigene (harboring epitopes), followed by fluorescence-activated cell sorting of T cells binding to epitope-MHC multimers [31]. Recent advances in single cell RNA sequencing (scRNA-seq) as well as numerous algorithms for read-mapping (scTCRseq, TRAPeS) have enabled the identification

of reproductive TCRαβ sequences, i.e., TCR sequences harboring complete V(D)J rearrangements, from single cells [308]. Such methods are not only fast but can also inform on the correct pairing of TCRα and β chains. The capture of single cells and reading depths of 500k, which are required for full recovery of reproductive TCR sequences [309], however, may pose a financial burden. Subsequently to the acquisition of TCR sequences, these are cloned and inserted into donor T cells. For this purpose, retro- and lentiviral vectors have already proven useful and safe tools with clinical precedence [310].

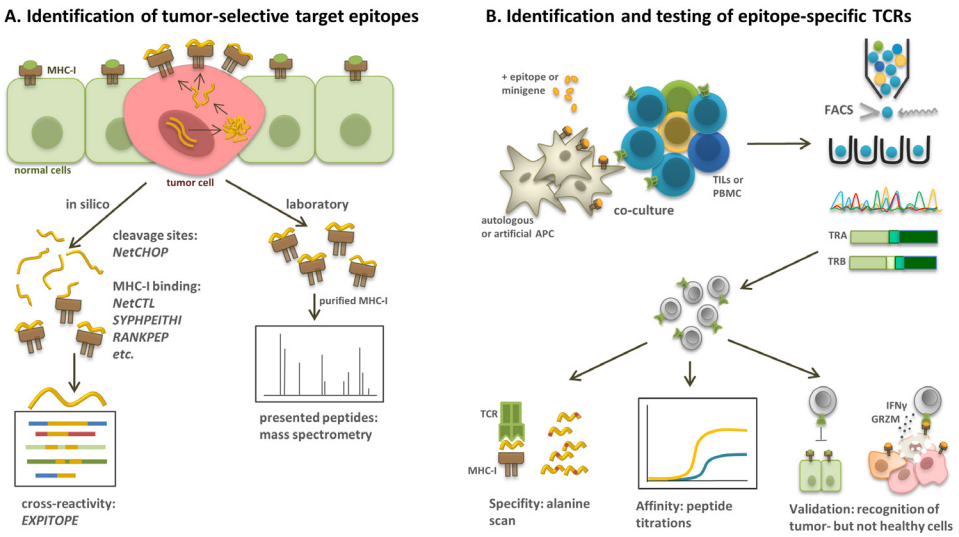

Figure 1. Selection of Target Epitopes and Corresponding T Cell Receptors. A. Workflow for epitope selection: Identification of immunogenic epitopes (yellow peptides) is accomplished using either in silico tools (left path, example tools in italic) for the prediction of HLA alleles, antigen processing and presentation, and cross-reactivity, or laboratory tools, such as mass spectrometry for the collection and analysis of HLA-presented epitopes (right path). **B**. Workflow for the identification and testing of TCRs: includes enrichment of epitope-specific T cells using epitope-loaded APCs, followed by FACSort of TCR positive cells (with epitope-MHC-multimers) and subsequent sequencing of TCR genes. TCR genes can then be cloned into donor T cells and tested for their specificity, affinity (e.g. alanine scan) and recognition of endogenously processed and presented epitopes. **Abbreviations**: APC: antigen presenting cell, FACS: fluorescence-activated cell sorting, IFNγ: interferon gamma, GRZM: granzyme B, MHC-I: major histocompatibility complex-I, PBMC: peripheral blood mononuclear cells, TCR: T cell receptor, TRA: T cell receptor alpha gene, TRB: T cell receptor beta gene.

In addition, TALEN or CRISPR-mediated gene editing may enable the replacement of endogenous TCRs by transgenes [311]. Such gene replacement can result in increased and more homogenous surface expression of TCR transgenes, while reducing mispairing with endogenous TCRs, thereby inducing a potent anti-tumor

Tool	parameter(s) tested	output	source
NetChop [376]	occurrence of c-terminal proteasomal cleavage sites	cleavage sites in FASTA sequence including probability score	http://www.cbs.dtu.dk/services/NetChop/
NetMHC [291]	-binding affinity for common HLA alleles	nanomolar affinity score for HLA allele	http://www.cbs.dtu.dk/services/NetMHC/
SYFPEITHI [377]	-epitopes and anchor residues for common HLA alleles	ranked binding score	http://www.syfpeithi.de/
RANKPEP [378]	-binding affinity for common HLA alleles -immune dominance (based on: peptide processing, MHC stability and TCR binding) -proteasomal cleavage sites -masking of sequence variability regions (i.e., mutational hotspots in virus)	integrated score and molecular weight	http://imed.med.ucm.es/Tools/rankpep.html
p-Vac-seq [379]	-MHC affinity of wild type and mutant epitopes -Filtering based on affinity score -Filtering based on RNA expression levels	neo-epitopes	Script available https://github.com/griffithlab/pVAC-Seq.
MuPeXi [380]	-Identification of mutated peptides -Similarity to wild type peptides -Binding affinities for common HLAs -Filtering based on RNA expression	Ranked neo-epiopes with annotation, HLA-affinity score and silmilarity to wild type epitope	http://www.cbs.dtu.dk/services/MuPeXI/
TIminer [381]	-Identification of neoantigens - expression of neoantigens -HLA typing and binding	neo-epitopes	Script available http://www.compbio.at/software/timiner/doc/
Fitness model [300]	-neoantigen expression -neoantigen clonality -binding affinities of mutant and wild type epitopes for common HLA alleles	neo-antigen fitness score	script available https://github.com/andre-wrech/antigen.garnish/tree/master/inst
Expitope [292]	-gene expression of antigen in healthy tissue -binding affinity for common HLA alleles -homology with self-epitopes	expression levels in healthy tissues and nanomolar affinity score for HLA allele of similar epitopes	http://webclu.bio.wzw.tum.de/expitope2/
MSIntrinsicEC [297]	-gene expression of antigen -MS peptide elution from HLA alleles -proteasomal cleavage sites	native presentation score	currently not publicly or commercially available
Reptiope [298]	-binding affinity for TCR based on amino acid contact profiles	immunogenicity score	R package https://github.com/masato-ogishi/Repitope/blob/master/R/TCRAnalysise_FastQDump.R

Table 2. Examples of Algorithms for Epitope Prediction. **Abbreviations:** HLA: Human leukocyte antigen; MHC: major histocompatibility complex; MS: Mass spectrometry, TCR: T cell receptor.

response and limiting potential off-target toxicities [312,313] without the need of viral vectors [314]. Finally, once the T cell product has been generated, we recommend a series of in vitro assays to assess efficacy and safety of the TCR T cell product prior to clinical implementation. Such assays [287], can include: an amino acid scan to determine the TCR's recognition motif; screens against allo-alleles and peptides eluted from the corresponding HLA allele to exclude cross-reactivity; titrations of cognate peptide to determine the TCR T cell's avidity; and T cell assays using tumor and healthy cells to validate recognition of endogenously presented peptides. The workflow for selecting epitope-specific TCRs is illustrated in **Figure 1B**.

5.3 Patient Stratification According to Local T Cell Immunity

Antagonizing Immune Suppressive TMEs: Not a Blind Choice Either

Solid tumors are not only heterogeneous with respect to antigen expression but also with respect to numbers, location and activation state of intra-tumoral T cells. Local T cell immunity is determined by multiple parameters and may provide predictive value of responsiveness to AT, that goes beyond markers of mere tumor antigenicity or mutational load. Parameters capturing local T cell immunity may include: influx and migration of T cells; antigen recognition by T cells; and/or function of T cells. These three categories may be defined by unique immune markers, and recent advances in in silico- and microscopy tools are expected to significantly boost immunophenotyping of tumors, and enable rational selections for co-treatments aiming to enhance efficacy of AT.

Influx and Migration of T Cells: The presence and intra-tumoral location of CD8 T cells can be considered as measurement of general immunogenicity of tumors as well as the ability of these cells to infiltrate the tumor. Vice versa, absence of CD8 T cells may either indicate a lack of immunogenicity or the presence of barriers that could hinder the infiltration of (adoptively transferred) T cells. Important for the recruitment of T cells are inflammatory chemokines, and while many chemokines may be present in the TME, the interferon (IFN)-inducible and epigenetically regulated C-X-C motif chemokines CXCL9 and CXCL10, which recruit CXCR3-positive CD8 T cells [317], may be of particular relevance to the AT setting. Notably, in a mouse model for spontaneous melanoma, basic leucine zipper ATF-like transcription factor 3 (BATF3)-dependent dendritic cells (DCs) were a major source of CXCL9 and CXCL10 and BATF3 gene knock-out abolished recruitment of adoptively transferred T cells [264]. In addition, the density of specialized vessels, such as high endothelial

venules (HEV), was found to correlate with numbers of TILs in human breast cancer [318], and these HEVs, which are equipped with adhesion molecules such as vascular cell adhesion molecule 1 (VCAM1), P-Selectin and E-Selectin [319], contribute to trans-endothelial migration of T cells into tumors. Of note, tumor endothelial cells with down-regulated surface expression of adhesion molecules, mediated for instance via vascular endothelial growth factor (VEGF), can inhibit trans-endothelial migration of T cells, whereas up-regulated surface expression of FAS ligand (FASL) on tumor endothelial cells (via anti-inflammatory mediators, such as interleukin (IL)-10) can lead to killing of FAS-expressing effector T cells ex vivo [320]. Moreover, infiltration and migration of T cells can be compromised by the collagen-density and structure of the extracellular matrix (ECM), which can provide a physical barrier to T cells, as evidenced by real time imaging of human T cells in lung and ovarian cancer [321]. ECM-mediated T cell exclusion has been attributed, at least in part, to an increased activity of cancer-associated fibroblasts (CAFs) and their production of cytokines, such as transforming growth factor beta (TGFβ) and IL6, since levels of which inversely correlated to the presence of TILs in urothelial cancer patients treated with anti-PDL1 antibody [277] and a mouse model of colon cancer, respectively.

Antigen Recognition by T Cells: A crucial factor contributing to efficient tumor clearance by CD8 T cells is antigen expression, processing and presentation. Down-regulation or loss of function (LOF) mutations in components of the antigen presentation pathway have been shown to be a major resistance mechanism to immune therapies, including AT in various human malignancie. LOF mutations frequently occur in (but are not limited to) B2M, TAP1 or HLA genes. In fact, a CRISPR-Cas 9 genome-wide screen in human melanoma cells pointed to antigen presentation and IFNγ-signaling being critical for effector functions of TCR-engineered T cells in vitro [324]. Interestingly, another study also demonstrated that LOF mutations in the novel marker APLNR (a G-protein coupled apelin receptor involved in JAK/STAT signaling) were present in human melanoma, which were refractory to immune therapies, and that knocking out the APLNR gene in mice resulted in enhanced melanoma tumor growth following AT with TCR-engineered T cells [325]. Besides gene mutations, epigenetic alterations represent another cause of limited type-I and type-II IFN signaling and decreased tumor immunogenicity, a notion that is supported by the observation that ablation of the histone demethylase LSD1 in mouse melanoma resulted in enhanced IFN signaling and CD8 T cell infiltration, and that expression of LSD1 in various human malignancies is inversely correlated with presence of CD8 TILs [326]. Yet another way to escape from antigen recognition by T cells is immune editing, where tumor relapse following AT is characterized by outgrowth of antigen-negative tumor

cell clones (for references, see **Table 1**).

Function of T Cells: The TME is often nutrient-deprived and hypoxic which can adversely modulate T cell development and function. For example, hypoxia and its downstream metabolites can reduce T cell proliferation and effector functions while increasing the expression of co-inhibitory receptors on T cells [327]. Moreover, hypoxia can induce the accumulation of extracellular adenosine, which in turn can promote tumor cell proliferation and metastasis, and inhibit the function of immune effector cells, including CD8 T cells [328]. Furthermore, increased glycolysis in tumor cells, as a result of the metabolic switch that can occur under hypoxic environments, or as a consequence of mutations in the phosphatase PTEN (pathway recognized for its contribution to cellular metabolism), has been found to limit the cytolytic capacities of T cells in vitro and to correlate with resistance to AT with TILs in melanoma and non-small cell lung cancer patients [215]. In extension, immune-compromised mice transplanted with human melanoma cells that lack PTEN, and show enhanced PI3K/AKT activation, revealed decreased T cell trafficking into tumors and resistance to CTL-induced apoptosis of tumor cells following AT with TCR engineered T cells [163]. Also, increased WNT/β-catenin signaling adversely affects numbers of TILs in melanoma patients, with the underlying mechanism being studied in mouse models of spontaneous melanoma and attributed to decreased CCL4 expression by tumor cells, impaired DC recruitment, and T cell priming [329]. From another angle, DCs expressing co-stimulatory ligands, such as, CD80, CD86, CD275 and CD252 can activate CD8 T cells in tumors [330]. In particular, a study with mouse breast cancer-derived BATF3 DCs demonstrated that these cells efficiently cross-present antigen and provide co-stimulation when compared to conventional DC in vitro, and a study with a mouse melanoma model demonstrated that BATF3 DCs are crucial contributors to T cell priming and anti-tumor T cell activity in vivo [59]. Moreover, DCs producing pro-inflammatory mediators such as nitric oxide have been found to accumulate in murine melanoma following AT, cross-present tumor antigens and activate CD8 T cells via CD40-CD40L interactions [332]. In fact, NOS2 and CD40LG gene expression correlated with survival in colorectal cancer patients [332]. By contrast, tumor cells, CAFs, M2 macrophages or myeloid-derived suppressor cells (MDSCs), have been reported to downregulate co-stimulatory ligands and upregulate co-inhibitory ligands such as programmed death-ligand 1 (PDL1), herpesvirus entry mediator (HVEM), and CD155, often leading to T cell dysfunction, which has generally been assessed in ex vivo co-cultures of mentioned cell types and T cells, or in situ stainings of different human malignancies. In addition, soluble factors released by tumor cells and immune suppressor cells, such as TGFβ and indoleamine 2,3-dioxygenase-1

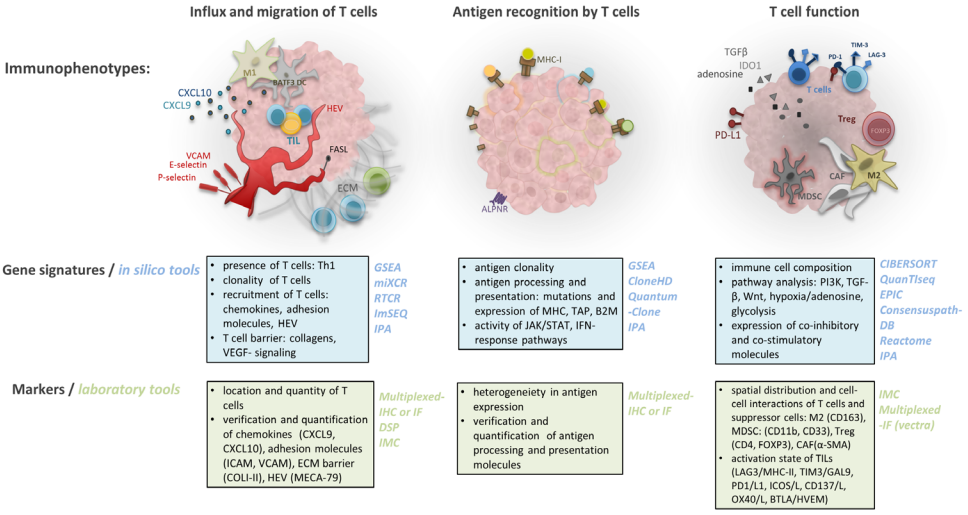

Figure 2. Charting Immune Micro-Environments Using In Silico and Laboratory Tools. Schematic illustration of immune evasive mechanisms. Immunophenotyping of tumors should include the evaluation of markers that predict: (1) influx and migration of T cells; (2) antigen recognition by T cells; and (3) the ability of T cells to sustain anti-tumor function. **Abbreviations**: α-SMA: alpha smooth muscle actin; APLNR: apelin receptor; BATF3 DC: basic leucine zipper ATF-Like transcription factor 3-positive dendritic cell; BTLA: B- and T lymphocyte attenuator; CAF: cancer associated fibroblast; CD: cluster of differentiation; CXCL9/10: chemokine (C-X-C motif) ligand 9/10, ECM: extracellular matrix; FASL: Fas ligand; FOXP3: forkhead box P3; GAL9: galectin-9, HEV: high endothelial venules; HVEM: herpesvirus entry mediator; ICAM-1: intercellular adhesion molecule 1; IDO-1: indoleamine 2,3-dioxygenase; LAG-3: lymphocyte activation gene 3; M1: M1 macrophage; M2: M2 macrophage; MDSC: myeloid derived suppressor cells; MHC: major histocompatibility complex; OX40: tumor necrosis factor receptor superfamily, member 4, PD-1: programmed cell death protein 1; PD-L1: programmed cell death protein 1 ligand; PI3K: phosphatidylinositol-3-kinase; TAP: transport-associated protein; B2M: beta-2-microglobulin; TGFβ: transforming growth factor beta; TIL: tumor infiltrating lymphocytes; TIM-3: T-cell immunoglobulin and mucin-domain containing molecule-3; Treg: regulatory T cell; VCAM-1: vascular cell adhesion protein 1; VEGF: vascular endothelial growth factor; WNT: wingless-type MMTV integration site family.

(IDO1), can also inhibit T cell proliferation and activation or lead to T cell apoptosis, respectively (reviewed in [335]).

Although there is still a vast amount of mechanistic understanding to be gained from immunophenotypes of various malignancies, particularly in terms of tissue-, tumor- and species-specific contexts, there is a strong rationale for evaluating markers related to influx and migration, antigen recognition and function of T cells. Such an evaluation potentially enables the stratification of patients, and tailoring of single or combination AT. Timely examples of markers and tools to assess these three categories of local T cell immunity are illustrated in **Figure 2**.

In Silico Tools for Immunophenotyping

Gene expression platforms and NGS technologies help determining the abundance of immune gene expression signatures, and, together with mutational and pathway analyses, are recommendable tools for a first screen of immune markers. Available databases and tools for functional annotation and pathway analyses include ConsensusPathDB [338], Reactome [339], DAVID [340] or IPA®. In addition, numerous in silico tools support dissection of the TME, such as those that characterize the cellular composition of immune cells or diversity of TCR sequences. An overview of in silico tools is given in **Table 3**.

For instance, the presence of effector T cells and immune suppressor cells can be extracted from microarray expression- or RNA-seq data of bulk-tumor tissues using computational approaches that take into account sets of immune-specific marker genes or expression signatures [294]. The most widely used approach is gene set enrichment analysis (GSEA). A limitation of GSEA-based methods is that they report enrichment scores that do neither reflect nor translate into proportions of the analyzed cell types [294]. Single sample GSEA (xCell) can address this shortcoming by calculating the abundance scores of immune cell types and calibrating these scores to resemble proportions [341]. Unlike GSEA, deconvolution methods such as CIBERSORT [203], EPIC [342] or quanTIseq [343] convert gene expression data into relative fractions of cell types according to cell type-specific expression profiles. Of note, quanTIseq combines deconvolution with image analyses of hematoxilin&eosin-stained samples thereby enabling “in silico multiplex staining” and prediction of immune cell densities [343]. Next to immune cell composition, algorithms such as MiXCR, IMSeq, and RTCR assess T cell clonality, which may serve as a marker for antigen recognition by CD8 T cells and tumor responsiveness towards immune therapies (reviewed in [208]).

Tool	performance	input	output
GSEAPreranked*	GSEA of 28 immune gene sets	ranked list of gene expression	enrichment scores for individual gene sets
xCell 341	GSEA of single samples	genome wide expression, RNAseq	relative abundance of 64 immune- and ECM cell subsets
CIBERSORT 203	deconvolution	genome wide expression	relative abundance and absolute (beta version) numbers of 22 immune cell subsets
EPIC 342	deconvolution	genome wide expression	relative abundance and absolute (beta version) numbers of 22 immune cell subsets

Tool	performance	input	output
QuanTIseq 343	deconvolution	RNAseq	relative abundance of 8 immune cell subsets, fibroblasts, and endothelial cells
Consesnus-pathDB338, DAVID340,Reac-tome339, IPA®	Functional annotation of genes and pathways	List of differentially expressed genes	Up- and down regulated genes and pathways, interaction maps, identified regulators
QuantumClone 382	Variant clustering based on frequency and tumor purity	DNAseq (>50x coverage)	Clonality, functional variants
CloneHD 383	Reconstruction of subclonal structure from short sequencing reads	DNAseq	
MiXCR, IMseq, RTCR, Vidjil 208	assignment of V(D)J genes and mapping on IMGT database	RNAseq (>150bp paired end reads)	V(D)J gene usage and number of CDR3 reads

Table 3. Examples of Omics Tools for Immunophenotyping. **Abbreviations:** ECM: extracellular matrix; GSEA: gene set enrichment analysis; IMGT: Immunogenetics, IPA: ingenuity pathway analyses.

*reference: http://software.broadinstitute.org/gsea/

Laboratory Tools for Immunophenotyping

New imaging techniques can enable quantitative and spatial assessment of multiple immune markers related to AT, which may be particularly important for the evaluation of the ability of CD8 T cells to infiltrate the tumor. Moreover, the activation state of TILs or cell to cell interactions can be assessed, which may provide insight into antigen recognition and T cell function. Multiplexed methods are either based on sequential imaging of single markers or simultaneous imaging of multiple markers. The former is time consuming, relies on image alignment, but does not require specialized equipment, whereas the latter has a higher degree of accuracy but does require sophisticated equipment and reagents (see **Table 4**). Sequential staining and imaging can be performed with IHC or IF protocols, such as cyclic immunofluorescence (CycIF) [344] and MxIF [345], which both use chemical inactivation and removal of fluorochromes, or multi-epitope ligand cartography (MELC), which uses photo-bleaching and has been reported to image up to 100 markers in a single sample [346]. More recently developed methods enable simultaneous staining of a high number of markers followed by a single image acquisition. For instance, Vectra®-based multiplexed IF (up to 8 markers) relies on consecutive steps of staining and stripping of antibodies (leaving behind immobilized fluorophores) (reviewed in [347]). Digital spa-

tial profiling (DSP) enables quantitation of up to 800 markers targeting DNAs, RNAs and proteins simultaneously with a near single cell resolution (1-4 cells) [348]. DSP uses the nCounter® barcoding technology (nucleic acids or antibodies labeled with an optical code) which relies on photo-cleavable tags that are digitally mapped back onto the tissue [348]. Finally, imaging CyTOF/ mass cytometry (IMC) [349] can provide unprecedented and detailed views of tissue heterogeneity. IMC combines CyTOF, in which cellular targets are labeled with metal-tagged antibodies and quantified by time-of-flight mass spectrometry, with IHC and high-resolution tissue laser ablation to image dozens (50+) of proteins at sub-cellular resolution (<1µm) [349]. Significant

Tool	performance(s)	required equipment	multiplex capacity	analysis software
Multiplex IHC [384]	sequential staining with enzyme-labeled reagents , imaging of whole slide, stripping of antibody and chromogen	conventional digital image scanner	12+	Cell Profiler, ImageJ, other
Cyclic IF [385]	sequential staining with fluorescently-labeled reagents, imaging of whole slide, chemical inactivation of fluorochromes	conventional epifluorescence microscope	30	ImageJ, Matlab,other
MxIF [345]	sequential staining with fluorescently-labeled reagents	conventional epifluorescence microscope	60	Axio Vision Mark & Find, ImageJ, other
MELC [346]	automated sequential staining with fluorescently-labeled reagents, imaging of whole slide, photo bleaching of fluorochrome	fluorescence microscope with robotic device	100	Matlab, Motiffinder, Motifanalyzer, IXCOSM, IMARIS for 3D images, other
Multiplex IF [347]	consecutive staining with fluorescently-labeled reagents, tyramide signal amplification (following each staining), stripping leaving fluorophores (following each staining)	Automated Quantitative Pathology Imaging System (Mantra, Vectra, Vectra Polaris)	8	InForm, TIBCO Spotfire, other
Imaging Mass Cytometry [349]	simultaneous staining with antibodies labeled with rare earth metal isotopes	Imaging mass cytometer (Hyperion)	52	Maxpar, Definiens, Cell Profiler, miCAT, histoCAT, other
Digital Spatial Profiling[348]	simultaneous staining with nucleic acids or antibodies tagged with optical barcode	NanoString high-plex digital IHC microscope	800	nCounter Analysis system, other

Table 4. Examples of Laboratory Tools for Immunophenotypingagen. Abbreviations: IF: immunofluorescence; IHC: immunohistochemistry.

advantages of IMC in comparison to the above-mentioned methods are the absence of sample autofluorescence and a wide dynamic range, which makes this method highly versatile and quantitative [349]. Highly multiplexed imaging methods, whatever the choice of method, generate complex multilevel data. Only with appropriate tools

and analysis software (summarized in **Table 4**) one can accurately and fully extract cellular phenotypes and spatial information such as cell-cell interaction networks, which together can be used to define clinically relevant features.

5.4 Adoptive T cell Therapy: Assessing TCRs and Designing Co-Treatments

Step-wise approaches for selecting safe target antigens and corresponding TCRs as well as co-treatments may further optimize AT. Once a target antigen, epitopes and corresponding TCRs have been identified and validated (as described above),

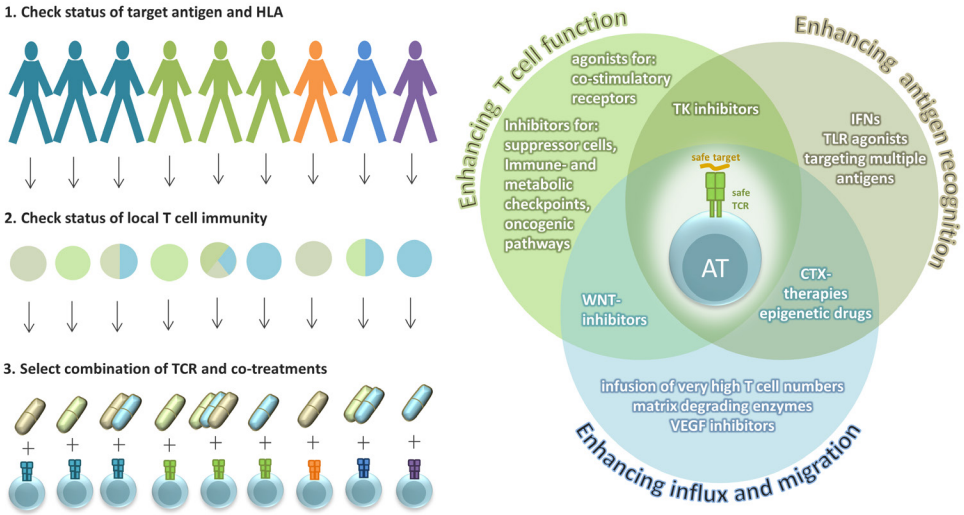

Figure 3. Patient Stratification According to TCRs and Co-Treatments. Proposed Workflow to stratify patients for combined AT (left). The color of patients represents the selected target antigen (shared: CGA or oncoviral antigens, patient specific: neo-antigens). Colored circles represent shortcomings in T cell immunity with respect to influx and migration (blue), antigen recognition (grey) and T cell function (green). Examples for co-treatments to counteract one or more (overlapping circles) immune evasive mechanisms are exemplified (right). **Abbreviations**: HLA: human leukocyte antigen; IFNs: interferons; TCR: T cell receptor; TK: tyrosine-kinase ; WNT: wingless-type MMTV integration site family.

patients can be screened for (single or combination) AT treatment. To this end, tumor biopsies (and patient's blood for matched normal DNA to identify mutated epitopes) are used to assess: first, the status of target antigens and HLA alleles that present epitopes and second, the status of local CD8 T cell immunity. In a third step, information of these two steps is used to design a combination AT treatment. These three steps can provide specific treatments for a patient (-subgroup) as illustrated in **Figure 3** and examples based on the three immunophenotypic categories (with respect

to local CD8 T cell immunity) are provided below. In case neo-antigens are targeted with AT, this treatment will be personalized regardless of the co-treatments.

Targeting oncoviral antigens or CGAs, however, warrants identification of groups of patients according to antigen and HLA expression. In general, antigens are measured by NGS or quantitative PCR, or in situ staining, when antibodies are available and staining protocols are operational. HLA alleles are mostly determined by genetic typing using PBMC-derived DNA. In the event no suitable antigen is expressed, a given patient may not be eligible for AT.

When intra-tumoral T cells are absent, one potential explanation may be the lack of chemokines or adhesion molecules due to endothelial quiescence (see previous section for references). In such a case, infusion of very high numbers of CD8 T cells may already be sufficient to induce endothelial cell activation (via complement activation), release of chemokines and subsequent homing of adoptively transferred T cells [350]. Other approaches for the normalization of the tumor vasculature include administration of VEGF-inhibitors[1], other tyrosine kinase inhibitors (TKI)* or epigenetic drugs*. The latter drugs, when exposed to ex vivo cultures of human ovarian cancer, have been reported to induce IFN-response genes and again trigger the release of chemokines, and, when administered to NSG mice transplanted with human ovarian cancer, and co-treated with TILs, resulted in improved survival [317]. In addition, combinations of TCR-engineered T cells with VEGF-inhibitors have resulted in increased numbers of intra-tumoral T cells in murine melanoma [351]. When the lack of intra-tumoral T cells is attributed to an enhanced ECM barrier, combinations that include matrix degrading enzymes may be considered, exemplified by enhanced CAR T cell infiltration ex vivo, and clearance of human neuroblastoma in mouse model by CAR T cells that are engineered to express heperanase [352].

When antigen expression or presentation is low, there is generally a rationale for combining AT with cytotoxic therapies (chemotherapy or radiation)* or epigenetic modifier treatment* (e.g. histone de-acetlyating agents or DNA de-methylating agents) [353]. Cytotoxic therapies increase immunogenic cell death and act synergistically with AT [354], and certain epigenetic drugs such as azacytidine or entinonstad have been found to enhance the expression of some tumor antigens, such as CGAs 183. If antigen expression is heterogeneous, or there is evidence for immune editing, one could opt to target multiple antigens simultaneously [355], each adhering to the criteria set out above. Lack of antigen recognition by T cells due to deficiencies in antigen processing and presentation downstream of genomic alterations, may imply that patients with such alterations are not eligible for AT. In case antigen processing and presentation is compromised due to epigenetic or transcriptional alterations,

one may opt for co-treatment with IFNs, TLR agonists1 (types: 2, 4, 7, 8 and 9), cytotoxic therapies, TKI, or epigenetic modifiers, as these have been reported to increase the expression of MHC- and/or co-stimulatory molecules in different human malignancies (reviewed in [356]).

Finally, when T cells are dysfunctional due to the accumulation of immune suppressor cells in tumor tissues, there may be a rationale for using drugs that could lead to macrophage depletion or re-polarization (CSF1R inhibitor and TNFα treatment, respectively) [225]; and/or depletion or blocking the recruitment of regulatory T cells (via CD25 and CCR4*, respectively) [357]. When immunophenotyping reveals that the activation state of intra-tumoral T cells is compromised, one may consider treatment with agonists for co-stimulatory receptors (CD137, OX40, ICOS). For instance, CD137 antibodies combined with AT resulted in increased T cell infiltration and better killing of murine melanoma, which was evidenced by intravital microscopy [358]. Alternative approaches include combinations with inhibitors of immune checkpoints (PD1*, CTLA4*), metabolic checkpoints (IDO1, adenosine1) or T cell inhibitory pathways (PI3K*, MAPK*, TGFβ*) [353]. Indeed, combinations of AT and PD1- and/or A2AR- inhibitors* resulted in increased CAR T cell efficacy in mouse models of breast cancer [359]. Along this line combinations with a BRAF-inhibitor1 have resulted in increased survival and in vivo cytolytic activity of TCR engineered T cells in murine melanoma models [360]. Yet another approach to overcome T cell dysfunction may be to execute ex vivo activation of T cells under hypoxic conditions, as hypoxic versus normoxic T cells demonstrate better proliferation, expression of granzyme-B and anti-tumor activity in murine melanoma models [361]. (*FDA approval for various malignancie).

Besides combining AT with other therapies, one might also include additional gene-engineering to generate T cells that exhibit enhanced resistance to immune escape mechanisms. This approach has already been clinically exploited for CARs, which often harbor intracellular co-signaling domains, have knocked out checkpoint molecules or are engineered to produce chemokines or matrix degrading enzymes upon antigen engagement. For a more complete overview of gene-engineering to enable T cells to enhance numbers and activity in an immune tolerant environment, see [362].

It is important to note that many of these approaches and combination regimens still require validation, and the assessment of toxicities and potential off-target effects. Consequent, extensive and robust testing is required to investigate these approaches, mechanisms of action and putative combination regimens.

5.6 Concluding Remarks

Major advances in NGS- and laboratory technologies are paving the way towards improved AT in immuno-oncology. It is remarkable that personalized AT targeting of neo-antigens in combination with checkpoint inhibition has not only been feasible for certain malignancies (e.g. solid tumors), but has also resulted in a complete durable response in a chemo-refractory, metastatic breast cancer patient [198]. These results indicate that patient-specific or patient group-specific AT might broaden the scope of responding tumor types, including those with low mutational burden, which are generally considered unresponsive to checkpoint blockade. Taken together, advanced immunophenotyping, which integrates NGS technologies, omics- and laboratory tools, is critically needed to provide a detailed characterization of T cell immunity in a patient's tumor and antitumor response. This, together with the selection of safe and effective epitopes and corresponding TCRs might provide optimal combination AT treatments with safe and effective clinical profiles. Although many questions remain (see **Outstanding Questions**), it will be quite exciting to follow how these technological advances contribute to catalyzing the future of personalized or group-specific AT with TCR-engineered T cells.

5.7 Acknowledgements

DM is supported by a grant from the Dutch Cancer Society (KWF); DR and ZT are supported by the Innsbruck Medical University and European Community (EU FP7 grant); JWMM and RD are supported by the Erasmus MC, and grants from Dutch Cancer Society (KWF), Dutch Scientific Council (NWO), and World Cancer Research (WCR).

5.8 Glossary

allo-alleles: non self-allele which can be recognized by TCRs independent of the bound peptide

algorithm: a sequence of operations in computer science, such as calculating, data processing and automated reasoning.

avidity: binding strength based on multiple receptor target interactions (for instance, T cell avidity includes combination of TCR-peptide:MHC and CD8).

Cancer Germline Antigens (CGAs): class of tumor antigens with expression re-

stricted to immune privileged tissues (germline) and tumors.

CAR T cells: T cells engineered to express a chimeric antigen receptor consisting of an extracellular antibody-domain, an intracellular TCR domain, and often a co-stimulatory domain.

cognate T cell epitope: A defined stretch of amino acids (9-11 amino acids) that is derived from intracellular proteins which is specifically recognized by a TCR. After processing by the (immune-) proteasome, peptides are presented by MHC molecules on the cell surface of target cells to the TCR on the cell surface of T cells.

cross-reactivity: T cell reactivity against an epitope other than the cognate epitope (often highly similar to cognate epitope and recognized with lower TCR affinity).

complement activation: chain reaction of protein cleavage that can result in the activation of immune cells.

differentiation antigens: class of tumor antigens that are expressed at different stages of tissue development or cell activation.

endothelial quiescence: inactive state of endothelial cells, generally with limited expression of chemokines, adhesion molecules, and co-stimulatory ligands, and consequently not favoring tissue entry of T cells.

immune suppressor cells: cells, including immune cells but also stromal cells, such as CAF, that can limit T cell function

immune checkpoints: receptors and ligands that upon ligation result in limiting activation of immune cells (i.e., putting immune cells in check).

immune editing: interplay between tumors and immune system resulting in loss of antigen-positive tumor cells upon selective pressure by T cells.

immunopeptidome: collection of all presented peptides by MHC molecules of a target cell(s) or tissue.

immunophenotyping: assessment of immunogenicity and immune evasive mechanisms by omics and/or laboratory tools.

M2 macrophages: innate immune cells that normally are specialized in engulfing aberrant cells and presenting antigens, but due to polarization, which may be a consequence of the tumor micro-environment, become immune suppressor cells.

neo-antigens: class of tumor antigens that are derived from mutated proteins.

next-generation sequencing: high throughput sequencing method of nucleic acids.

whole-exome sequencing: sequencing of all protein-coding genes of the genome.

omics: collection of sciences and necessary tools that focus on the structure and function, and related aspects, of defined groups of molecules (genomics: DNA; transcriptomics: RNA; proteomics: proteins; metabolomics: metabolites; immunomics: immune markers etc).

oncoviral antigens: class of tumor antigens which are derived from viral genes that had been integrated into the DNA of (pre-)malignant cells.

on-target toxicity: toxicity due to T cells targeting their cognate epitope outside tumor tissue.

off-target toxicity: toxicity due to cross-reactive T cells recognizing an epitope very similar to the cognate epitope outside tumor tissue.

read-mapping: locating of experimental sequences (called reads), through alignment with a set of reference sequences.

reading depths: number of sequences (called reads) that include a nucleotide of a reconstructed sequence, also referred to as coverage.

TALEN or CRISPR-mediated gene editing: technologies that enable targeted genome editing through different principles (TALEN (transcription activator-like effector nucleases) relies on modified restriction enzymes to cut out specific sequences from DNA; whereas CRISPR/Cas9 (clustered regularly interspaced short palindromic repeats) relies on guide RNA and a DNA endonuclease activity to remove specifc sequences from DNA).

TCR repertoire: diversity and abundance of TCR genes (often represented by β chain) used as a measure of T cell clonality; the more skewed a TCR repertoire, the more clonal the T cell response has been.

time-of-flight mass spectrometry: method to determine an ion's mass-to-charge ratio via acceleration in a known electric field, by time measurement.

TLR-agonists: natural or synthetic molecules that ligate to and stimulate Toll-Like Receptors (TLR), the latter being evolutionary conserved receptors generally expressed on innate immune cells and taking part in the recognition of pathogen-associated molecular patterns.

Tumor infiltrating lymphocytes: immune cells that are present in neoplastic tissue.

tumor selectivity: expression of tumor antigens by cancerous tissue but not healthy tissue (immune privileged tissues represent an exception in case of CGAs)

5.9 Outstanding Questions

1) What are the exact underlying biochemical rules that determine the immunogenicity of tumor antigens? What kind of data is required in order to improve epitope prediction algorithms for HLA-I, and ultimately also for HLA-II?

2) Are there categories of resistance to AT that are not captured by deviations in influx and migration-, antigen recognition and dysfunction of T cells? Are there subgroups of patients with certain genetic or environmental states (SNPs or composition of gut microbiota) that despite combination treatment do not respond to AT?

3) With respect to an effective anti-tumor response, is there a hierarchy of certain immune markers? And would this hierarchy of markers (when existing, this would greatly enhance our understanding of tumor immunity and facilitate charting immune evasion) hold true in a pan-cancer setting, or be it specific per tumor subtype or even patient?

4) Can acquired resistance or compensatory immune evasive mechanisms be fully prevented when targeting one category of T cell control? Should one opt to target multiple events within one or multiple categories, so for instance antagonize multiple types of suppressor cells instead of a single type of suppressor cell to limit renewed T cell evasion through compensatory mechanisms?

5) Since tumor-immune interactions are heterogeneous, not only across different tumor types, and within tumor subtypes, but also across different metastatic lesions within the same patients, would it be necessary to take biopsies from multiple sites prior to selecting co-treatments?

Chapter 6

PCT2° is a novel, tumor selective and highly prevalent target for T cell receptors against triple negative breast cancer°

Dora Hammerl[1*], Dian Kortleve[1*], Mieke Timmermans[2], Daan van Dorst[1], Mandy van Brakel[1], Anita M.C. Trapman-Jansen[2], Renée Foekens[2], Monique de Beijer[3], M Smid[2], Jeroen Demmers[4], Sonja Buschow[3], John W.M. Martens[2], R Debets[1]

[1]Laboratory of Tumor Immunology, [2]Department of Medical Oncology, and [3]Department of Gastroenterology, and [4]Department of Biochemistry, Erasmus MC-Cancer Institute, Rotterdam, the Netherlands; *joint first authors.

°This chapter has been amended due to patent filing (i.e., the target antigen (PCT2), epitopes and T cell receptor gene sequences have been coded).

Abstract

Triple negative breast cancer (TNBC) lacks classical targets for hormone and/or antibody therapy, and responses to immune checkpoint inhibitors are rare and generally not sustained. In TNBC the presence of tumor infiltrating CD8 lymphocytes, even though variable, has prognostic value, and TNBC often demonstrates antigenicity, making this disease amenable to adoptive T cell therapy. Here, we applied an integrative approach of in silico and laboratory tools to select and validate a tumor-selective intracellular target antigen, its corresponding immunogenic epitopes and TCRs. We observed that PCT2 showed absent RNA expression in 5 healthy tissue databases (n=1,709) and absent protein expression in tissues of >15 major healthy organs. Furthermore, PCT2 showed high RNA- and protein expression in >80% of TNBC patients in 3 independent cohorts (n=756). Epitope predictions according to immune-reactivity, together with epitope elutions and mass spectrometry analysis of an PCT2-expressing breast cancer cell line, enabled identification of 14 PCT2/HLA-A2 epitopes. T cell enrichments using the top 4 ranked epitopes based on HLA-A2 binding stability and subsequent molecular cloning yielded a TCR against epitope 12 that upon gene transfer into T cells specifically recognized epitope-positive target cells and demonstrated a stringent recognition motif towards this epitope. This TCR can be further exploited for the development of adoptive T cell therapy for TNBC patients.

6.1 Background

Triple negative breast cancer (TNBC) is an aggressive subtype, accounting for 15-20% of all breast cancer (BC) cases. TNBC is characterized by the absence of receptors for estrogen and progesterone and lack of human-epidermal growth factor receptor 2 (HER2), and is therefore not responding to current hormone receptor or HER2-targeting therapies[387]. Despite recent approval of immune checkpoint inhibitors (ICI) for PD-L1-positive TNBC, the majority of patients does not respond to this treatment[116]. Nevertheless, it has been recognized that TNBC is an immunogenic tumor type based on high numbers of tumor infiltrating lymphocytes (TILs), which are recognized for their prognostic and predictive value in TNBC[5,9,10,51,388]. Notably, TNBC shows a relatively high and frequent expression of tumor associated antigens[9]. These observations, together with the recent and partly disappointing outcomes of ICI treatment of this tumor type, suggest that TNBC may benefit from treatment with adoptively transferred tumor-specific T cells.

Adoptive T cell therapies (AT) generally rely on isolation of T cells from patients' blood, insertion of genes encoding either for a chimeric antigen receptor (CAR) or a T cell receptor (TCR) with pre-defined antigen specificity, expansion of these cells, and re-infusion of the engineered, autologous T cell product into patients. This strategy has been applied to different tumor types with variable successes, mainly depending on type of tumor, target antigen and type of transgenic receptor[28,31,32]. On the one hand, treatment with CAR-T cells is considered a breakthrough for B-cell malignancies (objective response rate (OR): 95%), and CD19 CAR T cell products (i.e., Kymriah, Yescarta, Tecartus) have recently been approved by the FDA and EMA to treat these malignancies. Unfortunately, the efficacy of CAR T cells to treat solid tumors is significantly lagging behind the efficacy observed for hematological malignancies. On the other hand, treatment with TCR-T cells has revealed clear clinical responses when used towards blood as well as solid tumor types[190,389]. For example, in melanoma, synovial sarcoma and multiple myeloma ORs of 55%, 61% and 80%, respectively, have been observed for AT with T cells expressing a NY-ESO1-specific TCR[283]. Despite these clinical success, a major challenge for the treatment with gene-engineered cells, CAR-T and TCR-T cells alike, is preventing treatment related toxicities. Such toxicities include on-target toxicities (i.e., engineered T cells recognizing targets outside tumor tissue) and off-target toxicities (i.e., engineered T cells recognizing epitopes that are highly similar to its cognate epitope)[287]. Treatment related toxicities generally depend on the choice of target antigen and transgenic receptor. For example, no treatment related toxicities have been observed for NY-ESO-specific TCRs, while CARs targeting the CAIX antigen have resulted in severe on-target toxicity[390], and treatment with affinity enhanced TCRs targeting the

MAGE-A3 antigen were accompanied by severe on- and off- target toxicities[30,375]. Another challenge, particularly for the treatment of solid tumors is lack of efficacy, which is mainly attributed to high level of antigen heterogeneity[391] and the immune-suppressive micro-environment; the latter often limiting T cell infiltration and/or activation of T cells inside solid tumors[31].

In the current study, we have carefully selected and validated intracellular targets antigens and their corresponding TCRs for TNBC, to which end we have set up and utilized a workflow consisting of in silico predictions and laboratory tools. We have applied a stringent selection process and demonstrated that PCT2 as well as its isoform PCT2B (>95% sequence overlap) are not expressed in a large series of healthy tissues, yet it is highly and homogeneously expressed in the vast majority of TNBC tissues. In silico epitope predictions as well as immunopeptidomics, combined with HLA-A2 binding avidity assays, enabled the identification of 9 to 11-mer PCT2/B T cell epitopes that were unique, immunogenic, and non-cross-reactive. T cell enrichments using these epitopes, yielded T cells specific for the HLA-A2-restricted epitope 12. Upon cloning, gene transfer and in vitro assays, we have identified and validated the TCR specifically recognizing this epitope and that can be further exploited for AT.

6.2 Results

PCT2 is absent from healthy tissues and shows abundant and homogenous expression in >80% of TNBC

To identify TNBC-specific target antigens for AT, we interrogated gene-expression values of >200 intracellular targets in 5 databases covering 66 healthy tissues derived from in total 1,735 individuals, and in 3 databases covering cancer tissues from 447 TNBC patients and 6,670 patients including 14 solid cancer types. Since NY-ESO1 (CTAG1B) has been successfully targeted with TCR-T cells without treatment related toxicities[283,392], its expression in healthy tissues was used as a reference value. These gene expressions (or their absence) were subsequently validated by qPCR and immunohistochemistry (IHC). Using this workflow, we have identified PCT2 as a target for AT to treat TNBC according to the following outcomes: First, PCT2 and its isoform PCT2B were not expressed in any healthy tissue tested (**Figure 1A**). Absent expression of both isoforms and the reference antigen (NY-ESO1) in major healthy tissues, was confirmed by qPCR using commercially obtained cDNA libraries of 48 healthy tissues pooled from 10 donors (**Figure 1B**) as well as IHC stainings of TMAs containing 16 major healthy tissues from 2-6 individuals (**Figure 1C**).

Figure1. PCT2 is not expressed in healthy tissues. A. Bars show PCT2 gene expression in healthy tissues according to TPM values and based on RNAseq of 6 different healthy tissue databases (colored boxes indicate presence of a tissue in corresponding database, see Materials and Methods for details), dashed, orange line shows expression of NY-ESO1, which was used as reference threshold. **B**. Dots (superimposed) show gene expression of PCT2 and its isoform PCT2B expressed as fold change in comparison to GAPDH in 48 healthy tissues according to qPCR using a cDNA library of healthy tissue samples. NY-ESO1 was taken along as a control. **C**. Panels show representative immune stainings of healthy tissues using PCT2/B- (top) or NY-ESO1 antibody (bottom) on tissue microarrays. (TMAs, n=63).

Second, PCT2/B was highly expressed by 84% of TNBC tissues (**Figure 2A**) as well as a melanoma (93%) and to a much lesser extent in a number of other solid tumor tissues (**Figure S1A**: urothelial cell carcinoma: 3%; lung squamous cell carcinoma: 5%; glioblastoma:3%). PCT2 gene-expression in high fraction of TNBC was confirmed in two additional gene-expression datasets (**Figure S1B**: TNBC Cohort A: 86%, n=66 patients; and TNBC Cohort B: 77%, n=183 patients). In comparison, NY-ESO1 was expressed in ≤14% of TNBC tissues, and expression levels were generally low (**Figure S1C**). In addition to gene expression, PCT2 protein expression was demonstrated in 88% of TNBC via immunohistochemical (IHC) staining of tumor tissue microarrays (TMAs, n=338 TNBC) (**Figure 2B**). Importantly, protein expression was homogenous in 83% of PCT2-positive TNBC, while NY-ESO1 was homogenously expressed in only 18% of NY-ESO1-positive TNBC (**Figure 2C, D**).

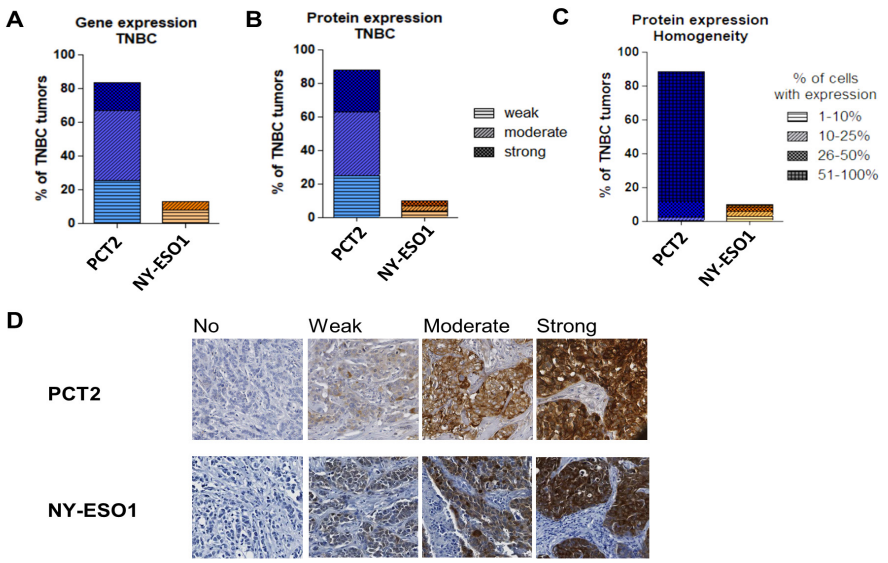

Figure 2. PCT2/B shows high and homogenous expression in TNBC. **A**. Bar graphs show fraction of TNBC tumors with weak (TPM 1-10), moderate (TPM 10-100) and strong (TPM >100) gene expression of PCT2/B (TCGA, RNAseq, n=122, see Materials and Methods for details). **B**. Bar graphs show fraction of TNBC tumors with weak, moderate and strong immune staining of PCT2/B (TMAs, n=338); scoring is performed as described in Materials and Methods as well as in panel **D**. **C**. Bar graphs show fraction of TNBC tumors with either 1-10%, 10-25%, 26-50% or 51-100% of the tumors cells positive for PCT2/B and NY-ESO1 protein. In gene and protein expression analyses, NY-ESO1 was taken along as a control.

Predicted and eluted PCT2-epitopes are avidly bound by HLA-A2

To select immunogenic T cell epitopes, we first performed a series of in silico predictions using the following tools: NetMHC, NetCTLpan, RANKPEP, and SYFPEITHI,

which are each biased towards various aspects of epitope presentation, such as presence of cleavage sites, affinity for transport of associated proteins (TAP), and affinity for binding to HLA (see **Figure 3A** and **3D** for an overview of epitope characterization and selection, see ref[201] for details on predicted features). Predicted epitopes were ranked per tool and the top 10 peptides of each tool were used to perform weighted ranking, resulting in 17 unique peptides. In a second approach, we used MDA-MB-231 cells (TNBC cell line with high HLA-A2 expression) that were gene-engineered to over-express PCT2 as a source for immunopeptidomics. To this end, we have generated the construct PCT2-2A-GFP, which was validated by sequence analysis, immune staining and flow cytometry (**Figure 3B**). Mass-spectrometry analysis of all HLA-I bound peptides (see Materials and Methods for details) yielded 2 additional unique HLA-peptides (**Figure 3B**). The total set of unique, potential epitopes (n=19) were screened for non-homology to other peptide sequences present in the human proteome using EXPITOPE (**Figure S2A**), which yielded 14 likely immunogenic, non-cross-reactive PCT2 peptides (i.e., peptides with >2 mismatches compared to any other peptide in the human proteome). These peptides, along with the NY-ESO1 peptide (SLLMWITQV) and a gp100 epitope with high HLA-A2 affinity (YLEPGPVTA), were tested for binding to HLA-A2 in vitro. In a first screen, all peptides were compared side-by-side using a saturating concentration (25µg/ml). Peptides that induced >1.1-fold change over baseline (considered a minimal inclusion criterion, **Figure 3C**) were subsequently used to assess binding stability to HLA-A2 according to peptide titrations (**Figure S2B**). Three predicted binders did not reach this cut off. Interestingly, epitope 1 (i.e., epi1, a 10-mer derived from immunopeptidome) did not bind to HLA-A2 (and was mapped to HLA-B40:01, also expressed by MDA-MB-231 cells), whereas epi11 (11-mer also derived from the immunopeptidome) bound to HLA-A2 with high affinity. Notably, the latter peptide was not identified via in silico predictions for A2 binding. Peptides that reached the >1.1 fold change threshold were subsequently ranked based on maximum HLA-A2-binding (amplitude) and EC50 values: peptides with > half-maximum binding of the reference epitope YLEPGPVTA and EC50 values lower than 10^{-5} were considered promising peptides to be used in T cell enrichment cultures (**Figure 3D**).

PCT2 epitope-specific CD8 T cells are enriched from healthy donor T cells

In order to enrich for PCT2-specific T cells, we used the 4 top-ranked epitopes (epi6, EC50: 3.3µM; epi10, EC50: 4.3µM; epi4, EC50: 5µM; epi12, EC50: 6.5µM) in co-cultures of T cells and artificial antigen presenting cells (aAPC, K562abc overexpressing HLA-A2, CD80 and CD86)393. These 4 epitopes had EC50 values similar to those as the NY-ESO1 peptide (SLLMWITQV, EC50: 5µM).

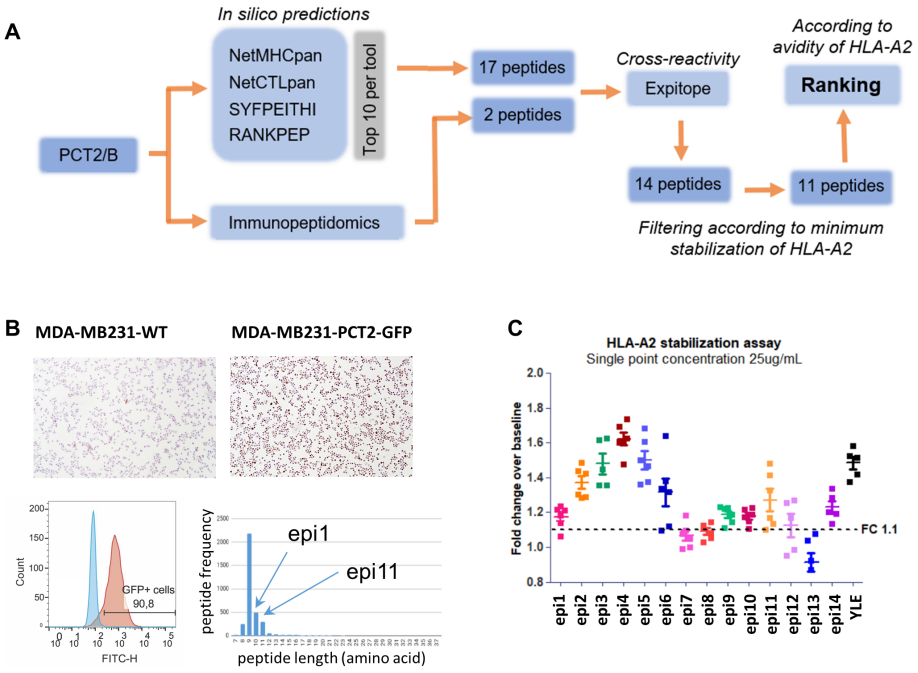

D

			Predicted immunogenicity				HLA-A2 binding			
Protein	Source	Peptides	NetMHCpan	NetCTLpan	SYFPEITHI	RANKPEP	Minimum stability	Amplitude	EC50	Ranking
PCT2/B	Predicted	epi6	15	4	92	97	1.32	2376.17	3.28E-06	1
PCT2/B		epi10	11	5	8	14	1.18	2620.56	4.35E-06	2
PCT2/B		epi4	9	3	5	6	1.62	3800.25	5.05E-06	3
PCT2B		epi12	2	6	12	11	1.13	3450.56	6.56E-06	4
PCT2B		epi5	1	-	1	1	1.50	2707.33	1.09E-05	6
PCT2/B		epi3	5	2	19	26	1.29	3478.36	1.14E-05	7
PCT2/B		epi9	8	9	21	20	1.19	2657.78	9.12E-05	8
PCT2B		epi14	3	8	6	8	1.16	3418.44	x	9
PCT2/B		epi2	7	7	2	5	1.37	2179.58	3.16E-06	10
PCT2B		epi8	24	16	30	7	1.09	x	x	
PCT2B		epi7	10	34	29	48	1.06	x	x	
PCT2/B		epi13	6	11	3	12	0.91	x	x	
PCT2/B	Eluted	epi1					1.17	665.91	x	11
PCT2/B		epi11					1.27	3174.78	6.99E-06	5
gp100 NY-ESO1	Reference	YLEPGPVTA SLLMWITQV					1.36	4480.34 4215.83	2.49E-06 5.08E-06	

Figure 3. Selection and ranking of PCT2 T cell epitopes according to immunogenicity and HLA-A2 stabilization. A. Flow chart of PCT2 peptide selection based on in silico predictions, peptide elution, check for non-cross-reactivity and HLA-A2 bindings (see Materials and Methods and supplementary figure 2C for details). **B**. PCT2 staining of MDA-MB231 TNBC cell line with and without PCT2 overexpression either grown on cytospins (upper panel) or in suspension (lower left panel, flowcytometry, red indicates % of GFP-positive cells of the overexpressing cell line, blue indicates % of GFP-positive cells of the negative control). Histogram (lower right panel) shows the total number of peptides (y-axis) and their length (x-axis) eluted from HLA-complexes of MDA-MB231-PCT2-2A-GFP cells. **C**. Head-to-head com-

parisons of unique (non-cross reactive) epitopes for HLA-A2 binding stability. Test was performed using single concentrations (25 μM); results are expressed as fold change of median fluorescent intensity (MFI) of HLA-A2 over baseline (T2 cells without addition of peptides), n=6. Peptides with fold change >1.1 were subsequently tested using titrated amounts (range from: 31nM to 31 μM) (see supplementary Figure 2B). D. Tabular overview of epitope rankings. Input comprised 2 reference peptides (gp100: YLE; NY-ESO1: SLL); and 14 non-cross-reactive PCT2 peptides. The table includes from left-to-right: in silico scores of each tool (provided as ranks); HLA-A2 binding parameters, such as minimum stability, amplitude (highest data point corrected for baseline point), and EC50 values (in M, calculated with GraphPad software 5); and final ranking of epitopes according to EC50 values see Materials and Methods for details).

T cells were either isolated from healthy donors or TILs derived from a PCT2/HLA-A2-positive BC patient, and following 4-5 enrichment cycles tested for epitope-specific IFNγ production (see for an overview of the T cell enrichment procedure **Figure 4A**). Along these lines, we have tested 3 HLA-A2-positive donors and were able to enrich for epi12- and epi4-epitope-specific T cells in 1 healthy donor (**Figure 4B**). Moreover, we observed epi4-specific T cell responses in TILs following 1 cycle of co-culture with aAPC (**Figure 4B**, right-hand side). Prolonged culture of TILs and subsequent isolation of TCR genes was challenged by low proliferation and survival of these T cells ex vivo. In contrast, T cells enriched from peripheral blood proliferated well and harbored 20% and 62% of T cells that bound epi12/HLA-A2 complexes after 4 and 5 cycles, respectively (**Figure 4B**). For T cells that bound epi4/HLA-A2 complexes these percentages were 10 and 49 (**Figure 4C**). Enriched T cells were either cloned through limiting dilutions following IFNγ capture (**Figure S3A**) or sorted through FACS using corresponding pMHC multimers (**Figure S3B**), and subsequently used to identify epitope-specific TCR genes via 5'RACE PCR (**Figure S3C**). The epi12-TCR genes contained 2 genes encoding for the variable TCRα chain (TRVA) and 1 gene encoding for the variable TCRβ chain (TRVB), whereas the epi4-TCR genes contained 4 TRVA genes and 1 TRVB sequence (**Figure 4D**).

Epi12 epitope-specific TCR is functionally expressed by healthy donor T cells

All TCR-α/β combinations (epi12 TCRs 1-2 as well as epi4 TCRs 1-4) were codon-optimized, and cloned into pMP71 in a TRB-2A-TRA format. Testing for surface expression in peripheral T cells from 2 healthy donors demonstrated that only epi12 TCR2 (**Figure 5A, B**), but none of the other 5 TCRs enabled binding of MHC complexed to the corresponding epitope (**Figure S4**). In subsequent experiments, epi12 TCR2 T cells were MACS-sorted using pMHC complexes, and this TCR was shown to mediate recognition of its cognate epitope with an affinity of 11nM but did not recognize an irrelevant epitope (**Figure 5C**). Furthermore, this TCR specifically recognized the epi12 epitope derived from PCT2 (containing an isoleucin at the 5th position) but not

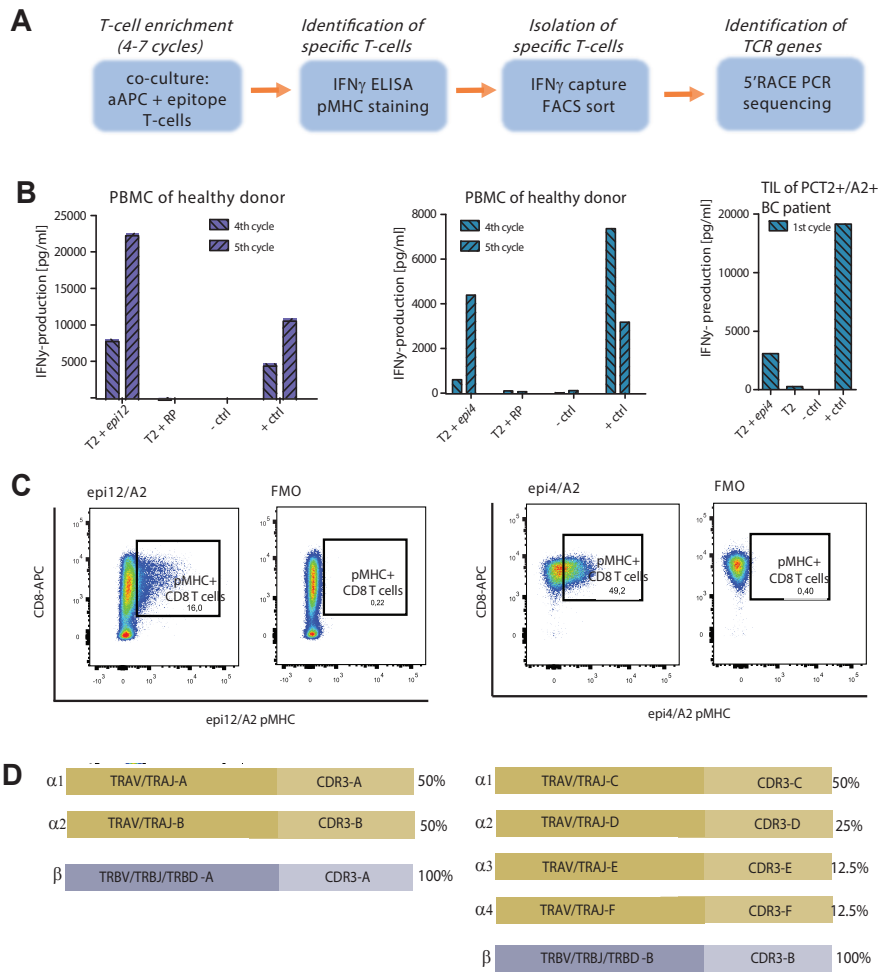

PCT2B (containing a methionine at the 5th position) (**Figure 5D**). Importantly, this

Figure 4. Enrichment of PCT2 epitope-specific CD8 T cells. **A**. Flow chart shows individual steps from T cell enrichment towards the identification of TCR genes. **B**. Boxplots show IFNγ production of epitope-stimulated T cells that were enriched following different rounds of co-culture with peptide-loaded aAPCs (see Materials and Methods for details; RP=random peptide,). Peripheral T cells from healthy donor that were enriched for epi12 specificity following 4 and 5 cycles (left); peripheral T cells from healthy donor that were enriched for epi4 specificity following 4 and 5 cycles (center); TILs from PCT2/HLA-A2-positive BC patient that were enriched for epi4 specificity following 1 cycle (right). **C**. Representative peptide:MHC-stainings of epi12-enriched (left) and epi4-enriched (right) peripheral T cells following 5 cycles of enrichment. pMHC+ CD8 T cells were gated based on fluorescence minus one (FMO, which contained all markers except for pMHC) D. Identified (coded) T cell receptor V-alpha (TRA V and J according to IMGT nomenclature; yellow) and beta genes (TRB V, D and J; blue) as well as corresponding C genes (starting and ending amino acids) cloned from T cells from (B); percentage reflects fraction of all identified colonies.

TCR showed a stringent recognition motif as determined by alanine scanning (see Materials and Methods for details). In fact, every amino acid, except for position 6,8 and 9 were assessed as being critical for TCR recognition (**Figure 5E**), and the resulting motif: 1-2-3-4-5-x-7-x-x (numbers indicate positions of critical amino acids) was not present in any other known sequence of the human proteome.

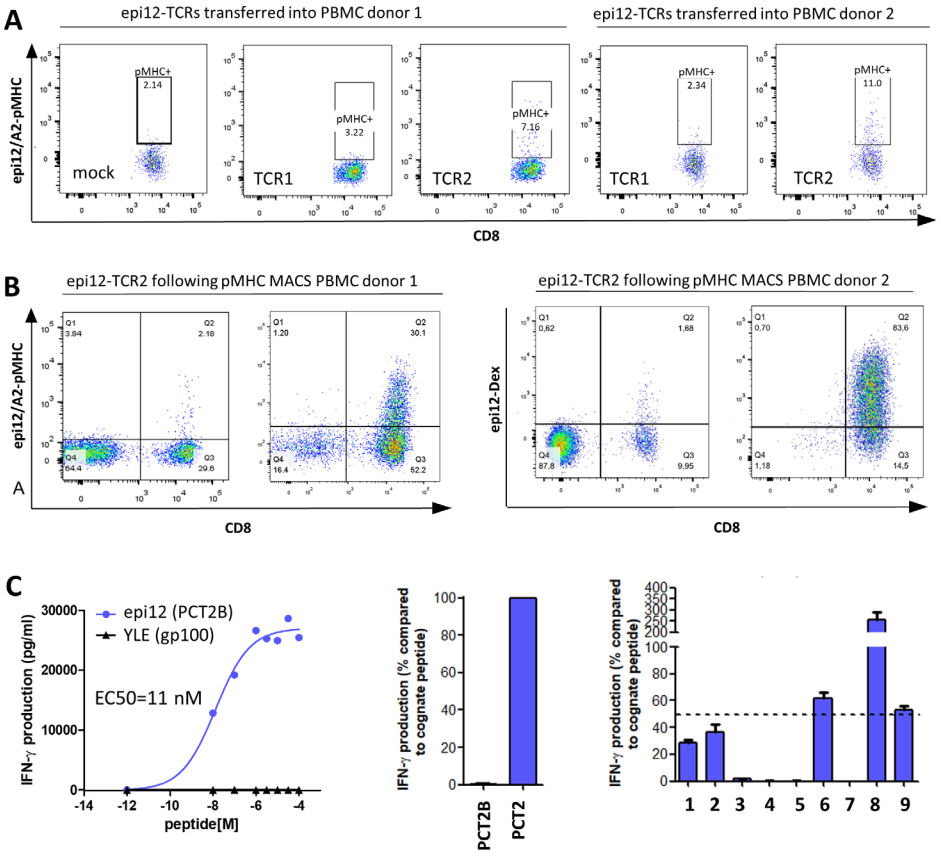

Figure 5. Surface expression and functionality of PCT2 epitope-specific TCR. A. Gene transfer of epi12-TCR1 and 2 in T cells from 2 healthy donors, and binding of epi12/A2 pMHC multimer by gene-engineered T cells. **B**. MACS-sort of epi12-TCR2 T cells from 2 healthy donors; panels show epi12/A2 pMHC binding before (left) and after MACS-sort with pMHC (right). **C**. Representative IFNγ response of epi12-TCR2 T cells (one out of 2 donors) upon stimulation with titrated amounts of epi12 and gp100 peptides (n=3). **D**. Bars show IFNγ-production by epi12-TCR2 T cells upon stimulation with epi12 PCT2B and the corresponding epitope from PCT2 (n=3). E. Bars show IFNγ production by epi12-TCR2 T cells upon stimulation with cognate peptide having alanine-mutations at each individual position (n=3).

6.3 Discussion

In the current study, we utilized a workflow of in silico and laboratory tools to identify a tumor-selective and immunogenic target antigen, its corresponding T cell epitopes and TCRs for the development of adoptive T cell treatment of TNBC. Importantly, with this workflow we aimed to address three challenges in the field of AT, namely: T cell-related toxicities; heterogeneous expression of target antigen; and selection of suboptimal T cell epitopes.

To address the risk for T cell-related toxicities, i.e., on- and off target toxicities, we utilized an approach that was aimed to minimize such risks. First, we have selected a target antigen with tumor-restricted expression. In other words, PCT2, was screened for absent expression in healthy tissues. Second, PCT2 epitopes were screened for non-homology to other peptide/protein sequences in the human proteome (EXPITOPE) to limit off-target toxicities. Third, the resulting TCR was screened for epitope specificity and absence of cross-reactivity. The generally low and heterogeneous expression of target antigens is considered to significantly contribute to the lack of sustained responses or relapse due to outgrowth of antigen-negative tumor cell clones[283,376,377]. PCT2 showed not only tumor-selective, but also high expression in >80% of TNBC (**Figures 1** and **2**), of which the majority had a strict homogeneous antigen expression, suggesting that it represents a safe and effective target for AT. To select immunogenic and non-cross reactive epitopes, we made use of multiple in silico and laboratory tools, and identified 6 epitopes, 4 of which were used for T cell enrichments, resulting in 2 TCRs. One TCR showed surface expression as well as a high level of epitope sensitivity as well as specificity and this TCR is currently scheduled for further testing towards clinical implementation to treat TNBC patients.

On a technical note, our data revealed little concordance among different techniques to select epitopes. For example, we have identified a naturally occurring HLA-A2-binding epitope (epi11) through immunopeptidome analysis (**Figure 3B**) that was not predicted to bind to HLA-A2. Vice versa, we observed T cell responses in healthy donors and a patient against predicted 9-mers (epi4, epi12, **Figure 4B**), which were not retrieved by immunopeptidome analysis. These observations point to the requirement of multiple tools to robustly enable identification of immunogenic epitopes. In addition to these tools, we argue that validation of HLA-binding in vitro is a prerequisite to exclude false positive epitopes and select towards immunogenicity since high HLA-affinity of epitopes generally enhances cross-presentation through antigen-presenting cells, which has proven an important feature of epitopes for effective anti-tumor T cell responses[397,398]. With respect to obtaining epitope-specific TCRs, from either TILs or healthy donor PBMCs is challenged by scarcity of tumor materials

and very low frequencies of antigen-specific T cells, respectively. Along this line, we were able to enrich for PCT2 specific T cells from TIL in 1 out of 1 patient (**Figure 4B**), yet, isolation of TCRs was challenged by poor cell viability, likely due to activation-induced cell death or terminal exhaustion of TILs[399,400]. In case of healthy donor PBMCs, we were able to enrich for PCT2-specific T cells in 1 out of 3 donors, requiring several enrichment cycles. Using the enriched T cells from this healthy donor, we were able to identify the same TCR genes through different approaches (**Figure S3**), which suggests that the PCT2-specific response in that donor originated from a single T cell. These observations indicate that high numbers of PBMC need to be used to enrich for tumor antigen-specific T cells from healthy donors, which is feasible based on our results. Collectively, our study advocates the sequential use of multiple tools identify unique and immunogenic epitopes and their corresponding TCRs.

To date, no studies have been conducted using AT with TCR-T cells in TNBC. CAR-T cells directed against the tyrosine kinase like orphan receptor 1 (ROR1) to treat TNBC are currently in clinical trials[401]. Preclinical studies have shown that these ROR1-CARs recognize and kill TNBC cells, which frequently overexpress ROR1[402]. Nevertheless, ROR1 is expressed in a variety of healthy tissues (according to human protein atlas), and we argue that ROR1 as a T cell target presents an increased risk for on-target toxicities. Furthermore, to date CAR T cells generally lack efficacy in solid tumors which has mainly been attributed to the immunosuppressive microenvironment[403,404]. We have recently shown that TNBC employs distinct T cell evasive mechanisms that are linked to differential spatial organizations of CD8 T cells (Chapter 4; Hammerl, in revision). In example, we observed that T cell evasion was either attributed to TGFβ/VEGF-mediated T cell exclusion, WNT-mediated absence of T cells or M2 macrophage-mediated suppression of intra-tumoral T cells. We argue that AT in TNBC would be most effective in combination with drugs that counteract spatial phenotype-specific T cell evasive mechanisms (further discussed in chapter 8).

6.4 Conclusion

We have established and utilized an effective workflow to identify and validate tumor-selective intracellular target antigens for AT, their epitopes and their corresponding TCRs. We were able to identify and isolate a PCT2-specific and HLA-A2-restricted TCR that is surface-expressed and mediates recognition of epitope 12 but not an irrelevant epitope. This TCR showed a stringent recognition amino acid motif that is not present in any other human protein. These data imply minimal risk for on- and off-target toxicities. Future studies such as screening peptide libraries, and stimu-

lation with healthy cell lines as well as in vitro and in vivo experiments to assess efficacy are needed to introduce this TCR into clinical AT studies.

6.5 Materials and Methods

Generation and culture of cell lines and T cells

To make a PCT2-overexpressing TNBC cell line, a PCT2-2A-GFP cDNA fragment was ordered via GeneArt (Regensburg, Germany) and PCR amplified using gene-specific primers that included 15bp extensions homologous to the PiggyBac PB510B-1 vector. The amplified fragment was cloned into PiggyBac vector (a kind gift from Dr. P.J. French, Erasmus MC, Rotterdam, the Netherlands) using In Fusion cloning kit (Takara). Subsequently, the MDA-MB231 cell line was stably transfected with PiggyBac PCT2-2A-GFP DNA using Lipofectamine (Invitrogen) and Transposase Expression vector DNA (System Biosciences). The transfected MDA-MB231 was FACSorted for GFP, after which expression of PCT2 was confirmed with PCR and immunohistochemical staining of cytospins (using rabbit anti-PCT2 antibody). The tumor cell lines MDA-MB231 and its PCT2-overexpressing variant were cultured in RPMI medium supplemented with 10% FBS, 200 mM L-glutamine and 1% antibiotics without and with 2µg/mL puromycin, respectively. The packaging cell lines 293T and Phoenix-Ampho were cultured in DMEM supplemented with 10% FBS, 200mM L-glutamine, nonessential amino acids, and 1% antibiotics (DMEM complete). T2 cells and BSM cells were cultured in RPMI medium supplemented with 10% FBS, 200 mM L-glutamine and 1% antibiotics. T cells were derived from PBMCs from healthy human donors (Sanquin, Amsterdam, the Netherlands) by centrifugation via Ficoll-Isopaque (density = 1.077 g/cm3; Amersham Pharmacia Biotech, Uppsala, Sweden), and cultured in RPMI 1640 medium supplemented with 25 mM HEPES, 6% human serum (Sanquin), 200 mM L-glutamine, 1% antibiotics (T cell medium) and 360 U/ml human rIL-2 (Proleukin; Chiron, Amsterdam, the Netherlands). T cells were stimulated every 2 weeks with a mixture of irradiated allogeneic feeder cells, as described elsewhere405.

Patient cohorts, databases and code of conduct

TGCA: Pan-cancer RNAseq data as well as sample annotation data were retrieved from the USCS Xena browser (n=10,495 of which 1,211 BC and 122 TNBC tumors, TPM normalized).

TNBC cohort A: BC with RNAseq (n=347 of which n=66 TNBC, geTMM normalized) accessible through European genome-phenome archive EGAS00001001178 (BASIS cohort).

TNBC cohort B: Primary BC with node-negative disease with microarray data (U133) who did not receive adjuvant systemic treatment (n=867 of which n=183 TNBC). Data retrieved from gene expression omnibus GSE2034, GSE5327, GSE11121, GSE2990 and GSE7390. Clinical details of the combined cohort have been described previously[9].

Healthy tissues: RNAseq data of 5 databases covering 66 healthy tissues (Uhlen's Lab: n=122 individuals, n=32 tissues; GTEx: n=1,315 individuals, n=63 tissues; Illumina body map: n=32 individuals, n=17 tissues; human proteome map: n=30 individuals, n=26 tissues; Synders Lab: n=210 individuals, n=32 tissues) were downloaded from Expression atlas (TPM normalized).

Code of conduct

This study was performed according the Declaration of Helsinki and the "Code for Proper Secondary Use of Human Tissue in The Netherlands" (version 2002, update 2011) of the Federation of Medical Scientific Societies (FMSF) (http://www.federa.org/). The latter codes aligns with authorized use of coded spare tissue for research. Data analysis and ex vivo analysis was approved by the medical ethical committee at Erasmus MC (MEC.02.953 and MEC-2020-0090, respectively). According to national guidelines, no informed consent was required for this study.

Expression analysis

Gene expression (RNAseq, microarray and qPCR): Expression of >200 intracellular target antigens was analyzed in healthy and tumor tissues. Expression of PCT2 was evaluated in 5 different public databases of healthy tissues and was considered expressed in a tissue when TPM values reached the threshold of TPM>0.2 in at least 2 cohorts (**Figure 2A**; threshold set according to expression of reference antigen, i.e., NY-ESO1). Expression in tumors (TCGA) was classified as follows: TPM values between 1-10, between10-100, and >100 were valued as low, moderate, and high expression, respectively. In case of or geTMM-normalized RNAseq data (TNBC cohort 1) or microarray data (TNBC Cohort 2), the expression cut off was set at the third quartile of all intracellular targets, and targets were subsequently ranked based on the percentage of positive tumors (**Figure S1C**). Quantitative PCR (qPCR) was

performed on normal human tissue cDNA panels (OriGene Technologies, Rockville, MD) using MX3000 to quantify PCT2 mRNA expression (TaqMan probe), PCT2B (Taqman probe) and GAPDH (TaqMan probe: Hs02758991_g1) of 48 healthy human tissues. Ct values of genes of interest were normalized to the Ct values of GAPDH and relative expression was expressed as 2-dCt.

Immunohistochemical staining

IHC stainings were performed using large cores of healthy tissues (2mm in diameter) covering 16 major tissues (see **Figure 1C**) from 2-6 individuals (derived from autopsy or resection, n=62, see supplementary Table 1 for details) as well as FFPE tissue microarrays of TNBC tumor tissue (n=338 patientswhich have been described previously)406 (see Figure 2D). Staining with anti-PCT2 antibody was performed following heat-induced antigen retrieval for 20 min, pH6 at 95 °C. After cooling to RT, staining was visualized by the anti-mouse EnVision+® System-HRP (DAB) (Dako-Cytomation, Glostrup, Denmark). Stainings were manually scored on intensity and percentage of positive tumor cells, using Distiller (SlidePath) software independently by DH, MDK and AMT.

Identification, selection and ranking of epitopes

Prediction and immunopeptidomics: Peptides were predicted according to different in silico methods that assessed different aspects of immune reactivity[201] (i.e., NetMHCpan[407], NetCTLpan[291], SYFPEITHI[408] and RANKPEP[379,409,410]). For immunopeptidomics, the PCT2-overexpressing MDA-MB231 cell line ($3x10^8$ cells) was treated with IFNγ for 24h and harvested using EDTA before immunoprecipitation of HLA-I complexes. Peptides were eluted and measured with mass spectrometry as described by (de Beijer et al., manuscript submitted). The top 10 predicted peptides per tool (n=17 unique peptides) as well as the unique peptides retrieved from immunopeptidomics (n=2) were checked for cross-reactivity with Expitope (see **Figure S2C**), and peptides with up to 2 amino acid mismatches were excluded from further analysis. Selected peptides (n=14) were ordered at ThinkPeptides (ProImmune, Oxford, United Kingdom), dissolved in 50-75% DMSO and stored at -20°C until use.

HLA-A2 stabilization assay and ranking of epitopes: The HLA-A2 stabilization assay was performed using T2 cells as described in[411]. In short, $0{,}15x10^6$ T2 cells (LCLxT lymphoblastoid hybrid cell line 0.1743CEM.T2) were incubated with different peptide concentrations for 3h at 37°C in serum-free RPMI medium supplemented with 3µg/mL β2-microglobulin (Sigma). Surface expressed HLA-A2 molecules were measured with flow cytometry using the HLA-A2 mAb BB7.2 (BD Pharmingen, 1:20).

To this end, T2 cells were washed, and stained using fluorescently labeled antibody, incubated 25 min on ice in the dark, and dissolved in 1% FBS PBS. Cells were gated for viability, events were acquired on a FACSCanto flow cytometer and analyzed using FlowJo software (TreeStar, Ashland, OR). T2 cells without peptide were used as a baseline measurement. In a first screen, peptides at a fixed concentration of 25µg/ml that induced >1.1-fold change over baseline (11 out of 14, see **Figure 2C**) were further titrated from 0,316 to 31,6 µg/ml (**Figure S2B**). Titrations yielded two parameters of binding avidity to HLA-A2, namely amplitude, which was calculated by the fluorescence intensity of the highest concentration subtracted by the fluorescence intensity of the baseline; and EC50, which was calculated using GraphPad Prizm software using dose-response fitting. Epitopes were selected when their amplitude was minimally half of the amplitude of the reference gp100 eptope YLEPGPVTA and EC50 was minimally $1E^{-5}$; remaining epitopes were finally ranked from low to high EC50 values (**Figure 2D**).

Enrichment of T cells

Isolation of TILs from PCT2/A2+ BC patient: Freshly excised tumor material was cut in small fragments (~1x1x1mm) and placed into 24-well plates containing T cell medium supplemented with 2,000IU human rIL2 and 0.3% 2-mercapto-ethanol. 200ul fresh T cell medium was added twice weekly. After 2 weeks, remaining fragments were removed and cells ($1.5x10^6$, 90% CD3+) were used for enrichment of epitope-specific T cells (see below).

Enrichment of PCT2 epitope-specific CD8 T cells from healthy donor PBMCs: Enrichment of epitope-specific CD8 T cells was performed principally according to the protocol described by Butler and colleagues[412], but included the following amendments. CD8 T lymphocytes were collected from PBMCs by magnetic-activated cell sorting (MACS) according to the CD8 isolation kit (Miltenyi Biotec). CD8 T cells with > 95% purity were subsequently cultured in T cell medium supplemented with IL-2 (36 IU/mL; but no gentamycin) for 1 day, after which expansion cycles started. K562ABC cells (kindly provided by Prof. Bruce Levine, University of Pennsylvania, PA) were loaded with 10 µg/ml epitope and incubated for 5h at RT in serum-free medium, after which cells were washed and fixed with 0,1% paraformaldehyde (PFA). After washing, K562ABC cells were suspended at $0.1x10^6$/mL and co-cultured with T cells in a 1:20 ratio. IL-2 (36IU/mL) and IL-15 (20ng/µL) were added at days 1 and 3 days after start of co-culture, and T cells were counted after 6 days, suspended at $2x10^6$/mL and rested for 1 day, after which the next cycle commenced (which was repeated up to 4 or 5 cycles). Following 4 and 5 cycles, T cells were stained with

pMHC multimers (HLA*0201/epi4 and HLA*0201/epi12, Immudex, Copenhagen, Denmark). T cells were pre-incubated with pMHC-PE at RT for 10 min followed by incubation with 7AAD, anti-CD3-FITC and anti-CD8-APC for 20 min. T cells were fixed with 1% paraformaldehyde and TCR surface expression was measured and analyzed using FlowJoX software. To test PCT2-specific IFNγ production, T2 cells ($4x10^6$/mL) were loaded with epitope (20ng/mL) for 30 min, and T cells ($2x10^5$) were cultured in a 1:1 ratio with T2 cells in a round bottom 96-wells plate. Supernatant was collected at 24h and IFN-γ production was measured with the Enzyme-linked immunosorbent assay (ELISA, Invitrogen) according to manufacturer's protocol. T2 cells without peptide were included as a negative control; and staphylococcal enterotoxin B (0.1µg, Sigma) was used as a positive control. To obtain PCT2-spepcific TCRs, enriched T cells were either single cell diluted following IFNγ secretion (Milentyi Biotec) or FACS-sorted with pMHC multimers. For the former procedure, T cells were stimulated with irradiated BSM cells, and IFNγ secreting cells were captured according manufacturers recommendations.

Obtaining and testing TCRs

TCR cloning and sequence identification: CD8 T cells were exposed to the SMARTerTM RACE cDNA Amplification Kit (Clontech) to identify PCT2 TCRα- and β- chains. In brief, RNA was isolated by spin column purification (NucleoSpin, Macherey-Nagel) after which 5'RACE ready cDNA was made as described previously[413], and PCR was performed to amplify TCR-V encoding regions. Initial products were re-amplified by nested PCRs, cloned into the TOPO 2.1 vector (Invitrogen), and subjected to DNA sequencing. TCRα and TCRβ sequences were verified in at least twelve colonies. Using the IMGT database and the HighV-QUEST tool (http://www.imgt.org), the TCR V, D, and J sequences were classified according to the Lefranc nomenclature.

TCR gene transfer and in vitro testing: TCRα and TCRβ genes were codon optimized (GeneArt, Regensburg, Germany) and cloned into the pMP71 vector (a kind gift of Prof. Wolfgang Uckert, MDC, Berlin, Germany) using a TCRβ-2A-TCRα cassette that was flanked by NotI and EcoRI restriction sites. Upon activation with anti-CD3 mAb OKT3, PBMCs from healthy donors were transduced with TCR-encoding retroviruses or empty vector that were produced by a co-culture of 293T and Phoenix-Ampho packaging cells, as described previously[414,415]. Staining of surface-expressed TCRs was performed as described above. Transduced T cells ($6×10^4$/well in a 96-well plate) were co-cultured with BSM cells (loaded with titrated amounts of epitope ranging from 1 pM to 1 µM) or tumor cells ($2×10^4$/well) in a total volume of 200

µl of T cell medium for 24h at 37°C. Half-maximal effective concentrations of PCT2 or control peptide gp100 (EC50) required for T cell IFN-γ production were calculated using GraphPad Prism 5 software using dose response curve-fitting. The recognition motif was determined in a co-culture of T2 cells loaded with peptides containing individual alanines as replacements at every single amino acid position in the cognate peptide. Critical positions were determined as >50% decrease in IFNγ-production compared to the cognate peptide. The resulting motif was scanned for occurrence in the humane proteome using https://prosite.expasy.org/scanprosite/.

6.6 Supplementary data

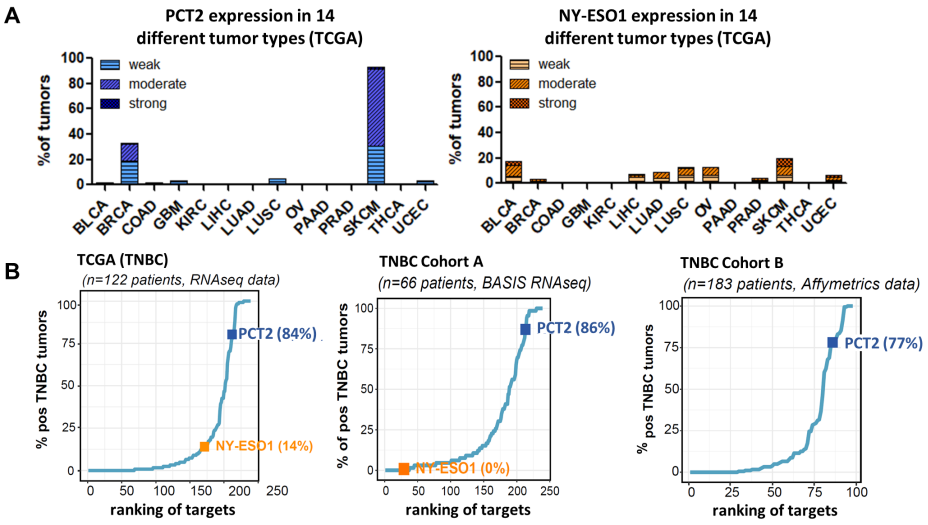

Supplementary figure 1. PCT2 mRNA is expressed in multiple tumors types. A. Bar graphs show fraction of tumors with weak (TPM 1-10), moderate (TPM 10-100) and strong (TPM >100) gene expression of PCT2 in 14 tumor types (TCGA, RNAseq data, n=6670). **B**. Ranking of targets according to percentage of TNBC tumors positive for PCT2. In both B and C, NY-ESO1 is taken along as a control. **Abbreviations**: BLCA, Bladder Urothelial Carcinoma; BRCA, Breast Carcinoma; COAD, Colon Adenocarcinoma; GBM, Glioblastoma Multiforme; KIRC, Kidney Renal Clear Cell Carcinoma; LIHC, Liver Hepatocellular Carcinoma; LUAD, Lung Adenocarcinoma; LUSC, Lung Squamous Cell Carcinoma; OV, Ovarian Serous Cystadenocarcinoma; PAAD, Pancreatic Adenocarcinoma; PRAD, Prostate Adenocarcinoma; SKCM, Skin Cutaneous Melanoma; THCA, Thyroid Carcinoma; UCEC, Uterine Corpus Endometrial Carcinoma.

A

Soure	Peptides	0 mismatch	1 mismatch	2 mismatch
Predicted	**epi5**	No	No	No
	epi12	No	No	No
	epi14	No	No	No
	epi15	No	No	5 proteins
	epi3	No	No	No
	epi13	No	No	No
	epi2	No	No	No
	epi9	No	No	No
	epi4	No	No	No
	epi7	No	No	No
	epi10	No	No	No
	epi16	No	No	3 proteins
	epi6	No	No	No
	epi17	No	No	1 protein
	epi8	No	No	No
	epi18	No	No	>5 proteins
	epi19	No	No	2 proteins
Eluted	**epi1**	No	No	No
	epi11	No	No	No

B

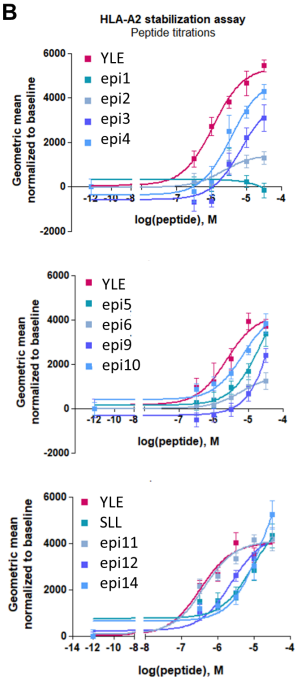

Supplementary Figure 2. Assessing cross-reactivity and avidity of HLA-A2 binding of PCT2 peptides. A. Predicted and eluted peptides tested for cross-reactivity with Expitope. **B**. Peptides with fold change >1.1 over no peptide (see Figure 3B) were tested using titrated amounts (range from: 31nM to 31 μM). EC50 values were calculated with GraphPad software 5 (n=3), see Figure 3D. Gp100 peptide YLEPGPVTA was used as a positive control and NY-ESO peptide SLLMWITQV as a reference peptide. Representative titration curves are shown.

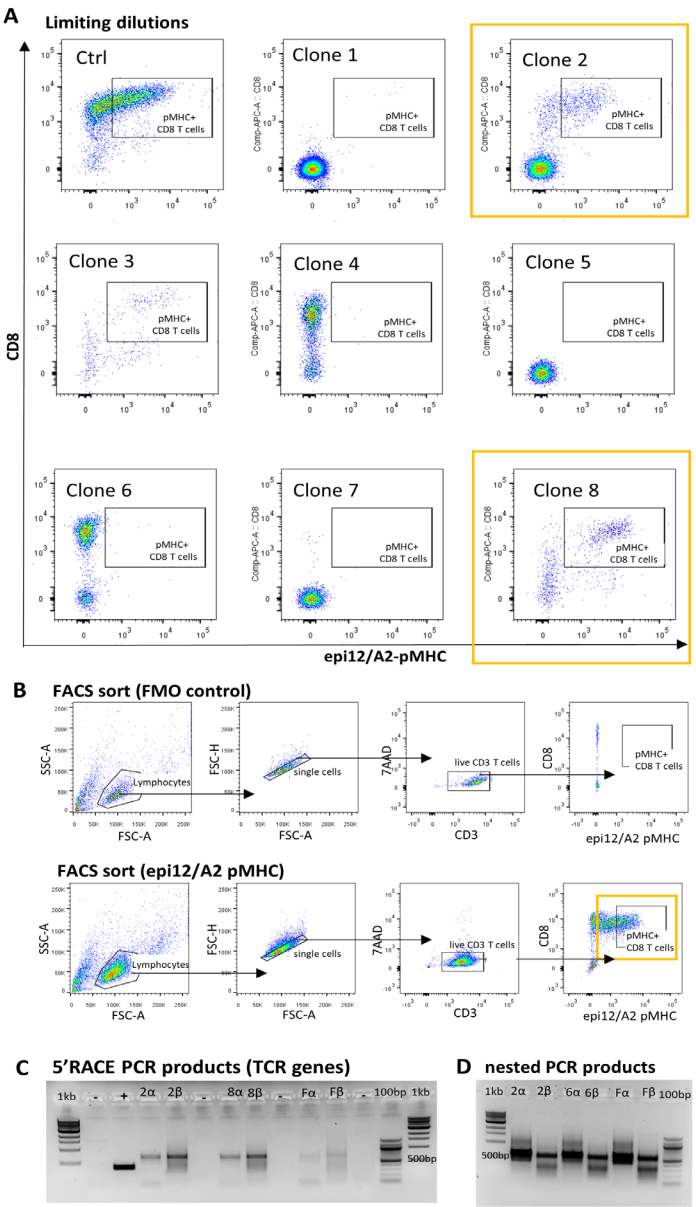

Supplementary Figure 3. Isolation of PCT2-specific TCRs. A. Flow cytometry plots show epi12/A2 pMHC staining of T cells directly after 5 cycles of enrichment (control) and T cells derived from different clones following IFNy capture (see Materials and Methods for details, clone 1-8). Samples with yellow squares were used for 5'RACE PCR and sequencing. **B**. Flow cytometry plots of T cells after 5 cycles of enrichment that were FACS-sorted with epi12/A2-pMHC multimers and corresponding fluorescence minus one (FMO) controls. Sample with yellow square was used for 5'RACE PCR and sequencing. **C**. Gel shows bands of 5'RACE products for TCR alpha and beta genes. + indicates positive PCR control; α and β indicate RACE products for TCR alpha and beta genes for clones 2 and 8 from limiting dilution and the pMHC FACS-sorted (F) population. **D** Gel shows an additional amplification step using nested primers.

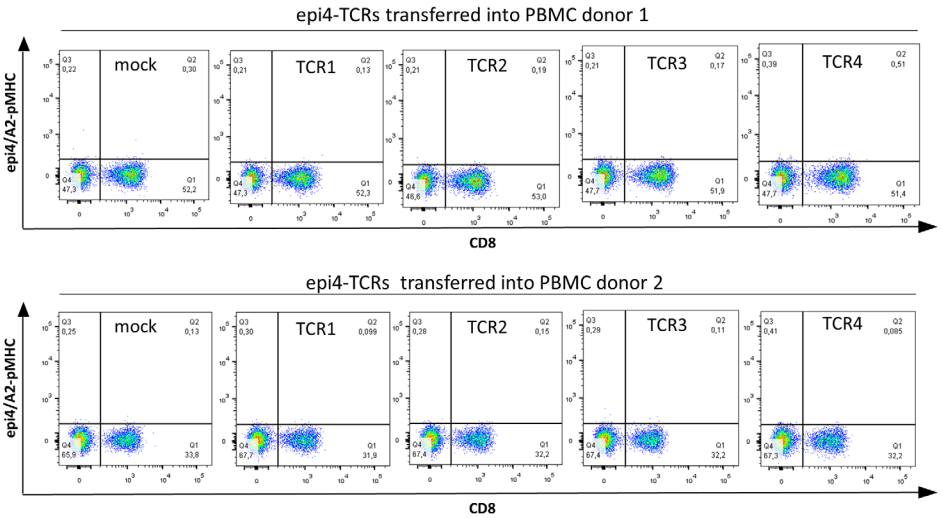

Supplementary Figure 4. Epi4 TCRs do not bind pMHC following gene transfer. Gene transfer of epi4/A2 TCR1-4 in T cells from 2 healthy donors, and lack of binding of epi4/A2 pMHC multimer.

TMA	tissue	origin
X	**X1**	
Y1	liver	resection/ adjacent normal
Y2	stomach	resection/ adjacent normal
Y3	lymph node	resection/ adjacent normal
Y4	heart	autopsy / normal
Y5	small intestine	autopsy / normal
Y6	skin	autopsy / normal
Y7	testis	resection/ adjacent normal
Y8	lung	resection/ adjacent normal
Y9	brain	autopsy / normal
Y10	pancreas	autopsy / normal
Y11	kidney	autopsy / normal
X	**X2**	
Y1	liver	resection/ adjacent normal
Y2	stomach	resection/ adjacent normal
Y3	lymph node	resection/ adjacent normal
Y4	intestine	resection/ adjacent normal
Y5	breast	resection/ adjacent normal
Y6	skin	autopsy / normal
Y7	testis	resection/ adjacent normal
Y8	lung	resection/ adjacent normal
Y9	brain	resection/ adjacent normal
Y10	pancreas	resection/ adjacent normal
Y11	kidney	resection/ adjacent normal
X	**X3**	
Y1	liver	resection/ adjacent normal
Y2	stomach	autopsy / normal
Y3	lymph node	resection/ adjacent normal
Y4	intestine	resection/ adjacent normal
Y5	breast	resection/ adjacent normal
Y6	skin/ nipple	resection/ adjacent normal
Y7	lung	autopsy / normal
Y8	muscle	autopsy / normal
Y9	brain	autopsy / normal
Y10	pancreas	autopsy / normal
Y11	kidney	resection/ adjacent normal

TMA	tissue	origin
X	**X4**	
Y1	liver	autopsy / normal
Y2	stomach	autopsy / normal
Y3	lymph node	autopsy / normal
Y4	small intestine	autopsy / normal
Y5	breast	resection/ adjacent normal
Y6	skin	resection/ adjacent normal
Y7	lung	resection/ adjacent normal
Y8	muscle	resection/ adjacent normal
Y9	pancreas	resection/ adjacent normal
Y10	kidney	resection/ adjacent normal
X	**X5**	
Y1	liver	autopsy / normal
Y2	stomach	autopsy / normal
Y3	thyroid	resection/ adjacent normal
Y4	large intestine	autopsy / normal
Y5	breast	resection/ adjacent normal
Y6	skin	resection/ adjacent normal
Y7	lung	resection/ adjacent normal
Y8	muscle	autopsy / normal
Y9	pancreas	resection/ adjacent normal
Y10	kidney	resection/ adjacent normal
X	**X6**	
Y1	liver	autopsy / normal
Y2	stomach	autopsy / normal
Y3	heart	autopsy / normal
Y4	intestine	resection/ adjacent normal
Y5	skin	resection/ adjacent normal
Y6	testis	resection/ adjacent normal
Y7	lung	resection/ adjacent normal
Y8	nipple	resection/ adjacent normal
Y9	pancreas	resection/ adjacent normal
Y10	kidney	resection/ adjacent normal

Supplementary Table 1. Overview of healthy tissue TMA. Table lists healthy tissues, their origin and whether derived from adjacent normal or completely normal tissues.

Chapter 7

Orthotopic T-cell engineering via CRISPR

Dian Kortleve, Dora Hammerl and Reno Debets

Laboratory of Tumor Immunology, Erasmus MC-Cancer Institute, Rotterdam, the Netherlands

Nature Biomedical Engineering, 2019, DOI: 10.1038/s41551-019-0490-4

The simultaneous removal of an endogenous T-cell receptor chain and the orthotopic placement of an exogenous receptor in human T cells via CRISPR gene editing prevents the mispairing between endogenous and transgenic receptors while preserving the cells' function.

Modifying human T cells for therapeutic purposes involves the ex vivo modification of a patient's T cells to make them express selected T-cell receptors (TCRs) specific for viral or tumour antigens, and the reinfusion of the modified cells back into the patient. The injected cells then mount an immune response to the specific pathogens or cancer cells[31]. Clinical trials for testing TCR-engineered T cells have shown promising results against various tumour types (in particular, melanoma, synovial sarcoma and multiple myeloma)[282,283], with objective response rates of 55–80% and complete response rates of 2–20% (ref.[31]). Because T cells express endogenous TCR αβ-chains, typical approaches for inserting exogenous TCRs in T cells may result in unwanted TCR combinations. In particular, TCR chain mispairing can occur when therapeutic TCR α-chains dimerize with endogenous TCR β-chains (or when therapeutic β-chains dimerize with endogenous α-chains), leading to mispaired heterodimers[411] with new (and often unknown) antigen specificities. Such TCR heterodimers may trigger autoimmune reactions or graft-versus-host disease[412]. Also, the introduced TCR chains can compete with endogenous chains for the limited pool of adapter CD3 molecules, which may result in reduced surface expression and function of the therapeutic TCR (ref. [413]). Moreover, the expression of the therapeutic TCR is often placed under the control of viral promotors, with loss of physiological regulation of TCR dynamics (including internalization and degradation of the TCR chains on antigen exposure[414]), which can result in tonic signalling of the therapeutic TCR, in decreased specificity, and in accelerated differentiation and exhaustion of the TCR-engineered T cells. Furthermore, the use of viral vectors to generate clinical T-cell products involves time-consuming production pipelines and high costs, and can cause the uncontrolled integration of the therapeutic TCR in the genome (with potential effects on the expression and function of other genes[415]). Reporting in Nature Biomedical Engineering, Dirk Busch and colleagues now show that the use of CRISPR- Cas9 gene editing to orthotopically insert a therapeutic TCR into the endogenous TCR α-chain (TRAC) locus of human T cells and the simultaneous deletion of the endogenous TCR β-chain locus (TRBC) abrogates the mispairing of TCR chains and preserves the physiological regulation of the inserted TCR (ref. [416]).

To study the assembly of individual TCR chains, Busch and colleagues used non-viral and viral gene-delivery methods to insert a fully human cytomegalovirus (CMV)-specific TCR, either via retroviral transduction (with or without knockout of TRAC)

or via CRISPR–Cas9-mediated knock-in into the endogenous TRAC locus. The engineered cells showed similar levels of cytokine production and peptide sensitivity regardless of the protocol used, raising the possibility that TCR mispairing still occurs in T cells expressing the endogenous TCR β-chain. Subsequent experiments for the identification of heterodimers of the inserted and endogenous TCR chains (in which the human therapeutic constant region of the TCR was replaced with a murine counterpart) showed no evidence of endogenous TCR expression (or of mispairing) when TRAC and TRBC were simultaneously targeted with CRISPR–Cas9 in human T cells. Notably, similarly to unmodified T cells, on antigen stimulation the engineered T cells produced cytokines and dynamically regulated the expression of TCR transgenes. Hence, appropriately paired TCRs with physiological dynamics, and better safety and functionality than virally transduced non-edited T cells, can be generated by shutting down the expression of both endogenous TCR chains and by inserting the therapeutic TCR orthotopically into the TRAC locus.

There are alternative strategies that diminish receptor mispairing and that enhance surface expression of the therapeutic TCR: in particular, TCR murinization, cysteine modification, the use of co-stimulatory domains[417], and the elimination of the endogenous TCR loci via microRNAs[418], zinc-finger nucleases[419], transcription activator-like effector nucleases[420] or CRISPR–Cas9. For instance, TRAC knockout via CRISPR–Cas9 and the viral introduction of template DNA encoding a CD19-specific chimeric antigen receptor into the same locus led to the regulation of the expression of the receptor by the endogenous TCR promoter (rather than by an exogenous viral promotor)[14]. Endowing an inserted TCR with an endogenous genetic regulatory domain led to the delaying of T-cell exhaustion and to enhanced performance of the engineered T cells for effective clearance of the target tumour in vivo[311]. Others performed TRBC knockout with CRISPR–Cas9, and lentivirally introduced a therapeutic TCR targeting the tumour-associated antigen NY-ESO-1; in this context the knockout T cells also showed increased expression and functionality of the therapeutic TCR when compared with T cells with intact endogenous TCR chains[421]. It is also possible to simultaneously perform non-viral TRAC knockout and TRAC knock-in of the TCR αβ-chains with CRISPR–Cas9 to generate TCR-modified T cells that target tumours expressing NY-ESO-1 (ref.[422]). Electroporation has also been used to knockout both TCR loci and to knock-in the TCR αβ-chains in the TRAC locus. Because TCRα and TCRβ chains may be regulated differently, it would be worthwhile to test the surplus value of knocking in an engineered TCR into both the TRAC and TRBC loci.

Busch and co-authors do not report the percentage of TRBC-knockout T cells when simultaneously editing the TRAC and TRBC loci. Yet they did not detect TCR mispairing, which is indicative of a high level of double-gene knockout. Although

knockout efficiencies of 50–90% are possible[311,421], it may be challenging to routinely achieve such high efficiencies in large-scale clinical settings without the need for additional screening, sorting, and method optimization. In addition, the evidence of homology-independent integration of the edited TRBC locus provided by the authors, together with the idea that the detection of random integration on a whole-genome level has low sensitivity, suggests that the system can still be optimized. Therapeutic T-cell engineering up to ~400 million TRAC knock-in cells can be generated after 10 days of in vitro expansion[16]; non-viral transfer of CRISPR–Cas9 and double-stranded DNA template may thus also be feasible in the clinical setting[422].

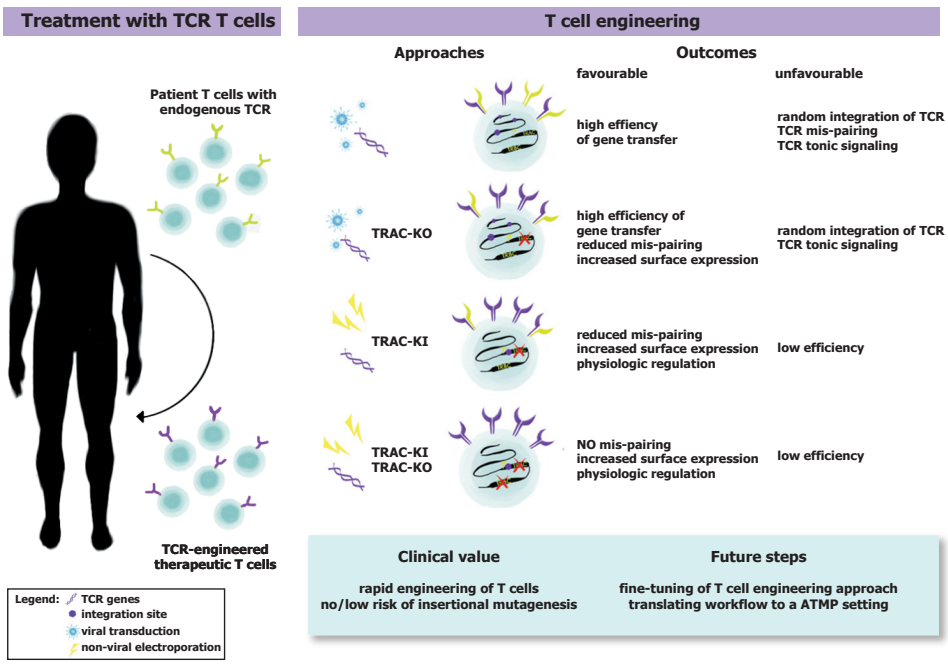

Fig. 1 | T-cell engineering for the generation of therapeutic T cells. The insertion of therapeutic T-cell receptors (TCRs) into human T cells can be done via viral and non-viral techniques (including the use of CRISPR-Cas9 gene editing with electroporation). Each approach has favourable and unfavourable outcomes, with simultaneous non-viral knock-in of the TCR alpha chain locus (TRAC-KI) and non-viral knockout of the TCR beta-chain locus (TRBC-KO) having particular advantages (although they will require optimization steps before they can be clinically implemented).

A drawback of non-viral delivery is its typically low gene-transfer efficiency; yet previous studies have shown that electroporated T cells are mostly viable and can be easily sorted prior to expansion. Although some of the procedures (CRISPR–Cas9 editing, cell sorting, and in vitro expansion of T cells) have been clinically applied,

cell manipulations may negatively affect cell viability and the sustained function of the engineered T cells. Studies of the long-term functionality of engineered T cells in preclinical models are limited because T-cell engineering methods have not been optimized for murine T cells, and new immune-competent models would need to be developed. Yet further insights may also come from clinical studies: for example, a phase-I trial (NCT03399448) in which virally delivered CRISPR–Cas9 is used for a triple knockout of the endogenous TRAC and TRBC loci and of the immune checkpoint factor programmed cell death-1, as well as of TRAC knock-in of NY-ESO1 TCR αβ-chains, is expected to shed light on the in-patient performance of the edited T cells. The next step would be non-viral editing and orthotopic delivery of TCR genes in a clinical setting. The optimization of technologies for the manufacturing of such T cells under requirements for advanced therapeutic medicinal products[423], the choice of safe antigen targets, and strategies to maximally sensitize tumours for T cells[201], provide a promising springboard for the clinical testing of improved engineered T cells.

Chapter 8

General Discussion

Chapter 8. General discussion

The major aims of this thesis were trying to close the knowledge-gap regarding T cell evasive mechanisms in breast cancer (BC, **Part 1**) and to identify new target antigens for adoptive T cell therapy to treat triple negative BC (TNBC, **Part 2**). This final chapter briefly summarizes and discusses the main outcomes, and puts them in perspective of future pre-clinical as well as clinical studies.

8.1 Outcomes Part 1: Charting T cell evasion

- Aspects of CD8 T cell immunity, such as antigen processing and presentation, co-signaling, clonality and subset distribution, and not mere numbers of CD8 T cells, determine patient survival of BC subtypes
- A gene classifier accurately assigns spatial immunophenotypes, is prognostic in TNBC, and various other cancers and predicts anti-PD1 response in metastatic TNBC
- Next to TNBC, also HER-2 and luminal-B subtypes show markers that reflect anti-tumor T cell responses which suggest that at least a subset of these BC subtypes can benefit from (combination) immune therapies
- Spatial immunophenotypes in TNBC are characterized by distinct T cell evasive pathways that advocate immune therapy in combination with drugs that provide phenotype-specific sensitization

Box 1. Major findings

Stratifying BC patients for immune therapies

As discussed in **Chapter 2** and based on the outcome of studies in **Chapter 3**, it is concluded that BC subtypes are not equally immunogenic, which is reflected by differential antigen load as well as differential prognostic values of tumor infiltrating lymphocytes (TIL). Antigenicity (i.e., expression of antigens, such as cancer germline antigens (CGAs) and neoantigens) and numbers of TILs are generally higher in the more aggressive ER-negative subtypes, especially in TNBC. Taken the differences in antigenicity into account, it is not surprising that initial ICI trials showed the best responses in ER- disease, whereas ER+ (luminal) BC is generally considered unresponsive to ICI. In contrast to other tumor types, antigenicity turns out not to be a predictor of ICI response in TNBC[19–21]. Interestingly, mutations in the DNA-damage repair genes BRCA1 or BRCA2, which have been linked to high frequencies of

neoantigens[424] and release of pro-inflammatory cytokines[425], however, were not predictive for ICI response in TNBC[218]. In fact, we showed in **Chapter 3** and in **Chapter 4** that neoantigens, irrespective of their type, only weakly correlate with numbers of TILs, and that BRCA status is not associated with a CD8 T cell inflamed phenotype. Notably, using node-negative, not systemically treated BC we observed that not TIL frequency per se, but rather markers reflecting an anti-tumor CD8 T cell response significantly impact prognosis in BC subtypes. Such markers include: (1) T cell subset distribution; (2) TCR clonality; (3) gene-expression of molecules that contribute to T cell-co inhibition and (4) antigen processing and presentation. Since the above markers are all measures of the effectiveness of an anti-tumor CD8 T cell response, we argue that these markers may serve well as predictive markers for ICI response in BC. In fact, TCR clonality has already been associated with anti-PD1 response in TNBC, and several studies have shown that PD-L1 expression (an immune checkpoint ligand that shows up-regulated expression following IFNy exposure) is correlated with response to ICI in TNBC and other BC subtypes. Furthermore, expression of the above-mentioned markers indicates that next to TNBC, at least a subset of HER2 and luminal-B subtypes may very well be immunogenic and responsive to immune therapies. Along this line, recent studies have shown that PD-L1+ HER2 subtypes as well as ER+ BC patients benefit from ICI: ORs in metastatic PD-L1+ HER2+ and PDL-1+ ER+ patients were 15% and 12%, respectively[219,426]. More trials are underway[427], and it is exciting to see how this type of therapy will further develop for different BC subtypes.

In a pan-cancer setting, it has become more and more evident that next to numbers and activation status of TILs, also their spatial localization matters with respect to survival and therapy responsiveness[27,244,246,249,251]. With this in mind, we have studied the spatial immune contexture in relation to clinical outcome in treatment-naïve TNBC and anti-PD1-treated metastatic TNBC (**Chapter 4**). In these studies, we have identified 3 dominant spatial immunophenotypes (covering nearly 100% of all tested cases), namely: the excluded immunophenotype, which was characterized by tumor margin-restricted localization of CD8 T cells; the ignored immunophenotype, which was characterized by absence of CD8 T cells; and the inflamed immunophenotype, which was characterized by the presence of intra-tumoral CD8 T cells that are evenly distributed among tumor margin and center. These spatial immunophenotypes could be captured by a gene-classifier, and had differential prognostic value in TNBC (i.e., the inflamed phenotype had the best survival, the ignored phenotype had the worst survival). Moreover, this gene-classifier also had prognostic value in cervical cancer, head and neck cancer, kidney cancer, bladder cancer and melanoma. We observed that the inflamed phenotype was enriched in those cancer types that generally respond well to ICI while the excluded and ignored phenotypes were

enriched in those cancer types that generally respond poorly to ICI. Importantly, the gene-classifier predicted response to anti-PD1 treatment in mTNBC with a negative predictive value of 0.9. In comparison, in the same dataset, PD-L1 expressed by immune cells, a currently and routinely used marker, had a negative predictive value of 0.4. Furthermore, we observed that assignment of different metastatic lesions from anti-PD1-treated TNBC resulted in a lower frequency of inflamed phenotypes, which is in line with recent reports[428,429]. This, together with the observation that assignment of these immunophenotypes did not depend on lesion site, argues that our gene-classifier may represent a viable and simple alternative to whole tissue stainings. In fact, the assignment of spatial phenotypes is based on the expression of 42 genes, which may be easily determined via standard molecular-based techniques and developed into a diagnostic tool. Collectively, these findings indicate that spatial immunophenotypes may improve patient stratification for ICI treatment and should be validated in other cohorts to test its value for incorporation into clinical practice.

Charting immune evasive mechanisms in BC

Despite the high number of studies on the prognostic and predictive value of TILs, up to now little emphasis has been given to immune evasive mechanisms in BC. In general terms, tumors may evade T cell control by: limiting T cell influx (i.e., down-regulation of expression of chemo-attractants or T cell adhesion molecules); halting the antigen processing and presentation machinery (i.e., selection for loss of function mutation); and lastly, suppressing T cell function (i.e., recruitment of suppressor cells, up-regulation of expression of co-inhibitory molecules and suppressive cytokines). New technologies, such as next-generation sequencing (NGS) and multiplexed imaging enable charting and identification of T cell evasive mechanisms (reviewed in **Chapter 5**). Along this line, we have studied the differential occurrence of T cell evasive pathways among BC subtypes using omics tools in **Chapter 3** and performed in-depth and integrated analysis of NGS and multiplexed images from primary TNBC in **Chapter 4**. These chapters pinpointed towards different T cell evasive strategies in BC subtypes, which are shortly discussed below, including possible consequences for treatment choices, and illustrated in **Figure 1**.

Multi-parameter omics analysis suggests that luminal-B BC is characterized by low numbers of TILs, which may be caused by decreased retention of T cells from the blood in line with our observation of low expression of T cell adhesion molecules. In this regard, luminal-B BC may benefit from therapies that facilitate T cell infiltration, such as the CDK4/6 inhibitors abemaciclib, ribiciclib, or palbociclib. These agents have significantly improved standard-of-care treatment of hormone receptor-positive

BC. Their mechanisms of action are considered to be modulation of the immune micro-environment via up-regulated expression of type-I IFN response genes, and antigen processing and presentation genes. Notably, these agents were shown to be able to reverse a gene program in BC cell lines, which is associated with CD8 T cell exclusion in melanoma[251,430]. These preclinical results are encouraging, and suggest that ER+ BC may be primed for ICI when pre-treated with CDK4/6 inhibitors. In fact, a combination of abemaciclib and pembrolizumab induced OR in 14% of unselected, metastatic HR+ HER2- BC patients[430,431]. Furthermore, in Luminal-B BC we have observed high frequencies of M2 macrophages and regulatory T cells which may represent additional targets for combination therapies. Besides potentially enhancing clinical benefit of ICIs, inhibition of M2 macrophage may also improve standard therapies for ER+ BC as preclinical models have revealed that M2 macrophages facilitate endocrine resistance in BC[432]. Nevertheless, M2 inhibition has not yet been assessed clinically in BC, a path that certainly warrants future testing.

Similarly, luminal-A BC is characterized by low numbers of TIL, and presence of M2 macrophages and regulatory T cells but in contrast to luminal-B BC, also low antigen load. This together with lack of prognostic value of immune parameters imply that this type of BC is unlikely to respond to immune therapies. Nevertheless, suppressor cells may represent actionable targets for combination therapies.

HER2+ BC showed high numbers of TILs yet relatively few signs of anti-tumor T cell reactivity (i.e., few expanded TCR clones, low expression of co-signaling genes, and low frequencies of immune-suppressor cells). This type of BC is standardly treated with HER2-blocking antibodies, such as trastuzumab, and their modes of action have at least in part been related to antibody-dependent cellular toxicity and reported to provide synergistic effects when combined with ICI in preclinical models[16]. Given the low numbers of tumor-specific CD8 T cells and a relatively high antigen load, we argue that HER2+ BC is amenable to adoptive T cell therapy targeting other antigens than HER2. Future studies may utilize the strategy we applied in **Part 2**, to identify safe and effective T cell targets in BC subtypes other than TNBC (see section 8.2).

When compared to other BC subtypes, TNBC showed the highest number of clonally expanded TCRs and also the highest expression of genes that represent immune-suppressive mediators, myeloid-derived suppressor cells and oncogenic and T cell evasive pathways. When zooming in on the 3 spatial immunophenotypes as introduced above, we have identified unique determinants and evasive pathways that would warrant immunophenotype-specific combination therapies to treat TNBC. In brief, the excluded phenotype, which was associated with resistance to anti-PD1, demonstrated: deposits of collagen-10 that likely provide a physical barrier to CD8 T cells; highest expression of genes related to glycolysis that may provide an un-

favorable environment for T cells; and highest gene-expression of serine protease inhibitors (SPI) that may limit T cell-mediated killing of tumor cells. All T cell evasive paths that occurred in the excluded phenotype were inversely correlated to the presence of CD8 T cells and associated with the activation of TGFβ/VEGF pathways. We argue that antagonizing TGFβ/VEGF pathways may limit T cell exclusion. In this regard, several inhibitors of the TGFβ/VEGF pathways are in clinical developments but have not yet been tested in combination with ICI in BC. Also, SPI represent interesting drug-targets as some members of this protein family (i.e., SERPINB3, SERPINB4 and SERPINB9) have been related to ICI resistance in melanoma[433,434], and certain SPI can inhibit granzymes and/or caspases and could thereby promote tumor survival[276,433]. Nevertheless, their exact role in T cell evasion remains elusive and requires further research. The ignored phenotype was also associated with resistance to anti-PD1 and demonstrated either high density of immune-suppressive M2 macrophages, which have been reported to suppress CD8 T cells, or activation of WNT/PPARγ pathways, which was inversely correlated to numbers of CD8 T cells and CLEC9A+ dendritic cells (DC). These observations suggest that antagonizing M2 macrophages or WNT/PPARγ pathways may promote CD8 T cell infiltration into ignored tumors and thereby sensitize them for immune therapies. In fact, a combination of WNT inhibition and ICI is currently being assessed in clinical trials including TNBC, albeit not stratified for presence of CD8 T cells. Finally, the inflamed phenotype, which was associated with response to anti-PD1, demonstrated signs of necrosis and a high density of CLEC9A+ DC that may trigger recruitment of CD8 T cells into the tumor. Also, the inflamed phenotypes showed a high TCR clonality that was independent of the quantity of neo-antigens. Notably, this phenotype showed signs of adaptive T cell evasion, such as enhanced expression of T-cell co-inhibitory receptors, high densities of M2 macrophages, and decreased expression of MHC molecules by tumor cells. Although the inflamed phenotype is generally most responsive to ICI, inflamed tumors may benefit from drugs that inhibit M2 macrophages or drugs that enhance antigen presentation, such as epigenetic drugs.

8.2 Outcomes Part 2: Exploring new targets for T cells

- Sequential use of new in silico as well as laboratory tools enable selection of potentially safe and effective target antigens, epitopes and TCRs
- PCT2 represents a highly and homogeneously expressed target antigen for adoptive T cell therapy in TNBC with little predicted risk for on-target toxicity

Box 2. Major findings Part 2

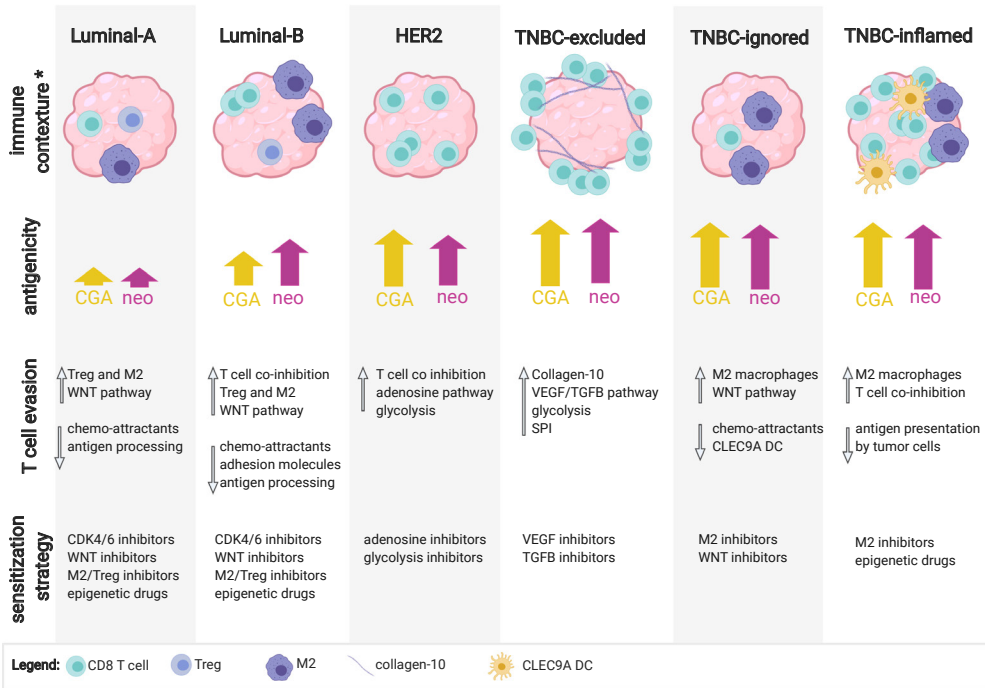

Figure 1. Charting T cell evasion in BC subtypes. Luminal-A, Luminal-B and HER2 BC were studied using multi-parameter omics analysis and TNBC were studied using omics tools and multiplexed imaging techniques, resulting in subdivision into 3 spatial immunophenotypes (TNBC-excluded, TNBC-ignored and TNBC-inflamed). Top panel shows most prominent differences in immune contextures per BC subtype; arrows in second panel show the relative frequency of cancer germline antigens (CGA) and neo-antigens (neo); arrows in third panel indicate a relative increase or decrease of different paths of T cell evasion; lowest panel lists possible combinations to sensitize tumors for immune therapies. * immune contexture of Luminal-A, Luminal-B and HER2 BC was studied based on transcriptome data only.

Is BC amenable for adoptive T cell therapy?

To date, only a hand full of studies were aimed to treat BC with adoptive T cell therapy. These studies mainly used CAR-T cells that target overexpressed antigens, such as HER2, mucin1 (MUC1), mesothelin and more recently the receptor tyrosine kinase-like orphan receptor 1 (ROR1). Notwithstanding promising preclinical results[398,435–437], the above treatments in humans were challenged by low objective response rates and treatment-related toxicities[438]. A disadvantage of CAR-T cells may be the limited pool of target antigens that are expressed on the tumor's cell surface, which compromises the selection of truly tumor-selective targets. In contrast, TCR-T cells are able to recognize extracellular as well as intracellular targets upon presentation via MHC-I or II, which maximizes the selection of target antigens. In this regard, CGAs, oncoviral or other tumor-selective intracellular targets may represent

interesting target candidates for TCR-T cell therapy. CGAs for example, are generally present in nucleus or intracellularly, some of which having potential roles in oncogenesis, and the thus far tested CGAs have shown clinical efficacy. In some cases, where CGAs were targeted with affinity-enhanced TCRs, overt toxicities were noted, whereas in other cases, where CGAs were targeted with natural TCRs against for example NY-ESO1, no toxicities were observed (see **Chapter 5** for details). This class of antigens is predominantly expressed in immune privileged tissues of the germline and often highly expressed in various malignancies. Interestingly, we observed that CGAs are frequently expressed in BC, particularly in TNBC (**Chapter 2** and **Chapter 3**), which potentially provides novel treatment options for this hard to treat BC subtype. Besides CGAs and other tumor-selective intracellular targets, the vast majority of TNBC also express at least 1 neoantigen[439] (i.e., non-self-antigens that are derived from nonsynonymous mutations), which can be recognized by T cells[440]. Nevertheless, neoantigens are rarely shared among patients and require personalized identification and selection of tumor-reactive TCRs. CGAs and oncoviral targets, however, are shared by a variety of patients and targeting this class of antigens enables stringent selection and testing of TCRs prior to patient inclusion, which in turn can be used as an “off-the shelf” cellular therapy.

Safety first!

In most cases, targets for TCRs are selected based on high expression in a given malignancy, whereas (limited) expression in healthy tissues is either accepted or neglected. T cells, however, are able to potently kill target antigens that express even very minute quantities of antigen[441], which, when targeting a self-antigen, have resulted in several clinical examples of severe on-target toxicities (a TCR’s cognate target that is expressed and recognized outside the tumor). In example, CAR-T cells targeting the overexpressed antigens CAIX and HER2 or TCR-T cells targeting MART1, gp100 or CEA have all resulted in severe on-target toxicities, which in some cases even resulted in fatalities (reviewed in [14,31,190]). To mitigate risks for on-target toxicities, we utilized a stringent selection process in **Chapter 6** which starts from absent expression of potential target antigens in healthy tissues (**Figure 2**). In case of intracellular targets, and using large public databases, we observed that PCT2 shows tumor-restricted expression, which many intracellular targets did not, arguing that TCR-targets should not be blindly chosen. Furthermore, we validated absent expression of PCT2 in healthy tissues using qPCR and immune stainings. In fact, we showed that PCT2 was expressed by 85% of TNBC patients and showed homogeneous expression in the majority of cases. The latter finding may potentially prevent immune editing (i.e., relapse of tumors following an initial response due to outgrowth

of antigen-negative clones). Our data so far suggest that PCT2 represents a safe and effective target antigen for AT in TNBC, which provided sufficient basis to continue our efforts to develop a PCT2-specific TCR.

Another safety concern of TCR engineering is off-target toxicity (a TCR's target that is highly similar yet not identical to cognate target, and expressed and recognized outside tumor). In order to mitigate the risk for off-target toxicity, we only consider protein-derived epitopes that were <80% identical with any other sequence in the human proteome. Furthermore, TCRs should not be affinity-enhanced and should be vigorously tested according to in vitro safety experiments as proposed in ref[287]. Such experiments have been performed for the PCT2 TCR as described in **Chapter 6**.

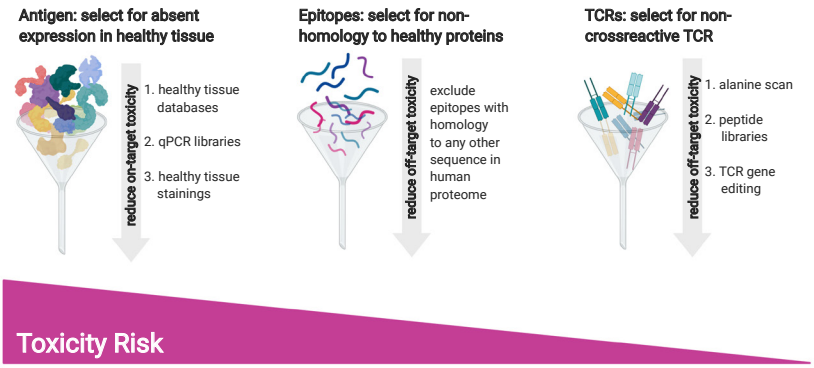

Figure 2. Risk reduction for AT-related toxicity through sequential in silico and in vitro assessment of antigens, epitopes and TCRs. Funnels illustrate filtering of target antigens (left), epitopes (middle) and TCRs (right) and include individual selection steps that are described in detail in Chapter 6.

In **Chapter 7** we have discussed recent developments regarding TCR editing technologies that potentially further minimize the risk for off-target toxicities. These developments include non-viral gene editing tools, such as CRISPR/CAS9, that enable insertion of TCR transgenes under the endogenous promoter while simultaneously knocking out the endogenous TCR loci[416]. Such TCR-edited cells have been shown to provide physiological regulation of TCR expression and at the same time prevent mispairing between exogenous TCR chains and endogenous TCR chains[312,416]. A recent study has shown that CRISPR-edited NY-ESO1 TCR T cells with simultaneous knock-out of endogenous TCR-α, TCR-β as well as PDCD1 genes were safely administered to 3 refractory cancer patients and resulted in long-term T cell engraftment, indicating that gene-editing is feasible in a clinical setting[442]. Clinical response has not been observed yet in this study, indicating that there are still challenges to address. Furthermore, the latter study used a viral delivery system, which, although

generally being more efficient, is considered less safe and has a higher regulatory burden for in-patient testing compared to non-viral delivery. Likely, some further optimizations are needed to efficiently produce edited T cells using non-viral editing techniques on a large scale under ATMP conditions. Taken together, this approach seems promising because it further improves safety of the T cell product and enables additional editing that potentially can enhance T cell fitness inside solid tumors.

Efficacy second!

Efficacy of AT does not only depend on the pharmacokinetics of the interaction between epitope and TCR, but also on the tumor micro-environment. Lack of efficacy of AT in solid tumors has been largely attributed to compromised T cell trafficking towards the tumor, reduced T cell persistence and reduced T cell activity due to the immune-suppressive microenvironment[31,225,443]. Similar to ICI in TNBC, AT is expected to require sensitization of tumors prior to infusion of T cells. To date, several trials investigate combinations of AT with chemotherapy, radiation, supplementation of cytokines or combination with ICI, but trials have not yet investigated combination treatments that are rationally selected based on their ability to counteract specific T cell evasive mechanisms. In particular, TNBC with an excluded or ignored immunophenotype may require combinations (as proposed in **Figure 1**) that facilitate infiltration of adoptively transferred T cells. TNBC tumors with an inflamed phenotype are likely to allow infiltration of T cells but once inside the tumor, adoptively transferred T cells may become functionally inhibited by M2 macrophages, which could represent a target of choice to sensitize inflamed tumors for AT.

8.3 Future perspective: the next steps towards effective immune therapies for breast cancer

Outstanding work

Part 1: It remains elusive whether spatial immunophenotypes can evolve and change over time due to immune-editing or upon selected treatments. In line, it is of interest whether different metastatic lesions can show different spatial phenotypes, as has been observed in ovarian cancer[444,445], which would challenge patient stratification and selection of optimal treatments based on spatial phenotype of a single biopsy. Finally, the above described evasive mechanisms, though generally recognized, should be functionally validated and phenotype-specific combinations with immune therapies should be evaluated in clinical trials.

Part2: In order to develop an optimal form of AT, more TCRs need be obtained and tested for their efficacy and safety using pre-clinical models. With respect to combinatorial approaches it is of interest whether the in Part 1 identified prognostic and predictive markers also apply for AT and whether spatial immunophenotypes turn out to be stable or evolve into another phenotype upon adoptive transfer of TCR-T cells. In case spatial phenotypes are stable, in particular excluded and ignored phenotypes likely require combinatorial approaches that enable effective T cell influx of TCR engineered cells.

Based on the outstanding work, future research should include a series of ex vivo and in vivo studies as illustrated in Figure 3 and briefly exemplified and described below. The clinical value of spatial immunophenotypes, and its relation to T cell evasion and immune-editing, is inherently linked to the question whether intra-patient heterogeneity with respect to spatial immunophenotypes exists. To this end, it is recommended to study spatial phenotypes in different metastatic lesions and monitor such phenotypes over time. In this regard, our spatial phenotype gene-classifier represents a fast and simple way to assign spatial immunophenotypes based on (serial-) biopsies from different lesions. CD8 immune stainings on the other hand yield more confident assignments, yet the latter method depends on the availability of whole tissue sections. Next, the proposed combinatorial approaches to counteract T cell evasion and to modulate spatial immunophenotypes require functional validation. To this end, short term ex-vivo studies in which tumor pieces (from a tumor with known spatial immunophenotype/T cell evasive mechanism) may be cultured together with autologous TIL or PBMC. Exposure of such a culture to the above proposed drugs may reveal whether the spatial architecture of the TME can be remodelled or not. Direct administration of immune modulators into tumor lesions via microinjections[446], may represent another approach to study modulation of immunophenotypes in patients. This approach requires sequential biopsies and assignment of spatial immunophenotypes pre- and post-injection.

With respect to AT, in addition to experiments performed in **Chapter 6**, future studies should include TCR-editing of cells as well as in vitro assays to ensure safety (screen for recognition of peptide libraries and panels of healthy cell lines) and potency of TCR T cells (recognition of BC cell lines, circulating tumor cells and organoids). Safe and effective TCRs should then further advance into murine studies in order to test their efficacy in a patient-derived xenograft (PDX) model. Furthermore, PDX mouse models will also shed light on the modulation of spatial immunophenotypes upon administration of tumor-specific T cells. Finally, the most safe and effective TCR should be tested in combination with the most effective immune modulator (which may be different per spatial immunophenotype).

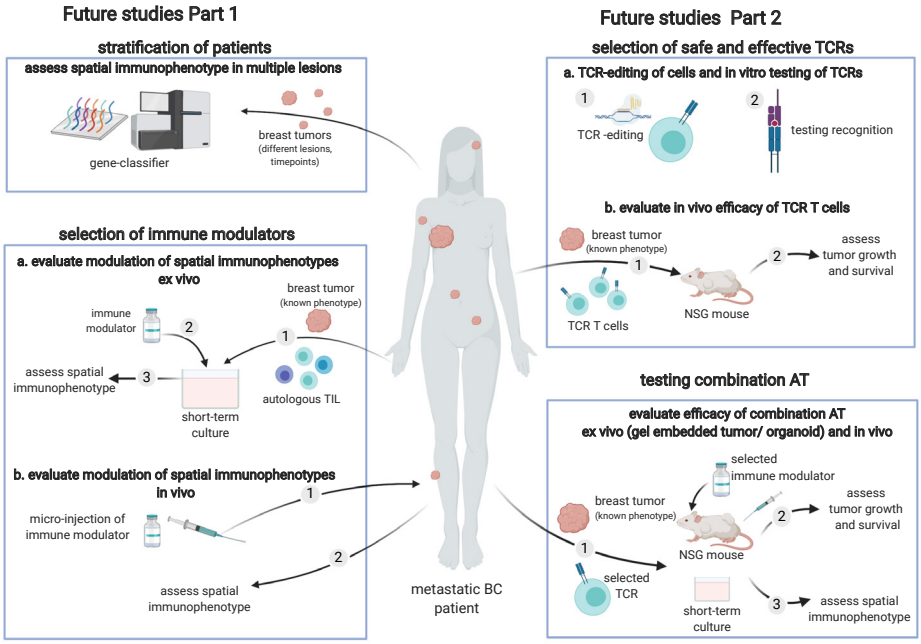

Figure 3. Future studies to select immune modulators and TCRs. Individual boxes visualize approaches to pursue the outstanding work based on research from Part 1 (left) and Part 2 (right) of this thesis. Arrows and numbers illustrate sequence of events.

8

Once optimal TCRs and drugs have been selected and validated, different immunophenotype-specific combinatorial approaches should advance into clinical trials. In the clinical setting (exemplified in **Figure 4**), a patients' biopsy can be transcriptome profiled in order to assign the spatial immunophenotype using the gene-classifier, the HLA-status with in silico typing algotithms (see also **Chapter 5**) and to assess expression of TCR target antigens. In case the patient expresses HLA-A2 as well as the target antigen, she could advance to AT combined with immunophenotype-specific modulators. In case the patient is not eligible for AT, she could advance to ICI in combination with immunophenotype-specific modulators.

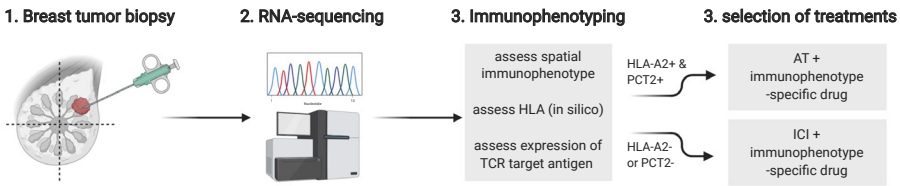

Figure 4. Patient and treatment selections into clinical practice. Flow-chart shows proposed individual steps for selection of (combination) immune therapies to treat BC.

8

References

References

1. Yang SX, Polley EC. Systemic treatment and radiotherapy, breast cancer subtypes, and survival after long-term clinical follow-up. *Breast Cancer Res Treat*. 2019;175(2):287-295. doi:10.1007/s10549-019-05142-x

2. Fragomeni SM, Sciallis A, Jeruss JS. Molecular Subtypes and Local-Regional Control of Breast Cancer. *Surg Oncol Clin N Am*. 2018;27(1):95-120. doi:10.1016/j.soc.2017.08.005

3. Moo T, Sanford R, Dang C, et al. Overview of Breast Cancer Therapy. 2019;13(3):339-354. doi:10.1016/j.cpet.2018.02.006.Overview

4. Luen SJ, Salgado R, Fox S, et al. Tumour-infiltrating lymphocytes in advanced HER2-positive breast cancer treated with pertuzumab or placebo in addition to trastuzumab and docetaxel: a retrospective analysis of the CLEOPATRA study. *Lancet Oncol*. 2017;18(1):52-62. doi:10.1016/S1470-2045(16)30631-3

5. Loi S, Drubay D, Adams S, et al. Tumor-Infiltrating Lymphocytes and Prognosis: A Pooled Individual Patient Analysis of Early-Stage Triple-Negative Breast Cancers. *J Clin Oncol*. 2019;37(7):559-569. doi:10.1200/JCO.18.01010

6. Ignatiadis M, Van den Eynden G, Roberto S, et al. Tumor-Infiltrating Lymphocytes in Patients Receiving Trastuzumab/Pertuzumab-Based Chemotherapy: A TRYPHAENA Substudy. *JNCI J Natl Cancer Inst*. 2018;111:69-77. doi:10.1093/jnci/djy076

7. Loi S, Michiels S, Salgado R, et al. Tumor infiltrating lymphocytes are prognostic in triple negative breast cancer and predictive for trastuzumab benefit in early breast cancer: Results from the FinHER trial. *Ann Oncol*. 2014;25(8):1544-1550. doi:10.1093/annonc/mdu112

8. Savas P, Salgado R, Denkert C, et al. Clinical relevance of host immunity in breast cancer: from TILs to the clinic. *Nat Rev Clin Oncol*. 2015. doi:10.1038/nrclinonc.2015.215

9. Hammerl D, Massink MPG, Smid M, et al. Clonality, antigen recognition and suppression of CD8+ T cells differentially affect prognosis of breast cancer subtypes. *Clin Cancer Res*. 2019. doi:10.1158/1078-0432.CCR-19-0285

10. Denkert C, von Minckwitz G, Darb-Esfahani S, et al. Tumour-infiltrating lymphocytes and prognosis in different subtypes of breast cancer: a pooled analysis of 3771 patients treated with neoadjuvant therapy. *Lancet Oncol*. 2018;19(1):40-50. doi:10.1016/S1470-2045(17)30904-X

11. Jang N, Kwon HJ, Park MH, Kang SH, Bae YK. Prognostic Value of Tumor-Infiltrating Lymphocyte Density Assessed Using a Standardized Method Based on Molecular Subtypes and Adjuvant Chemotherapy in Invasive

Breast Cancer. *Ann Surg Oncol*. 2018;25(4):937-946. doi:10.1245/s10434-017-6332-2

12. Hollingsworth RE, Jansen K. Turning the corner on therapeutic cancer vaccines. *npj Vaccines*. 2019;4(1):1-10. doi:10.1038/s41541-019-0103-y

13. Ganesan S, Mehnert J. Biomarkers for Response to Immune Checkpoint Blockade. *Annu Rev Cancer Biol*. 2020;4(1):331-351. doi:10.1146/annurev-cancerbio-030419-033604

14. Guedan S, Ruella M, June CH. Emerging Cellular Therapies for Cancer. *Annu Rev Immunol*. 2019;37(1):145-171. doi:10.1146/annurev-immunol-042718-041407

15. Russel L, Peng K. The emerging role of oncolytic virus therapy against cancer. *Clhin Clin Oncol*. 2018;176(1):139-148. doi:10.1016/j.physbeh.2017.03.040

16. Planes-Laine G, Rochigneux P, Bertucci F, et al. PD-1/PD-l1 targeting in breast cancer: The first clinical evidences are emerging. a literature review. *Cancers (Basel)*. 2019;11(7):1-25. doi:10.3390/cancers11071033

17. Kim HS, Seo HK. Immune checkpoint inhibitors for urothelial carcinoma. *Investig Clin Urol*. 2018;59(5):285-296. doi:10.4111/icu.2018.59.5.285

18. Regzedmaa O, Zhang H, Liu H, Chen J. Immune checkpoint inhibitors for small cell lung cancer: Opportunities and challenges. *Onco Targets Ther*. 2019;12:4605-4620. doi:10.2147/OTT.S204577

19. Marra A, Viale G, Curigliano G. Recent advances in triple negative breast cancer: The immunotherapy era. *BMC Med*. 2019;17(1):1-9. doi:10.1186/s12916-019-1326-5

20. Samstein RM, Lee CH, Shoushtari AN, et al. Tumor mutational load predicts survival after immunotherapy across multiple cancer types. *Nat Genet*. 2019;51(2):202-206. doi:10.1038/s41588-018-0312-8

21. Molinero L, Li Y, Chang CW, et al. Tumor immune microenvironment and genomic evolution in a patient with metastatic triple negative breast cancer and a complete response to atezolizumab. *J Immunother Cancer*. 2019;7(1):1-9. doi:10.1186/s40425-019-0740-8

22. P. Schmid, J. Cortés, R. Dent, L. Pusztai, H.L. McArthur, S. Kuemmel, J. Bergh, C. Denkert, Y.H. Park, R. Hui, N. Harbeck, M. Takahashi, T. Foukakis, P.A. Fasching, F. Cardoso, L. Jia, V. Karantza, J. Zhao, G. Aktan JO. KEYNOTE-522: PHASE 3 STUDY OF PEMBROLIZUMAB (PEMBRO) + CHEMOTHERAPY (CHEMO) VS PLACEBO (PBO) + CHEMO AS NEOADJUVANT TREATMENT, FOLLOWED BY PEMBRO VS PBO AS ADJUVANT TREATMENT FOR EARLY TRIPLE-NEGATIVE BREAST CANCER (TNBC). 2019:Annals of Oncology (2019) 30 (suppl_5): v851-v934.

23. Bartoschek M, Oskolkov N, Bocci M, et al. Spatially and functionally distinct subclasses of breast cancer-associated fibroblasts revealed by single cell RNA sequencing. *Nat Commun*. 2018;9(1):5150. doi:10.1038/s41467-018-07582-3

24. Berthel A, Zoernig I, Valous NA, et al. Detailed resolution analysis reveals spatial T cell heterogeneity in the invasive margin of colorectal cancer liver metastases associated with improved survival. *Oncoimmunology*. 2017;6(3):1-10. doi:10.1080/2162402X.2017.1286436

25. Corredor G, Wang X, Zhou Y, et al. Spatial architecture and arrangement of tumor-infiltrating lymphocytes for predicting likelihood of recurrence in early-stage non-small cell lung cancer. *Clin Cancer Res*. 2018:clincanres.2013.2018. doi:10.1158/1078-0432.CCR-18-2013

26. Lazarus J, Maj T, Smith JJ, et al. Spatial and phenotypic immune profiling of metastatic colon cancer. *JCI insight*. 2018;3(22). doi:10.1172/jci.insight.121932

27. Gruosso T, Gigoux M, Manem VSK, et al. Spatially distinct tumor immune microenvironments stratify triple-negative breast cancers. *J Clin Invest*. 2019;129(4):1785-1800. doi:10.1172/JCI96313

28. Johnson LA, June CH. Driving gene-engineered T cell immunotherapy of cancer. *Cell Res*. 2017;27(1):38-58. doi:10.1038/cr.2016.154

29. Robbins PF, Kassim SH, Tran TLN, et al. A pilot trial using lymphocytes genetically engineered with an NY-ESO-1-reactive T cell receptor: Long term follow up and correlates with response. *Clin Cancer Res*. 2015;21(5):1019–1027. doi:10.1161/CIRCRESAHA.116.303790.The

30. Cameron BJ, Gerry AB, Dukes J, et al. Identification of a Titin-Derived HLA-A1-Presented Peptide as a Cross-Reactive Target for Engineered MAGE A3-Directed T Cells. *Sci Transl Med*. 2013;5(197):197ra103-197ra103. doi:10.1126/scitranslmed.3006034

31. Debets R, Donnadieu E, Chouaib S, Coukos G. TCR-engineered T cells to treat tumors: Seeing but not touching? *Semin Immunol*. 2016;28(1):10-21. doi:10.1016/j.smim.2016.03.002

32. Sadelain M, Rivière I, Riddell S. Therapeutic T cell engineering. *Nature*. 2017;545(7655):423-431. doi:10.1038/nature22395

33. Farkona S, Diamandis EP, Blasutig IM. Cancer immunotherapy: the beginning of the end of cancer? *BMC Med*. 2016;14(1):73. doi:10.1186/s12916-016-0623-5

34. Angelova M, Charoentong P, Hackl H, et al. Characterization of the immunophenotypes and antigenomes of colorectal cancers reveals distinct tumor escape mechanisms and novel targets for immunotherapy. *Genome*

Biol. 2015;16(1):64. doi:10.1186/s13059-015-0620-6

35. Charoentong P, Finotello F, Angelova M, Mayer C. Pan-cancer immunogenomic analyses reveal genotype-immunophenotype relationships and predictors of response to checkpoint blockade. *bioRxiv*. 2016:056101. doi:10.1101/056101

36. Chang L-S, Leng C-H, Yeh Y-C, et al. Toll-like receptor 9 agonist enhances anti-tumor immunity and inhibits tumor-associated immunosuppressive cells numbers in a mouse cervical cancer model following recombinant lipoprotein therapy. *Mol Cancer*. 2014;13(1):60. doi:10.1186/1476-4598-13-60

37. Liu XS, Mardis ER. Applications of Immunogenomics to Cancer. *Cell*. 2017;168(4):600-612. doi:10.1016/j.cell.2017.01.014

38. Degnim AC, Brahmbhatt RD, Radisky DC, et al. Immune cell quantitation in normal breast tissue lobules with and without lobulitis. *Breast Cancer Res Treat*. 2014;144(3):539-549. doi:10.1007/s10549-014-2896-8

39. Atabai K, Sheppard D, Werb Z. Roles of Innate Immune System in Mammary Gland Remodeling During Involution. *J Mammary Gland Biol Neoplasia*. 2007;March(12):37-45. doi:10.1097/OPX.0b013e3182540562.The

40. Hussein MR, Hassan HI. Analysis of the mononuclear inflammatory cell infiltrate in the normal breast, benign proliferative breast disease, in situ and infiltrating ductal breast carcinomas: preliminary observations. *J Clin Pathol*. 2006;59(9):972-977. doi:10.1136/jcp.2005.031252

41. Alfonso JCL, Schaadt NS, Schönmeyer R, Brieu N, Forestier G, Wemmert C. In-silico insights on the prognostic potential of immune cell infiltration patterns in the breast lobular epithelium. *Nat Publ Gr*. 2016;(April):1-18. doi:10.1038/srep33322

42. Beckmann MW, Niederacher D, Schnüren HG, Gusterson BA, Bender HG. Multistep carcinogenesis of breast cancer and tumour heterogeneity. *J Mol Med*. 1997;75(6):429-439. doi:10.1007/s001090050128

43. Kristensen VN, Vaske CJ, Ursini-Siegel J, et al. Integrated molecular profiles of invasive breast tumors and ductal carcinoma in situ (DCIS) reveal differential vascular and interleukin signaling. *Proc Natl Acad Sci U S A*. 2012;109(8):2802-2807. doi:10.1073/pnas.1108781108

44. Pruneri G, Lazzeroni M, Bagnardi V, et al. The prevalence and clinical relevance of tumor-infiltrating lymphocytes (TILs) in ductal carcinoma in situ of the breast. *Ann Oncol*. 2016;(September):mdw623. doi:10.1093/annonc/mdw623

45. Gil Del Alcazar CR, Huh SJ, Ekram MB, et al. Immune Escape in Breast Cancer During In Situ to Invasive Carcinoma Transition. *Cancer Discov*. 2017:CD-17-0222. doi:10.1158/2159-8290.CD-17-0222

46. Thompson E, Taube JM, Elwood H, et al. The immune microenvironment of breast ductal carcinoma in situ. *Mod Pathol*. 2016;29(3):249-258. doi:10.1038/modpathol.2015.158

47. Mohammed ZM, Going JJ, Edwards J, Elsberger B, McMillan DC. The relationship between lymphocyte subsets and clinico-pathological determinants of survival in patients with primary operable invasive ductal breast cancer. *Br J Cancer*. 2013;109(6):1676-1684. doi:10.1038/bjc.2013.493

48. Wasserman JK, Parra-Herran C. Regressive change in high-grade ductal carcinoma in situ of the breast: Histopathologic spectrum and biologic importance. *Am J Clin Pathol*. 2015;144(3):503-510. doi:10.1309/AJCPW4EADZ9BNXXM

49. Denkert C, Loibl S, Noske A, et al. Tumor-Associated Lymphocytes As an Independent Predictor of Response to Neoadjuvant Chemotherapy in Breast Cancer. *J Clin Oncol*. 2010;28(1):105-113. doi:10.1200/JCO.2009.23.7370

50. García-Martínez E, Gil GL, Chaves Benito A, et al. Tumor-infiltrating immune cell profiles and their change after neoadjuvant chemotherapy predict response and prognosis of breast cancer. *Breast Cancer Res*. 2014;16:1-17. doi:10.1186/s13058-014-0488-5

51. Dushyanthen S, Beavis PA, Savas P, et al. Relevance of tumor-infiltrating lymphocytes in breast cancer. *BMC Med*. 2015;13:202. doi:10.1186/s12916-015-0431-3

52. Miyan M, Schmidt-Mende J, Kiessling R, et al. Differential tumor infiltration by T-cells characterizes intrinsic molecular subtypes in breast cancer. *J Transl Med*. 2016;14(1):227. doi:10.1186/s12967-016-0983-9

53. Varn FS, Andrews EH, Mullins DW, Cheng C. Integrative analysis of breast cancer reveals prognostic haematopoietic activity and patient-specific immune response profiles. *Nat Commun*. 2016;7:10248. doi:10.1038/ncomms10248

54. Nagalla S, Chou JW, Willingham MC, et al. Interactions between immunity, proliferation and molecular subtype in breast cancer prognosis. *Genome Biol*. 2013;14(4):R34. doi:10.1186/gb-2013-14-4-r34

55. Alistar A, Chou JW, Nagalla S, Black MA, D'Agostino R, Miller LD. Dual roles for immune metagenes in breast cancer prognosis and therapy prediction. *Genome Med*. 2014;6(10):80. doi:10.1186/s13073-014-0080-8

56. Salgado R, Denkert C, Demaria S, et al. The evaluation of tumor-infiltrating lymphocytes (TILs) in breast cancer: recommendations by an International TILs Working Group 2014. *Ann Oncol*. 2015;26(2):259-271. doi:10.1093/annonc/mdu450

57. Denkert C, Wienert S, Poterie A, et al. Standardized evaluation of tumor-infiltrating lymphocytes in breast cancer: results of the ring studies of the international immuno-oncology biomarker working group. *Mod Pathol*. 2016;29(10):1155-1164. doi:10.1038/modpathol.2016.109

58. Mao Y, Qu Q, Chen X, Huang O, Wu J, Shen K. The prognostic value of tumor-infiltrating lymphocytes in breast cancer: A systematic review and meta-analysis. *PLoS One*. 2016;11(4):1-13. doi:10.1371/journal.pone.0152500

59. Liu S, Lachapelle J, Leung S, Gao D, Foulkes WD, Nielsen TO. CD8+ lymphocyte infiltration is an independent favorable prognostic indicator in basal-like breast cancer. *Breast Cancer Res*. 2012;14(2):R48. doi:10.1186/bcr3148

60. Mohammed ZMA, Going JJ, Edwards J, McMillan DC. The role of the tumour inflammatory cell infiltrate in predicting recurrence and survival in patients with primary operable breast cancer. *Cancer Treat Rev*. 2012;38(8):943-955. doi:10.1016/j.ctrv.2012.04.011

61. Chen Z, Chen X, Zhou E, et al. Intratumoral CD8+ cytotoxic lymphocyte is a favorable prognostic marker in node-negative breast cancer. *PLoS One*. 2014;9(4). doi:10.1371/journal.pone.0095475

62. Liu S, Foulkes WD, Leung S, et al. Prognostic significance of FOXP3+ tumor-infiltrating lymphocytes in breast cancer depends on estrogen receptor and human epidermal growth factor receptor-2 expression status and concurrent cytotoxic T-cell infiltration. *Breast Cancer Res*. 2014;16(5):432. doi:10.1186/s13058-014-0432-8

63. Mulligan AM, Raitman I, Feely L, et al. Tumoral Lymphocytic Infiltrate and Expression of the Chemokine CXCL10 in Breast Cancers from the Ontario Familial Breast Cancer Registry. *Clin Cancer Res*. 2013;January 15(19(2)):336-346. doi:10.1097/OPX.0b013e3182540562.The

64. West NR, Kost SE, Martin SD, et al. Tumour-infiltrating FOXP3(+) lymphocytes are associated with cytotoxic immune responses and good clinical outcome in oestrogen receptor-negative breast cancer. *Br J Cancer*. 2013;108(1):155-162. doi:10.1038/bjc.2012.524

65. Linsley PS, Chaussabel D, Speake C. The relationship of immune cell signatures to patient survival varies within and between tumor types. *PLoS One*. 2015;10(9):1-19. doi:10.1371/journal.pone.0138726

66. Jia W, Wu J, Jia H, et al. The peripheral blood neutrophil-to-lymphocyte ratio is superior to the lymphocyte-to-monocyte ratio for predicting the long-term survival of triple-negative breast cancer patients. *PLoS One*. 2015;10(11):1-13. doi:10.1371/journal.pone.0143061

67. Ali HR, Chlon L, Pharoah PDP, Markowetz F, Caldas C. Patterns of Immune

Infiltration in Breast Cancer and Their Clinical Implications: A Gene-Expression-Based Retrospective Study. *PLoS Med*. 2016;13(12):1-24. doi:10.1371/journal.pmed.1002194

68. Bergenfelz C, Larsson AM, Von Stedingk K, et al. Systemic monocytic-MDSCs are generated from monocytes and correlate with disease progression in breast cancer patients. *PLoS One*. 2015;10(5). doi:10.1371/journal.pone.0127028

69. Diaz-montero CM, Salem ML, Nishimura MI, Garett-Mayer E, Cole DJ, Montero AJ. Increased circulating myeloid-derived suppressor cells correlate with clinical cancer stage, metastasic burden, and doxorubicin-cyclophosphamide chemotherapy. *Cancer Immunol Immunother*. 2009;58(1):49-59. doi:10.1007/s00262-008-0523-4.Increased

70. Solito S, Falisi E, Diaz-montero CM, et al. A human promyelocytic-like population is responsible for the immune suppression mediated by myeloid-derived suppressor cells. *Blood*. 201AD;118(8):1-4. doi:10.1182/blood-2010-12-325753.The

71. Xing C. The neutrophil lymphocyte ratio is associated with breast cancer prognosis : an updated systematic review and meta-analysis. 2016:5567-5575.

72. Verma C, Kaewkangsadan V, Eremin JM, et al. Natural killer (NK) cell profiles in blood and tumour in women with large and locally advanced breast cancer (LLABC) and their contribution to a pathological complete response (PCR) in the tumour following neoadjuvant chemotherapy (NAC): differential rest. *J Transl Med*. 2015;13(1):180. doi:10.1186/s12967-015-0535-8

73. Gentles AJ, Newman AM, Liu CL, et al. The prognostic landscape of genes and infiltrating immune cells across human cancers. *Nat Med*. 2015;21(8):938-945. doi:10.1038/nm.3909

74. Jiang X, Shapiro DJ. The immune system and inflammation in breast cancer. *Mol Cell Endocrinol*. 2014;382(1):673-682. doi:10.1002/aur.1474. Replication

75. Iglesia MD, Vincent BG, Parker JS, et al. Prognostic B-cell signatures using mRNA-seq in patients with subtype-specific breast and ovarian cancer. *Clin Cancer Res*. 2014;20(14):3818-3829. doi:10.1158/1078-0432.CCR-13-3368

76. Ali HR, Chlon L, Pharoah PDP, et al. Innate and adaptive immune cells in the tumor microenvironment. *Nat Immunol*. 2015;13(10):1014-1022. doi:10.1038/ni.2703.Innate

77. Ye J, Ma C, Wang F, et al. Specific recruitment of γδ regulatory T cells in human breast cancer. *Cancer Res*. 2013;73(20):6137-6148. doi:10.1158/0008-5472.CAN-13-0348.Specific

78. Ma C, Zhang Q, Ye J, et al. Tumor-infiltrating γδ T lymphocytes predict clinical outcome in human breast cancer. *J Immunol*. 2012;189(10):5029-5036. doi:10.4049/jimmunol.1201892

79. Peiris-Pagès M, Sotgia F, Lisanti MP. Chemotherapy induces the cancer-associated fibroblast phenotype, activating paracrine Hedgehog-GLI signalling in breast cancer cells. *Oncotarget*. 2015;6(13):10728-10745. doi:10.18632/oncotarget.3828

80. Ignatiadis M, Singhal SK, Desmedt C, Haibe-kains B, Criscitiello C. Gene Modules and Response to Neoadjuvant Chemotherapy in Breast Cancer Subtypes : A Pooled Analysis. 2012;30(16). doi:10.1200/JCO.2011.39.5624

81. Sota Y, Naoi Y, Tsunashima R, et al. Construction of novel immune-related signature for prediction of pathological complete response to neoadjuvant chemotherapy in human breast cancer. *Ann Oncol*. 2014;25(1):100-106. doi:10.1093/annonc/mdt427

82. Denkert C, von Minckwitz G, Darb-Esfahani, S Ingold, Heppner B, et al. Evaluation of tumor-infiltrating lymphocytes (TILs) as predictive and prognostic biomarker in different subtypes of breast cancer treated with neoadjuvant therapy - A metaanalysis of 3771 patients. *San Antonia Breast Cancer Symp*. 2016;Abstract S.

83. Gu-Trantien C, Loi S, Garaud S, et al. CD4+ follicular helper T cell infiltration predicts breast cancer survival. *J Clin Invest*. 2013;123(7):1-20. doi:10.1172/JCI67428.Traditionally

84. Wang K, Xu J, Zhang T, Xue D. Tumor-infiltrating lymphocytes in breast cancer predict the response to chemotherapy and survival outcome : A meta-analysis. 2016;7(28).

85. Verma R, Foster RE, Horgan K, et al. Lymphocyte depletion and repopulation after chemotherapy for primary breast cancer. *Breast Cancer Res*. 2016;18(1):10. doi:10.1186/s13058-015-0669-x

86. West NR, Milne K, Truong PT, Macpherson N, Nelson BH, Watson PH. Tumor-infiltrating lymphocytes predict response to anthracycline-based chemotherapy in estrogen receptor-negative breast cancer. *Breast Cancer Res*. 2011;13(6):R126. doi:10.1186/bcr3072

87. Standish LJ, Torkelson C, Hamill FA, et al. Immune defects in breast cancer patients after radiotherapy. *J Soc Integr Oncol*. 2008;6(3):110-121. doi:10.2310/7200.2008.0018

88. Bernal-Estévez D, Sánchez R, Tejada RE, Parra-López C. Chemotherapy and radiation therapy elicits tumor specific T cell responses in a breast cancer patient. *BMC Cancer*. 2016;16(1):591. doi:10.1186/s12885-016-2625-2

89. Zheng LH, Zhao YH, Feng HL, Liu YJ. Endocrine resistance in breast can-

cer. *Climacteric*. 2014;17(5):522-528. doi:10.3109/13697137.2013.864268

90. Selli C, Dixon JM, Sims AH. Accurate prediction of response to endocrine therapy in breast cancer patients: current and future biomarkers. *Breast Cancer Res*. 2016;18(1):118. doi:10.1186/s13058-016-0779-0

91. Engels CC, Charehbili A, van de Velde CJH, et al. The prognostic and predictive value of Tregs and tumor immune subtypes in postmenopausal, hormone receptor-positive breast cancer patients treated with adjuvant endocrine therapy: a Dutch TEAM study analysis. *Breast Cancer Res Treat*. 2015;149(3):587-596. doi:10.1007/s10549-015-3269-7

92. Behjati S, Frank MH. The effects of tamoxifen on immunity. *Curr Med Chem*. 2009;16(24):3076-3080. doi:10.2174/092986709788803042

93. Arnould L, Gelly M, Penault-Llorca F, et al. Trastuzumab-based treatment of HER2-positive breast cancer: an antibody-dependent cellular cytotoxicity mechanism? *Br J Cancer*. 2006;94(2):259-267. doi:10.1038/sj.bjc.6602930

94. Andre F, Dieci M V., Dubsky P, et al. Molecular pathways: involvement of immune pathways in the therapeutic response and outcome in breast cancer. *Clin Cancer Res*. 2013;19(1):28-33. doi:10.1158/1078-0432.CCR-11-2701

95. Varadan V, Gilmore H, Miskimen KLS, et al. Immune signatures following single dose trastuzumab predict pathologic response to preoperativetrastuzumab and chemotherapy in HER2-positive early breast cancer. *Clin Cancer Res*. 2016;22(13):3249-3259. doi:10.1158/1078-0432.CCR-15-2021

96. Kim S-R, Gavin PG, Pogue-Geile KL, et al. A surrogate gene expression signature of tumor infiltrating lymphocytes (TILs) predicts degree of benefit from trastuzumab added to standard adjuvant chemotherapy in NSABP (NRG) trial B-31 for HER2+ breast cancer. *Proc 106th Annu Meet Am Assoc Cancer Res*. Philadelph(75(15 Suppl):Abstract nr 2837).

97. Perez EA, Ballman K V, Tenner KS, et al. Association of Stromal Tumor-Infiltrating Lymphocytes With Recurrence-Free Survival in the N9831 Adjuvant Trial in Patients With Early-Stage HER2-Positive Breast Cancer. *JAMA Oncol*. 2016;2(1):56-64. doi:10.1001/jamaoncol.2015.3239

98. Perez EA, Thompson EA, Ballman K V., et al. Genomic analysis reveals that immune function genes are strongly linked to clinical outcome in the North Central Cancer Treatment Group N9831 adjuvant trastuzumab trial. *J Clin Oncol*. 2015;33(7):701-708. doi:10.1200/JCO.2014.57.6298

99. Adams S. ENlisting the immune system to cure breast cancer—a recipe for success. *JAMA Oncol*. 2016;2(1):25-27. doi:10.1001/jamaoncol.2015.3236. Conflict

100. Gingras I, Azim HA, Ignatiadis M, C. Sotiriou. Immunology and breast cancer: Toward a new way of understanding breast cancer and de-

veloping novel therapeutic strategies. *Clin Adv Hematol Oncol*. 2015;13(6):372-382. http://www.embase.com/search/results?subaction=viewrecord&from=export&id=L604934317%5Cnhttp://sfx.library.uu.nl/utrecht?sid=EMBASE&issn=15430790&id=doi:&atitle=Immunology+and+breast+cancer:+Toward+a+new+way+of+understanding+breast+-cancer+and+developing+no.

101. Kang J, Demaria S, Formenti S. Current clinical trials testing the combination of immunotherapy with radiotherapy. *J Immunother Cancer*. 2016;4(1):51. doi:10.1186/s40425-016-0156-7

102. Tamkus D, Joginpally T. Therapeutic strategies to reverse immunosuppressive breast cancer microenvironment. *Oncol Discov*. 2016;4(1):1. doi:10.7243/2052-6199-4-1

103. Czerniecki BJ, Koski GK, Koldovsky U, et al. Targeting HER-2/neu in early breast cancer development using dendritic cells with staged interleukin-12 burst secretion. *Cancer Res*. 2007;67(4):1842-1852. doi:10.1158/0008-5472.CAN-06-4038

104. Koski GK, Koldovsky U, Xu S, et al. A Novel Dendritic Cell-Based Immunization Approach for the Induction of Durable Th1-polarized Anti-HER2/neu Responses in Women With Early Breast Cancer. *J Immunother*. 2013;35(1):54-65. doi:10.1097/CJI.0b013e318235f512.A

105. Sharma A, Kodolsky U, Xu S, et al. Her-2 Pulsed Dendritic Cell Vaccine Can Eliminate HER-2 Expression and Impact DCIS. *Cancer*. 2012;118(17):4354-4362. doi:10.1016/j.pestbp.2011.02.012.Investigations

106. Bernhard H, Neudorfer J, Gebhard K, et al. Adoptive transfer of autologous, HER2-specific, cytotoxic T lymphocytes for the treatment of HER2-overexpressing breast cancer. *Cancer Immunol Immunother*. 2008;57(2):271-280. doi:10.1007/s00262-007-0355-7

107. Lum LG, Thakur a., Al-Kadhimi Z, et al. Targeted T cell Therapy in Stage IV Breast Cancer: A Phase I Clinical Trial. *Clin Cancer Res*. 2015:2305-2314. doi:10.1158/1078-0432.CCR-14-2280

108. Hardy NM, Mossoba ME, Steinberg SM, et al. Phase I trial of adoptive cell transfer with mixed-profile type-I/type-II allogeneic T cells for metastatic breast cancer. *Clin Cancer Res*. 2011;17(21):6878-6887. doi:10.1158/1078-0432.CCR-11-1579

109. Geller M a, Cooley S, Judson PL, et al. A Phase II Study of Allogeneic Natural Killer Cell Therapy to Treat Patients With Recurrent Ovarian and Breast Cancer. *Cytotherapy*. 2013;13(1):98-107. doi:10.3109/14653249.2010.515582.A

110. Vonderheide RH, Lorusso PM, Khalil M, et al. Tremelimumab in combina-

tion with exemestane in patients with advanced breast cancer and treatment-associated modulation of inducible costimulator expression on patient T cells. *Clin Cancer Res*. 2010;16(13):3485-3494. doi:10.1158/1078-0432.CCR-10-0505

111. Nanda R, Chow LQM, Dees EC, et al. Pembrolizumab in patients with advanced triple-negative breast cancer: Phase Ib keynote-012 study. *J Clin Oncol*. 2016;34(21):2460-2467. doi:10.1200/JCO.2015.64.8931

112. Adams S, Loi S, Toppmeyer D, et al. Phase 2 study of pembrolizumab as first-line therapy for PD-L1-positive metastatic triple-negative breast cancer (mTNBC):Preliminary data from KEYNOTE-086 cohort B. *J Clin Oncol*. 2017;35(suppl; abstr 1088).

113. Augusto Santa-Maria C, Kato T, Park Y-H, et al. Durvalumab and tremelimumab in metastatic breast cancer (MBC): Immunotherapy and immunopharmacogenomic dynamics. *J Clin Oncol*. 2017;35(suppl; abstr 3052).

114. Brahmer JR, Tykodi SS, Chow LQM, et al. Safety and Activity of Anti-PD-L1 Antibody in Patients with Advanced Caancer. *N Engl J Med*. 2012;366(26):2455-2465. doi:10.1056/NEJMoa1200694.Safety

115. Dirix L, Takacs I, Nikolinakos P, et al. Avelumab (MSB0010718C), an anti-PD-L1 antibody, in patients with locally advanced or metastatic breast cancer: A phase Ib JAVELIN solid tumor trial. *38th Annu San Antonio Breast Cancer Symp*. 2015;abstract:10718.

116. Dua I, Tan AR. Immunotherapy for Triple-Negative Breast Cancer : A Focus on Immune Checkpoint Inhibitors. :20-27.

117. Loi S et al. LBA13 - Relationship between tumor infiltrating lymphocyte (TIL) levels and response to pembrolizumab (pembro) in metastatic triple-negative breast cancer (mTNBC): results from KEYNOTE-086. *ESMO Annu Meet*. 2017;September(Abstract LBA13).

118. Nanda R, Liu MC, Yau C, et al. Pembrolizumab plus standard neoadjuvant therapy for high-risk breast cancer (BC): Results from I-SPY 2. *J Clin Oncol*. 2017;35(suppl, abstr: 506).

119. Adams S, Diamond JR, Hamilton EP, et al. Phase Ib trial of atezolizumab in combination with nab-paclitaxel in patients with metastatic triple-negative breast cancer (mTNBC). *J Clin Oncol*. 2016;ASCO Annua(suppl. abstr: 1009).

120. Brignone C, Gutierrez M, Mefti F, et al. First-line chemoimmunotherapy in metastatic breast carcinoma: combination of paclitaxel and IMP321 (LAG-3Ig) enhances immune responses and antitumor activity. *J Transl Med*. 2010;8(1):71. doi:10.1186/1479-5876-8-71

121. Park JW, Melisko ME, Esserman LJ, Jones LA, Wollan JB, Sims R. Treat-

ment with autologous antigen-presenting cells activated with the HER-2 -based antigen lapuleucel-T: Results of a phase I study in immunologic and clinical activity in HER-2-overexpressing breast cancer. *J Clin Oncol*. 2007;25(24):3680-3687. doi:10.1200/JCO.2006.10.5718

122. Qi CJ, Ning YL, Han YS, et al. Autologous dendritic cell vaccine for estrogen receptor (ER)/ progestin receptor (PR) double-negative breast cancer. *Cancer Immunol Immunother*. 2012;61(9):1415-1424. doi:10.1007/s00262-011-1192-2

123. Svane IM, Pedersen AE, Nikolajsen K, Zocca MB. Alterations in p53-specific T cells and other lymphocyte subsets in breast cancer patients during vaccination with p53-peptide loaded dendritic cells and low-dose interleukin-2. *Vaccine*. 2008;26(36):4716-4724. doi:10.1016/j.vaccine.2008.06.085

124. Tiriveedhi V, Fleming TP, Goedegebuure PS, et al. Mammaglobin-A cDNA Vaccination of Breast Cancer Patients Induces Antigen-Specific Cytotoxic CD4+ICOShi T Cells. *Breast Cancer Res Treat*. 2013;138(1):109-118. doi:10.1007/s10549-012-2110-9.Mammaglobin-A

125. Mittendorf EA, Clifton GT, Holmes JP, et al. Clinical Trial Results of the HER-2/neu (E75) Vaccine to Prevent Breast Cancer Recurrence in High-Risk Patients. 2013;118(10):2594-2602. doi:10.1002/cncr.26574.Clinical

126. Dols A, Smith 2nd JW, Meijer SL, et al. Vaccination of women with metastatic breast cancer, using a costimulatory gene ({CD80)-modified}, {HLA-A2-matched}, allogeneic, breast cancer cell line: clinical and immunological results. *Hum Gene Ther*. 2003;14(11):1117-1123. doi:10.1089/104303403322124828

127. Gates JD, Clifton GT, Benavides LC, et al. Circulating regulatory T cells (CD4+CD25+FOXP3+) decrease in breast cancer patients after vaccination with a modified MHC class II HER2/neu (AE37) peptide. *Vaccine*. 2010;28(47):7476-7482. doi:10.1016/j.vaccine.2010.09.029

128. Vassilaros S, Tsibanis A, Tsikkinis A, Pietersz G a, McKenzie IFC, Apostolopoulos V. Up to 15-year clinical follow-up of a pilot Phase III immunotherapy study in stage II breast cancer patients using oxidized mannan-MUC1. *Immunotherapy*. 2013;5(11):1177-1182. doi:10.2217/imt.13.126

129. Meraviglia S, Eberl M, Vermijlen D, et al. In vivo manipulation of V9V2 T cells with zoledronate and low-dose interleukin-2 for immunotherapy of advanced breast cancer patients. *Clin Exp Immunol*. 2010;161(2):290-297. doi:10.1111/j.1365-2249.2010.04167.x

130. Melero I, Gaudernack G, Gerritsen W, et al. Therapeutic vaccines for cancer : an overview of clinical trials. *Nat Publ Gr*. 2014. doi:10.1038/nrclinonc.2014.111

131. Criscitiello C. Tumor-associated antigens in breast cancer. *Breast Care*. 2012;7(4):262-266. doi:10.1159/000342164

132. Glenn WK, Heng B, Delprado W, Iacopetta B, Whitaker NJ, Lawson JS. Epstein-Barr Virus, Human Papillomavirus and Mouse Mammary Tumour Virus as Multiple Viruses in Breast Cancer. *PLoS One*. 2012;7(11). doi:10.1371/journal.pone.0048788

133. Wang-Johanning F, Li M, Esteva FJ, et al. Human endogenous retrovirus type K antibodies and mRNA as serum biomarkers of early-stage breast cancer. *Int J Cancer*. 2013;134(3):587-595. doi:10.1002/ijc.28389

134. Ariad S, Milk N, Bolotin A, Gopas J, Sion-Vardy N, Benharoch D. Measles virus antigens in breast cancer. *Anticancer Res*. 2011;31(3):913-920.

135. Taher C, de Boniface J, Mohammad A-A, et al. High prevalence of human cytomegalovirus proteins and nucleic acids in primary breast cancer and metastatic sentinel lymph nodes. *PLoS One*. 2013;8(2):e56795. doi:10.1371/journal.pone.0056795

136. Michaelis M, Doerr HW, Cinatl J. The Story of Human Cytomegalovirus and Cancer: Increasing Evidence and Open Questions. *Neoplasia*. 2009;11(1):1-9. doi:10.1593/neo.81178

137. Taylor M, Bolton LM, Johnson P, Elliott T, Murray N. Breast cancer is a promising target for vaccination using cancer-testis antigens known to elicit immune responses. *Breast Cancer Res*. 2007;9(4):R46. doi:10.1186/bcr1749

138. Saini S, Jagadish N, Gupta A, Bhatnagar A, Suri A. A Novel Cancer Testis Antigen, A-Kinase Anchor Protein 4 (AKAP4) Is a Potential Biomarker for Breast Cancer. *PLoS One*. 2013;8(2). doi:10.1371/journal.pone.0057095

139. Chen YT, Ross DS, Chiu R, et al. Multiple cancer/testis antigens are preferentially expressed in hormone-receptor negative and high-grade breast cancers. *PLoS One*. 2011;6(3):1-9. doi:10.1371/journal.pone.0017876

140. Adams S, Greeder L, Reich E, et al. Expression of cancer testis antigens in human BRCA-associated breast cancers: Potential targets for immunoprevention? *Cancer Immunol Immunother*. 2011;60(7):999-1007. doi:10.1007/s00262-011-1005-7

141. Balafoutas D, zur Hausen A, Mayer S, et al. Cancer testis antigens and NY-BR-1 expression in primary breast cancer: prognostic and therapeutic implications. *BMC Cancer*. 2013;13(1):271. doi:10.1186/1471-2407-13-271

142. Yang F, Zhou X, Miao X, et al. MAGEC2, an epithelial-mesenchymal transition inducer, is associated with breast cancer metastasis. *Breast Cancer Res Treat*. 2014;145(1):23-32. doi:10.1007/s10549-014-2915-9

143. Gjerstorff MF, Andersen MH, Ditzel HJ, Gjerstorff MF, Andersen MH, Ditzel HJ. Oncogenic cancer/testis antigens: prime candidates for immunotherapy. *Oncotarget*. 2015;6(18):15772-15787. doi:10.18632/oncotarget.4694

144. Alexandrov LB, Nik-Zainal S, Wedge DC, et al. Signatures of mutational processes in human cancer. *Nature*. 2013;500:415-421. doi:10.1038/nature12477

145. Schumacher TN, Schreiber RD. Neoantigens in cancer immunotherapy. *Science (80-)*. 2015;348(6230):69-74. doi:10.1126/science.aaa4971

146. Budczies J, Bockmayr M, Denkert C, et al. Classical pathology and mutational load of breast cancer - integration of two worlds. *J Pathol Clin Res*. 2015;1(4):225-238. doi:10.1002/cjp2.25

147. Cescon DW, Haibe-Kains B, Mak TW. APOBEC3B expression in breast cancer reflects cellular proliferation, while a deletion polymorphism is associated with immune activation. *Proc Natl Acad Sci U S A*. 2015;112(9):2841-2846. doi:10.1073/pnas.1424869112

148. Sieuwerts AM, Willis S, Burns MB, et al. Elevated APOBEC3B Correlates with Poor Outcomes for Estrogen-Receptor-Positive Breast Cancers. 2014:405-413. doi:10.1007/s12672-014-0196-8

149. Smid M, Rodríguez-González FG, Sieuwerts AM, et al. Breast cancer genome and transcriptome integration implicates specific mutational signatures with immune cell infiltration. *Nat Commun*. 2016;7:12910. doi:10.1038/ncomms12910

150. Kotoula V, Lakis S, Vlachos IS, et al. Tumor infiltrating lymphocytes affect the outcome of patients with operable triple-negative breast cancer in combination with mutated amino acid classes. *PLoS One*. 2016;11(9):1-17. doi:10.1371/journal.pone.0163138

151. Dunn GP, Bruce AT, Ikeda H, Old LJ, Schreiber RD. Cancer immunoediting : from immuno- surveillance to tumor escape. 2002;3(11):991-998.

152. Rooney MS, Shukla SA, Wu CJ, Getz G, Hacohen N. Molecular and genetic properties of tumors associated with local immune cytolytic activity. *Cell*. 2015;160(1-2):48-61. doi:10.1016/j.cell.2014.12.033

153. Forero A, Li Y, Chen D, et al. Expression of the MHC Class II Pathway in Triple-Negative Breast Cancer Tumor Cells Is Associated with a Good Prognosis and Infiltrating Lymphocytes. *Cancer Immunol Res*. 2016:1-11. doi:10.1158/2326-6066.CIR-15-0243

154. Kaneko K, Ishigami S, Kijima Y, et al. Clinical implication of HLA class I expression in breast cancer. *BMC Cancer*. 2011;11(1):454. doi:10.1186/1471-2407-11-454

155. da Silva GBRF, Silva TGA, Duarte RA, et al. Expression of the Classical and Nonclassical HLA Molecules in Breast Cancer. *Int J Breast Cancer*. 2013;2013:250435. doi:10.1155/2013/250435

156. Harada A, Ishigami S, Kijima Y, et al. Clinical implication of human leukocyte antigen (HLA) -F expression in breast cancer. *Pathol Int*. 2015;65:569-574. doi:10.1111/pin.12343

157. Vitale M, Rezzani R, Rodella L, Down-regulation TAP, Breast HP, Zauli G. HLA Class I Antigen and Transporter Associated with Antigen Processing (TAP1 and TAP2) Down-Regulation in High-Grade Primary Breast Carcinoma Lesions HLA Class I Antigen and Transporter Associated with Antigen Processing. *Cancer Res*. 1998;58(914):737-742.

158. Palmisano GL, Pistillo MP, Capanni P, et al. Investigation of HLA class I downregulation in breast cancer by RT-PCR. *Hum Immunol*. 2001;62(2):133-139. doi:10.1016/S0198-8859(00)00241-X

159. Shin DS, Zaretsky JM, Escuin-ordinas H, et al. Primary Resistance to PD-1 Blockade Mediated by JAK1 / 2 Mutations. 2016. doi:10.1158/2159-8290. CD-16-1223

160. Zaretsky JM, Garcia-Diaz A, Shin DS, et al. Mutations Associated with Acquired Resistance to PD-1 Blockade in Melanoma. *N Engl J Med*. 2016;375(9):819-829. doi:10.1056/NEJMoa1604958

161. Yates LR, Knappskog S, Wedge D, et al. Genomic Evolution of Breast Cancer Metastasis and Relapse. *Cancer Cell*. 2017;32(2):169-184.e7. doi:10.1016/j.ccell.2017.07.005

162. Luen S, Virassamy B, Savas P, Salgado R, Loi S. The genomic landscape of breast cancer and its interaction with host immunity. *Breast*. 2016;29:241-250. doi:10.1016/j.breast.2016.07.015

163. Peng W, Chen JQ, Liu C, et al. Loss of PTEN promotes resistance to T cell–mediated immunotherapy. *Cancer Discov*. 2016;6(2):202-216. doi:10.1158/2159-8290.CD-15-0283

164. Loi S, Dushyanthen S, Beavis PA, et al. RAS/MAPK activation is associated with reduced tumor-infiltrating lymphocytes in triple-negative breast cancer: Therapeutic cooperation between MEK and PD-1/PD-L1 immune checkpoint inhibitors. *Clin Cancer Res*. 2016;22(6):1499-1509. doi:10.1158/1078-0432.CCR-15-1125

165. Yan Mao, Evan T. Keller, David H. Garfield, Kunwei Shen and JW. Stroma Cells in Tumor Microenvironment and Breast Cancer. *Cancer Metastasis Rev*. 2013;32(0):303-315. doi:10.1007/s10555-012-9415-3.Stroma

166. Esquivel-Velázquez M, Ostoa-Saloma P, Palacios-Arreola MI, Nava-Castro KE, Castro JI, Morales-Montor J. The Role of Cytokines in Breast Cancer

Development and Progression. *J Interf Cytokine Res*. 2015;35(1):1-16. doi:10.1089/jir.2014.0026

167. Ward R, Sims AH, Lee A, et al. Monocytes and macrophages, implications for breast cancer migration and stem cell-like activity and treatment. *Oncotarget*. 2015;6(16):14687-14699. doi:10.18632/oncotarget.4189

168. Lindau D, Gielen P, Kroesen M, Wesseling P, Adema GJ. The immunosuppressive tumour network: myeloid-derived suppressor cells, regulatory T cells and natural killer T cells. *Immunology*. 2013;138(2):105-115. doi:10.1111/imm.12036

169. Law AMK, Lim E, Ormandy CJ, Gallego-Ortega D. The innate and adaptive infiltrating immune systems as targets for breast cancer immunotherapy. *Endocr Relat Cancer*. 2017;24(4):R123-R144. doi:10.1530/ERC-16-0404

170. Smith EL, Zamarin D, Lesokhin AM. Harnessing the immune system for cancer therapy. *Curr Opin Oncol*. 2014;26(6):600-607. doi:10.1097/CCO.0000000000000128

171. Trella E, Droeser RA, Muenst S, et al. Expression of programmed death ligand 1 (PD-L1) is associated with poor prognosis in human breast cancer. 2014;1. doi:10.1007/s10549-014-2988-5

172. Bertucci F, Finetti P, Colpaert C, et al. PDL1 expression in inflammatory breast cancer is frequent and predicts for the pathological response to chemotherapy. 6(15).

173. Mittendorf EA, Philips A V., Meric-Bernstam F, et al. PD-L1 Expression in Triple Negative Breast Can. *Cancer Immunol Res*. 2014;2(4):361-370. doi:10.1158/2326-6066.CIR-13-0127.PD-L1

174. Sabatier R, Finetti P, Mamessier E, et al. Prognostic and predictive value of PDL1 expression in breast cancer. *Oncotarget*. 2014;6(7).

175. Kolacinska A, Obrzut BC, Pakula L, et al. Immune checkpoints : Cytotoxic T-lymphocyte antigen 4 and programmed cell death protein 1 in breast cancer surgery. 2015:1079-1086. doi:10.3892/ol.2015.3321

176. Buisseret L, Garaud S, Wind A De, Eynden G Van Den, Boisson A, Solinas C. Tumor-in fi ltrating lymphocyte composition , organization and PD-1 / PD-L1 expression are linked in breast cancer. *Oncoimmunology*. 2017;6(1).

177. Bottai G, Raschioni C, Losurdo A, et al. An immune stratification reveals a subset of PD-1/LAG-3 double-positive triple-negative breast cancers. *Breast Cancer Res*. 2016;18(1):121. doi:10.1186/s13058-016-0783-4

178. Zhu S, Lin J, Qiao G, Wang X, Xu Y. Tim-3 identifies exhausted follicular helper T cells in breast cancer patients. *Immunobiology*. 2016:1-8. doi:10.1016/j.imbio.2016.04.005

179. Arnedos M, Filleron T, Dieci MV, et al. 351OGENOMIC AND IMMUNE CHARACTERIZATION OF METASTATIC BREAST CANCER (MBC): AND ANCILLARY STUDY OF THE SAFIR01 & MOSCATO TRIALS. *Ann Oncol*. 2014;25(suppl_4):iv116-iv116. doi:10.1093/annonc/mdu329.1

180. VOUTSADAKIS IA. Immune Blockade Inhibition in Breast Cancer. *Anticancer Res*. 2016;36(11):5607-5622. doi:10.21873/anticanres.11145

181. Demaria S, Volm MD, Shapiro RL, et al. Development of Tumor-infiltrating Lymphocytes in Breast Cancer after Neoadjuvant Paclitaxel Chemotherapy Development of Tumor-infiltrating Lymphocytes in Breast Cancer after Neoadjuvant Paclitaxel Chemotherapy 1. *Clin Cancer Res*. 2001;7(October):3025-3030.

182. Karpf AR. Potential role for epigenetic modulatory drugs in the enhancement of cancer/germ-line antigen vaccine efficacy. *Epigenetics*. 2006;1(3):116-120. doi:10.4161/epi.1.3.2988

183. Dunn J, Rao S. Epigenetics and immunotherapy: The current state of play. *Mol Immunol*. 2017;87(April):227-239. doi:10.1016/j.molimm.2017.04.012

184. Mazzone R, Zwergel C, Mai A, Valente S. Epi-drugs in combination with immunotherapy: a new avenue to improve anticancer efficacy. *Clin Epigenetics*. 2017;9(1):59. doi:10.1186/s13148-017-0358-y

185. Liontos M, Anastasiou I, Bamias A, Dimopoulos M-A. DNA damage, tumor mutational load and their impact on immune responses against cancer. *Ann Transl Med*. 2016;4(14):264-264. doi:10.21037/atm.2016.07.11

186. Kok M et al. Adaptive phase II randomized non-comparative trial of nivolumab after induction treatment in triple negative breast cancer: TONIC-trial. *Present Eur Soc Med Oncol 2017 Congr Madrid, Spain*. 2017;September(Abstract LBA14).

187. Butt AQ, Mills KHG. Immunosuppressive networks and checkpoints controlling antitumor immunity and their blockade in the development of cancer immunotherapeutics and vaccines. *Oncogene*. 2013;33(38):4623-4631. doi:10.1038/onc.2013.432

188. Camisaschi C, Vallacchi V, Vergani E, et al. Targeting Immune Regulatory Networks to Counteract Immune Suppression in Cancer. :1-17. doi:10.3390/vaccines4040038

189. Borcherding N, Kolb R, Gullicksrud J, Vikas P, Zhu Y, Zhang W. Keeping Tumors in Check: A Mechanistic Review of Clinical Response and Resistance to Immune Checkpoint Blockade in Cancer. *J Mol Biol*. 2018;430(14):2014-2029. doi:10.1016/j.jmb.2018.05.030

190. Johnson LA, June CH. Driving gene-engineered T cell immunotherapy of cancer. *Cell Res*. 2017;27(1):38-58. doi:10.1038/cr.2016.154

191. Hammerl D, Smid M, Timmermans AM, Sleijfer S, Martens JWM, Debets R. Breast cancer genomics and immuno-oncological markers to guide immune therapies. *Semin Cancer Biol*. 2018;52. doi:10.1016/j.semcancer.2017.11.003

192. Foekens JA, Martens JWM, Sleijfer S. Are immune signatures a worthwhile tool for decision making in early-stage human epidermal growth factor receptor 2 - Positive breast cancer? *J Clin Oncol*. 2015;33(7):673-675. doi:10.1200/JCO.2014.59.5058

193. Ascierto ML, Kmieciak M, Idowu MO, et al. A signature of immune function genes associated with recurrence-free survival in breast cancer patients. *Breast Cancer Res Treat*. 2012;131(3):871-880. doi:10.1007/s10549-011-1470-x

194. Athreya K, Ali S. Advances on immunotherapy in breast cancer. *Transl Cancer Res*. 2017;6(1):30-37. doi:10.21037/tcr.2017.01.09

195. Kwa MJ, Adams S. Checkpoint inhibitors in triple-negative breast cancer (TNBC): Where to go from here. *Cancer*. 2018;124(10):2086-2103. doi:10.1002/cncr.31272

196. Paquet ER, Hallett MT. Absolute assignment of breast cancer intrinsic molecular subtype. *J Natl Cancer Inst*. 2015;107(1):1-9. doi:10.1093/jnci/dju357

197. Dai X, Li T, Bai Z, et al. Breast cancer intrinsic subtype classification, clinical use and future trends. *Am J Cancer Res*. 2015;5(10):2929-2943. doi:www.ajcr.us/ISSN:2156-6976/ajcr0014158

198. Zacharakis N, Chinnasamy H, Black M, et al. Immune recognition of somatic mutations leading to complete durable regression in metastatic breast cancer. *Nat Med*. 2018;01. doi:10.1038/s41591-018-0040-8

199. Brown SD, Warren RL, Gibb EA, et al. Neo-antigens predicted by tumor genome meta-analysis correlate with increased patient survival. *Genome Res*. 2014;24(5):743-750. doi:10.1101/gr.165985.113

200. Stevanović S, Pasetto A, Helman SR, et al. Landscape of immunogenic tumor antigens in successful immunotherapy of virally induced epithelial cancer. *Science (80-)*. 2017;356(6334):200-205. doi:10.1126/science.aak9510

201. Hammerl D, Rieder D, Martens JWM, Trajanoski Z, Debets R. Adoptive T Cell Therapy: New Avenues Leading to Safe Targets and Powerful Allies. *Trends Immunol*. 2018;xx:1-16. doi:10.1016/j.it.2018.09.004

202. Bolotin DA, Poslavsky S, Mitrophanov I, et al. MiXCR: Software for comprehensive adaptive immunity profiling. *Nat Methods*. 2015;12(5):380-381. doi:10.1038/nmeth.3364

203. Newman AM, Liu CL, Green MR, et al. Robust enumeration of cell subsets from tissue expression profiles. *Nat Methods*. 2015;12(MAY 2014):1-10. doi:10.1038/nmeth.3337

204. Reuben A, Gittelman RM, Gao J, et al. TCR Repertoire Intratumor Heterogeneity in Localized Lung Adenocarcinomas: an Association with Predicted Neoantigen Heterogeneity and Postsurgical Recurrence. *Cancer Discov*. 2017;(OctOber):CD-17-0256. doi:10.1158/2159-8290.CD-17-0256

205. Fuertes MB, Kacha AK, Kline J, et al. Host type I IFN signals are required for antitumor CD8 $^{+}$ T cell responses through CD8α $^{+}$ dendritic cells. *J Exp Med*. 2011;208(10):2005-2016. doi:10.1084/jem.20101159

206. Massink MPG, Kooi IE, Martens JWM, Waisfisz Q, Meijers-Heijboer H. Genomic profiling of CHEK2*1100delC-mutated breast carcinomas. *BMC Cancer*. 2015;15(1):877. doi:10.1186/s12885-015-1880-y

207. Hammerl D, Smid M, Timmermans AM, Sleijfer S, Martens JWM, Debets R. Breast cancer genomics and immuno-oncological markers to guide immune therapies. *Semin Cancer Biol*. 2018;52(July):178-188. doi:10.1016/j.semcancer.2017.11.003

208. Heather JM, Ismail M, Oakes T, Chain B. High-throughput sequencing of the T-cell receptor repertoire: pitfalls and opportunities. *Brief Bioinform*. 2017;(February):bbw138. doi:10.1093/bib/bbw138

209. Scheper W, Kelderman S, Fanchi LF, et al. Low and variable tumor reactivity of the intratumoral TCR repertoire in human cancers. *Nat Med*. 2019;25(1):89-94. doi:10.1038/s41591-018-0266-5

210. Kong DH, Kim YK, Kim MR, Jang JH, Lee S. Emerging roles of vascular cell adhesion molecule-1 (VCAM-1) in immunological disorders and cancer. *Int J Mol Sci*. 2018;19(4):13-17. doi:10.3390/ijms19041057

211. Zitvogel L, Galluzzi L, Kepp O, Smyth MJ, Kroemer G. Type I interferons in anticancer immunity. *Nat Rev Immunol*. 2015;15(7):405-414. doi:10.1038/nri3845

212. Savas P, Virassamy B, Ye C, et al. Single-cell profiling of breast cancer T cells reveals a tissue-resident memory subset associated with improved prognosis. *Nat Med*. 2018;24(7):986-993. doi:10.1038/s41591-018-0078-7

213. Stefani Spranger, Robbert M. Spaapen, Yuanyuan Zha, et al. Up-Regulation of PD-L1, IDO, and Tregs in the Melanoma Tumor Microenvironment Is Driven by CD8+ T Cells. *Sci Transl Med*. 2013;5(200):200ra116. doi:10.1126/scitranslmed.3006504

214. Shou D, Wen L, Song Z, Yin J, Sun Q, Gong W. Suppressive role of myeloid-derived suppressor cells (MDSCs) in the microenvironment of breast cancer and targeted immunotherapies. *Oncotarget*. 2016;7(39).

doi:10.18632/oncotarget.11352

215. Cascone T, McKenzie JA, Mbofung RM, et al. Increased Tumor Glycolysis Characterizes Immune Resistance to Adoptive T Cell Therapy. *Cell Metab*. 2018;27(5):977-987.e4. doi:10.1016/j.cmet.2018.02.024

216. Li W, Tanikawa T, Kryczek I, et al. Aerobic Glycolysis Controls Myeloid-Derived Suppressor Cells and Tumor Immunity via a Specific CEBPB Isoform in Triple-Negative Breast Cancer. *Cell Metab*. 2018;28(1):87-103.e6. doi:10.1016/j.cmet.2018.04.022

217. Castagnoli L, Cancila V, Cordoba-Romero SL, et al. WNT signaling modulates PD-L1 expression in the stem cell compartment of triple-negative breast cancer. *Oncogene*. 2019;38(21):4047-4060. doi:10.1038/s41388-019-0700-2

218. Voorwerk L, Slagter M, Horlings HM, et al. Immune induction strategies in metastatic triple-negative breast cancer to enhance the sensitivity to PD-1 blockade: the TONIC trial. *Nat Med*. 2019. doi:10.1038/s41591-019-0432-4

219. Loi S, Giobbie-Hurder A, Gombos A, et al. Pembrolizumab plus trastuzumab in trastuzumab-resistant, advanced, HER2-positive breast cancer (PANACEA): a single-arm, multicentre, phase 1b–2 trial. *Lancet Oncol*. 2019;0(0). doi:10.1016/S1470-2045(18)30812-X

220. P. Schmid, S. Adams, H.S. Rugo, A. Schneeweiss, C.H. Barrios, H. Iwata, V. Diéras, R. Hegg, S.-A. Im, G. Shaw Wright, V. Henschel, L. Molinero, S.Y. Chui, R. Funke, A. Husain, E.P. Winer, S. Loi and LAE. Atezolizumab and Nab-Paclitaxel in Advanced Triple-Negative Breast Cancer. *N Engl J Med*. 2018;379(22):2108-2121. doi:10.1056/nejmoa1809615

221. Emens L, Powderly J, Fong L, et al. Abstract CT119: CPI-444, an oral adenosine A2a receptor (A2aR) antagonist, demonstrates clinical activity in patients with advanced solid tumors. *Cancer Res*. 2017;77(13 Supplement):CT119 LP-CT119. doi:10.1158/1538-7445.AM2017-CT119

222. Najjar YG, Finke JH. Clinical perspectives on targeting of myeloid derived suppressor cells in the treatment of cancer. *Front Oncol*. 2013;3(March):49. doi:10.3389/fonc.2013.00049

223. Priceman SJ, Tilakawardane D, Jeang B, et al. Regional delivery of chimeric antigen receptor-engineered T cells effectively targets HER2+breast cancer metastasis to the brain. *Clin Cancer Res*. 2018;24(1):95-105. doi:10.1158/1078-0432.CCR-17-2041

224. Goel S, Decristo MJ, Watt AC, et al. CDK4/6 inhibition triggers anti-tumour immunity. *Nature*. 2017;548(7668):471-475. doi:10.1038/nature23465

225. Lanitis E, Dangaj D, Irving M, Coukos G. Mechanisms regulating T-cell infiltration and activity in solid tumors. *Ann Oncol*. 2017;28(September

2017):xii18-xii32. doi:10.1093/annonc/mdx238

226. Wang Y, Klijn JGM, Zhang Y, et al. Gene-expression profiles to predict distant metastasis of lymph-node-negative primary breast cancer. *Lancet*. 2005;365(9460):671-679. doi:10.1016/S0140-6736(05)70933-8

227. Minn AJ, Gupta GP, Padua D, et al. Lung metastasis genes couple breast tumor size and metastatic spread. *Proc Natl Acad Sci*. 2007;104(16):6740-6745. doi:10.1073/pnas.0701138104

228. Schmidt M, Böhm D, Von Törne C, et al. The humoral immune system has a key prognostic impact in node-negative breast cancer. *Cancer Res*. 2008;68(13):5405-5413. doi:10.1158/0008-5472.CAN-07-5206

229. Sotiriou C, Wirapati P, Loi S, et al. Gene expression profiling in breast cancer: Understanding the molecular basis of histologic grade to improve prognosis. *J Natl Cancer Inst*. 2006;98(4):262-272. doi:10.1093/jnci/djj052

230. Desmedt C, Piette F, Loi S, et al. Strong time dependence of the 76-gene prognostic signature for node-negative breast cancer patients in the TRANSBIG multicenter independent validation series. *Clin Cancer Res*. 2007;13(11):3207-3214. doi:10.1158/1078-0432.CCR-06-2765

231. McCall MN, Bolstad BM, Irizarry RA. Frozen robust multiarray analysis (fRMA). *Biostatistics*. 2010;11(2):242-253. doi:10.1093/biostatistics/kxp059

232. Johnson WE, Li C, Rabinovic A. Adjusting batch effects in microarray expression data using empirical Bayes methods. *Biostatistics*. 2007;8(1):118-127. doi:10.1093/biostatistics/kxj037

233. Nik-Zainal S, Davies H, Staaf J, et al. Landscape of somatic mutations in 560 breast cancer whole-genome sequences. *Nature*. 2016;534(7605):47-54. doi:10.1038/nature17676

234. Nagel JHA, Peeters JK, Smid M, et al. Gene expression profiling assigns CHEK2 1100delC breast cancers to the luminal intrinsic subtypes. *Breast Cancer Res Treat*. 2012;132(2):439-448. doi:10.1007/s10549-011-1588-x

235. Sims AH, Smethurst GJ, Hey Y, et al. The removal of multiplicative, systematic bias allows integration of breast cancer gene expression datasets – improving meta-analysis and prediction of prognosis. *BMC Med Genomics*. 2008;1(1):42. doi:10.1186/1755-8794-1-42

236. Gendoo DMA, Ratanasirigulchai N, Schröder MS, et al. Genefu: An R/Bioconductor package for computation of gene expression-based signatures in breast cancer. *Bioinformatics*. 2016;32(7):1097-1099. doi:10.1093/bioinformatics/btv693

237. Ritchie ME, Phipson B, Wu D, et al. Limma powers differential expression analyses for RNA-sequencing and microarray studies. *Nucleic Acids Res*.

2015;43(7):e47. doi:10.1093/nar/gkv007

238. Schmid P, Rugo HS, Adams S, et al. Atezolizumab plus nab-paclitaxel as first-line treatment for unresectable, locally advanced or metastatic triple-negative breast cancer (IMpassion130): updated efficacy results from a randomised, double-blind, placebo-controlled, phase 3 trial. *Lancet Oncol*. 2020;21(1):44-59. doi:10.1016/S1470-2045(19)30689-8

239. Schmid P, Cortes J, Pusztai L, et al. Pembrolizumab for Early Triple-Negative Breast Cancer. *N Engl J Med*. 2020;382(9):810-821. doi:10.1056/NEJMoa1910549

240. Savas P, Loi S. Expanding the Role for Immunotherapy in Triple-Negative Breast Cancer. *Cancer Cell*. 2020;37(5):623-624. doi:https://doi.org/10.1016/j.ccell.2020.04.007

241. Emens LA, Cruz C, Eder JP, et al. Long-term Clinical Outcomes and Biomarker Analyses of Atezolizumab Therapy for Patients with Metastatic Triple-Negative Breast Cancer: A Phase 1 Study. *JAMA Oncol*. 2019;5(1):74-82. doi:10.1001/jamaoncol.2018.4224

242. Relationship Between Tumor-Infiltrating Lymphocytes and Outcomes in the KEYNOTE-119 Study of Pembrolizumab Versus Chemotherapy for Previously Treated , Metastatic Triple-Negative Breast Cancer. 2019:2019.

243. Savas P, Virassamy B, Ye C, et al. Single-cell profiling of breast cancer T cells reveals a tissue-resident memory subset associated with improved prognosis. *Nat Med*. 2018:1. doi:10.1038/s41591-018-0078-7

244. Keren L, Bosse M, Marquez D, et al. A Structure Tumor-Immune Microenvironment in Triple Negative Breast Cancer Revealed by Multiplexed Ion Beam imaging. *Submitted*. 2018;174(6):1373-1387.e19. doi:10.1016/j.cell.2018.08.039

245. Galon J, Costes A, Sanchez-Cabo F, et al. Type, Density, and Location of Immune Cells Within Human Colorectal Tumors Predict Clinical Outcome Je´roˆme. 2006;336(April):61-64. doi:10.1126/science.1206034

246. Galon J, Bruni D. Approaches to treat immune hot, altered and cold tumours with combination immunotherapies. *Nat Rev Drug Discov*. 2019:1. doi:10.1038/s41573-018-0007-y

247. Kalbasi A, Ribas A. Tumour-intrinsic resistance to immune checkpoint blockade. *Nat Rev Immunol*. 2020;20(1):25-39. doi:10.1038/s41577-019-0218-4

248. Sharma P, Hu-Lieskovan S, Wargo JA, Ribas A. Primary, Adaptive, and Acquired Resistance to Cancer Immunotherapy. *Cell*. 2017;168(4):707-723. doi:10.1016/j.cell.2017.01.017

249. Joyce JA, Fearon DT. T cell exclusion, immune privilege, and the tumor

microenvironment. *J Chem Inf Model*. 2015;53(9):1689-1699. doi:10.1017/CBO9781107415324.004

250. Sweis RF, Spranger S, Bao R, et al. Molecular drivers of the non- T-cell-inflamed tumor microenvironment in urothelial bladder cancer. *Cancer Immunol Res*. 2016;4(7):563-568. doi:10.1158/2326-6066.CIR-15-0274

251. Jerby-Arnon L, Shah P, Cuoco MS, et al. A Cancer Cell Program Promotes T Cell Exclusion and Resistance to Checkpoint Blockade. *Cell*. 2018;175(4):984-997.e24. doi:10.1016/j.cell.2018.09.006

252. Spranger S, Bao R, Gajewski TF. Melanoma-intrinsic β-catenin signalling prevents anti-tumour immunity. *Nature*. 2015;523(7559):231-235. doi:10.1038/nature14404

253. Stefani Spranger, Robbert M. Spaapen, Yuanyuan Zha, et al. Up-Regulation of PD-L1, IDO, and Tregs in the Melanoma Tumor Microenvironment Is Driven by CD8+ T Cells. *Sci Transl Med*. 2013;5(200):200ra116. doi:10.1126/scitranslmed.3006504

254. Lanitis E, Dangaj D, Irving M, Coukos G. Mechanisms regulating T-cell infiltration and activity in solid tumors. *Ann Oncol*. 2017;28(May):xii18-xii32. doi:10.1093/annonc/mdx238

255. Trujillo JA, Sweis RF, Bao R, Luke JJ. T Cell–Inflamed versus Non-T Cell–Inflamed Tumors: A Conceptual Framework for Cancer Immunotherapy Drug Development and Combination Therapy Selection. *Cancer Immunol Res*. 2018;6(9):990-1000. doi:10.1158/2326-6066.CIR-18-0277

256. Cabrita R, Lauss M, Sanna A, et al. Tertiary lymphoid structures improve immunotherapy and survival in melanoma. *Nature*. 2020;(February). doi:10.1038/s41586-019-1914-8

257. Helmink BA, Reddy SM, Gao J, et al. B cells and tertiary lymphoid structures promote immunotherapy response. *Nature*. 2020;(February). doi:10.1038/s41586-019-1922-8

258. Seymour L, Bogaerts J, Perrone A, et al. iRECIST: guidelines for response criteria for use in trials testing immunotherapeutics. *Lancet Oncol*. 2017;18(3):e143-e152. doi:10.1016/S1470-2045(17)30074-8

259. Hegde PS, Karanikas V, Evers S. The where, the when, and the how of immune monitoring for cancer immunotherapies in the era of checkpoint inhibition. *Clin Cancer Res*. 2016;22(8):1865-1874. doi:10.1158/1078-0432.CCR-15-1507

260. Riaz N, Havel JJ, Makarov V, et al. Tumor and Microenvironment Evolution during Immunotherapy with Nivolumab. *Cell*. 2017;171(4):934-949.e15. doi:10.1016/j.cell.2017.09.028

261. Hugo W, Zaretsky JM, Sun L, et al. Genomic and Transcriptomic Features of Response to Anti-PD-1 Therapy in Metastatic Melanoma. *Cell*. 2016;165(1):35-44. doi:10.1016/j.cell.2016.02.065

262. Nasser MW, Wani NA, Ahirwar DK, et al. RAGE mediates S100A7-induced breast cancer growth and metastasis by modulating the tumor microenvironment. *Cancer Res*. 2015;75(6):974-985. doi:10.1158/0008-5472.CAN-14-2161

263. Coffelt SB, Kersten K, Doornebal CW, et al. IL-17-producing γδ T cells and neutrophils conspire to promote breast cancer metastasis. *Nature*. 2015;522(7556):345-348. doi:10.1038/nature14282

264. Spranger S, Dai D, Horton B, Gajewski TF. Tumor-Residing Batf3 Dendritic Cells Are Required for Effector T Cell Trafficking and Adoptive T Cell Therapy. *Cancer Cell*. 2017;31(5):711-723.e4. doi:10.1016/j.ccell.2017.04.003

265. Zhu Y, Fu H, Liu Z, Zhang J, Ye D. Immune-desert, immune-excluded and inflamed phenotypes predict survival and adjuvant chemotherapy response in patients with MIBC. *Eur Urol Suppl*. 2018;17(2):e128-e130. doi:10.1016/s1569-9056(18)30940-0

266. Knudson KM, Hicks KC, Luo X, Chen JQ, Schlom J, Gameiro SR. M7824, a novel bifunctional anti-PD-L1/TGFβ Trap fusion protein, promotes anti-tumor efficacy as monotherapy and in combination with vaccine. *Oncoimmunology*. 2018;7(5):1-14. doi:10.1080/2162402X.2018.1426519

267. Lee J, Zimmer ADS, Lipkowitz S, et al. Phase I study of the PD-L1 inhibitor, durvalumab (MEDI4736; D) in combination with a PARP inhibitor, olaparib (O) or a VEGFR inhibitor, cediranib (C) in women's cancers (NCT02484404). *J Clin Oncol*. 2019;34(15_suppl):3015-3015. doi:10.1200/jco.2016.34.15_suppl.3015

268. Rini BI, Plimack ER, Stus V, et al. Pembrolizumab plus axitinib versus sunitinib for advanced renal-cell carcinoma. *N Engl J Med*. 2019;380(12):1116-1127. doi:10.1056/NEJMoa1816714

269. Finn RS, Qin S, Ikeda M, et al. Atezolizumab plus Bevacizumab in Unresectable Hepatocellular Carcinoma. *N Engl J Med*. 2020;382(20):1894-1905. doi:10.1056/NEJMoa1915745

270. Yu J, Goetz MP, Wang L, et al. DNA methyltransferase expression in triple- negative breast cancer predicts sensitivity to decitabine Find the latest version : The Journal of Clinical Investigation DNA methyltransferase expression in triple-negative breast cancer predicts sensitivity to. 2018;128(6):2376-2388.

271. Chapman KB, Prendes MJ, Sternberg H, et al. COL10A1 expression is elevated in diverse solid tumor types and is associated with tumor vasculature.

Futur Oncol. 2012;8(8):1031-1040. doi:10.2217/fon.12.79

272. Li T, Huang H, Shi G, et al. TGF-β1-SOX9 axis-inducible COL10A1 promotes invasion and metastasis in gastric cancer via epithelial-to-mesenchymal transition. *Cell Death Dis*. 2018;9(9). doi:10.1038/s41419-018-0877-2

273. Huang H, Li T, Ye G, et al. High expression of COL10A1 is associated with poor prognosis in colorectal cancer. *Onco Targets Ther*. 2018;11:1571-1581. doi:10.2147/OTT.S160196

274. Li X, Gruosso T, Zuo D, et al. Infiltration of CD8 + T cells into tumor cell clusters in triple-negative breast cancer. *Proc Natl Acad Sci U S A*. 2019;116(9):3678-3687. doi:10.1073/pnas.1817652116

275. Lim SO, Li CW, Xia W, et al. EGFR signaling enhances aerobic glycolysis in triple-negative breast cancer cells to promote tumor growth and immune escape. *Cancer Res*. 2016;76(5):1284-1296. doi:10.1158/0008-5472.CAN-15-2478

276. Lu F, Lamontagne J, Sun A, Pinkerton M, Block T, Lu X. Role of the inflammatory protein serine protease inhibitor Kazal in preventing cytolytic granule granzyme A-mediated apoptosis. *Immunology*. 2011;134(4):398-408. doi:10.1111/j.1365-2567.2011.03498.x

277. Mariathasan S, Turley SJ, Nickles D, et al. TGFβ attenuates tumour response to PD-L1 blockade by contributing to exclusion of T cells. *Nature*. 2018;554(7693):544-548. doi:10.1038/nature25501

278. Atala A. Re: Evasion of Immunosurveillance by Genomic Alterations of PPARγ/RXRα in Bladder Cancer. *J Urol*. 2018;199(5):1115-1116. doi:10.1016/j.juro.2018.02.015

279. Chang K, Creighton CJ, Davis C, et al. The Cancer Genome Atlas Pan-Cancer analysis project. *Nat Genet*. 2013;45(10):1113-1120. doi:10.1038/ng.2764

280. Smid M, Coebergh van den Braak RRJ, van de Werken HJG, et al. Gene length corrected trimmed mean of M-values (GeTMM) processing of RNA-seq data performs similarly in intersample analyses while improving intrasample comparisons. *BMC Bioinformatics*. 2018;19(1):1-13. doi:10.1186/s12859-018-2246-7

281. Nik-Zainal S, Davies H, Staaf J, et al. Landscape of somatic mutations in 560 breast cancer whole-genome sequences. *Nature*. 2016;534(7605):47-54. doi:10.1038/nature17676

282. Robbins PF, Kassim SH, Tran TLN, et al. A pilot trial using lymphocytes genetically engineered with an NY-ESO-1-reactive T-cell receptor: Long-term follow-up and correlates with response. *Clin Cancer Res*. 2015;21(5):1019-1027. doi:10.1158/1078-0432.CCR-14-2708

283. Rapoport AP, Stadtmauer EA, Binder-Scholl GK, et al. NY-ESO-1-specific TCR-engineered T cells mediate sustained antigen-specific antitumor effects in myeloma. *Nat Med*. 2015;21(8):914-921. doi:10.1038/nm.3910

284. Johnson L a, Morgan R a, Dudley ME, et al. regression and targets normal tissues expressing cognate antigen Gene therapy with human and mouse T cell receptors mediates cancer regression and targets normal tissues expressing cognate antigen. *Hematology*. 2009;114(3):535-547. doi:10.1182/blood-2009-03-211714

285. Linette GP, Stadtmauer EA, Maus M V, et al. Cardiovascular toxicity and titin cross-reactivity of af fi nity-enhanced T cells in myeloma and melanoma. *Blood*. 2013;122(6):863-872. doi:10.1182/blood-2013-03-490565.G.P.L.

286. Coulie PG, Van Den Eynde BJ, Van Der Bruggen P, Boon T. Tumour antigens recognized by T lymphocytes: At the core of cancer immunotherapy. *Nat Rev Cancer*. 2014;14(2):135-146. doi:10.1038/nrc3670

287. Kunert A, Obenaus M, Lamers CH, Blankenstein T, Debets R. T cell receptors for clinical therapy: *in vitro* assessment of toxicity risk. *Clin Cancer Res*. 2017;31(0):clincanres.1012.2017. doi:10.1158/1078-0432.CCR-17-1012

288. Caballero OL, Chen YT. Cancer/testis (CT) antigens: Potential targets for immunotherapy. *Cancer Sci*. 2009;100(11):2014-2021. doi:10.1111/j.1349-7006.2009.01303.x

289. Hirahata M, Abe T, Tanaka N, et al. Genome Information Broker for Viruses (GIB-V): Database for comparative analysis of virus genomes. *Nucleic Acids Res*. 2007;35(SUPPL. 1):339-342. doi:10.1093/nar/gkl1004

290. Kapushesky M, Emam I, Holloway E, et al. Gene expression Atlas at the European Bioinformatics Institute. *Nucleic Acids Res*. 2009;38(SUPPL.1):690-698. doi:10.1093/nar/gkp936

291. Stranzl T, Larsen MV, Lundegaard C, Nielsen M. NetCTLpan: pan-specific MHC class I pathway epitope predictions. *Immunogenetics*. 2010;62(6):357-368. doi:10.1007/s00251-010-0441-4

292. Jaravine V, Mösch A, Raffegerst S, Schendel DJ, Frishman D. Gene expression Expitope 2.0 : a tool to assess immunotherapeutic antigens for their potential cross-reactivity against naturally expressed proteins in human tissues. *BMC Cancer*. 2017:1-7. doi:10.1186/s12885-017-3854-8

293. Shao W, Pedrioli PGA, Wolski W, et al. The SysteMHC Atlas project. *Nucleic Acids Res*. 2018;46(D1):D1237-D1247. doi:10.1093/nar/gkx664

294. Hackl H, Charoentong P, Finotello F, Trajanoski Z. Computational genomics tools for dissecting tumour-immune cell interactions. *Nat Rev Genet*. 2016;17(8):441-458. doi:10.1038/nrg.2016.67

295. Mittal D, Gubin MM, Schreiber RD, Smyth MJ. New insights into cancer immunoediting and its three component phases-elimination, equilibrium and escape. *Curr Opin Immunol*. 2014;27(1):16-25. doi:10.1016/j.coi.2014.01.004

296. Efremova M, Finotello F, Rieder D, Trajanoski Z. Neoantigens generated by individual mutations and their role in cancer immunity and immunotherapy. *Front Immunol*. 2017;8(November):1-8. doi:10.3389/fimmu.2017.01679

297. Abelin JG, Keskin DB, Sarkizova S, et al. Mass Spectrometry Profiling of HLA-Associated Peptidomes in Mono-allelic Cells Enables More Accurate Epitope Prediction. *Immunity*. 2017;46(2):315-326. doi:10.1016/j.immuni.2017.02.007

298. Ogishi M. TCR-peptide contact profile determines immunogenicity in pathogen/tumor-derived MHC-I epitopes. *bioRxiv*. 2017:1-50. http://biorxiv.org/content/biorxiv/early/2017/06/25/155317.full.pdf.

299. Dash P, Fiore-Gartland AJ, Hertz T, et al. Quantifiable predictive features define epitope-specific T cell receptor repertoires. *Nature*. 2017;547(7661):89-93. doi:10.1038/nature22383

300. Luksza M, Riaz N, Makarov V, et al. A neoantigen fitness model predicts tumour response to checkpoint blockade immunotherapy. *Nature*. 2017;551(7681):517-520. doi:10.1038/nature24473

301. Müller M, Gfeller D, Coukos G, Bassani-Sternberg M. “Hotspots” of antigen presentation revealed by human leukocyte antigen ligandomics for neoantigen prioritization. *Front Immunol*. 2017;8(OCT):1-14. doi:10.3389/fimmu.2017.01367

302. Pearson H, Daouda T, Granados DP, et al. MHC class I – associated peptides derive from selective regions of the human genome. *J Clin Invest*. 2016;126(12):1-12. doi:10.1172/JCI91302

303. Melief CJM, Kessler JH. Novel insights into the HLA class I immunopeptidome and T-cell immunosurveillance. *Genome Med*. 2017;9(1):10-12. doi:10.1186/s13073-017-0439-8

304. Smith SN, Wang Y, Baylon JL, et al. Changing the peptide specificity of a human T-cell receptor by directed evolution. *Nat Commun*. 2014;5:5223. doi:10.1038/ncomms6223

305. Song I, Gil A, Mishra R, Ghersi D, Selin LK, Stern LJ. Broad TCR repertoire and diverse structural solutions for recognition of an immunodominant CD8+ T cell epitope. *Nat Struct Mol Biol*. 2017;24(4):395-406. doi:10.1038/nsmb.3383

306. Antunes DA, Rigo MM, Freitas M V., et al. Interpreting T-Cell cross-reactivity through structure: Implications for TCR-based cancer immunotherapy. *Front*

Immunol. 2017;8(OCT):1-16. doi:10.3389/fimmu.2017.01210

307. Stronen E, Toebes M, Kelderman S, et al. Targeting of cancer neoantigens with donor-derived T cell receptor repertoires. *Science (80-)*. 2016;352(6291):1337-1341. doi:10.1126/science.aaf2288

308. Afik S, Yates KB, Bi K, et al. Targeted reconstruction of T cell receptor sequence from single cell RNA-seq links CDR3 length to T cell differentiation state. *Nucleic Acids Res*. 2017;45(16):1-13. doi:10.1093/nar/gkx615

309. Redmond D, Poran A, Elemento O. Single-cell TCRseq: paired recovery of entire T-cell alpha and beta chain transcripts in T-cell receptors from single-cell RNAseq. *Genome Med*. 2016;8(1):80. doi:10.1186/s13073-016-0335-7

310. Marcucci KT, Jadlowsky JK, Hwang WT, et al. Retroviral and Lentiviral Safety Analysis of Gene-Modified T Cell Products and Infused HIV and Oncology Patients. *Mol Ther*. 2018;26(1):269-279. doi:10.1016/j.ymthe.2017.10.012

311. Eyquem J, Mansilla-Soto J, Giavridis T, et al. Targeting a CAR to the TRAC locus with CRISPR/Cas9 enhances tumour rejection. *Nature*. 2017;543(7643):113-117. doi:10.1038/nature21405

312. Legut M, Dolton G, Mian AA, Ottmann O, Sewell A. CRISPR-mediated TCR replacement generates superior anticancer transgenic T-cells. *Blood*. 2017;6:blood-2017-05-787598. doi:10.1182/blood-2017-05-787598

313. Knipping F, Osborn MJ, Petri K, et al. Genome-wide Specificity of Highly Efficient TALENs and CRISPR/Cas9 for T Cell Receptor Modification. *Mol Ther - Methods Clin Dev*. 2017;4(March):213-224. doi:10.1016/j.omtm.2017.01.005

314. Roth TL, Puig-saus C, Yu R, et al. Reprogramming human T cell function and specificity with non- viral genome targeting. 2017. doi:https://doi.org/10.1101/183418

315. Straetemans T, Berrevoets C, Coccoris M, et al. Recurrence of Melanoma Following T Cell Treatment: Continued Antigen Expression in a Tumor That Evades T Cell Recruitment. *Mol Ther*. 2015;23(2):396-406. doi:10.1038/mt.2014.215

316. Donia M, Harbst K, Van Buuren M, et al. Acquired immune resistance follows complete tumor regression without loss of target antigens or IFNγ signaling. *Cancer Res*. 2017;77(17):4562-4566. doi:10.1158/0008-5472.CAN-16-3172

317. Peng D, Kryczek I, Nagarsheth N, et al. Epigenetic silencing of TH1-type chemokines shapes tumour immunity and immunotherapy. *Nature*. 2015;527(7577):249-253. doi:10.1038/nature15520

318. Martinet L, Garrido I, Filleron T, et al. Human solid tumors contain high endothelial venules: Association with T- and B-lymphocyte infiltration and favorable prognosis in breast cancer. *Cancer Res*. 2011;71(17):5678-5687. doi:10.1158/0008-5472.CAN-11-0431

319. Ager A, May MJ. Understanding high endothelial venules: Lessons for cancer immunology. *Oncoimmunology*. 2015;4(6). doi:10.1080/2162402X.2015.1008791

320. Motz GT, Santoro SP, Wang LP, et al. Tumor endothelium FasL establishes a selective immune barrier promoting tolerance in tumors. *Nat Med*. 2014;20(6):607-615. doi:10.1038/nm.3541

321. Bougherara H, Mansuet-Lupo A, Alifano M, et al. Real-time imaging of resident T cells in human lung and ovarian carcinomas reveals how different tumor microenvironments control T lymphocyte migration. *Front Immunol*. 2015;6(OCT). doi:10.3389/fimmu.2015.00500

322. Kato T, Noma K, Ohara T, Kashima H, Katsura Y. Cancer-Associated Fibroblasts Affect Intratumoral CD8 + and FoxP3 + T Cells via Interleukin 6 in the Tumor Microenvironment. 2018. doi:10.1158/1078-0432.CCR-18-0205

323. Manguso RT, Pope HW, Zimmer MD, et al. In vivo CRISPR screening identifies Ptpn2 as a cancer immunotherapy target. *Nature*. 2017;547(7664):413-418. doi:10.1038/nature23270

324. Patel SJ, Sanjana NE, Kishton RJ, et al. Identification of essential genes for cancer immunotherapy. *Nature*. 2017;548(7669):537-542. doi:10.1038/nature23477

325. Sheng W, Lafleur MW, He HH, Sharpe AH. Article LSD1 Ablation Stimulates Anti-tumor Immunity and Enables Checkpoint Blockade. *Cell*. 2018:1-15. doi:10.1016/j.cell.2018.05.052

326. Antonioli L, Blandizzi C, Pacher P, Haskó G. Immunity, inflammation and cancer: a leading role for adenosine. *Nat Rev Cancer*. 2013;13(12):842-857. doi:10.1038/nrc3613

327. Cekic C, Linden J. Adenosine A2A receptors intrinsically regulate CD8+ T cells in the tumor microenvironment. *Cancer Res*. 2014;74(24):7239-7249. doi:10.1158/0008-5472.CAN-13-3581

328. Spranger S, Bao R, Gajewski TF. Melanoma-intrinsic β-catenin signalling prevents anti-tumour immunity. *Nature*. 2015;523(7559):231-235. doi:10.1038/nature14404

329. Hubo M, Trinschek B, Kryczanowsky F, Tuettenberg A, Steinbrink K, Jonuleit H. Costimulatory molecules on immunogenic versus tolerogenic human dendritic cells. *Front Immunol*. 2013;4(APR):1-14. doi:10.3389/fimmu.2013.00082

330. Broz ML, Binnewies M, Boldajipour B, et al. Dissecting the Tumor Myeloid Compartment Reveals Rare Activating Antigen-Presenting Cells Critical for T Cell Immunity. *Cancer Cell*. 2014;26(5):638-652. doi:10.1016/j.ccell.2014.09.007

331. Marigo I, Zilio S, Desantis G, et al. T Cell Cancer Therapy Requires CD40-CD40L Activation of Tumor Necrosis Factor and Inducible Nitric-Oxide-Synthase-Producing Dendritic Cells. *Cancer Cell*. 2016;30(3):377-390. doi:10.1016/j.ccell.2016.08.004

332. Ballbach M, Dannert A, Singh A, et al. Expression of checkpoint molecules on myeloid-derived suppressor cells. *Immunol Lett*. 2017;192(August):1-6. doi:10.1016/j.imlet.2017.10.001

333. Li J, Lee Y, Li Y, et al. Co-inhibitory Molecule B7 Superfamily Member 1 Expressed by Tumor-Infiltrating Myeloid Cells Induces Dysfunction of Anti-tumor CD8+T Cells. *Immunity*. 2018;48(4):773-786.e5. doi:10.1016/j.immuni.2018.03.018

334. van der Woude LL, Gorris MAJ, Halilovic A, Figdor CG, de Vries IJM. Migrating into the Tumor: a Roadmap for T Cells. *Trends in Cancer*. 2017;3(11):797-808. doi:10.1016/j.trecan.2017.09.006

335. Charoentong P, Finotello F, Angelova M, et al. Pan-cancer Immunogenomic Analyses Reveal Genotype-Immunophenotype Relationships and Predictors of Response to Checkpoint Blockade. *Cell Rep*. 2017;18(1):248-262. doi:10.1016/j.celrep.2016.12.019

336. Linch M, Goh G, Hiley C, et al. Intratumoural evolutionary landscape of high-risk prostate cancer: The PROGENY study of genomic and immune parameters. *Ann Oncol*. 2017;28(10):2472-2480. doi:10.1093/annonc/mdx355

337. Ayers M, Lunceford J, Nebozhyn M, et al. IFN- γ – related mRNA profile predicts clinical response to PD-1 blockade. *J Clin Invest*. 2017;127(15):1-11. doi:10.1172/JCI91190

338. Kamburov A, Stelzl U, Lehrach H, Herwig R. The ConsensusPathDB interaction database: 2013 Update. *Nucleic Acids Res*. 2013;41(D1):793-800. doi:10.1093/nar/gks1055

339. Croft D, O'Kelly G, Wu G, et al. Reactome: A database of reactions, pathways and biological processes. *Nucleic Acids Res*. 2011;39(SUPPL. 1):691-697. doi:10.1093/nar/gkq1018

340. Huang DW, Sherman BT, Tan Q, et al. The DAVID Gene Functional Classification Tool: A novel biological module-centric algorithm to functionally analyze large gene lists. *Genome Biol*. 2007;8(9). doi:10.1186/gb-2007-8-9-r183

341. Aran D, Hu Z, Butte AJ. xCell: Digitally portraying the tissue cellular heterogeneity landscape. *Genome Biol*. 2017;18(1):1-14. doi:10.1186/s13059-017-1349-1

342. Racle J, de Jonge K, Baumgaertner P, Speiser DE, Gfeller D. Simultaneous enumeration of cancer and immune cell types from bulk tumor gene expression data. *Elife*. 2017;6(0):e26476. doi:10.7554/eLife.26476

343. Finotello F, Mayer C, Plattner C, et al. We introduce quanTIseq, a method to quantify the tumor immune contexture, determined by the type and density of tumor-infiltrating immune cells. quanTIseq is based on a novel deconvolution algorithm for RNA sequencing data that was validated with independ. 2017.

344. Lin JR, Fallahi-Sichani M, Sorger PK. Highly multiplexed imaging of single cells using a high-throughput cyclic immunofluorescence method. *Nat Commun*. 2015;6:1-7. doi:10.1038/ncomms9390

345. Gerdes MJ, Sevinsky CJ, Sood A, Adak S, Bello MO. Highly multiplexed single-cell analysis of formalin- fi xed , paraf fi n-embedded cancer tissue. *Proc Natl Acad Sci U S A*. 2013;110(29):11982-11987. doi:10.1073/pnas.1300136110/-/DCSupplemental.www.pnas.org/cgi/doi/10.1073/pnas.1300136110

346. Schubert W, Bonnekoh B, Pommer AJ, et al. Analyzing proteome topology and function by automated multidimensional fluorescence microscopy. *Nat Biotechnol*. 2006;24(10):1270-1278. doi:10.1038/nbt1250

347. Stack EC, Wang C, Roman KA, Hoyt CC. Multiplexed immunohistochemistry, imaging, and quantitation: A review, with an assessment of Tyramide signal amplification, multispectral imaging and multiplex analysis. *Methods*. 2014;70(1):46-58. doi:10.1016/j.ymeth.2014.08.016

348. Pollock SB, Hu A, Mou Y, et al. Highly multiplexed and quantitative cell-surface protein profiling using genetically barcoded antibodies. *Proc Natl Acad Sci*. 2018;115(11):2836-2841. doi:10.1073/pnas.1721899115

349. Giesen C, Wang HAO, Schapiro D, et al. Highly multiplexed imaging of tumor tissues with subcellular resolution by mass cytometry. *Nat Methods*. 2014;11(4):417-422. doi:10.1038/nmeth.2869

350. Facciabene A, De Sanctis F, Pierini S, et al. Local endothelial complement activation reverses endothelial quiescence, enabling t-cell homing, and tumor control during t-cell immunotherapy. *Oncoimmunology*. 2017;6(9):1-15. doi:10.1080/2162402X.2017.1326442

351. Shrimali RK, Yu Z, Theoret MR, Chinnasamy D, Restifo NP, Rosenberg SA. Antiangiogenic agents can increase lymphocyte infiltration into tumor and enhance the effectiveness of adoptive immunotherapy of cancer. *Cancer*

Res. 2010;70(15):6171-6180. doi:10.1158/0008-5472.CAN-10-0153

352. Caruana I, Savoldo B, Hoyos V, et al. Heparanase promotes tumor infiltration and antitumor activity of CAR-redirected T lymphocytes. *Nat Med*. 2015;21(5):524-529. doi:10.1038/nm.3833

353. Foley KC, Nishimura MI, Moore T V. Combination immunotherapies implementing adoptive T-cell transfer for advanced-stage melanoma. *Melanoma Res*. 2018;28(3):171-184. doi:10.1097/CMR.0000000000000436

354. Chia W-K, Teo M, Wang W-W, et al. Adoptive T-cell Transfer and Chemotherapy in the First-line Treatment of Metastatic and/or Locally Recurrent Nasopharyngeal Carcinoma. *Mol Ther*. 2014;22(1):132-139. doi:10.1038/mt.2013.242

355. Vyas M, Müller R, von Strandmann EP. Antigen loss variants: Catching hold of escaping foes. *Front Immunol*. 2017;8(FEB):1-7. doi:10.3389/fimmu.2017.00175

356. de Charette M, Marabelle A, Houot R. Turning tumour cells into antigen presenting cells: The next step to improve cancer immunotherapy? *Eur J Cancer*. 2016;68:134-147. doi:10.1016/j.ejca.2016.09.010

357. Liu C, Workman CJ, Vignali DAA. Targeting regulatory T cells in tumors. *FEBS J*. 2016;283:2731-2748. doi:10.1111/febs.13656

358. Weigelin B, Bolaños E, Rodriguez-Ruiz ME, Martinez-Forero I, Friedl P, Melero I. Anti-CD137 monoclonal antibodies and adoptive T cell therapy: a perfect marriage? *Cancer Immunol Immunother*. 2016;65(5):493-497. doi:10.1007/s00262-016-1818-5

359. Beavis PA, Henderson MA, Giuffrida L, et al. Targeting the adenosine 2A receptor enhances chimeric antigen receptor T cell efficacy. 2017;127(3):929-941. doi:10.1172/JCI89455

360. Koya RC, Mok S, Otte N, et al. BRAF inhibitor vemurafenib improves the antitumor activity of adoptive cell immunotherapy. *Cancer Res*. 2012;72(16):3928-3937. doi:10.1158/0008-5472.CAN-11-2837

361. Gropper Y, Feferman T, Shalit T, Salame TM, Porat Z, Shakhar G. Culturing CTLs under Hypoxic Conditions Enhances Their Cytolysis and Improves Their Anti-tumor Function. *Cell Rep*. 2017;20(11):2547-2555. doi:10.1016/j.celrep.2017.08.071

362. Kunert A. Engineering T cells for adoptive therapy: outsmarting the tumor. *Curr Opin Immunol*. 2018;in press.

363. Mesri EA, Feitelson MA, Munger K. Human viral oncogenesis: A cancer hallmarks analysis. *Cell Host Microbe*. 2014;15(3):266-282. doi:10.1016/j.chom.2014.02.011

364. Hartmaier RJ, Charo J, Fabrizio D, et al. Genomic analysis of 63,220 tumors reveals insights into tumor uniqueness and targeted cancer immunotherapy strategies. *Genome Med*. 2017;9(1):1-9. doi:10.1186/s13073-017-0408-2

365. Flippot R, Malouf GG, Su X, Khayat D, Spano JP. Oncogenic viruses: Lessons learned using next-generation sequencing technologies. *Eur J Cancer*. 2016;61:61-68. doi:10.1016/j.ejca.2016.03.086

366. Manzo T, Heslop HE, Rooney CM. Antigen-specific T cell therapies for cancer. *Hum Mol Genet*. 2015;24(R1):R67-R73. doi:10.1093/hmg/ddv270

367. Gnjatic S, Nishikawa H, Jungbluth AA, et al. NY-ESO-1: Review of an Immunogenic Tumor Antigen. *Adv Cancer Res*. 2006;95(May 2014):1-30. doi:10.1016/S0065-230X(06)95001-5

368. Vansteenkiste JF, Cho BC, Vanakesa T, et al. Efficacy of the MAGE-A3 cancer immunotherapeutic as adjuvant therapy in patients with resected MAGE-A3-positive non-small-cell lung cancer (MAGRIT): a randomised, double-blind, placebo-controlled, phase 3 trial. *Lancet Oncol*. 2016;17(6):822-835. doi:10.1016/S1470-2045(16)00099-1

369. Lucas S, De Plaen E, Boon T. MAGE-B5, MAGE-B6, MAGE-C2, and-MAGE-C3: four new members of theMAGE family with tumor-specific expression. *Int J Cancer*. 2000;87(1):55-60. doi:10.1002/1097-0215(20000701)87:1<55::AID-IJC8>3.0.CO;2-J

370. Cherkasova E, Weisman Q, Childs RW. Endogenous Retroviruses as Targets for Antitumor Immunity in Renal Cell Cancer and Other Tumors. *Front Oncol*. 2013;3(September):1-5. doi:10.3389/fonc.2013.00243

371. Tran E, Turcotte S, Gros A, et al. Cancer Immunotherapy Based on. *Science (80-)*. 2014;9(May):641-645. doi:10.1126/science.1251102

372. Stevanović S, Draper LM, Langhan MM, et al. Complete regression of metastatic cervical cancer after treatment with human papillomavirus-targeted tumor-infiltrating T cells. *J Clin Oncol*. 2015;33(14):1543-1550. doi:10.1200/JCO.2014.58.9093

373. Morgan RA, Chinnasamy N, Abate-daga DD, et al. Cancer regressions and neurologic toxicity following anti-MAGE-A3 TCR gene therapy. *J Immunother*. 2014;36(2):133-151. doi:10.1097/CJI.0b013e3182829903.Cancer

374. Verdegaal EME, De Miranda NFCC, Visser M, et al. Neoantigen landscape dynamics during human melanoma-T cell interactions. *Nature*. 2016;536(7614):91-95. doi:10.1038/nature18945

375. Timm J, Walker CM. Mutational escape of CD8+ T cell epitopes: implications for prevention and therapy of persistent hepatitis virus infections. *Med Microbiol Immunol*. 2015;204(1):29-38. doi:10.1007/s00430-014-0372-z

376. Keşmir C, Nussbaum AK, Schild H, Detours V, Brunak S. Prediction of proteasome cleavage motifs by neural networks. *Protein Eng*. 2002;15(4):287-296. doi:10.1093/protein/15.4.287

377. Rammensee HG, Bachmann J, Emmerich NPN, Bachor OA, Stevanović S. SYFPEITHI: Database for MHC ligands and peptide motifs. *Immunogenetics*. 1999;50(3-4):213-219. doi:10.1007/s002510050595

378. Reche PA, Glutting JP, Zhang H, Reinherz EL. Enhancement to the RANKPEP resource for the prediction of peptide binding to MHC molecules using profiles. *Immunogenetics*. 2004;56(6):405-419. doi:10.1007/s00251-004-0709-7

379. Hundal J, Carreno BM, Petti AA, et al. pVAC-Seq: A genome-guided in silico approach to identifying tumor neoantigens. *Genome Med*. 2016;8(1):1-11. doi:10.1186/s13073-016-0264-5

380. Bjerregaard AM, Nielsen M, Hadrup SR, Szallasi Z, Eklund AC. MuPeXI: prediction of neo-epitopes from tumor sequencing data. *Cancer Immunol Immunother*. 2017;66(9):1123-1130. doi:10.1007/s00262-017-2001-3

381. Tappeiner E, Finotello F, Charoentong P, Mayer C, Rieder D, Trajanoski Z. TIminer: NGS data mining pipeline for cancer immunology and immunotherapy. *Bioinformatics*. 2017;33(19):3140-3141. doi:10.1093/bioinformatics/btx377

382. Deveau P, Colmet Daage L, Oldridge D, et al. QuantumClone: clonal assessment of functional mutations in cancer based on a genotype-aware method for clonal reconstruction. *Bioinformatics*. 2018;34(January):1808-1816. doi:10.1093/bioinformatics/bty016

383. Fischer A, Vázquez-García I, Illingworth CJR, Mustonen V. High-definition reconstruction of clonal composition in cancer. *Cell Rep*. 2014;7(5):1740-1752. doi:10.1016/j.celrep.2014.04.055

384. Blom S, Paavolainen L, Bychkov D, et al. Systems pathology by multiplexed immunohistochemistry and whole-slide digital image analysis. *Sci Rep*. 2017;7(1):15580. doi:10.1038/s41598-017-15798-4

385. Lin J-R, Fallahi-Sichani M, Chen J-Y, Sorger PK. Cyclic Immunofluorescence (CycIF), A Highly Multiplexed Method for Single-cell Imaging. 2017;8(4):251-264. doi:10.1126/science.1249098.Sleep

386. Yao H, He G, Yan S, et al. Triple-negative breast cancer: Is there a treatment on the horizon? *Oncotarget*. 2017;8(1):1913-1924. doi:10.18632/oncotarget.12284

387. Salgado R, Loi S. Tumour infiltrating lymphocytes in breast cancer: increasing clinical relevance. *Lancet Oncol*. 2018;19(1):3-5. doi:10.1016/S1470-2045(17)30905-1

388. Kunert A, Straetemans T, Govers C, et al. TCR-Engineered T Cells Meet New Challenges to Treat Solid Tumors: Choice of Antigen, T Cell Fitness, and Sensitization of Tumor Milieu. *Front Immunol*. 2013;4(November):1-16. doi:10.3389/fimmu.2013.00363

389. Lamers CHJ, Sleijfer S, Van Steenbergen S, et al. Treatment of metastatic renal cell carcinoma with CAIX CAR-engineered T cells: Clinical evaluation and management of on-target toxicity. *Mol Ther*. 2013;21(4):904-912. doi:10.1038/mt.2013.17

390. Majzner RG, Mackall CL. Tumor antigen escape from car t-cell therapy. *Cancer Discov*. 2018;8(10):1219-1226. doi:10.1158/2159-8290.CD-18-0442

391. Robbins PF, Kassim SH, Tran TLN, et al. A pilot trial using lymphocytes genetically engineered with an NY-ESO-1-reactive T-cell receptor: Long-term follow-up and correlates with response. *Clin Cancer Res*. 2015. doi:10.1158/1078-0432.CCR-14-2708

392. Butler MO, Friedlander P, Milstein MI, et al. Establishment of Antitumor Memory in Humans Using in Vitro-Educated CD8+ T Cells. *Sci Transl Med*. 2011;3(80):80ra34-80ra34. doi:10.1126/scitranslmed.3002207

393. Engels B, Engelhard VH, Sidney J, et al. Relapse or eradication of cancer is predicted by peptide-major histocompatibility complex affinity. *Cancer Cell*. 2013;23(4):516-526. doi:10.1016/j.ccr.2013.03.018

394. Kammertoens T, Blankenstein T. It's the peptide-mhc affinity, stupid. *Cancer Cell*. 2013;23(4):429-431. doi:10.1016/j.ccr.2013.04.004

395. Arakaki R, Yamada A, Kudo Y, Hayashi Y, Ishimaru N. Mechanism of activation-induced cell death of T cells and regulation of FasL expression. *Crit Rev Immunol*. 2014;34(4):301-314. doi:10.1615/critrevimmunol.2014009988

396. Zhang Z, Liu S, Zhang B, Qiao L, Zhang Y, Zhang Y. T Cell Dysfunction and Exhaustion in Cancer. *Front Cell Dev Biol*. 2020;8(February). doi:10.3389/fcell.2020.00017

397. Specht JM, Lee SM, Turtle C, et al. Abstract P2-09-13: A phase I study of adoptive immunotherapy for ROR1+ advanced triple negative breast cancer (TNBC) with defined subsets of autologous T cells expressing a ROR1-specific chimeric antigen receptor (ROR1-CAR). *Cancer Res*. 2019;79(4 Supplement):P2-09-13 LP-P2-09-13. doi:10.1158/1538-7445.SABCS18-P2-09-13

398. Wallstabe L, Göttlich C, Nelke LC, et al. ROR1-CAR T cells are effective against lung and breast cancer in advanced microphysiologic 3D tumor models. *JCI Insight*. 2019;4(18). doi:10.1172/jci.insight.126345

399. Martinez M, Moon EK. CAR T cells for solid tumors: New strategies for finding, infiltrating, and surviving in the tumor microenvironment. *Front Immu-*

nol. 2019;10(FEB):1-21. doi:10.3389/fimmu.2019.00128

400. Riddell shivani S and SR. CAR T Cell Therapy: Challenges to Bench-to-Bedside Efficacy. *Physiol Behav*. 2017;176(5):139-148. doi:10.1016/j.physbeh.2017.03.040

401. VAN DE GRIEND RJ, BOLHUIS RLH. RAPID EXPANSION OF ALLOSPECIFIC CYTOTOXIC T CELL CLONES USING NONSPECIFIC FEEDER CELL LINES WITHOUT FURTHER ADDITION OF EXOGENOUS IL2. *Transplantation*. 1984;38(4):401-406. doi:10.1097/00007890-198410000-00017

402. Liu NQ, De Marchi T, Timmermans AM, et al. Ferritin heavy chain in triple negative breast cancer: A favorable prognostic marker that relates to a cluster of differentiation 8 positive (CD8+) effector t-cell response. *Mol Cell Proteomics*. 2014;13(7):1814-1827. doi:10.1074/mcp.M113.037176

403. Hoof I, Peters B, Sidney J, et al. NetMHCpan, a method for MHC class i binding prediction beyond humans. *Immunogenetics*. 2009;61(1):1-13. doi:10.1007/s00251-008-0341-z

404. Reche PA, Glutting JP, Reinherz EL. Prediction of MHC class I binding peptides using profile motifs. *Hum Immunol*. 2002;63(9):701-709. doi:10.1016/S0198-8859(02)00432-9

405. Reche PA, Reinherz EL. Prediction of peptide-MHC binding using profiles. *Methods Mol Biol*. 2007;409:185-200. doi:10.1007/978-1-60327-118-9_13

406. Miles KM, Miles JJ, Madura F, Sewell AK, Cole DK. Real time detection of peptide-MHC dissociation reveals that improvement of primary MHC-binding residues can have a minimal, or no, effect on stability. *Mol Immunol*. 2011;48(4):728-732. doi:10.1016/j.molimm.2010.11.004

407. Butler MO, Lee JS, Ansén S, et al. Long-lived antitumor CD8+ lymphocytes for adoptive therapy generated using an artificial antigen-presenting cell. *Clin Cancer Res*. 2007;13(6):1857-1867. doi:10.1158/1078-0432.CCR-06-1905

408. Kunert A, van Brakel M, van Steenbergen-Langeveld S, et al. MAGE-C2-Specific TCRs Combined with Epigenetic Drug-Enhanced Antigenicity Yield Robust and Tumor-Selective T Cell Responses. *J Immunol*. 2016;197(6):2541-2552. doi:10.4049/jimmunol.1502024

409. Straetemans T, … MVB-C and, 2012 undefined. TCR gene transfer: MAGE-C2/HLA-A2 and MAGE-A3/HLA-DP4 epitopes as melanoma-specific immune targets. *downloads.hindawi.com*.

410. Lamers CHJ, Willemsen R a, van Elzakker P, van Krimpen B a, Gratama JW, Debets R. Phoenix-ampho outperforms PG13 as retroviral packaging cells to transduce human T cells with tumor-specific receptors: impli-

cations for clinical immunogene therapy of cancer. *Cancer Gene Ther*. 2006;13(5):503-509. doi:10.1038/sj.cgt.7700916

411. Willemsen RA, Weijtens MEM, Ronteltap C, et al. Grafting primary human T lymphocytes with cancer-specific chimeric single chain and two chain TCR. *Gene Ther*. 2000;7(16):1369-1377. doi:10.1038/sj.gt.3301253

412. Bendle GM, Linnemann C, Hooijkaas AI, et al. Lethal graft-versus-host disease in mouse models of T cell receptor gene therapy. *Nat Med*. 2010;16(5):565-570. doi:10.1038/nm.2128

413. Ahmadi M, King JW, Xue SA, et al. CD3 limits the efficacy of TCR gene therapy in vivo. *Blood*. 2011;118(13):3528-3537. doi:10.1182/blood-2011-04-346338

414. Gallegos AM, Xiong H, Leiner IM, et al. Control of T cell antigen reactivity via programmed TCR downregulation. *Nat Immunol*. 2016;17(4):379-386. doi:10.1038/ni.3386

415. Fraietta JA, Nobles CL, Sammons MA, et al. Disruption of TET2 promotes the therapeutic efficacy of CD19-targeted T cells. *Nature*. 2018;558(7709):307-312. doi:10.1038/s41586-018-0178-z

416. Schober K, Müller TR, Gökmen F, et al. Orthotopic replacement of T-cell receptor α- and β-chains with preservation of near-physiological T-cell function. *Nat Biomed Eng*. 2019. doi:10.1038/s41551-019-0409-0

417. Govers C, Sebestyén Z, Coccoris M, Willemsen RA, Debets R. T cell receptor gene therapy: strategies for optimizing transgenic TCR pairing. *Trends Mol Med*. 2010;16(2):77-87. doi:10.1016/j.molmed.2009.12.004

418. Clauss J, Obenaus M, Miskey C, et al. Efficient Non-Viral T-Cell Engineering by Sleeping Beauty Minicircles Diminishing DNA Toxicity and miRNAs Silencing the Endogenous T-Cell Receptors. *Hum Gene Ther*. 2018;29(5):569-584. doi:10.1089/hum.2017.136

419. Provasi E, Genovese P, Lombardo A, et al. Editing T cell specificity towards leukemia by zinc finger nucleases and lentiviral gene transfer. *Nat Med*. 2012;18(5):807-815. doi:10.1038/nm.2700

420. Berdien B, Mock U, Atanackovic D, Fehse B. TALEN-mediated editing of endogenous T-cell receptors facilitates efficient reprogramming of T lymphocytes by lentiviral gene transfer. *Gene Ther*. 2014;21(6):539-548. doi:10.1038/gt.2014.26

421. Legut M, Dolton G, Mian AA, Ottmann OG, Sewell AK. *CRISPR-Mediated TCR Replacement Generates Superior Anticancer Transgenic T Cells*.; 2018.

422. Roth TL, Puig-Saus C, Yu R, et al. Reprogramming human T cell

function and specificity with non-viral genome targeting. *Nature*. 2018;559(7714):405-409. doi:10.1038/s41586-018-0326-5

423. Leong W, Nankervis B, Beltzer J. Automation: what will the cell therapy laboratory of the future look like? *Cell Gene Ther Insights*. 2018;4(9):679-694. doi:10.18609/cgti.2018.067

424. Wen WX, Leong CO. Association of BRCA1- And BRCA2-deficiency with mutation burden, expression of PD-L1/ PD-1, immune infiltrates, and T cell-inflamed signature in breast cancer. *PLoS One*. 2019;14(4):1-16. doi:10.1371/journal.pone.0215381

425. Heijink AM, Talens F, Jae LT, et al. BRCA2 deficiency instigates cGAS-mediated inflammatory signaling and confers sensitivity to tumor necrosis factor-alpha-mediated cytotoxicity. *Nat Commun*. 2019;10(1). doi:10.1038/s41467-018-07927-y

426. Rugo HS, Delord JP, Im SA, et al. Safety and antitumor activity of pembrolizumab in patients with estrogen receptor–positive/human epidermal growth factor receptor 2–negative advanced breast cancer. *Clin Cancer Res*. 2018;24(12):2804-2811. doi:10.1158/1078-0432.CCR-17-3452

427. Ayoub NM, Al-Shami KM, Yaghan RJ. Immunotherapy for HER2-positive breast cancer: Recent advances and combination therapeutic approaches. *Breast Cancer Targets Ther*. 2019;11:53-69. doi:10.2147/BCTT.S175360

428. He TF, Yost SE, Frankel PH, et al. Multi-panel immunofluorescence analysis of tumor infiltrating lymphocytes in triple negative breast cancer: Evolution of tumor immune profiles and patient prognosis. *PLoS One*. 2020;15(3):1-15. doi:10.1371/journal.pone.0229955

429. Szekely B, Bossuyt V, Li X, et al. Immunological differences between primary and metastatic breast cancer. *Ann Oncol*. 2018;29(11):2232-2239. doi:10.1093/annonc/mdy399

430. Page DB, Bear H, Prabhakaran S, et al. Two may be better than one: PD-1/PD-L1 blockade combination approaches in metastatic breast cancer. *npj Breast Cancer*. 2019;5(1):1-9. doi:10.1038/s41523-019-0130-x

431. Tolaney SM, Kabos P, Dickler MN, et al. Updated efficacy, safety, & PD-L1 status of patients with HR+, HER2- metastatic breast cancer administered abemaciclib plus pembrolizumab. *J Clin Oncol*. 2018;36(15_suppl):1059. doi:10.1200/JCO.2018.36.15_suppl.1059

432. Castellaro AM, Rodriguez-Baili MC, Di Tada CE, Gil GA. Tumor-associated macrophages induce endocrine therapy resistance in ER+ breast cancer cells. *Cancers (Basel)*. 2019;11(2):1-29. doi:10.3390/cancers11020189

433. Jiang P, Gu S, Pan D, et al. Signatures of T cell dysfunction and exclusion predict cancer immunotherapy response. *Nat Med*. 2018;24(10):1550-1558.

doi:10.1038/s41591-018-0136-1

434. Riaz N, Havel JJ, Kendall SM, et al. Recurrent SERPINB3 and SERPINB4 mutations in patients who respond to anti-CTLA4 immunotherapy. *Nat Genet*. 2016;48(11):1327-1329. doi:10.1038/ng.3677

435. Zhou R, Yazdanifar M, Roy L Das, et al. CAR T cells targeting the tumor MUC1 glycoprotein reduce triple-negative breast cancer growth. *Front Immunol*. 2019;10(MAY):1-12. doi:10.3389/fimmu.2019.01149

436. Szoor A, Toth G, Zsebik B, et al. Trastuzumab derived HER2-specific CARs for the treatment of trastuzumab-resistant breast cancer: CAR T cells penetrate and eradicate tumors that are not accessible to antibodies. *Cancer Lett*. 2020. doi:10.1016/j.canlet.2020.04.008

437. Tóth G, Szöllősi J, Abken H, Vereb G, Szöőr Á. A small number of HER2 redirected CAR T cells significantly improves immune response of adoptively transferred mouse lymphocytes against human breast cancer xenografts. *Int J Mol Sci*. 2020;21(3):1-10. doi:10.3390/ijms21031039

438. Liu X, Zhang N, Shi H. Driving better and safer HER2-specific CARs for cancer therapy. *Oncotarget*. 2017;8(37):62730-62741. doi:10.18632/oncotarget.17528

439. Narang P, Chen M, Sharma AA, Anderson KS, Wilson MA. The neoepitope landscape of breast cancer: Implications for immunotherapy. *BMC Cancer*. 2019;19(1):1-10. doi:10.1186/s12885-019-5402-1

440. Zhang X, Kim S, Hundal J, et al. Breast cancer neoantigens can induce CD8+ T-cell responses and antitumor immunity. *Cancer Immunol Res*. 2017;5(7):516-523. doi:10.1158/2326-6066.CIR-16-0264.Breast

441. Huang J, Brameshuber M, Zeng X, et al. A Single peptide-major histocompatibility complex ligand triggers digital cytokine secretion in CD4+ T Cells. *Immunity*. 2013;39(5):846-857. doi:10.1016/j.immuni.2013.08.036

442. Stadtmauer EA, Fraietta JA, Davis MM, et al. CRISPR-engineered T cells in patients with refractory cancer. *Science (80-)*. 2020;367(6481):eaba7365. doi:10.1126/science.aba7365

443. Kunert A, Debets R. Engineering T cells for adoptive therapy: outsmarting the tumor. *Curr Opin Immunol*. 2018;51:133-139. doi:10.1016/j.coi.2018.03.014

444. Dötzer K, Schlüter F, Bo Schoenberg M, et al. Immune heterogeneity between primary tumors and corresponding metastatic lesions and response to platinum therapy in primary ovarian cancer. *Cancers (Basel)*. 2019;11(9):1-14. doi:10.3390/cancers11091250

445. Jiménez-Sánchez A, Memon D, Pourpe S, et al. Heterogeneous Tumor-Im-

mune Microenvironments among Differentially Growing Metastases in an Ovarian Cancer Patient. *Cell*. 2017;170(5):927-938.e20. doi:10.1016/j.cell.2017.07.025

446. Klinghoffer RA, Bahrami SB, Hatton BA, et al. HHS Public Access simultaneously within a patient ' s tumor. 2016;7(284):1-12. doi:10.1126/scitranslmed.aaa7489.A

Summary
Samenvatting

Summary

Cancer immunotherapy represents a collection of effective new treatment options for a number of tumor types. Nevertheless, not all tumor types respond equally well to current immune therapies. Zooming in on breast cancer, this type of tumor is currently confronted by a number of gaps in its treatment portfolio, namely: low response rates and lack of predictive markers for immune therapies; lack of druggable targets that counteract T cell evasion; and lack of safe and effective target antigens for adoptive T cell therapies.

Chapter 1 provides a short introduction to the thesis' research which includes a brief overview of standard treatment as well as immunotherapeutic approaches and their current challenges in breast cancer. According to these challenges, this thesis followed 2 main research lines:

-**Charting T cell evasion**: In Part 1 of this thesis (**Chapter2-4**) we focused on the knowledge gap regarding T cell evasive mechanisms, which, provides a basis for patient stratification and selection of combination therapies.

-**Exploring new targets for T cells**: In Part 2 of this thesis (**Chapter 5-7**) we focused on the identification and selection of safe and effective target antigens and corresponding TCRs for adoptive T cell therapy for TNBC (one of the subtypes of breast cancer).

In **Chapter 2** we reviewed recent literature regarding the composition of TILs, their prognostic and predictive value, and the antigenicity of breast cancer subtypes (Luminal-A, Luminal-B, HER2 and TNBC), which suggest that BC subtypes are not equally immunogenic and do not equally respond to immune therapies. Furthermore, we provided an overview of recent immune therapy trials in BC and propose a strategy to select ER+ and ER- patients for (combination-) immune therapies.

In **Chapter 3** we studied large cohorts of breast cancer subtypes for the differential prognostic value of various immune parameter and the occurrence of immune evasive strategies in silico. Our data suggest that not merely CD8 T cell presence itself, but rather clonality, subset distribution, and co-inhibition of T cells as well as antigen presentation reflect the occurrence of a CD8 T cell response in BC subtypes. According to our data, such CD8 T cell responses have been aborted by distinct T cell suppressive mechanisms, such as alteration in metabolic pathways, decreased expression of T cell adhesion molecules, enhanced expression of immunosuppressive mediators, or recruitment of different types of suppressor cells. Furthermore,

our data indicates that next to TNBC also HER2 and a subset of luminal B patients may benefit from immune therapies with subtype-specific combinations.

In **Chapter 4** we zoomed in on TNBC and studied the prognostic and predictive value of spatial immune contextures in untreated and anti-PD1 treated TNBC. We identified 3 immunophenotypes based on the spatial localization of CD8 T cells: excluded (T cells restricted to the invasive margin), ignored (no T cells present) and inflamed (T cells present in tumor center). We were able to capture these immunophenotypes by a gene classifier that predicts survival in untreated TNBC and various other cancers as well as anti-PD1 response of metastatic TNBC and melanoma. Importantly, our in-depth analyses revealed distinct T cell evasive pathways that advocate spatial immunophenotype-specific combinations, such as blockade of TGFb- or VEGF-pathways in case of the excluded phenotype, or blockade of M2 macrophages or WNT-pathway in case of the ignored phenotype to boost the efficacy of ICI in TNBC.

in **Chapter 5**, we reviewed in silico as well as laboratory tools and strategies to select target antigens, epitopes and TCRs for adoptive T cell therapy as well as tools that enable charting of T cell evasive mechanisms which can be used to select combination therapies.

In **Chapter 6**, we applied these technologies to large proprietary and public databases covering transcriptome data from tumor and healthy tissues and identified PCT2, as a TNBC-selective inracellular target antigen. We verified absent expression in healthy tissue and high- and homogenous expression in TNBC using qPCR and immune stainings. Furthermore, we selected unique and immunogenic target epitopes using a series of in silico predictions, HLA-peptidome analysis and in vitro binding assays. Finally, we identified a PCT2-specific TCR which can be further exploited for the development of adoptive T cell therapy for TNBC.

In **Chapter 7** we listed and described recent developments with respect to TCR-editing technologies that enable insertion of TCR transgenes into the endogenous TCR loci thereby facilitating endogenous regulation of TCR transgenes. Furthermore, these technologies enable simultaneous knock out of endogenous TCRα and TCRβ which reduces mispairing of TCR chains, which in turn limits toxicity risks of TCR engineered cells.

In **Chapter 8**, the main findings of Parts 1 and 2 were discussed in a broader context. Outstanding questions were formulated, and according to these questions, future research developments were proposed.

Samenvatting

Immunotherapie is een effectieve nieuwe behandelingsoptie voor kanker. In de regel houdt deze therapie in dat je tumorcellen niet direct behandeld, maar indirect door de immuun cellen van de patiënt te activeren, waardoor deze cellen, met name T cellen, de tumor aanvallen. Echter, niet alle tumortypen reageren even goed op deze therapieën. Zo reageert bij borstkanker slechts een relatief kleine fractie van de patiënten op immunotherapie, en dit varieert sterk afhankelijk van het borstkanker subtype. Het gebrek aan kennis hoe we het beste immunotherapie in borstkanker kunnen ondersteunen, dwz onderzoek naar de onderliggende reden waarom T cellen hun taak niet uitvoeren, en hoe we dit kunnen verbeteren, is het onderwerp van dit proefschrift.

Hoofdstuk 1 leidt het onderzoek in, en geeft een kort overzicht van zowel standaardbehandelingen als immunotherapiën bij borstkanker. Ondanks vooruitgang in klinische effecten door immunotherapie, is er duidelijk ruimte voor verbetering. Hiertoe is in dit proefschrift onderzoek gedaan volgens 2 hoofdlijnen:

-**In kaart brengen van redenen waarom T cellen hun taak niet uitvoeren**: In deel 1 van dit proefschrift (hoofdstuk 2-4) hebben we ons gericht op mechanismen van borstkanker die T cellen om de tuin leiden, en welke een basis kunnen bieden voor de ontwikkeling van factoren welke voorspellen of een patiënt wel/niet gaat reageren, en hoe het beste combinatietherapieën te kiezen.

-**Verkenning van nieuwe targets voor T-cellen**: In deel 2 van dit proefschrift (hoofdstuk 5-7) hebben we ons gericht op de identificatie en selectie van veilige en effectieve doelwit-antigenen en bijbehorende T cel receptoren (TCRs; receptoren waarmee T cellen antigenen op tumorcellen herkennen) voor adoptieve T-celtherapie bij TNBC.

In **Hoofdstuk 2** hebben we recente literatuur samengevat en besproken met betrekking tot de samenstelling van tumor-infiltrerende immuuncellen, hun voorspellende waarde wat betreft patiënt overleving, en immunogeniciteit van borstkanker subtypen. Verder hebben we een overzicht gegeven van recente klinische studies die gericht zijn op immunotherapie in borstkanker, en een strategie voorgesteld om zogenaamde oestrogeen receptor-positieve en negatieve patiënten te selecteren voor (combinatie-) immunotherapieën.

In **Hoofdstuk 3** hebben we grote patiëntcohorten van verschillende borstkanker

subtypen bestudeerd wat betreft verschillende immuun parameters en het optreden van T cel ontwijkende mechanismen. Onze gegevens suggereren dat niet alleen de aanwezigheid van CD8 T-cellen, maar eerder functionele karakteristieken bepalend zijn voor het optreden van een effectieve anti-tumor T-cel respons. Interessant is dat in de verschillende subtypen, functionele T cel responsen op verschillende wijzen ontweken lijken te worden. Bovendien geven onze gegevens aan dat naast het TNBC subtype ook HER2 en een subset van luminale B-patiënten baat kunnen hebben bij immunotherapieën die ondersteund worden met subtype-specifieke behandeling.

In **Hoofdstuk 4** hebben we TNBC uitgelicht, en hebben we de ruimtelijke verdeling van immuun cellen in onbehandelde en anti-PD1 behandelde patiënten bestudeerd. We identificeerden 3 fenotypen op basis van de ruimtelijke lokalisatie van CD8 T-cellen. Naast immuun kleuringen konden we deze fenotypen vaststellen met een serie genen (een zogenaamde classifier) die de overleving in TNBC voorspelt, evenals de anti-PD1-respons van uitgezaaid TNBC. Belangrijk is dat onze diepgaande analyses verschillende T-cel ontwijkende routes aan het licht brachten welke pleiten voor het belang van ruimtelijke informatie wat betreft CD8 T cellen om juiste behandel keuzes te maken voor TNBC.

In **Hoofdstuk 5** hebben we computer en laboratoriumtechnieken besproken om doelwit-antigenen, epitopen en TCRs te selecteren voor adoptieve T-celtherapie, evenals up-to-date technieken om T-cel ontwijking in kaart te brengen. Slimme keuzes van dergelijke technieken maakt het mogelijk op rationele wijze combinatietherapieën te selecteren.

In **Hoofdstuk 6** hebben we deze technologieën toegepast op grote databases die transcriptoom data van tumor en gezonde weefsels bevatten en op deze wijze PCT2 geïdentificeerd als een TNBC-selectief doelwit-antigeen. We verifieerden afwezige expressie van dit antigeen in gezond weefsel en toonden hoge en homogene expressie in TNBC. Verder selecteerden we unieke en immunogene epitopen, en tot slot hebben we een PCT2 specifieke TCR geïdentificeerd die verder kan worden getest voor de ontwikkeling van adoptieve T-celtherapie.

In **Hoofdstuk 7** hebben we recente technische noviteit besproken die endogene regulering toelaat van TCR-transgenen, zogenaamde TCR-gene editing. Deze technologie zorgt verder voor uit-knocking van endogene TCR genen waardoor risico's van toxiciteit sterk vermindert.

In **Hoofdstuk 8** werden de belangrijkste bevindingen van deel 1 en 2 bediscussieert. Openstaande onderzoeksvragen zijn geformuleerd, en aan de hand van deze vragen is toekomstige onderzoek is voorgesteld.

Acknowledgements

Acknowledgements

Despite that this thesis displays a single name on its cover, it would not have been possible to create it without the help of many people:

To my promotors, prof. Reno Debets and **prof. John W. M. Martens**:

Dear **Reno**, I'd like to express my gratitude for all your trust and support over the past years. You really did a great job in guiding my scientific path towards obtaining my PhD degree. I'd like to thank you for all the good scientific discussions that pushed the work in this thesis; the time and effort you took to answer every email (even in the middle of the night, or during your vacation ;-)) and of course the laughs and positivity during work meetings and lab-outings. I truly admire your dedication to science, everything you do for the team and that your family and even Frodo always come first! Thanks for everything and I'm looking forward to more exciting science and PCT adventures.

Dear **John**, thank you so much for being a great co-promotor. I always appreciated your direct and honest view during work discussions. Even tough immunology was not your primary expertise, you had great suggestions and your out-of-the-box thinking was always very much appreciated. I admire, the way you run your lab, collaborate with many people, always push science while maintain scientific integrity. Thanks for all your input, help and support, random jokes and I hope we can continue working together on many projects.

To prof. Stefan Sleijfer: Dear Stefan, you were my promoter during the first year and I would like to thank you for not only the scientific input and for trying to maintain timelines but also for asking me about my career goals. While at that time I did not know where I saw myself in 10 years, it made me think and realize that I do really want to pursue a career in academia. I'd also like to thank you and the *scout and behoud commissie* for your trust and the opportunity to pursue this ambition.

To the reading committee: prof. Peter Sillevis-Smitt, prof. Roberto Salgado and **prof. Ton Langerak** thank you for thoroughly reading and assessing my thesis.

To the remaining members: dr. Caroline van Deurzen; dr. Sonja Buschow; dr.

Martijn Lolkema; prof. Guido Jenster, prof. Stefan Sleijfer, prof. Georges Coukos, thank you for taking part in the committee.

To the lab-members: Rebecca, thanks for all your help and the fun hours petting mice and watching beautiful pictures on the Vectra. I truly admire your organization skills, leakless memory and directness. You are a great colleague, on a scientific as well as personal level! **Mandy**, the first memory of you was a huge belly and a huge smile! You are not only a great role model in the lab but also as a working mom. Thanks for all your help with in vitro experiments and of course the chats that always made we forget with what question I came to your office. **Cor B**, we did not really collaborate on a project, but I really enjoyed having you around doing your own thing (starting from different kind of music to sometimes doing experiments somewhat different than you first had in mind). I always enjoyed talking about sports, culture, or life in general. **Astrid**, we did not work much together either, but I really appreciate your support with the FACS and for always being super helpful. You are a great addition to our lab as well as lab-outings! **Emrah**, thanks for your help with VECTRA and image analysis and for always promoting lab outings and of course for feeding us! Also you are a great addition to the lab, scientifically as well as personally. **Cor L**, thanks for your help with METC related questions, your awesome dance moves that made every conference party more fun. You are being missed in the lab. **Pim**, please come by more often!

Mieke, thank you for always making time for me, prioritizing our project when it was needed, and for being nice and caring in general. I really enjoyed working together including spending hours watching tissues and scoring slides and of course our chats. Thanks a lot, and I am really happy that you are my paraminf. **Anita** and **Renée**, thank you for all your help with stainings etc. I admire your dedication and scientific accuracy. I really appreciate that, and always enjoyed working together. **Marcel**, thank you for all your help and answering all my bioinformatics questions. I really appreciate your help, input and jokes and am impressed how you always manage to keep your promise regarding timelines. I've heard the following a lot and could not agree more: *we all need more Marcels* (and then I mean clones, not just people called the same name ;-)).

To all other lab members and colleagues in the JNI, thanks for your help and collaboration and for creating such a great work atmosphere that made coming to work just a little bit nicer!

To my fellow (ex-) PhD students: Yarne and **André**, you gave me a warm welcome when I started my PhD. I love thinking back to the time in the cave (except for the view and the smell, obviously). It was our safe room and we shared all of our excitement as well as setbacks. You are both super smart and fun but also very different. **André**, thanks for always being there and pushing me (indirectly) to remember other peoples birthday and be more kind in general. **Yarne**, thanks for your help with R, the loughs and for pushing me physically into walls and for pushing Cor Bs' buttons during the breaks.

Maud and **Priscilla**, with you the cave slowly turned into a warm nest (including slightly better smells -thanks!) and I had so much fun talking girls stuff and even doing shopping nights after work. We were all in a similar stage in our PhD and life in general and it was awesome to come into such a warm nest every morning. **Dian**, you came here as my student and you became a colleague and even my paranimf. Thanks for always being yourself and making our lab a better place with your smile, enthusiasm and by just being you! Please never change that! Of course, I also would like to thank you for your help in the lab and I really enjoy working together. **Shweta**, you always make me smile when you come into the room with a waaay to happy "good morning". Besides all the effort and hard work, you inspire me to be a better person with your view on life and your goals for later in life. **Chumut**, even though we were colleagues for a while we only got to know each other a little better when you moved to our office. Also you make me smile when you come in and I appreciate your kindness and great attitude.

To my master students: Daan and **Alex**, I enjoyed sharing my knowledge and lab skills with you. Thanks for all your enthusiasm and help!

A

To our collaborators: Sonja, Monique, Morten, Mikkel, Zlatko, Dietmar, Marleen, Leonie, Iris, Hugo, Roberto, Carolien, **Maxine**, **Guido, Harmen** and **Job**, I would like to thank you for your help, useful discussions and/or critical review. I enjoyed collaborating on different projects and papers and very much hope that it will continue this way.

To my family and friends: Richard and **Silla**, thanks for raising me in a way that made me believe that I can achieve and do anything in life, and for being great parents and role models in many ways. To you and the rest of our crazy *patchwork*

family, I'd like to thank you for all the love and support throughout the years.

Gerle, we spent the past 9 years together and lately much of my time and energy went into my PhD. I really appreciate your support, for moving to Leiden, to the US and for accepting a little less attention when I was working in the weekends or at night. I also would like to thank you for being my rock (and sometimes water) and for making me laugh and feeling loved when I needed it. A big *thank you* also the rest of the Ykema-family for all your love, support and for making me truly feel at home in the Netherlands.

To all my friends, in Austria, the US and the Netherlands, many thank for being a great distraction from the phD stress, for always being there for me and for all the fun during (video-) calls, on the sand, in the water and of course while traveling.

PhD Portfolio

PhD portfolio

General information:

Name:	Dora Hammerl
Research school:	Molecular Medicine
Period:	01-01-2016 until 01-07-2020
Promotor 1:	prof. Reno Debets
Promotor 2:	prof. John Martens

1. PhD training	Year	Time	ECTS
1.1 General academic skills			
1.2 Research skills			
1.3 In-depth courses (e.g. Research school, medical training)			
• Advanced Immunology course, Erasmus MC, March 15-24	2016	8d	3
• Article 9 acc to Dutch law on animal experimentation, Rotterdam, April 4-22	2016	3wk	4,2
1.4.1 Poster Presentations			
• Keystone Symposium, 24-28 January, Vancouver, Canada	2016	14h	0,5
• VIB Cell Symposium, 11-13 December, Ghent, Belgium	2016	14h	0,5
• AACR-CIMT, 6-9 September, Mainz, Germany	2017	14h	0,5
• SABCS, 4-8 December, San Antonio USA	2018	14h	0,5
• Keystone Symposium, 10-14 March, Whistler, Canada	2019	14h	0,5

1.4.2 Oral Presentations			
• Tumor Immunology Platform (TIP) Erasmus MC bi-annual	2016	28h	1
• Keystone Symposium, January 24-28, Vancouver, Canada	2016	28h	1
• JNI scientific research meeting, October 17, Erasmus MC	2016	28h	1
• TCC meeting, January 12, Erasmus MC	2017	28h	1
• CGC meeting, January 13, Utrecht, the Netherlands	2017	28h	1
• Wetenschapsmiddag, June 16, Erasmus MC	2017	28h	1
• DTIM, June 22, Breukelen, the Netherlands	2017	28h	1
• Talk/chairing MORM meeting, June 8, Erasmus MC	2017	28h	1
• NVVI, December 2017, Noordwijkerhout, the Netherlands	2017	28h	1
• EMCCR day, October 29, Erasmus MC	2017	28h	1
• Talk/chairing MORM meeting, Sept 5, Erasmus MC	2018	28h	1
• JNI scientific research meeting, June 19, Erasmus MC	2018	28h	1
• Healthy Ideas Healthy Returns, May 8, Ghent, Belgium	2018	28h	1
• ACE Tumor Immunology meeting, June 25, Erasmus MC	2019	28h	1
• TCC meeting, November 28, Erasmus MC	2019	28h	1
• NVVI December 10-11, Noordwijkerhout	2020	28h	1
• ACE Breast Cancer, June 29, Erasmus MC	2020	28h	1
1.5 *International conferences*			
• Keystone Symposium, January 24-28, Vancouver, Canada	2016	1wk	1,4
• VIB Cell Symposium, December 11-13, Ghent, Belgium	2016	3d	1
• AACR-CIMT-meeting, September 6-9, Mainz, Germany	2017	4d	1
• SABCS, 4-8 December, San Antonio, USA	2018	1wk	1
• Keystone Symposium, March10-14, Whistler, Canada	2019	1wk	1

1.6 Seminars and workshops			
• Course: R, Erasmus MC	2016	4d	1
• Course: Gene expression analysis in R, Erasmus MC	2016	1wk	1,4
• Workshop in Pathology and Digital quantification, Erasmus MC	2016	4h	0,15
• Course: IPA pathway analysis, Erasmus MC	2016	8h	0,3
• Scientific integrity, Erasmus MC	2017	8h	0,3
• Personal Grant Charities	2019	8h	0,3
• NWO VENI workshop	2020	8h	0,3
1.7 Didactic skills			
1.8 Other 2016-2020			
• T cell consortium (TCC) meetings (~6x yearly), Erasmus MC	4 years	6h	0,8
• JNI scientific research meetings (~36x yearly), Erasmus MC	4 years	36h	6
• Tumor Immunology Platform (TIP) meetings (~36x yearly), Erasmus MC, an interdepartmental journal club and project meeting on tumor immunology, Rotterdam	4 years	36h	6
• Medical Oncology Research Meeting (MORM) (~6x yearly), Erasmus MC	4 years	12h	2
2. Teaching activities			
2.1 Lecturing			
• Molmed Lecture on Immunotherapy for solid tumors	2017	12h	0,5
• Molmed Lecture on Immunotherapy for solid tumors	2018	12h	0,5
• Nanobiology Course on Tumor Immunology	2019	12h	0,5
• Nanobiology Course on Tumor Immunology	2020	12	0,5
2.2 Supervising practical's and excursions			
• Ellis Eikenboom, Research Minor, 4wk	2016	36h	1,5
• Daan van Dorst, Research Master, 6 months	2017	108h	3
• Dian Kortleve, Research Master, 9 months	2018	108h	3
• Alexandre Marraffa, Research Master, 9 months	2019	108h	3

2.3 Supervising theses			
• Laura Moonen, BSc, 6months	2016	28h	1
• Anniek Meesters, BSc, 6months	2017	28h	1
• Daan van Dorst, MSc, 6months	2017	28h	1
• Dian Kortleve, MSc, 9months	2018	28h	1
• Alexandre Marraffa, MSc, 9month	2020	28h	1
2.4 Other			
Subtotal	66,15		
(28 hours workload = 1 ECTS) Total ECTS	ECTS		

List of Publications

List of publications

Hammerl D, Smid M, Timmermans M, Sleijfer S, Martens J, Debets R
'Breast cancer genomics and immuno-oncological markers to guide immune therapies' Special Issue in Seminars in Cancer Biology on Immuno-oncological Biomarkers. 2018 Oct;52(Pt 2):178-188

Hammerl D, Massink M, Smid M, van Deurzen CMH, Meijers-Heijboer H, Waisfisz Q, Debets R*, Martens JWM*; *joint senior authors
'Differential prognostic value in breast cancer subtypes: not T cell abundance, rather T cell influx, antigen recognition and suppression'
Clinical Cancer Research, 2020 Jan 15;26(2):505-517

Hammerl D, Rieder D, Smid M, Martens JWM, Trajanoski Z, Debets R
'Adoptive T cell Therapy: new avenues leading to safe targets and powerful allies'
Trends in Immunology, Nov;39(11):921-936

Kortleve D, Hammerl D and Debets R
'Orthotopic editing of T-cell receptors'
Nature Biomedical Engineering, 2019 Dec;3(12):949-950.

Agahozo MC , Hammerl D, Debets R, Kok M, van Deurzen CHM
'The role of the immune system during ductal carcinoma in situ of the breast'. Modern Pathology, 2018 Jul;31(7):1012-1025
Uhr K, Sieuwerts AM, de Weerd V, Smid M, Hammerl D, Foekens JA, and Martens JWM
'Association of microRNA-7 and its binding partner CDR1-AS with the prognosis and prediction of 1st-line tamoxifen therapy in breast cancer'. Scientific Reports. 2018 Jun 25;8(1):9657

Submitted manuscripts

Hammerl D, Timmermans A, Martens JWM, Smid M, Trapman-Jansen A, Foekens R, Isaeva OI, Voorwerk L, Balcioglu HE, Wijers R, Salgado R, Nederlof I, Horlings H, Kok M, Debets R
'Spatial immunophenotypes predict response to anti-PD1 in Triple Negative Breast Cancer capture distinct paths of CD8 T cell evasion'
Nature Communication, in revision.

Mutsaers P, Kuipers R, Hammerl D, van Duin M, van der Holt R, Zweegman S, Cornelissen J, Debets R, Sonneveld P.
'Multiple myeloma escapes T-cell evasion by differential expression genes responsible for T-cell co-signaling, adhesion molecules and autophagy'
JCI, under review.

Manuscripts in preperation

Hammerl D, Kortleve D, Timmermans A, van Brakel M, van Dorst D, Martens JWM and Debets R
'PCT2 is a novel, tumor selective and highly prevalent target for T cell receptors against triple negative breast cancer' Manuscript in preparation

van Riet J, Hammerl D, van Gelder M, van de Werken HJG, Jenster G and Debets R
'An exploratory study into the immunogenetics and immunotherapy potential in prostate-cancer'
Manuscript in preparation.

Timbergen MJM, Grünhagen DJ, Verhoef C, Sleijfer S, Smid M, Chibon F, Hammerl D, Debets R, Wiemer EAC
'Defining the immune microenvironment of desmoid-type fibromatosis'
Manuscript in preparation.

Additional dutch publications

Wilting S, van Deurzen CHM, Meijer TG, Hammerl D, Martens JWM, Bos M
"Moleculaire diagnostiek van het mammacarcinoom ten behoeve van de praktijk".
Pfijzer Oncologie Special 2019, PP-ONC-NLD-0583

About the author

About the author

Dora was born in 1989 and grew up in a small town called Oberwart in south-east Austria. Despite, having a passion for art and sports she graduated high school with majors in English, biology, physics and psychology. Dora was curious about nature and a series of fatal illnesses of friends and family, sparked her interest to learn more about cancer. In 2008 Dora moved to Vienna to pursue her studies in molecular biology at the University of Vienna. After receiving her BSc degree in 2012, she moved to the Netherlands where she obtained a MSc Diploma (cum laude) in biopharmaceutical sciences at Leiden University. Dora always dreamed about living in a tropical place, and didn't think twice when she got the opportunity in 2015 to work at La Jolla Institute located in San Diego. After moving to the US, she studied ways to activate the immune system against cancer by targeting adenosine receptors (PI: prof. Joel Linden). Regardless of countless joyful hours working at a cutting-edge research institute, endless sunset surfing sessions and good memories, she felt the need to move on and obtain a doctorate degree. Dora found a vacancy to obtain a PhD in the field of tumor immunology at one of the leading research university medical centres in Europe, the Erasmus MC Cancer Institute. In 2016 she moved back to the Netherlands and started a PhD position at the laboratory of Tumor Immunology (PI: prof. Reno Debets in collaboration with prof. John Martens) and put all her energy into understanding the interplay between cancer cells and immune cells, and finding new targets in order to boost T cell immunity in breast cancer. From July 2020 onwards, she continued to work at the laboratory of Tumor Immunology as a postdoctoral fellow, in order to work towards clinical translation of the research presented in this thesis.